THE UNIVERSITY OF MELBOURNE

DOCTORAL THESIS

Mechanochromic Polymeric Materials Based on Spiropyran

Wenlian Qiu

ORCID: 0000-0002-4903-9219

January 2020

Polymer Science Group

Department of Chemical Engineering

Submitted in total fulfilment of the requirements of the degree of Doctor of Philosophy

Abstract

Smart chromic materials which change colour due to an external stimulus such as light, mechanical force, temperature and humidity have great potential in commercial applications including as sensors, coatings and drug delivery. Mechanochromic polymeric materials, those polymeric materials which respond to an applied force, are one of the most widely studied and one strategy for their preparation is to covalently bond a mechanochromophore such as spiropyran (SP) into a polymer matrix. Spiropyran when constrained in this way, undergoes a ring-opening reaction to form brightly coloured merocyanine (MC) isomer when subjected to an external force. Although SP has been integrated into a wide range of polymers, lacking the detailed understanding of the factors that affect their mechanochromic properties and challenges in achieving high mechanochromic sensitivity of these systems have limited their practical applications.

The goals of this thesis were to explore the factors affecting the mechanochromic efficiency of SP to MC and design advanced polymer architectures to improve their mechano-sensitivity. In Chapter 2, a new tri-functional SP (SP3) combining the attachment positions of the two most commonly used SPs (SP1 and SP2) was synthesized. The three SPs (SP1-3) were subsequently crosslinked into the same non-polar polydimethylsiloxane (PDMS) polymer and their mechanochromic properties induced by compression and tension were evaluated. The influence of varying the functional group attachment to the matrix resulting in the geometric and electronic changes on their mechanochromic properties were investigated. The outcome of this investigation determined that of the two factors influencing the mechanochromic responsiveness of the materials, the geometric effect was more dominant than the electronic effect. Typically the majority of mechanochromic SPs are conjugated in non-polar matrices for their studies, however in Chapter 3, we studied the incorporation of SPs (SP1-3) into polar poly(hydroxyethyl acrylate) (PHEA) polymer and studied their unique mechanochromic properties and negative photochromism due to the polar environment. In this investigation the mechanochromic materials were triggered by the force induced by swelling in water. The results demonstrated that SP3 with more attachment points was the least affected by the polar environment and it showed the fastest mechano-activation during swelling.

Following on from the swelling-induced mechanochromic advantages observed for SP3, in Chapter 4, a multi-network structure of polyacrylates was adopted to incorporate this mechanophore into a pre-stretched first-network. The resultant double network presented a remarkable mechanochromic activity, where the corresponding SP-linked single network showed no colour change. The activation energy was further reduced by the formation of a third-network. This SP-linked triple-network was shown to display the lowest activation energy compared to previously reported SP-linked elastomers, demonstrating a significant improvement in the mechanochromic sensitivity of these materials due to advanced architectural design.

This thesis therefore provides insights into the factors influencing the ring-opening efficiency of SP to MC through the design of a new SP, and led to a new strategy towards the fabrication of highly sensitive mechanochromic SP-linked polymer. The outcomes of this research will be useful for the design of mechanochromic materials for targeted applications such as force sensors and authentication devices.

Declaration of Authorship

I, Wenlian Qiu, declare that this PhD thesis titled, “Mechanochromic Polymeric Materials based on Spiropyran” and the research work presented in it are my own work. I confirm that:

- This thesis comprises only my original research work towards my PhD degree at this University.
- Due acknowledgement has been made in the text to all other materials used.
- The thesis is less than 100,000 words in length, exclusive of tables, maps, bibliographies and appendices.

Wenlian Qiu

Preface

Assistance with DFT calculations described in Chapter 2 were given by Dr. Gabriel da Silva.

Acknowledgements

Finally, I am standing at the terminal of PhD study! It's impossible for me to reach where I am now without a lot of people's help. Thank all the people that I have met during this trip. First and foremost, I would like to thank my main supervisor Prof. Greg Qiao for providing me with the opportunity to do research in Polymer Science Group and giving me a lot of support and guidance. Thank him for the encouragement of pursing truth and jumping out of the box for scientific research. And I would also like to thank my co-supervisor Dr. Paul Gurr for his patience of teaching me various experimental skills, helping me analyse data and revising the manuscripts. Also thank Paul for his management of the lab to ensure that we can conduct experiments safely and smoothly.

I would like to express my gratitude to Dr. Gabriel da Silva for conducting molecular modelling for my research project. Appreciation is extended to my PhD committee Chair Prof. Dave Dunstan for guiding me on the right track during my PhD journey. Thank the technicians and colleagues in the Department of Chemical Engineering and the Department of Chemistry for the assistance of materials characterization, and the staff in physics workshop for efficiently creating the experimental moulds for me. I would like to thank all the past and present group members in Polymer Science Group for giving me a lot of experimental help, laughs and joy.

I have received several scholarships supporting my PhD study and trips for conference. I would like to thank The University of Melbourne for providing me with the Melbourne International Fee Remission Scholarship (MIFRS) and Melbourne International Research Scholarship (MIRS). Thank the Melbourne School of Engineering for offering me the Travelling Scholarship and Clive Pratt Scholarship, and Particulate Fluids and Processing Center (PFPC) for providing me with PFPC Travel Grant.

Outside of the research, I would like to say thank you to my besties in Melbourne and in China for being there with me through all the frustrating moments and sharing joy with me. Most importantly, I would like to give my deepest gratitude to my family for their unconditional love and ongoing support no matter what I am. I can't express in words my appreciation to them, and I hope I can be strong to likewise support them in the future.

List of Publications

Publications obtained from this thesis

Note that the publication copies are included at the end of the thesis.

Wenlian Qiu, Paul A. Gurr, Gabriel da Silva, Greg G. Qiao. "Insights into the Mechanochromism of Spiropyran Elastomers", *Polymer Chemistry*, 2019, 10, 1650–1659. (**Chapter 2**)

Wenlian Qiu, Paul A. Gurr, and Greg G. Qiao. "Colour-Switchable Polar Polymeric Materials", *ACS Applied Materials & Interfaces*, 2019, 11, 29268–29275. (**Chapter 3**)

Wenlian Qiu, Paul A. Gurr, and Greg G. Qiao. "Regulating Color Activation Energy of Mechanophore-linked Multi-network Elastomers", *Macromolecules*, in press, DOI: 10.1021/acs.macromol.0c00477. (**Chapter 4**)

Other publications not included in this thesis

Jianhua Zhao, Ke Xie, Liang Liu, Min Liu, **Wenlian Qiu**, Paul A. Webley. "Enhancing plasticization-resistance of mixed-matrix membranes with exceptionally high CO2/CH4 selectivity through incorporating ZSM-25 zeolite", *Journal of Membrane Science*, 2019, 583, 23-30.

Alicia Rasines Mazo, Stephanie Allison-Logan, Fatemeh Karimi, Nicholas Jun-An Chan, **Wenlian Qiu**, Wei Duan, Neil M. O'Brien-Simpson, Greg G. Qiao. "Polypeptides via ring opening polymerization of α-amino acids: recent advances in synthesis, architecture and applications of polypeptides and their hybrids", *Chemical Society Reviews*, 2020, DOI:10.1039/c9cs00738e.

Conference Proceedings

"Insight into the Mechanical Response of Spiropyran in Elastomers"

Wenlian Qiu, Paul A. Gurr, Gabriel da Silva, Greg G. Qiao

European Polymer Congress 2019 (EPF 2019), Crete, Greece, June 2019. (**Oral presentation**)

"Colour switchable polar polymers based on spiropyran"

Wenlian Qiu, Paul A. Gurr, Greg G. Qiao

37th Australasian Polymer Symposium (37APS), Sunshine Coast, Australia, November 2019. (**Oral presentation**)

Table of Contents

List of Schemes

Lists of Figures

Figure 1.9. Synthesis of a crosslinked SP-PDMS network via platinum-catalysed hydrosilylation reaction among vinyl-terminated SP and PDMS oligomers and a hydrosilane copolymer.[64]

Figure 1.10. Non-covalently bonded systems carrying SP for mechanochromism. (A) Complexation of a stable SP with cyclodextrin achieves mechanochromism.[107] (B) Schematic illustration of preparing SP-ZnO/polythiourethane composite.[108]

Figure 1.11. Setup of ultrasound apparatus for mechano-activation. (A) Assembly of ultrasound equipment for mechanical activation of SP-linked PMA dissolved in solvent by ultrasound.[36] (B) Schematic diagram of a flow system coupled with the ultrasound equipment with a UV-Vis spectrometer and a peristaltic pump for transporting polymer solution to achieve in-situ measurement.[86] (C) Schematic diagram of sonication setup for mechanical activation of naphthopyran-linked elastomer.[109]

Figure 1.12. Schematic diagram of mechanical testing instruments. (A) Tensile test and (B) compression test. (C) Apparatus for in situ fluorescence imaging of SP-linked polymers under stretching.[84]

Figure 1.13. Swelling-induced colour activation of SP-linked polymers. (A) Schematic illustration and optical images of SP cross-linked PMMA before and after swelling in organic solvents: acetone (ACT), acetonitrile (ACN), tetrahydrofuran (THF), and dimethylformamide (DMF).[110] (B) Preparation of SP cross-linked PDEA microgel which can swell in water purged with CO_2 due to the protonation of tertiary amine groups. Optical images showing the colour change by alternatively purging with CO_2 and N_2, and DLS data showing the size change of the microgel.[111]

Figure 1.14. Study of the effect of varying attachment positions or substituents on SP on mechano-activation. (A) Force-separation curves of two SP copolymer samples varying attachment positions on the indoline ring, measured by a single molecule force spectroscopy.[91] (B) Plot of blue/green colour intensity ratio against strain of three SP-PDMS samples varying attachment positions on the benzopyran moiety.[103] (C) Force-extension curves of three SP copolymer samples varying substituent at the 6-position, measured by a single molecule force spectroscopy.[67]

Figure 1.15. (A) Optical images of SP-linked P*n*BA$_n$ (*n*=3, 7, 10, 16, 30) dissolved in solution after ultrousoud activation.[65] (B) Optical images of the randomly aligned-fibre and fibre-aligned P(SP-*alt*-C_{10})-PDMS composites under stretch in vertical and perpendicular directions.[75] (C) Images of SP-linked PMMA specimens after uniaxial tensile test at various temperature. Scale bar = 6 mm.[84]

Figure 1.16. Mechano-responses enhanced by micellization. (A) Change in the absorbance at peak wavelength as a function of sonication time for the PNIPAM-P*t*BA-SP-P*t*BA-PNIPAM formed micelles in THF/water and dissolved in THF.[89] (B) Synthesis of poly(AM-*co*-MA/SP) hydrogel via micellar copolymerization, and tensile stress-strain curves of the hydrogels using SP or EGDMA as crosslinkers or without crosslinkers.[82]

Figure 1.17. Enhanced mechanical properties by introduction of hydrogen bonding. (A) Chemical structure of SP covalently linked PU with UPy motifs integrated along the backbone. Hydrogen bonding is formed due to dimerization of UPy units.[96] (B) The left figure represents stress-strain curves of SP-PU elastomers end-capped with UPy units (U10 and U20) and urethane motifs (E10 and E20). The figure on the right shows the change of normalized fluorescence intensity against tensile strain, and the onset of mechano-activation is determined by the intersection of the two tangent lines.[95]

Figure 1.18. Regulable mechanochromic properties by adjusting hard domains. (A) Tensile stress-strain curves of PS-P*n*BA-SP-P*n*BA-PS triblock copolymers varying the ratio of soft/hard blocks, and the corresponding images before and after tensile test.[65] (B) Tensile stress-strain curve of PBA-SP-PS and change of colour intensity as a function of strain. The inset figure indicates the onset of colour activation strain.[66]

Figure 1.19. Effect of strain rate on mechanochromic properties. (A) Tensile stress-strain curves of dual cross-linked SP-PU elastomers varying strain rates, and optical images of the corresponding specimens stretched to a strain of 600%.[97] (B) Stress-strain curves of PBA-SP-PS polymer at various tensile strain rate, and the corresponding change of blue colour intensity against strain.[66]

Figure 1.20. Applications using mechanochromic SP-linked PDMS. (A) Images of a three-arm gripper robot before, during and after inflation, with the appearance of purple colour indicating the "at-risk" regions.[102] (B) Laminated structure of an electro-mechano-chemically responsive system, before and after applied with an electric field, and image of fluorescent patterns observed due to the mechano-activation. Scale bar = 250 μm.[101] (C) A pressure-sensitive touch screen with colour change in response to dynamic writing.[113] (D) A dual-mode force sensor with mechanochromic and triboelectric functions using a porous nanoparticle-in-micropore SP-PDMS, enabling spatiotemporal detection of writing force and speed.[114] (E) Metallic nanowires embedded in mechanochromic SP-PDMS for indicating failure.[68]

Figure 1.21. 3D printing technique applied to SP-linked mechanochromic polymers. (A) CAD representation of a "dog bone" shaped tensile specimen consisting of a difunctional SP-linked PCL filament responsive to both UV and mechanical force (red strips) embedded in a monofunctional SP-linked filament only responsive to UV, and optical images of the specimen before and after stretched and UV irradiation. Scale bar = 20 mm.[90] (B) So-gel transition is observed under mixing of microbead suspensions with bi-alkene SP, forming uncured silicone ink for extrusion 3D printing (top figure). A schematic illustration of 3D printed cone cylinder and the optical images displaying the colour change of the cone before and after compression (bottom figure).[129]

Figure 1.22. Schematic illustration of preparing P(BA-*co*-MMA-*co*-SP-*co*-VTES) latexes via emulsion polymerization, and images of the latex film under stretch at various strains.[133]

Figure 1.23. Research theme of this thesis: three SP varying attachment positions and numbers were synthesized and crosslinked into non-polar PDMS and polar PHEA for mechanochromic purpose, to study the effect of SP geometry. A multi-network made of poly acrylates was adopted to covalently link tri-functional SP3 in the pre-stretched first-network, to reduce the energy of mechano-activation.

Figure 1.24. Chapter 2: SPs crosslinked into non-polar PDMS and their mechano-responses under compression represented by the plot of blue/red channel intensity as a function of strain and the inset images showing the samples under a strain of 68%.

Figure 1.25. Chapter 3: SPs incorporated into polar PHEA and their negative photochromic performances and mechano-responses when swollen in water.

Figure 1.26. Chapter 4: (A) First-network SP-poly(butyl acrylate) was swollen in monomer followed by white light polymerization to prepare DN elastomers. (B) A plot of U_A against strain of SP-linked elastomers presented in this work (red colour) and reported in the literature (blue colour).

Figure 2.1. Spiropyrans with varying attachment points, for **SP1**: R_1 and R_3; **SP2**: R_2 and R_3; **SP3**: R_1, R_2 and R_3 (this paper). Force, heat and UV light can be the external stimuli to activate the ring-closed SP to ring-open MC.

Figure 2.2. Chemical structures of three vinyl terminated SPs (SP1, SP2 and SP3) with different attachment points.

Figure 2.3. (A) Corresponding B/R value (bule channel intensity/red channel intensity) as a function of compressive strain for SP samples (conc. = 5.0 μmol/g), and the inset images of SP samples at 68% strain; (B) Chromaticity diagram (standard CIE 1931) of SP samples showing the colour change directions under compression (strain: 0% to 70%), relaxation and recovery (SP1-3: conc. = 5.0 μmol/g).

Figure 2.4. UV-Vis absorption spectra of SP elastomers at concentrations of 5.0 μmol/g, (A) SP1, (B) SP2, (C) SP3 as increasing compressive strain. (D) Plot of absorption intensity vs compressive strain of SP. (E) Parameters from UV-Vis absorption spectra of a-c, where λ_{max} refers to the maximum absorption wavelength at the strain of 62%.

Figure 2.5. UV-Vis spectra of SP1-3 (conc. = 9.4 μmol/g) under tensile strain (≈ 2) and unloading. (A) SP1, width: 5 mm, thickness: 0.8 mm, (B) SP2, width: 4 mm, thickness: 0.8 mm, (C) SP3, width: 4 mm, thickness: 0.8 mm.

Figure 2.6. (A) Plot of absorption intensity/maximum absorption intensity vs relaxation time in darkness after unloading from 62% compressive strain for SP1, SP2 and SP3 (conc. = 9.4 μmol/g). (B) Decolouration parameters from UV-Vis spectra, where $T_{1/2}$ represents relaxation time at Abs/Abs_{max} = 0.5, T_{Abs} < 0.1 is the relaxation time at 0.1 absorption intensity, and k_d is the decolouration rate.

Figure 2.7. Hypothesized paths for merocyanine (MC) isomers of SP1 and SP2 model compounds under force and relaxation.

Figure 3.1. (A) Absorbance spectra of SP1-3 dissolved in HEA after absorption plateaued in darkness and the corresponding images, and (B) the absorption intensity at the maximum wavelength of 542nm, 549nm and 553nm respectively.

Figure 3.2. (A) Plot of absorbance at λ_{max} versus time in the dark for SP1-3 with 1 mol % crosslinkers (inserted pictures of SP1-PHEA/PHEA film in "Yin-Yang" symbol shape before and after being stored in the dark overnight, diameter: ~ 5 cm), and (B) images showing the colour change of SP1-3 relative to time.

Figure 3.3. Absorbance as a function of the swelling time in water for SP1-3 samples with 1 mol % crosslinker (λ_{max} of SP1 at 522 nm, SP2 at 532 nm and SP3 at 540 nm): (A) over 3hr and (B) over 50 hr (pictures of a SP3-PHEA/PHEA film in "Yin-Yang" shape before and after swelling in water for 1.5 hr as inserted, scale bar: 1 cm); (C) volume and mass change ratio of the three samples versus the immersing time in water; (D) the representative images showing the colour change relative to the swelling time (images are not to scale).

Figure 3.4. Decrease of absorbance at λ_{max} of SP1-3 PHEA (1 mol % crosslinkers) swollen films under white light irradiation in (A) swollen and (B) corresponding dehydrated states. Colour fading time t_f is defined as the intersection of two tangent lines (dot lines).

Figure 3.5. (A) Scheme of cyclic absorbance measurements between SP and MC by white light irradiation and subsequent storage in the dark for recovery, and the absorption plot of the SP1-3 films (1 mol % crosslinkers) in water; (B) scheme of cyclic absorbance measurements between SP and MC by swelling in water, dehydration in the dark at ambient conditions and white light irradiation, and the absorption plot of the SP1-3 films. The absorbance is normalized based on the maximum value in the swollen state.

Figure 3.6. (A) Influence of crosslinking density on absorption intensity as a function of the swelling time for SP3-PHEA films (1 mol %, 2.5%, 5% and 10%), and the inset images of different crosslinked films swelling over 1 day; (B) swelling ratio of the SP3-PHEA films at different crosslinking density.

Figure 4.1. (A) Tensile stress-strain curves of SNs prepared in the presence/absence of toluene (BA_T and BA_0) and DN ($BA_{0.83}BA$). (B) A plot of rBc as a function of tensile strain for $BA_{0.83}BA$ with ε_{MC} determined by the intersection of two tangent lines. The colour activation energy U_A is calculated by integration of the area underneath the onset of colour change on stress-strain curve. (C) Images of the two SNs and DN $BA_{0.83}BA$ under tension prior to fracture.

Figure 4.2. (A) Tensile stress-strain curves of DN samples with SP concentration of 0.5, 0.83, 1.17 mol % in the first-network. (B) Colour change plots of rBc against strain for the three samples, and the onset strain of colour activation ε_{MC} determined by the intersection of the two tangent lines. (C) Images of the three samples under tensile at a strain of 338%, 330% and 332%, respectively.

Figure 4.3. (A) Tensile stress-strain curves of DN samples prepared with various toluene volume in the first-network, 40%, 50% and 60%, respectively, and SP concentration of 0.83 mol %. (B) Colour change curves of rBc against strain for the three samples, and the onset of colour activation strain ε_{MC} indicated by green lines.

Figure 4.4. Cyclic tensile test on a specimen of $BA_{0.83}BA$ until rupture. (A) Loading-unloading curves obtained at a strain rate of 0.5mm s^{-1} and the dissipated energy for each cycle in the inset figure. (B) The rBc value as a function of loading-unloading cycles and the inset images of the sample under a strain of 250% for the 1^{st}, 3^{rd}, 5^{th}, and 7^{th} cycle, without MC returning to SP upon relaxation for each cycle. (C) A plot of normalized absorbance intensity against loading-unloading cycles, with MC recovering to SP under exposure to room light for 30-40 min for each cycle. The sample was subjected to a specific strain for 4-5 times before increasing the elongation, and the numbers show the value of strain corresponding to each dashed line.

Figure 4.5. Tensile stress-strain curves and colour change plot of rBc against strain for (A) $BA_{0.83}BA$ and (B) $BA_{0.83}MA$. The onset of colour activations ε_{MC} are indicated by the arrows. Inset pictures showed a blue colour when the samples were under stretching prior to fracture.

Figure 4.6. Absorbance spectra of (A) $BA_{0.83}BA$ and (B) $BA_{0.83}MA$ activated by UV light until plateaued and by stretching upon fracture. The inset figures presented the absorbance intensity at the peak wavelength at 580 nm.

List of Tables

List of Abbreviations

Abs	Absorption intensities
AgNW	Silver nanowire
ATRP	Atom transfer radical polymerization
CD	Cyclodextrin
CL	ε-caprolactone
COGEF	Constrained Geometries Simulate External Force
DEA	2-(Diethylamino)ethyl-methacrylate
DFT	Density functional theory
3D	Three-dimensional
DLP	Digital light processing
DN	Double-network
DSC	Differential scanning calorimetry
EGDMA	Ethylene glycol dimethacrylate
HDI	Hexamethylene diisocyanate
HIFU	High-intensity focused ultrasound
LC-MS	Liquid chromatography mass spectrometry
MC	Merocyanine
MDI	Diphenyldiisocyanate
MS	Mass Spectrometry
***n*BA**	*n*-Butyl acrylate
NIPAM	*N*-isopropylacrylamide
NMR	Nuclear magnetic resonance spectroscopy
PCL	Polycaprolactone
PDMS	Polydimethylsiloxane
PEGDMA	Poly(ethylene glycol) dimethacrylate
PEOC	Poly(ethylene-octene)
PEVA	Poly(ethylene-vinyl acetate)
PHEA	Poly(hydroxyethyl acrylate)
PMA	Poly methyl acrylate
PMMA	Poly methyl methacrylate

POSS	Polyhedral oligomeric silsesquioxanes
PS	Polystyrene
PTMG	Poly(tetramethylene glycol)
PU	Polyurethanes
RAFT	Reversible addition fragmentation chain transfer polymerization
ROMP	Ring opening metathesis polymerization
ROP	Ring-opening polymerization
SET-LRP	Single electron transfer living radical polymerization
SGP	Step growth polymerization
SMFS	Single molecule force spectroscopy
SN	Single network
SNPs	Silica nanoparticles
SP	Spiropyran
SPC	Suzuki polycondensation
THF	Tetrahydrofuran
TN	Triple-network
T-ZnO	Tetrapodal zinc oxide
UPy	Ureidopyrimidinone
UV	Ultra Violet
UV-Vis	UV–visible spectroscopy
VTEA	Vinyltriethoxysilane

Chapter 1: Introduction, Literature Review and Research Objectives

1.1 Mechanochemistry and Mechanochromophores

Chemical reactions can be categorized based on their source of free energy, into photo-, thermo-, electro- and mechano-chemistry.[1] Mechanochemistry although relatively new among these categories, has been intensively developed in recent years. Chemically, external forces can selectively impact weak bonds of molecules, leading to chemical activations such as decomposition and radical generation upon bond cleavage.[2] The molecules that undergo structural change triggered by mechanical force are referred as mechanophores.[3] Either bond cleavage or isomerization of the mechanophore will occur when the weak bonds or strained rings of the molecules are subjected to pressure. When the mechanophores are covalently linked within a polymer matrix, the functional groups generated from mechanical activation can provide possibilities for a range of chemical reactions. An example is the *ortho*-quinodimethide generated from benzocyclobutene which reacts with bismaleimide to form a gel when under stress.[4, 5] More specifically, when the mechanical activation of the mechanophores is accompanied by an optical colour change, absorption or emission (fluorescence or luminescence), the molecules are referred as mechanochromophores.[6]

The two main types of mechanochromophores subjected to chemically structural change are based on ring-opening (isomerization) and radical generation mechanisms.[3, 6-8] Isomerization-based mechanochromophores consist of a spiro-junction that undergoes ring-opening under external force, resulting in resonance structures exhibiting a change in colour (**Figure 1.1**). Mechanochromophores of spiropyran (SP),[9] spirothiopyran,[10] rhodamine[11, 12] and naphthopyran[13, 14] are within the ring-opening category. The ring-opening and ring-closure processes are reversible under loading and unloading. This category based on a bond rupture mechanism has been widely studied and their integration into a range of polymer matrices for stress/strain sensing purposes have been reported. Mechanochromophores based on radical generation are less reported for macroscopic visualization applications. This class of mechanochromophores comprises of a dynamic carbon-carbon (C-C) “bridge” bond connecting two identical moieties and

goes through a homolytic bond cleavage under deformation leading to radical formation at the two fragment molecules with a change in colour. Some reported radical-type mechanochromophores include diarylbibenzofuranone (DABBF),[15-18] diarylbibenzothiophenonyl,[19, 20] difluorenylsuccinonitrile[21] and tetraarylsuccinonitrile,[22-24] with DABBF conjugated to polymers, being the most reported. The reversible reaction of dissociation and recombination of the dynamic C-C bond not only affords the function of colour switching, but also provides great opportunities for use as self-healing agents.[18, 25, 26] Bis(adamantyl) dioxetane is an example of the third less reported class of mechanochromophores, known as chemiluminescents, which generate luminescence without a visible colour change upon bond breakage.[27, 28] The chemiluminescence is due to one of the decomposed moieties staying in an electronically excited state. Unlike the above-mentioned mechanochromophores with reversible colour changing behaviour under loading and unloading, the light emission process of luminescent mechanochromophores is irreversible.

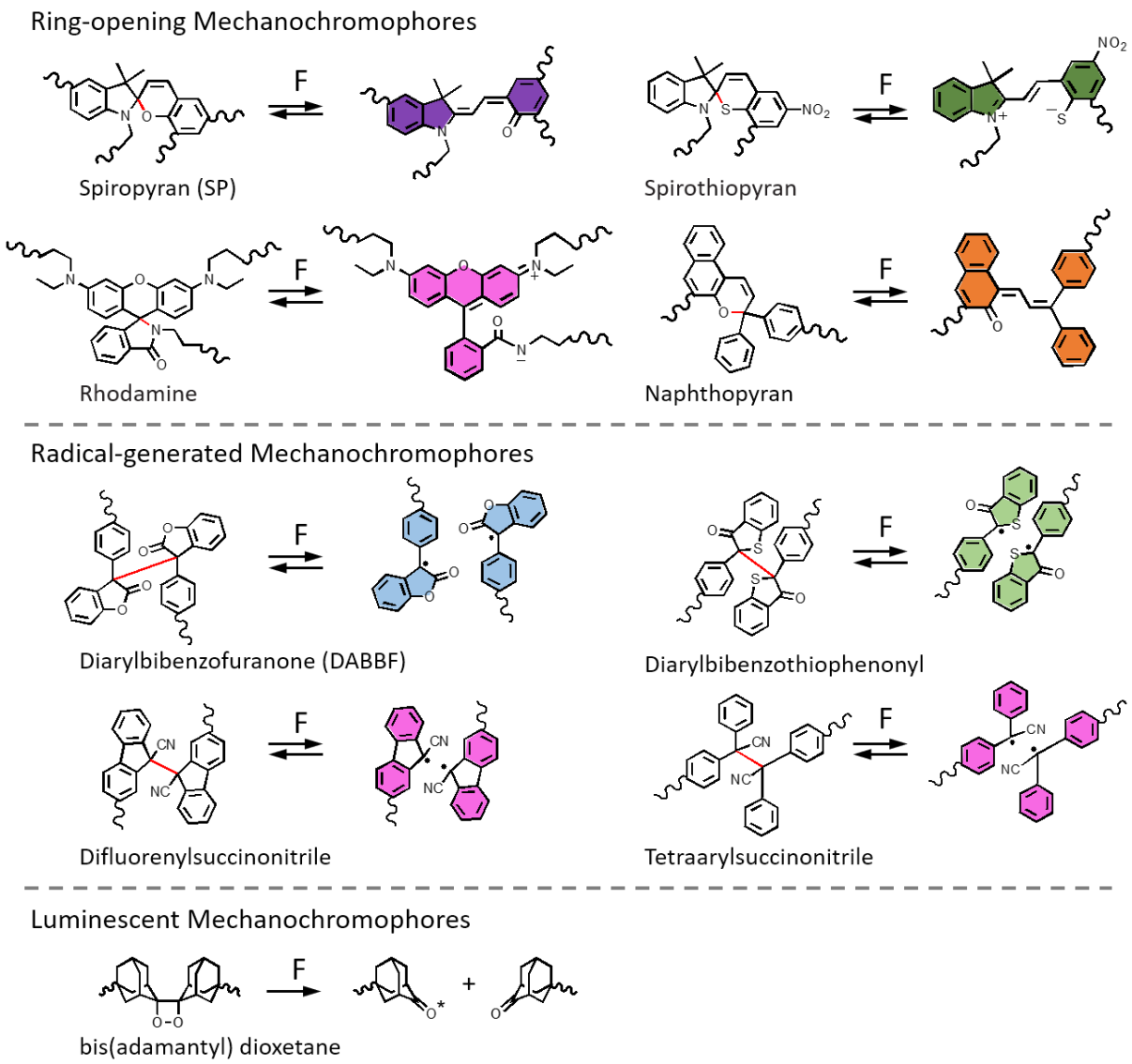

Figure 1.1 Chemical structures of the reported mechanochromophores and their bond cleavage reactions under force. The mechanically weak bond is labelled in red for the ring-opening and radical-generated type mechanochromophores.

1.2 Spiropyran (SP)

Among the mechanochromophores mentioned, spiropyran and its derivatives have been widely studied with well-established synthetic approaches. Spiropyran was first discovered in 1926 for its thermochromism[29] and has been widely investigated for its photochromic properties.[9, 30-35] More recently, in 2007, SP covalently linked into poly(methyl acrylate) dissolved in acetonitrile was found to undergo a colour change when subjected to ultrasound, which imparts a mechanical force.[36] In 2009, the first

mechanochromic SP covalently linked bulk polymer was reported by the Moore group,[37] which has opened the door to intensive exploration of the mechanochromic properties of spiropyran. Due to its fast mechano-responsiveness and relatively low-pressure requirements, SP-linked polymers have become the main mechanochromic materials in this field.

As shown in **Figure 1.2**, SP molecule consists of an indoline ring and a benzopyran moiety, which are connected perpendicularly via a weak C-O bond. The colourless SP converts into its coloured and ring-open isomer merocyanine (MC) upon the C-O bond breaking under an external stimulus, such as UV irradiation, elevated temperature, force or changes in pH.[9, 38-40] The MC can be in a zwitterionic or quinoidal form as shown in **Figure 1.2**, both of which exist in the mechanochromic process. The ring-closure reaction is a thermodynamic process which occurs upon cessation of the external stimuli. This isomerization process brings fascinating potential for a range of applications, not only because of the resultant optical change but also for the distinct physical and chemical properties between SP and MC. Regarding their optical properties, SP shows no absorbance signal in the visible range, whereas MC shows an absorption peak at 500 – 600 nm. Similarly no fluorescence is generated from SP, unlike MC. Moreover, SP is a highly hydrophobic molecule whereas MC is hydrophilic, which lends themselves to their implementation in the field of self-assembly,[41, 42] drug delivery,[43, 44] and wettability control and cell adhesion.[45, 46] The difference in the size of MC compared to SP has been used for microfluidic applications.[47, 48] The transition from a neutral to charged molecule has also been exploited for metal ion detection[49, 50] and electrochemistry.[51, 52] Most of these applications rely on light control, benefiting from the photochromism of SP. The equilibrium between SP and MC is affected by the environmental polarity, with a polar environment stabilizing the more hydrophilic MC, even in the absence of UV stimulus, and it has been defined as negative photochromism.[53-55] The polar environment can be due to the solvents,[56] bulk materials[57] and the attached polymers.[58] Multi-responsive and functional materials can be achieved combining the photochromic and thermochromic properties of SP.[59, 60]

For photochromic purposes, only one side of either the indoline or benzopyran rings needs to be attached to the polymer chains, when incorporated into covalently linked systems. However, for mechano-responsive SP polymeric materials, both the indoline

ring and the benzopyran moiety are required to be attached to the polymer matrix, so that the applied force can be transferred along the C-O bond resulting in its cleavage. There are several linkage points on the spiropyran where polymers can be attached (**Figure 1.2**), with the attachment at 1'- or 5'- position on the indoline ring and 6- or 8-position on the benzopyran ring, being the most commonly reported.

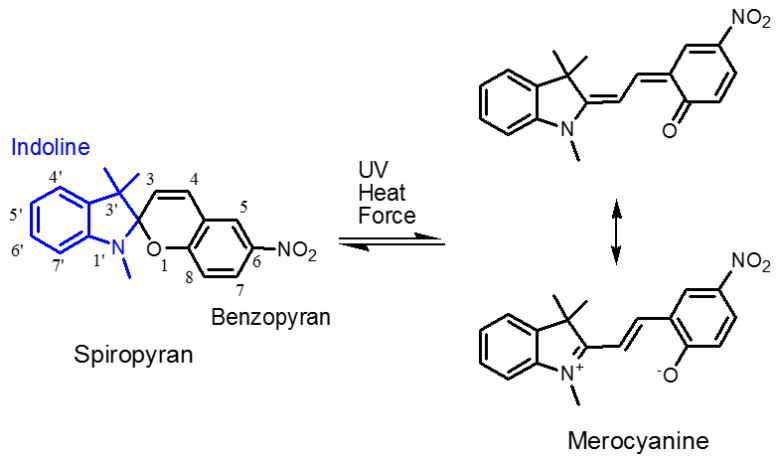

Figure 1.2. Chemical structure of SP and its ring-opening reaction under external stimuli.

1.3 Synthesis of SP-based Mechanochromic Materials

Spiropyran-based materials can be prepared in covalently or non-covalently bonding approaches, of which the former is the dominant class.

1.3.1 SP Covalently Bonded Systems

The majority of mechanochromic materials bearing SP are covalently bonded systems which can facilitate the eternal force transmitted to the spiro-junction to induce the ring-opening reaction. SP covalently bonded polymeric materials have been prepared using similar synthetic approaches. The synthesis of SP molecules and the range of polymerization approaches used to bind them will be summarised separately.

1.3.1.1 Synthesis and Modification of SP

SP is generally synthesized by the condensation of salicylaldehyde derivatives and indolium salts in ethanol under basic conditions (piperidine or triethylamine).

Accordingly, the functional groups on SP can be manipulated by designing the substitution of the salicylaldehyde and the indolium salt precursors.

6-Nitro-SP mechanophores have been widely studied, and the most common functionalities are hydroxy groups at the 5'- and 8-positions ($SP_{5',8\text{-}OH}$) (**Table 1.1a**).[37, 61, 62] Functional groups on the indoline ring can be introduced at the 1'-position, by conjugating 2-iodoethanol to the indolium forming salt before condensation ($SP_{1',8\text{-}OH}$) (**Table 1.1b&c**).[63-65] Hydroxyl groups can provide modifiable moieties leading to the introduction of a range of crosslinking chemistries. The functionalities can also be achieved before the condensation step by modifying the salicylaldehyde and indoline derivatives. Jia *et al.* synthesized indoline derivatives with alkyl bromide group and salicylaldehyde derivatives with methacrylate groups, which subsequently underwent condensation to afford SP consisting of an alkyl bromide group at the 5'-position and methacrylate group at the 8-position ($SP_{5'\text{-}Br\text{-}8\text{-}MA}$) (**Table 1.1g**).[66] 6-bromide-SP with hydroxy functionalities at the 1'- and 8-positions was synthesized (**Table 1.1f**)[67] to compare with the corresponding 6-nitro-SP and 6-hydrogen-SP (**Table 1.1e**)[68] on the substituent effects. A SP with bromine groups at the 5'- and 8-positions was synthesized by Sommer's group, using indolium salts and salicylaldehyde derivatives with bromide groups ($SP_{5',8\text{-}Br}$) (**Table 1h**).[69] A similar SP with iodide groups ($SP_{5',8\text{-}I}$) was reported in 2006 for photochromism.[70] SP without a nitro group at the 6-position has also been developed for UV inactive purpose. Salicylaldehyde derivatives without nitro but alkyl alcohol group at 6-position react with indolium salts with alkyl alcohol at the 1'-position to afford di-hydroxyl SP ($SP_{1',6\text{-}OH}$) (**Table 1.1d**).[71] For a different attachment position on the indoline side, a SP with a bromine group at the 5'- and 6-positions was developed ($SP_{5',6\text{-}Br}$) (**Table 1.1i**).[69, 72-75]

Table 1.1. A summary of synthetic compounds to synthesize spiropyran with functional groups designed for mechanochromism via condensation

Entry	Indolium (salts)	Salicylaldehyde derivatives	Spiropyran (after condensation)	Ref.
a	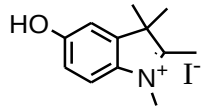	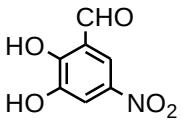	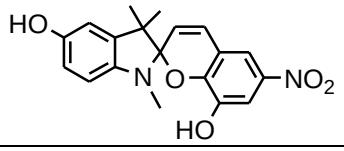	37, 61, 62
b	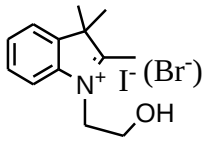		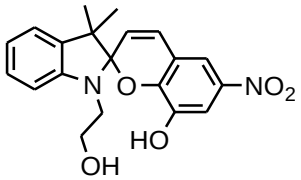	64
c		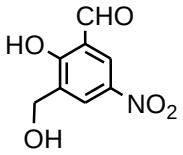	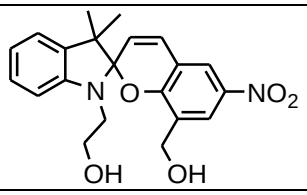	63, 65
d		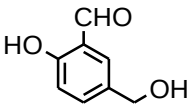	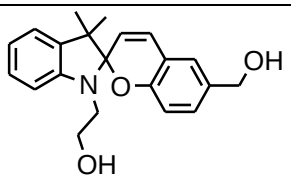	71
e		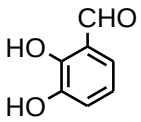	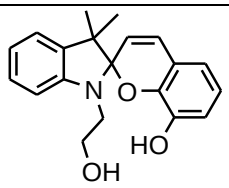	68
f		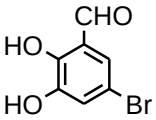	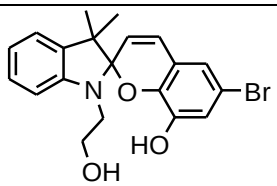	67
g	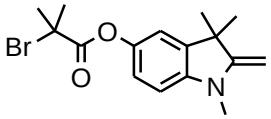	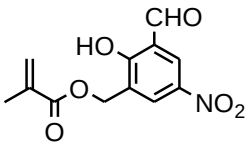	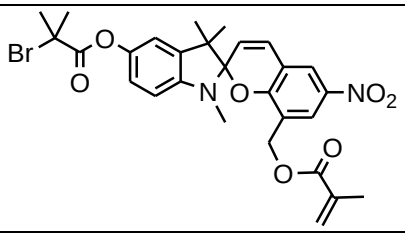	66
h	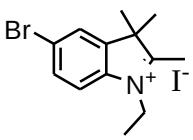	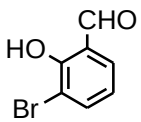	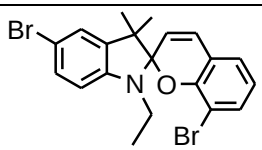	69
i		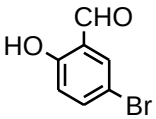	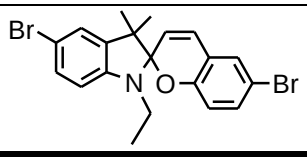	69, 72-75

The reactive hydroxyl groups on SP can be further modified to afford other functional groups, such as methacryloyl ester, alkene and bromoisobutyryloxy groups (**Scheme 1.1**). The modification of hydroxyl to methacryloyl ester groups can be achieved by nucleophilic addition with methacryloyl chloride[37] or esterification with methacrylic anhydride in the presence of either TEA or 4-(dimethylamino)pyridine.[61] Similarly, bromoisobutyryloxy functionality can be introduced from the hydroxy-SP with 2-bromo-2-methylpropionyl bromide under similar conditions.[37] The alkene groups are obtained via esterification with the corresponding alkenyl anhydride. Craig's group has been using this method to functionalize di-hydroxyl $SP_{1',8\text{-}OH}$.[64] TEA was not employed during the reaction but only DMAP was acting as a base and catalyst, which can be referred to modify the esterification with methacrylic anhydride without the presence of TEA.

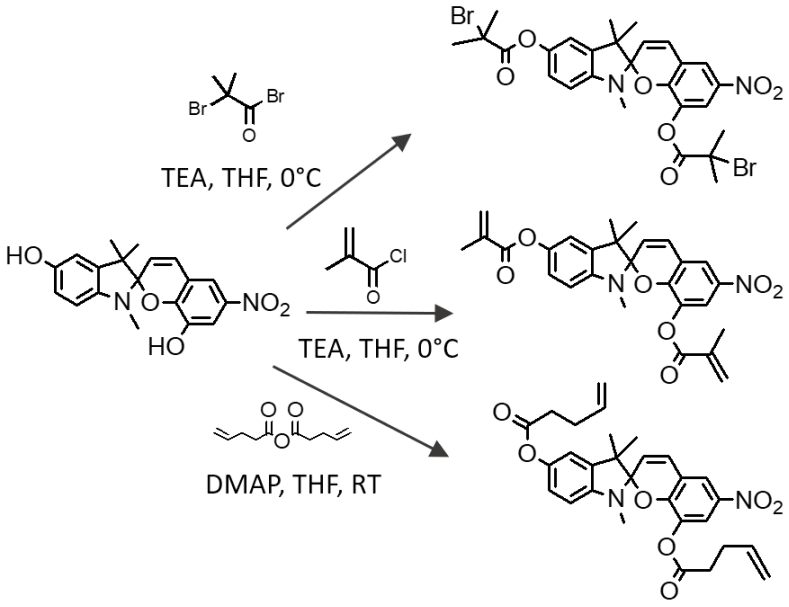

Scheme 1.1. Modification of di-hydroxyl SP with other functionalities.

It should be noted that the synthesis and modification of SP are not trivial, but the difficulty is converting the functionalized SPs, exclusive of dihydroxyl SP, into their ring-closed form. The basic condition of the reaction promotes the equilibrium SP ↔ MC towards MC and the polar eluent required for chromatography also favours MC, due to solvatochromism. The product in its MC form can also aggregate, due to the zwitterionic structure and π-stacking,[9] and can degrade via oxidation and radical attack;[76, 77] thus, the most stable form for storage is the ring-closed SP. The most common approach is recrystallization of the obtained functional mechanophores in hexane after column chromatography.[37] The ring-closed SP favours the non-polar hexane resulting in the

crude purple oil product turning to yellow, indicating the majority mechanophores in their ring-closed version. The drawbacks of recrystallization include time consuming and yield loss. To overcome those issues caused by recrystallization, in the synthesis of alkene functionalised SP, an approach to avoid recrystallization was to increase the ratio of non-polar solvent prior to evaporation by rotary evaporation following column chromatography.[78]

1.3.1.2 Polymerization Approaches of Covalently Bonding SP

With functional groups attached, covalent incorporation of SPs into polymer matrices are readily achieved. The reactions of incorporation cover various common polymerization methods, including free radical polymerization (photo and thermal), atom transfer radical polymerization (ATRP), single electron transfer living radical polymerization (SET-LRP) step growth polymerization (SGP), ring-opening polymerization (ROP), hydrosilylation, reversible addition fragmentation chain transfer polymerization (RAFT) and Suzuki polycondensation (SPC). A summary of the approaches used in this manner and the resultant architectures are presented in **Table 1.2**. With SPs functionalised with suitable functionalities, they can be used as an initiator in ATRP, SET-LRP, RAFT and ROP polymerisations, resulting in a single SP centred in one polymer chain as illustrated in **Figure 1.3A**, or as a monomer to form multiple SPs along each polymer chain by SGP and SPC (**Figure 1.3B**); while SP is a crosslinker, crosslinked polymer can be prepared via free radical polymerization and hydrosilylation (**Figure 1.3C**). Linear polymers containing SP are generally obtained as powders after precipitation then hot pressed to fabricate bulk samples. Crosslinked SP polymers are generally obtained in bulk with the polymerization occurring in a mould.

Table 1.2. A summary of polymerization methods for synthesizing SP-based mechanochromic polymeric materials

Method	Role of SP	Polymer	M_w (kDa)	Architecture	Ref.
Free radical polymerization	Crosslinker	PMMA	-	Crosslinked	37, 79-81
		P(AM-*co*-MA/SP) hydrogels	-		82
		PEVA, PEOC	-		83
SET-LRP	Initiator	PMA	170,[36]	Linear, single SP	37
ATRP	Initiator	PMMA	180, 260	Linear, single SP	84, 85
		PMA	230[85], 156[86]		37, 85-87
		PEA	177		86
		P*n*BA	139		86
		P*i*BA	152		86
		P*t*BA	124		86
		PS	160		88
		PS-P*n*BA-SP-P*n*BA-PS	36-48	Triblock copolymer, single SP	65
		PNIPAM-P*t*BA-SP-P*t*BA-PNIPAM	39.9	Linear, single SP	89
		PBA-SP-PS	21.1	Graft copolymer, single SP	66
ROP	Initiator	PCL		Linear, single SP	63, 90
ROMP	Monomer	P(SP-*co*-epoxidized cyclooctadiene)	105-118	Linear, multiple SP	67, 91
Step grow polymerization	Monomer	PU	50-70,[92] 20.5[93]	Linear, multiple SP	92-94
		PU-UPy	10-20[95]		95, 96
		PU-UPy		Crosslinked	97
		PU-BTP	30	Linear, multiple SP	98
		Waterborne PU	33		99
		POSS-PU		Crosslinked	100
Suzuki polycondensation	Monomer	P(SP-*alt*-F8)	100	Linear, multiple SP	69
		Polyarylene	96		74
		P(SP-*alt*-C_{10})	34.8		73
		P(SP-*alt*-C_{10}) nanofiber	78.9		75
Hydrosilylation	Crosslinker	PDMS	-	Crosslinked	64, 67, 101-104
RAFT	Initiator	PBA-SP-PS	21.1	Graft copolymer, single SP	66

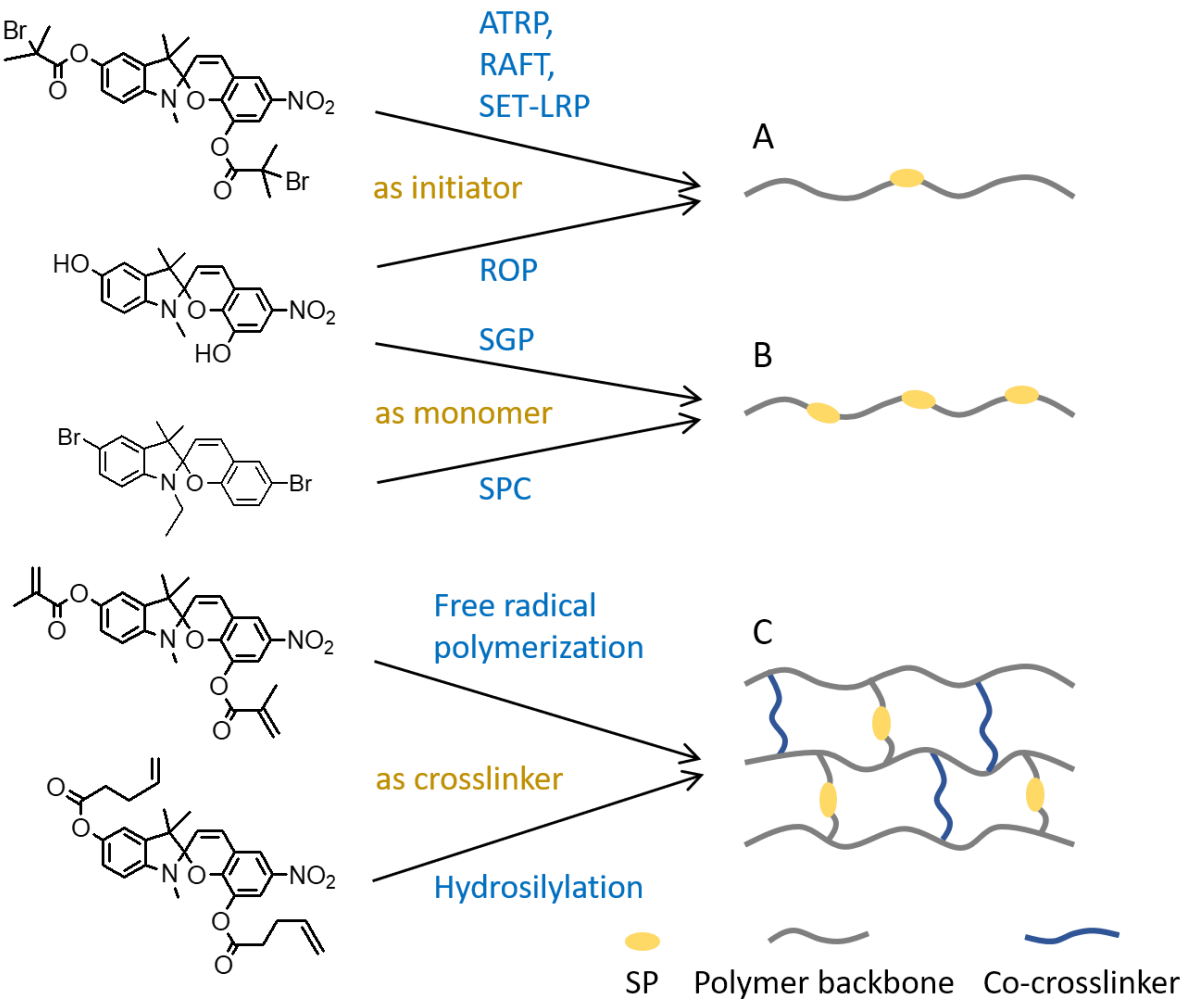

Figure 1.3. Schematic illustration of (A) linear polymer with single SP in the centre of polymer chain obtained by ATRP, SET-LRP, RAFT or ROP with SP as initiator, (B) linear polymer with multiple SPs along a polymer backbone with SP as monomer, synthesized via SGP or SPC, and (C) crosslinked polymer with SPs as crosslinkers through free radical polymerization or hydrosilylation.

Linear polymers with single SP in the chain centre

Moore's group have pioneered the development of covalently linked spiropyran in polymers for mechanochromism and published many subsequent papers on the topic. They were the first to report that spiropyran covalently linked into poly methyl acrylate (PMA) in solution underwent a colour change, when subjected to ultrasound, which imparted a mechanical force.[36] Bis-bromo-SP (α-bromo-α-methylpropionyloxy-spiropyran) (**Figure 1.4A**) as initiator was reacted with methyl acrylate in DMSO in the

presence of catalyst of Cu(0) and tris(2-dimethylaminoethyl)amine (Me_6-TREN) as a ligand via ATRP. After the removal of Cu(0), the linear polymer SP-PMA was obtained through precipitation in methanol. The linear SP-PMA polymer was then processed in bulk by hot-compression in a mould.[37, 85, 87] Linear SP-PMMA (poly methyl methacrylate) was synthesized in a similar copper based-ATRP method using 2,2'-bipyridine (bpy) as a ligand, resulting in a polymer with molecular weight up to 260 kDa.[84, 85] SP-PMMA specimens were prepared by moulding them above their melting point under 200 psi. The same copper-based ATRP method can be used to incorporate bis-α-bromo ester SP into a variety range of poly acrylates (**Figure 1.4B**).[86] SP-linked polystyrene (PS) was also synthesized using bis-α-bromo ester SP as initiator via ATRP.[88] The obtained polymer with SP in the centre of polymer chain reached a molecular weight of 160 kDa. Compression moulding and spin coating were employed to prepare bulk samples and thin films respectively.

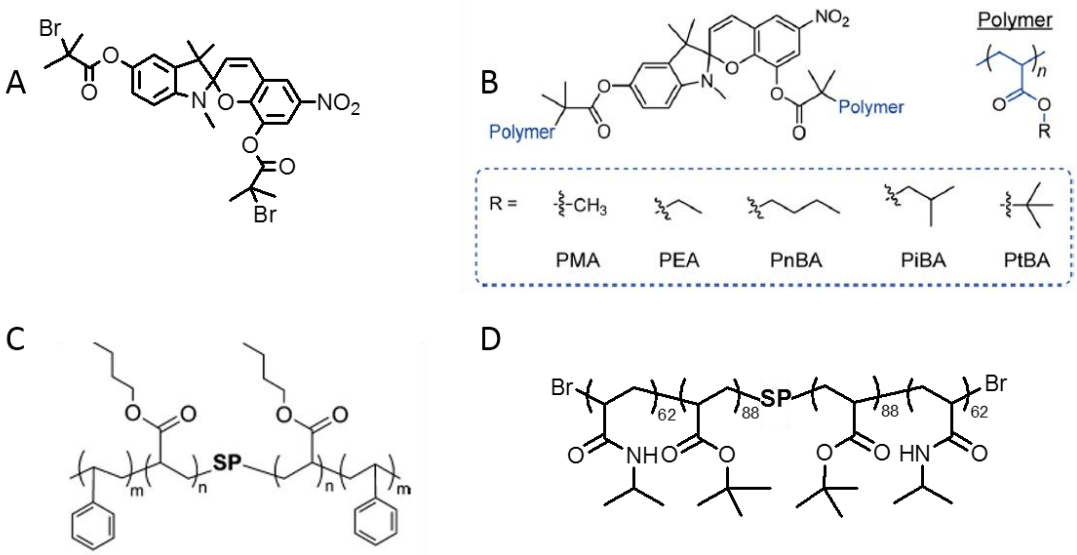

Figure 1.4. Chemical structure of (A) bis-α-bromo ester SP,[36] (B) SP linked in chain centre of various polyacrylates via ATRP,[86] (C) SP conjugated block polymer with P*n*BA and PS blocks via ATRP,[65] (D) SP conjugated amphiphilic block polymer with P*t*BA and PNIPAM blocks via SET-LRP and ATRP.[89]

Weng's group designed a triblock copolymer bearing SP in the chain centre.[65] Bis-α-bromo ester SP as an initiator was first polymerized with *n*-butyl acrylate (*n*BA) via ATRP, followed conjugation with PS blocks (**Figure 1.4C**). The molecular weight of the PS blocks was changed with a constant P*n*BA length, to vary the ratio of hard and soft blocks,

resulting in different microphase separated structures having different mechanical responses. Tensile samples were prepared by solvent casting. Wang *et al.* synthesized a SP linked amphiphilic triblock copolymer via SET-LRP and ATRP.[89] SP was conjugated with hydrophobic *t*-butyl acrylate (*t*BA) before polymerized with temperature sensitive *N*-isopropylacrylamide (NIPAM), leading to an amphiphilic block copolymer (**Figure 1.4D**) which formed micelles below its critical micelle temperature.

Di-hydroxyl SP as an initiator polymerized with ε-caprolactone (CL) via ROP, leading to one SP per polymer backbone (**Figure 1.5A**), was reported by O'Bryan and co-workers.[63] The beige coloured powder with M_w 60 kDa was obtained by precipitation into cold methanol after ROP, and processed into thin sheets by hot-pressing. A polymer chain alignment step was required to achieve sufficient mechanochromic response, by stretching the pristine sheet to 20% of its original thickness and heating to 50 °C in a water bath. Peterson and co-workers made use of 3D-printing technology to fabricate mechanochromic SP-PCL bulk samples.[90] Two dihydroxyl SPs, $SP_{1'\text{-}8\text{-}OH}$ and nitro-absent $SP_{1'\text{-}6\text{-}OH}$, were integrated into PCL via ROP (M_w 90 and 82.5 kDa) (**Figure 1.5B**), followed by mixing with 50% - 90% (w/w) commercial PCL to form filaments through melt extrusion. 3D samples were built up in the vertical z axis with printing layers in alternating x and y axis, with extrusion heads set at 110 °C. Despite the high printing temperature, neither thermal activation of the SP or polymer degradation (by M_w analysis) was observed. This work highlighted the capability of constructing specially designed mechanochromic materials in irregularly shape via 3D-printing.

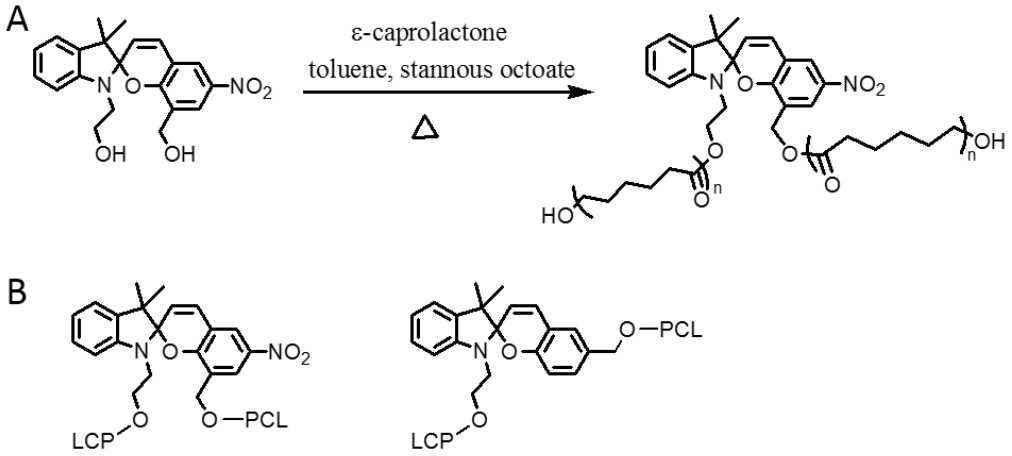

Figure 1.5. Di-hydroxyl SP as an initiator for SP linked within a PCL chain. (A) Synthesis of SP-PCL via ROP.[63] (B) Chemical structures of two SP-PCL synthesized for 3D printable mechanochromic polymers.[90]

Linear Polymers with Multiple SPs along a Backbone

Dihydroxy SPs have been reported to be used as a monomer in the preparation of mechanochromic polyurethanes (PU) via SGP. This results in a linear block copolymer with multiple SPs distributed within the polymer chain. PU is a widely used and versatile engineering polymer, as such this approach of incorporating SP into PU provides the opportunity to fabricate mechanochromic polymers on a large scale. In this process, the diol-SP reacts with diisocyanates (hard segment), followed by polyether polyol (soft segment), and finally chain extender to form PU elastomers. Since isocyanates react readily with water producing CO_2, the raw materials need to be anhydrous with the bulk samples prepared under an inert atmosphere. Moore's group has utilized diphenyldiisocyanate (MDI) as a hard segment to conjugate $SP_{5',8\text{-}OH}$, poly(tetramethylene glycol) (PTMG) (M_n = 650) as a soft segment and hexamethylene diisocyanate (HDI) as a chain extender to prepare SP-PU elastomers (**Figure 1.6A**).[92] PU samples containing 0.03 wt % SP were able to generate significant colour change when stretched. In order to align the polymer chains before activation, tensile samples were pre-strained to neck and then cold-drawn. Upon deformation, irreversible phase separation occurs due to the incompatible segments. SP integrated in either soft or hard segments of PU were synthesized, to investigate the influence of SPs location on the force distribution for mechano-activation.[94] The same research group also synthesized SP-PU employing PEG 200 as a soft segment.[93]

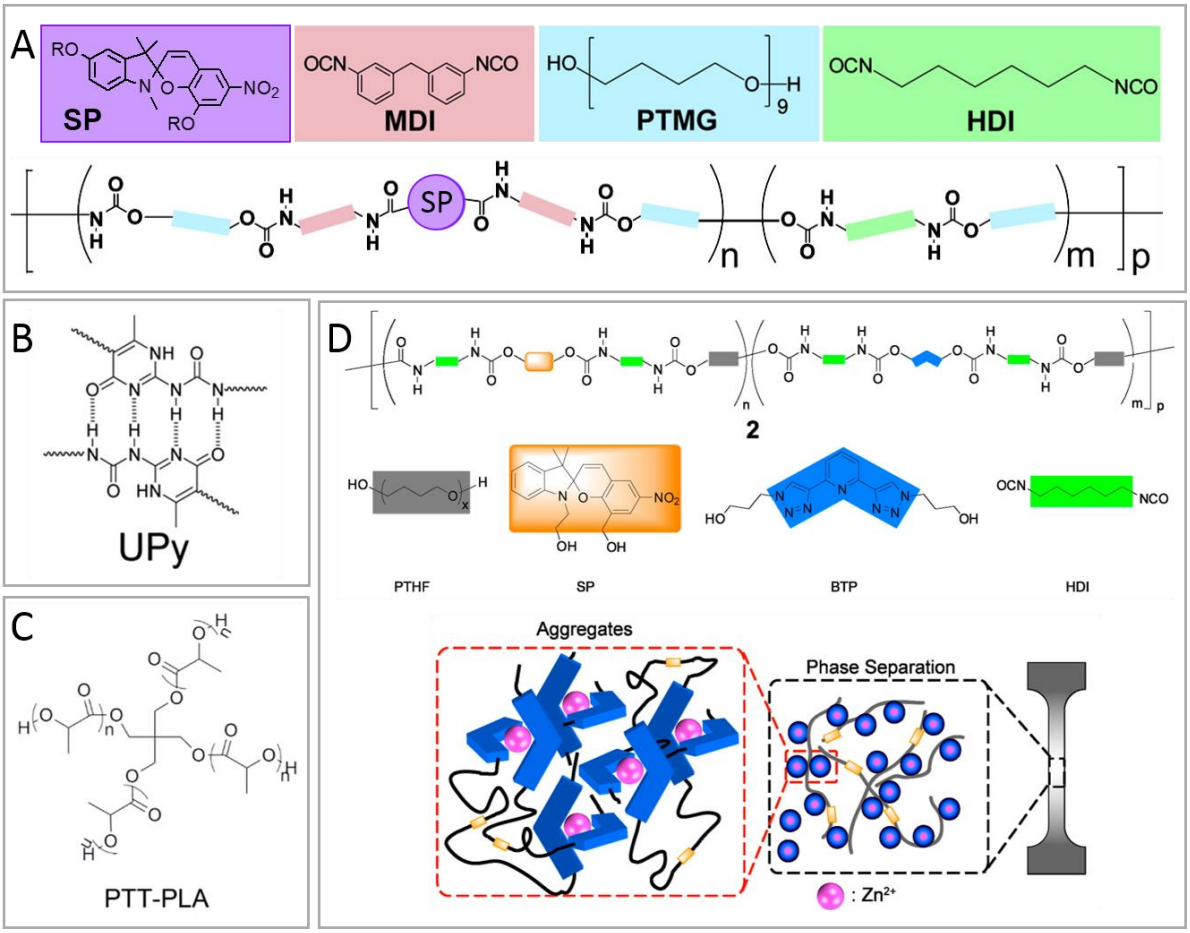

Figure 1.6. SP linked in PU backbone. (A) SP integrated into PU via SGP where m >> n.[92] (B) Chemical structure of ureidopyrimidinone motif which is incorporated into PU leading to enhanced mechanical properties via hydrogen boding formation.[96] (C) Chemical structure of oligo-poly(lactic acid) end-capped pentaerythritol as chemical crosslinker.[97] (D)BTP ligands incorporated into SP-PU backbone and formation of metal-ligand complexes.[98]

Weng's group focused on modifying SP-PUs to achieve higher mechanical properties with the aim to achieve better mechanochemical responses. Ureidopyrimidinone (UPy) motifs (**Figure 1.6B**) were introduced into the polymer backbone as a chain extender by reaction with SP/HDI precursors, followed by addition of PTMG (M_n = 2000) and HDI in DMF.[96] The resultant polymer was moulded into thin films by solvent casting. The tensile samples displayed excellent mechanical properties with ultimate strength of 23.7 MPa and large breaking strain at 970% (0.05 s^{-1} strain rate), which was due to the hydrogen bonding formation of dimeric UPy moieties (**Figure 1.6B**). The hard domains formed by stacking of UPy dimers resulted in formation of loops along the polymer chains, which

could dissipate energy when dissociating under strain. The UPy dimer stacks as hard domains also benefited the orientation of the polymer chains, facilitating the mechanical activation of SP contained within the backbone. The location of UPy was then adjusted by being end-capped in the PU chain.[95] The sample with or without end-capped UPy differed in mechanical properties and SP mechanical activation, as the former showed higher strength (45.7 MPa with strain at break of 1050%) , a higher strain for SP ring-opening and a higher ratio of SP-to-MC conversion. They concluded that the difference was due to the hydrogen bonding formation resulting in chain alignment and strain induced crystallization. Making use of the physical crosslinking (hydrogen bonding) from UPy dimers, a chemical crosslinking was introduced to the SP-PU elastomer to form a dual crosslinked elastomer.[97] A prepolymer of SP reacted with UPy-diisocyanate, HDI and PTMG was crosslinked with oligo-poly(lactic acid) end-capped pentaerythritol (**Figure 1.6C**) with bulk samples prepared in Teflon moulds. The strength of the elastomer was about 27 MPa breaking at 900% strain under strain rate of 0.05 s^{-1}. Additionally, Weng's group also developed a healable SP-PU by incorporation of ligand 2,6-bis(1,2,3-triazol-4-yl)pyridine (BTP), which can form complex with metal, into polymer backbone (**Figure 1.6D**).[98] The linear SP-BTP-PU polymer was obtained by precipitation in methanol and then coordinated with metal ion of Zn^{2+} or Eu^{3+} in chloroform to form metallosupramolecular polymers, which were processed into films by solvent casting. The metallosupramolecular film containing Zn^{2+} with a notch could fully recover to its original mechanical properties in the presence of solvent for 3 hours whereas the film with Eu^{3+} did not show healing ability.

Zhang *et al.* reported a waterborne SP-PU for mechanochromism based on the mentioned SP-PU systems.[99] Dimethylolpropionic acid was introduced to the polymer backbone constructed by SP, MDI, PTMG and isophorone diisocynate (IPDI), followed by neutralisation with TEA. The resultant ionic waterborne PU formed an emulsion in water, which became a film once water was removed. The obtained film had a strength of 16 MPa with a breaking strain of 880%. Xing *et al.* developed a SP-PU with an enhanced thermal aging stability by employing polyhedral oligomeric silsesquioxanes (POSS) as crosslinker.[100]

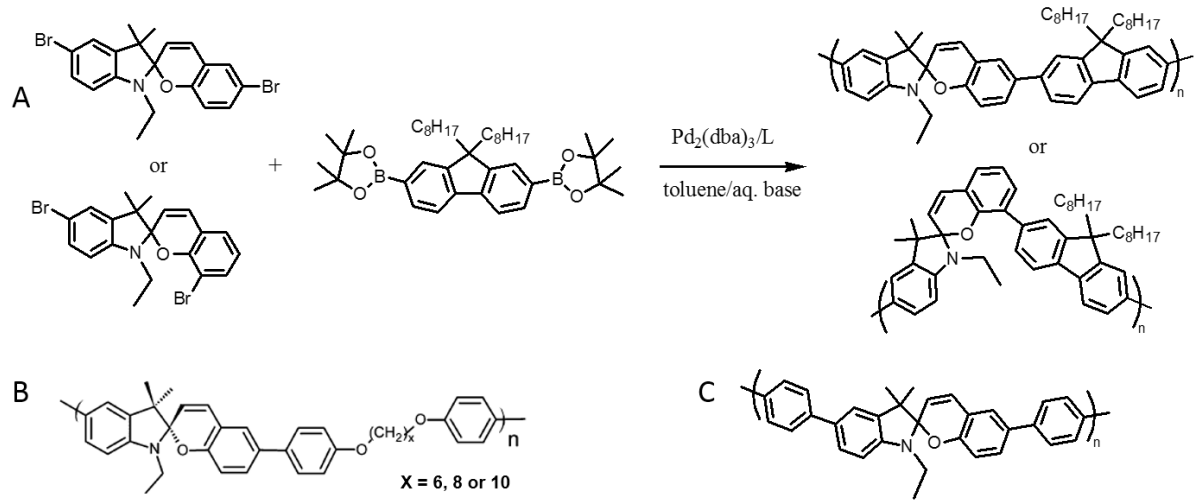

Figure 1.7. SP conjugated in copolymers via Suzuki polycondensation. (A) Two di-bromo SP copolymerized with 9,9-dioctylfluorene.[69] Structure of (B) SP-linked polymers with phenol-based alkyl linker with 6-10 carbons[72] and (C) SP-linked polyarylene.[75]

Di-bromo SP was synthesized for preparing alternating SP linked with stiff fluorene units in polymer backbone via Suzuki polycondensation (SPC) reported by Sommer and co-workers.[69] Two di-bromo SPs ($SP_{5',8\text{-}Br}$ and $SP_{5',6\text{-}Br}$ without nitro groups) were copolymerized with 9,9-dioctylfluorene (F8) boronate ester using palladium as a catalyst and a base to afford SP linked fluorene copolymers P(SP-*alt*-F8) (**Figure 1.7A**). The obtained polymers dissolved in solvent, when subjected to ultrasound, showed a distinct colour change. By replacing the co-monomer, a phenol-based alkyl linker (6-10 carbon) was conjugated alternately with SP via SPC to form mechanochromic P(SP-*alt*-C_x), and the structure is shown in **Figure 1.7B**.[72] In a subsequent paper the same research group used microwave heating to synthesize P(SP-*alt*-C_{10}), with a molecular weight M_W up to 174 kDa (M_n 34.8 kDa).[73] They also synthesized a SP-linked polyarylene via SPC (**Figure 1.7C**), with a molecular weight of 96 kDa.[74] The SP-polyarylene exhibited excellent mechanical properties with a Young's modulus of 0.9 GPa and a breaking strain at 300%. The blue colour induced from stretching, returned to its original pale pink colour transiently upon unloading, due to the lack of the nitro group and the electronic effect of the phenyl moiety destabilizing the MC structure.

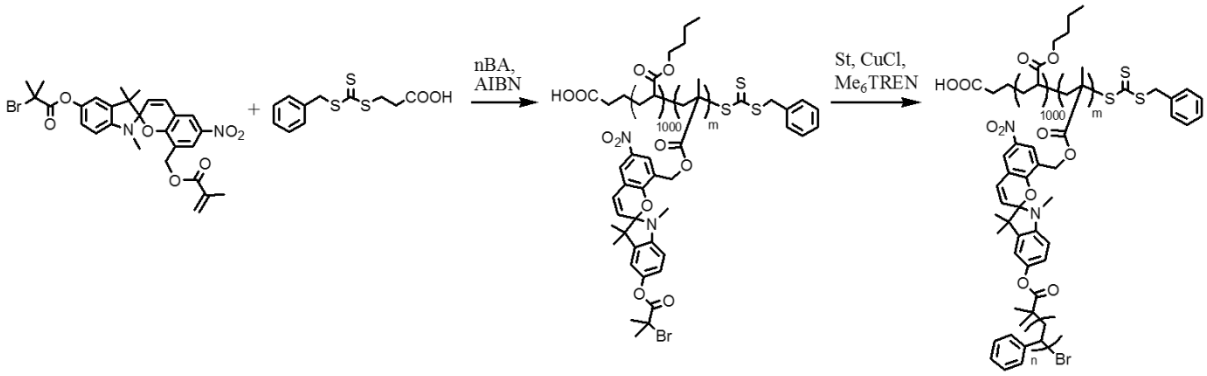

Figure 1.8. Synthesis of comb-structured graft copolymer via two steps: SP consisting of methacrylate and bromo ester functionalities polymerized with *n*BA via RAFT, followed by polymerization with styrene via ATRP.[66]

In other approach, the work by Zhu and co-workers reported the incorporation of SP moieties into the side chain of comb-like structures. SPs containing methacrylate and bromo ester functionalities were synthesized and used as a co-monomer with *n*BA to polymerize a comb-like structure via RAFT. Initiation via the bromo- functionality under ATRP conditions afforded PS grafted P*n*BA-SP-PS (**Figure 1.8**).[66] The resultant polymers had multiple SPs as a part of the side chain. Thin film samples were prepared by solvent casting and these thermoplastic elastomers with SP content of 0.15 - 0.34 wt % (M_w = 143 – 181 kDa) were shown to afford bright colour changes upon mechanical activation.

Crosslinked polymers with SP as crosslinker

The functionalized SPs with acrylate or alkene groups can be used as crosslinking precursors to prepare crosslinked polymers.

As an example, the functionality of bis-methyl acrylate on SP made it simple to be conjugated in a PMMA matrix via free radical polymerization. In this case, SP acting as the crosslinker resulted in a crosslinked SP-polymer network in bulk. Benzoyl peroxide was used as a radical initiator and *N*,*N*-dimethylaniline (DMA) acting as an activator allowed for the thermo-curing to occur at room temperature.[37, 79] Other examples have used co-crosslinkers such as ethylene glycol dimethacrylate (EGDMA)[37, 79-81] and poly(ethylene glycol) dimethacrylate (PEGDMA).[79]

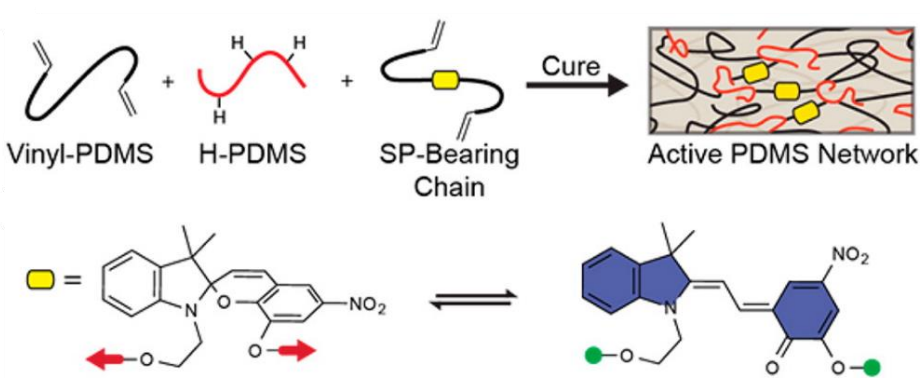

Figure 1.9. Synthesis of a crosslinked SP-PDMS network via platinum-catalysed hydrosilylation reaction among vinyl-terminated SP and PDMS oligomers and a hydrosilane copolymer.[64]

Commercial PDMS (Sylgard 184) was used to conjugate bis-alkene functionalized SP via platinum-catalysed hydrosilylation to form a crosslinked network.[64, 67, 101-104] Vinyl-terminated SP and PDMS reacted with hydrosilane PDMS copolymer under platinum catalysis by thermal-curing at 65 °C **(Figure 1.9**). Strict conditions, e. g. oxygen-free, are not necessary for the reaction as the facile preparation involved mixing the two components of the commercial PDMS with SP allowing for large scale fabrication.

Di-methyl acrylate SP was also crosslinked into two polyolefins, including poly(ethylene-vinyl acetate) (PEVA) and poly(ethylene-octene) (PEOC), by free radical polymerization using dicumyl peroxide as initiator under hot press.[83] Radicals formed on the secondary and tertiary carbon of PEVA and PEOC during the hot press triggering the crosslinking of SP and the polymer substrates. Interestingly, the SP without a nitro group can resist the high processing temperature (160 °C) without turning dark, whereas the SP with a nitro group became dark red after the hot press with the colouration being irreversible. The thermal inactive property was attributed to the lack of electron withdrawing nitro group. This preparation method of mechanochromic polymers via hot press presented a facile fabrication and facilitates the development of mechanochromic polyolefins.

1.3.2 SP Non-covalently Bonded Systems

Although external force transmitted along polymer chains to SP guarantees the ring-opening of SP-linked mechanochromic systems, there are a few examples where SPs have not been covalently bonded. For these systems, the loading area needs be small to subject

high pressure such as impact, and the colour switch is not distributed over the whole specimen when loaded.

Cyclodextrin (CD) has been widely used as a host to bear guest molecules thanks to the well-defined cavity structure.[105, 106] For this reason CD-SPs have been used to act as a host-guest system capable of mechanochromism.[107] A stable SP bearing benzoic acid at the 1'-position and carboxyl group at 5'-position was synthesized and included into γ-CD to form supramolecular complex (**Figure 1.10A**). The inclusion complex was cast onto glass substrates to form films, which switched colour from colourless to purple upon grinding. The pressure of grinding required for colour activation using CP-SP was reduced to 2.2 kg from more than 10 kg without complexation with CD. The dominant strong hydrogen bonding between SP and CD resulted in "locking" SP into the CD and induced SP ring-opening. The matching geometric conformation of CD and SP was crucial in this ability for mechanochromism. Replacement of γ-CD with α-CD or β-CD increased the activating force required to 5.6 kg and 5.2 kg respectively. This non-covalently bonded system based on supramolecules provided a simple way to prepare SP-mechanochromic materials, however as the product was in the form of a powder and grinding was required as the triggering force, it limits its practical applicability.

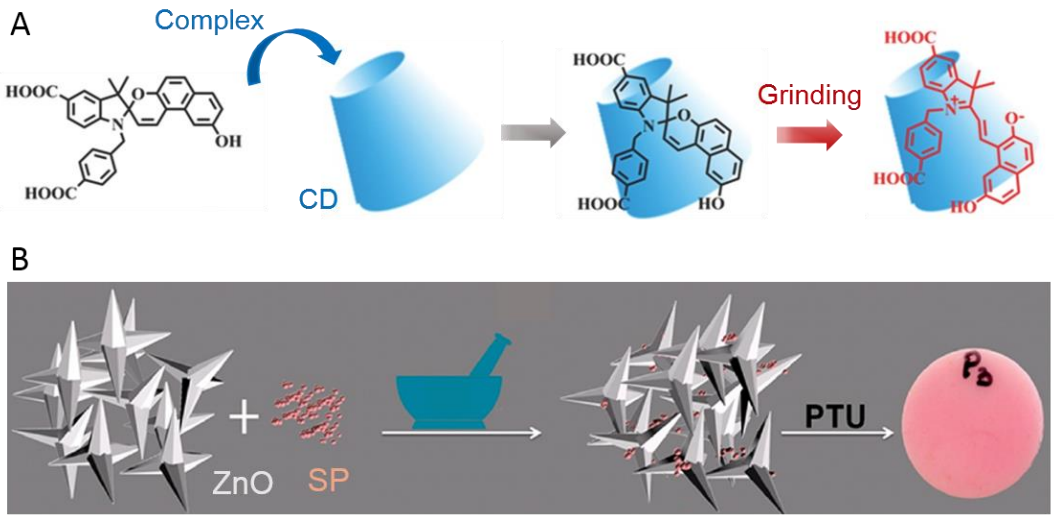

Figure 1.10. Non-covalently bonded systems carrying SP for mechanochromism. (A) complexation of a stable SP with cyclodextrin achieves mechanochromism.[107] (B) Schematic illustration of preparing SP-ZnO/polythiourethane composite.[108]

Another example was the incorporation of SP with zinc oxide into polythiourethane to afford mechanochromic composites.[108] All of the components were commercially

available except for tetrapodal zinc oxide (T-ZnO). The incorporation of T-ZnO allows for the formation of a 3D network which improves the mechanical stability of the polymer matrix leading to high impact resistance. Bulk samples were obtained by thermo-curing the mixture of all the ingredients (**Figure 1.10B**). The area subjected to the impact of a hammer underwent a colour change from yellow-orange to purple. The appearance of pressure induced cracks increased with increasing contents of T-ZnO. Noticeably, the specimen without T-ZnO also showed colour change under impact, however the activating force required for the samples with or without T-ZnO was not reported.

1.4 Sources of Mechanical Force Inducing Mechano-activation

Since the coloured ring-open MC shows an absorption signal in the visible range as well as a fluorescence when excited by green light, it can be quantified by RGB colour intensity from optical images, absorbance measurements and fluorescence imaging accordingly. There are various types of mechanical force that can be used to induce the ring-opening reaction of SP, with tension being the most common.

1.4.1 Ultrasound

The mechanochromism of SP covalently linked to a polymer matrix, induced by ultrasound was first reported by Moore's group.[36] The synthesized SP-PMA (170 kDa) was dissolved in acetonitrile followed by being subjected to pulsed ultrasound (0.5 s on, 1 s off, 8.7 W/cm^2, 20 kHz) at 8 °C, resulting in a pink solution which was originally colourless. The existence of ring-open MC in the pink solution was proven by the UV-Vis absorbance peak at 550 nm. The ultrasound system used in this procedure is shown in **Figure 1.11A**. A Suslick cell was used in direct contact with the solution, with a constant distance between the titanium tip and the bottom of the cell. The system is required to be kept cool in an ice bath to avoid thermo-activation of SP induced by the generated heat. In this case, the force generated by ultrasound is sufficient to activate the SP located in the centre of the polymer chain. Different acrylate monomers were also used to conjugate SP into linear chains to study the effect of polymerization (degree or molecular weight) on mechanochromic activation induced by ultrasound.[86] The ultrasound equipment was coupled with a UV-Vis spectrometer equipped with a flow-cell (**Figure 1.11B**). The sample solution was transported from the Suslick cell to UV-Vis spectrometer through a

peristaltic pump and then returned to the cell, to achieve in situ measurement of the activation of SP to MC and thus determine the kinetics of ultrasonic activation. A similar flow system was used by Wang *et al.* to investigate the ultrasonic activation of SP centred in an amphiphilic block copolymer which self-assembled into micelles.[89] SP embedded in waterborne polyurethane (WPU) which formed emulsion in THF/water also displayed ultrasonic response.[99] A P(SP-*alt*-F8) polymer conjugated with multiple SPs in the chain has also been shown to exhibit mechanochromic properties triggered by pulsed ultrasound (0.5 s on and off, 230 W/cm^2).[69]

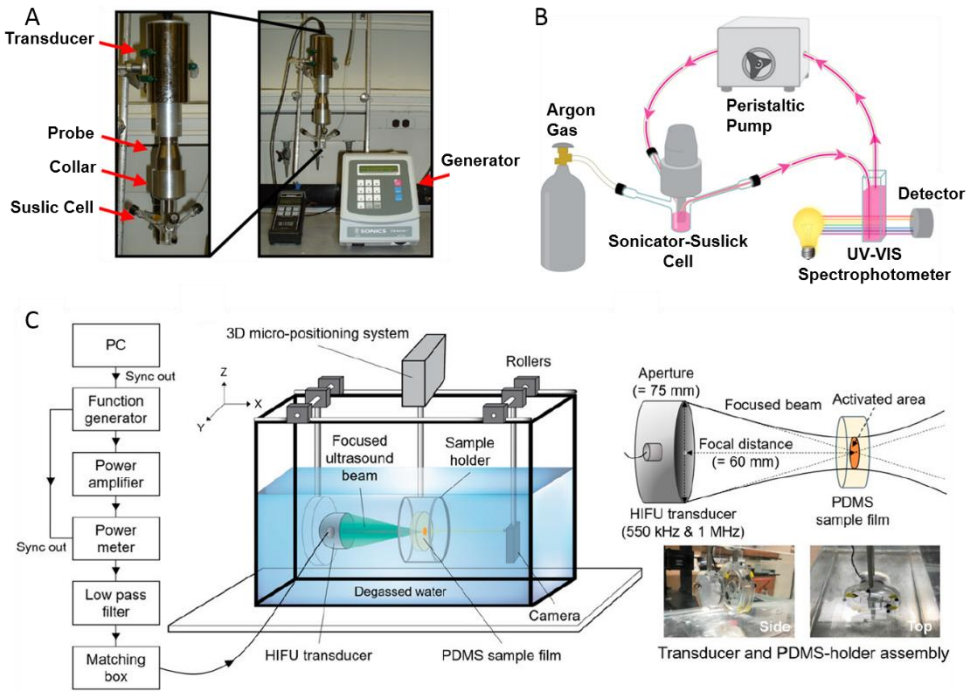

Figure 1.11. Setup of ultrasound apparatus for mechano-activation. (A) Assembly of ultrasound equipment for mechanical activation of SP-linked PMA dissolved in solvent by ultrasound.[36] (B) Schematic diagram of a flow system coupled with the ultrasound equipment with a UV-Vis spectrometer and a peristaltic pump for transporting polymer solution to achieve in-situ measurement.[86] (C) Schematic diagram of sonication setup for mechanical activation of naphthopyran-linked elastomer.[109]

Mechano-activation by ultrasound has been shown to be as achievable in bulk materials as in solution. In this case SP was replaced with another mechanochromophore naphthopyran, in which ultrasound was shown to induce colour change in a mechano-activating elastomer .[109] Naphthopyran was cross-linked into PDMS elastomer which was subjected to high-intensity focused ultrasound (HIFU) to induce the ring-opening

reaction. The setup of HIFU comprised components for controlling the sonication pressure, location and duration to provide a non-invasive activation approach (**Figure 1.11C**). The frequency of the spherically-focused transducer was 550 kHz and 1MHz. The mechano-active naphthopyran-linked elastomer showed colour change under a pressure over 3.4 MPa (376 $W \cdot cm^{-2}$) but the control naphthopyran-linked PDMS (monofunctionalized naphthopyran) also indicated colour change under such a pressure due to the generated heat. To avoid the thermo-induced activation, the sonication intensity was required to be lower or equal to 333 $W \cdot cm^{-2}$.

1.4.2 Tension and Compression

For SP-linked polymers which are synthesized in bulk or processed into bulk samples by solvent casting or hot-pressing, the mechanochromism can be activated by uniaxial tension and compression.[62-64] These materials are generally processed into dumbbell shapes for tensile testing and cylindrical shapes for compression testing. For this reason, there are limitations to this method of testing. Unlike the experimental requirements of ultrasound activation, where only a tiny amount of sample is required, tensile and compression testing requires relatively large amounts of material. In addition, despite being the most common loading modes for mechanochromic activation, they are only applicable for elastic polymers tested at room temperature. External forces cannot be transferred across the spiro-junction on SP embedded in materials being too soft (energy dissipated on straightening polymer chains) or brittle (fracture before mechanochromic activation). For glassy polymers, the testing temperature is elevated to increase the mobility of polymer chains to achieve mechao-activation.[62, 84]

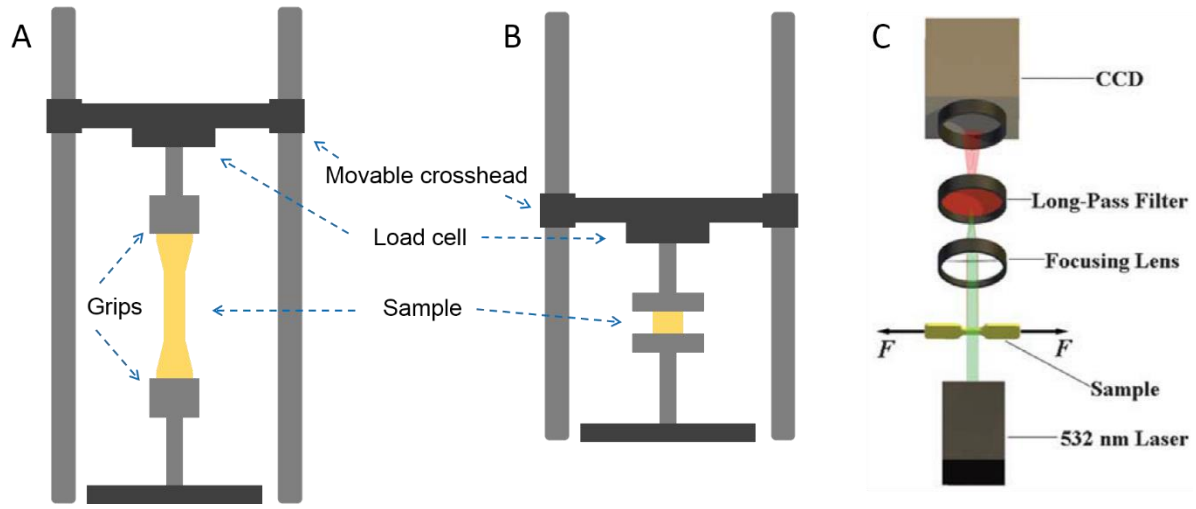

Figure 1.12. Schematic diagram of mechanical testing instruments. (A) Tensile test and (B) compression test. (C) Apparatus for in situ fluorescence imaging of SP-linked polymers under stretching.[84]

The tensile testing apparatus consists of load cells with various force capacities which apply a macroscopic force to the mechanochromic samples, with the elongation rate precisely controlled with a movable crosshead (**Figure 1.12A&B**). Stress-strain curves are then obtained to quantify the mechanical properties, including stress/strain at break and Young's modulus. An optical camera can be equipped to capture the colour transition in situ as the sample is deformed, thus the RGB colour intensity values can be determined through combining the images with the stress-strain curves.[64, 71] In addition to optical image recording, Moore's group designed an optical setup for in situ fluorescence imaging of the stretched samples which mainly consisted of a load cell, a green diode laser for sample excitation, focusing lens, a light filter and a CCD detector (**Figure 1.12C**).[84, 85, 87]

1.4.3 High Strain Rate Loading and Shearing

Although the commonly used tensile/compression loading methods are not ideal for mechano-activation of SP-linked glassy polymers, the high strain rate of loading allows these SP-linked polymers to be measured. Moore's group reported that shockwaves induced by acoustic pulses with extremely high strain rates at 1×10^7 to 10^8 s^{-1} (calculated with applied stresses and time frames) could induce mechano-activation when applied to SP-linked PS samples.[88] The activation was captured by *ex-situ* fluorescence imaging and the comparison of the active SP-linked PS to the control

samples determined that the force was the key for the activation rather than the generated heat. Another study employing a fast-compressive loading rate (1×10^2 to 10^4 s^{-1}) for activating SP-linked PMMA was reported by Hemmer *et al*.[61] A split Hopkinson pressure bar was used for the mechanical response measurement. The high rate impact results in fragmentation of the bulk samples with a visual colour observed around the fracture surfaces. Colour activation was also observed for a mechanically inert but thermally active sample by fluorescence imaging, suggesting that the localized heat resulted from the high strain impact also caused the conversion of SP to MC. In this case, the thermal activation rather than mechanical activation dominated the colour change under high strain rate measurement. These high strain rate-induced optical activations could provide glassy polymers the potential for crack indicating applications under extreme conditions.

Deformation caused by shearing has also been shown to induce the ring-opening of SP embedded into a polymer matrix.[79] Torsion testing was performed using a rheometer equipped with a fluorescence imaging set-up, and colour and fluorescence changes were generated under shearing after bulk polymer yielding. Crosslinked PMMA samples with different length crosslinkers, showed that the shear-induced activation of the specimens with longer primary crosslinkers required a lower activation stress but a larger strain at a higher shear rate (0.1 rad s^{-1}). This shearing activation method provided a new testing protocol for investigating the effect of polymer architecture on mechano-responsiveness.

Apparatus equipped with fluorescence imaging components are only available to a few research groups and for this reason its use in studying mechanochromic polymers are limited. Easy-to-establish and reliable testing approaches are called for to expand the development of this field.

1.4.4 Swelling

The mechanochromic activation by tension/compression suggests that a mechanical deformation is essential for the force transfer. As another source of force, the deformation generated during polymer swelling was first shown by Moore's group to be sufficient to activate mechanophore SP crosslinked in a PMMA polymer matrix. (**Figure 1.13A**).[110] Different organic solvents were used to swell SP-linked PMMA, and it demonstrated that swelling speed played a key role in the mechanochromic performance. Solvents with

moderate polarity were shown to efficiently induce a significant colour change, whereas highly polar solvents such as water and apolar solvents such as toluene showed minor colour change due to a limited swelling ratio or a slow swelling rate. Although samples in chloroform produced a significant colour change, the specimen fragmented due to an extremely fast swelling speed. The mechanochromic behaviour of the samples with different cross-link densities measured by fluorescence imaging, demonstrated that the colour intensity was directly related to the swelling ratio. However, reversibility of the colour change by removal of the solvents was not reported.

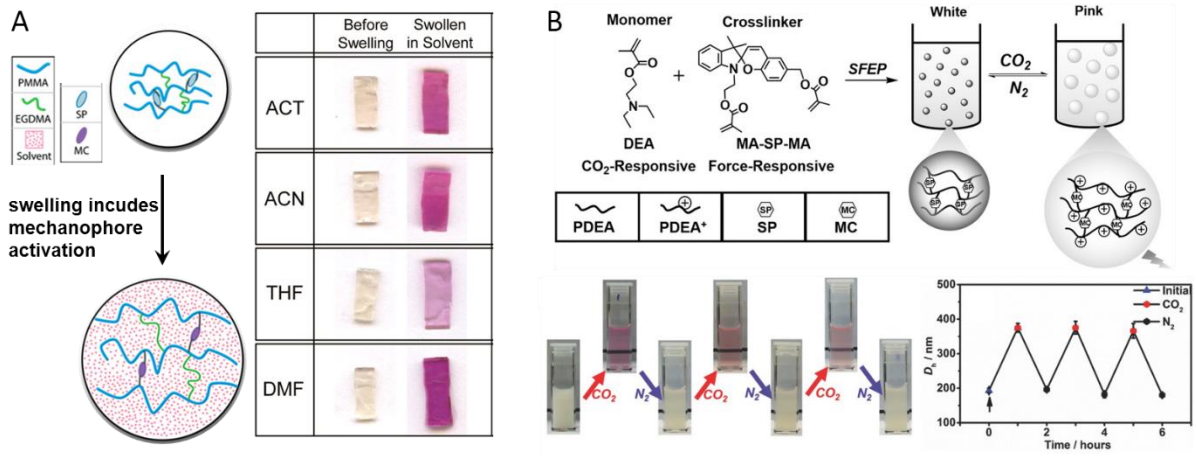

Figure 1.13. Swelling-induced colour activation of SP-linked polymers. (A) Schematic illustration and optical images of SP cross-linked PMMA before and after swelling in organic solvents: acetone (ACT), acetonitrile (ACN), tetrahydrofuran (THF), and dimethylformamide (DMF).[110] (B) Preparation of SP cross-linked PDEA microgel which can swell in water purged with CO_2 due to the protonation of tertiary amine groups. Optical images showing the colour change by alternatively purging with CO_2 and N_2, and DLS data showing the size change of the microgel.[111]

Aside from bulk materials swollen in solvents, CO_2 gas has also been used to cause mechano-activation of SP crosslinked microgels consisting of SP and 2-(diethylamino)ethyl-methacrylate (DEA). (**Figure 1.13B**).[111] The microgels synthesized through soap-free emulsion polymerization were swollen due to the protonation of tertiary amine groups on PEDA under CO_2 treatment resulting in a transition from water non-swellable to water swellable. The colour change was reversible and deprotonation of the amine groups by purging with N_2 gas led to deswelling of the microgels, resulting in colour fading.

Aside from these few reports, little has been published regarding the SP-ring activation due to solvent swelling and as such this area offers great potential for further exploration with the aim to develop practical applications.

1.5 Factors Influencing Mechanical Conversion of SP-to-MC

Moore's group were the first to report that the selective breakage of the spiro-junction at C-O under external force led to the mechanochromic activation of SP and this theory was developed using first-principles steered molecular dynamic and Constrained Geometries Simulate External Force (COGEF) at a density functional theory (DFT) level to further understand the influences of mechanochromism.[37] The C-O distance was calculated under simulated pulling at the attachment points of SP and the relative energy determined. To improve the efficiency of the mechanochromic function, it is important to understand the influencing factors. Varying the attachment positions on SP molecules leads to changes in geometry and electronic distribution which affects the equilibrium between SP and MC, however a detailed study to systematically quantify the two has been rarely reported. More studies about impact of polymer architectures on the force transmission to the covalently bonded SP have been reported for different efficiency of the SP ring-opening.

1.5.1 Geometric and Substituent Effects on SP

As the mechanochromic activation requires both the indoline ring and benzopyran moiety connected to polymer chains, the covalent-linked positions on SP (geometry or regiochemical effect) are vital for the force translation to induce SP ring-opening. The Craig group adopted a single molecule force spectroscopy (SMFS) to investigate the energy of ring-opening of two 6-nitro-SPs with different linkage positions on the indoline ring ($SP_{5',8}$ and $SP_{1',8}$).[91] SP-linked copolymers were synthesized via ring opening metathesis polymerization (ROMP) with cyclooctadiene monomer (9-oxabicyclo[6.1.0]non-4-ene), which increased their adhesion with the AFM tip. The single polymer chains of the obtained SP-linked copolymers were pulled by the AFM tips and the subsequent force-extension curves revealed that $SP_{1',8}$ required less force and shorter extension for the bond breakage than $SP_{5',8}$ (**Figure 1.14A**), demonstrating that the geometry of $SP_{1',8}$ is more advantageous in the mechano-activation. This study provides

insights into the geometric effect on the mechanochromism from a molecular level. More recently, the macroscopic mechanical response of these two SPs conjugated in PDMS were reported by the Moore group.[112] Despite computational calculations indicating that the $SP_{1',8}$ is more advantageous for the mechano-response than $SP_{5',8}$, the mechanochromic reactivity (onset stress/strain and fluorescence intensity at a certain strain) of these two SP-PDMS systems were indistinguishable.

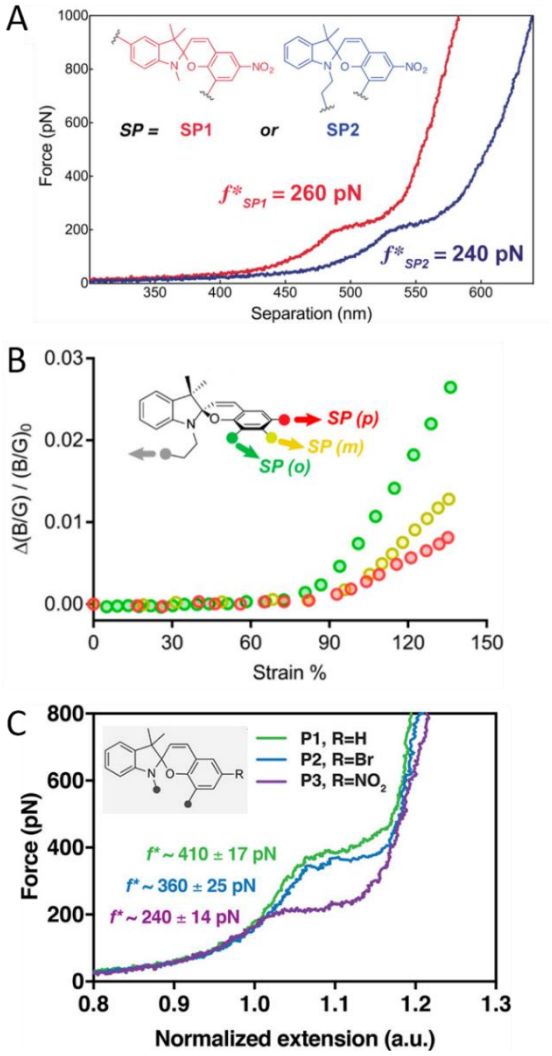

Figure 1.14. Study of the effect of varying attachment positions or substituents on SP on mechano-activation. (A) Force-separation curves of two SP copolymer samples varying attachment positions on the indoline ring, measured by a single molecule force spectroscopy.[91] (B) Plot of blue/green colour intensity ratio against strain of three SP-PDMS samples varying attachment positions on the benzopyran moiety.[103] (C) Force-extension curves of three SP copolymer samples varying substituent at the 6-position, measured by a single molecule force spectroscopy.[67]

Another investigation of the geometric effect on mechanochromism performed by the Craig group varied the attachment positions on the benzopyran moiety ($SP_{1',6}$, $SP_{1',7}$ and $SP_{1',8}$) from the perspective of macroscopic response (**Figure 1.14B**).[103] Three SPs without nitro groups were covalently incorporated into PDMS. Uniaxial tensile tests demonstrated that the order of colourimetric response was $SP_{1',8}$ > $SP_{1',7}$ > $SP_{1',6}$ but the onset of colour activation was indistinguishably occurring at around 90% strain. The results of COGEF modelling indicated that the mechanical response was contour length dependant, with the order of the change in the length of $SP_{1',8}$ > $SP_{1',7}$ > $SP_{1',6}$, same as the order of colour intensity under a given strain.

Varying the substituents on SP (electron donating/withdrawing groups) also affects the equilibrium between SP and MC leading to different mechanochromic properties. Synthetic SP mechanophores contain either no nitro groups or nitro substituents on the benzopyran moiety. The SP without a nitro substituent at the 6-position is UV inactive[71, 90] and processes a faster backwards reaction from MC to SP[113, 114] due to the absence of strong electron-withdrawing group. The Craig group investigated the effect of substituents on the mechano-reactivity by synthesizing SP mechanophores ($SP_{1',8}$) substituted with H, Br or NO_2 at the 6-position (**Figure 1.14C**). The strategy of copolymerizing the SP with cyclooctadiene via ROMP and the characterization of force-induced response by SMFS was applied. The force-extension curves revealed that the trend of critical force for C-O rupture was H > Br > NO_2, which was consistent with a theoretical study[115] showing that electron withdrawing groups (EWG) on the para position to O atom enhanced the conversion of SP to MC due to a stabilization of the negative charge at O. The backward reaction from MC to SP followed the opposite trend with NO_2 > Br > H, suggesting that the EWG stabilization of MC is more advantageous for the forward reaction and unfavourable for the backward reaction.

1.5.2 Polymer Architecture

It has been shown that the mechanochromic reactivity can be altered by regulating the attachment positions and substituents on SP. Another approach to alter this reactivity which have been reported more is using the polymer architecture attached to the spiropyran. As an example, ultrasound activation of SP-linked P*n*BA was shown to be polymer chain length dependent.[65] When the *n*BA repeating unit on each side of SP was

lower than 10, the colour change was not distinguishable (**Figure 1.15A**). For the repeating unit higher than 30, the chain was too long to induce a bright colour, due to the force inefficiently transferring to the SP which was in the chain centre. Another study further investigated the effect of molecular weight and polymerization degree using ultrasound, by conjugating SP to different acrylate monomers.[86] Absorbance measurements showed that the degree of polymerization mainly determined the mechanochromic performance rather than the molecular weight or the type of side chains.

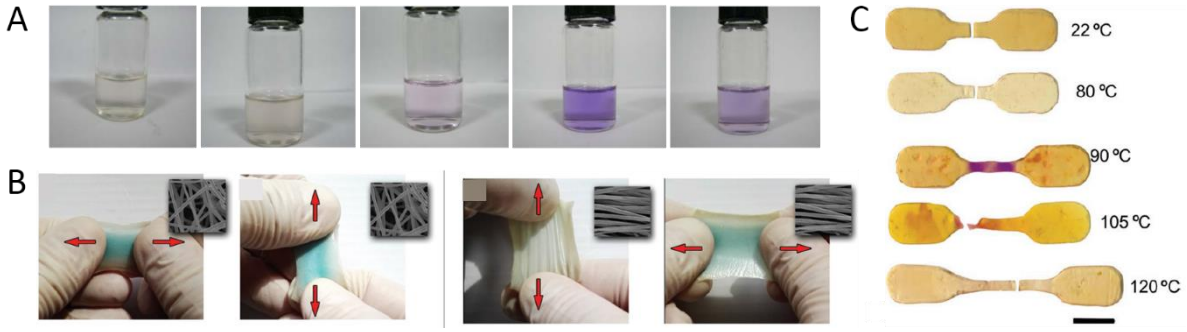

Figure 1.15. (A) Optical images of SP-linked P*n*BA$_n$ (*n*=3, 7, 10, 16, 30) dissolved in solution after ultrousoud activation.[65] (B) Optical images of the randomly aligned-fibre and fibre-aligned P(SP-*alt*-C$_{10}$)-PDMS composites under stretch in vertical and perpendicular directions.[75] (C) Images of SP-linked PMMA specimens after uniaxial tensile test at various temperature. Scale bar = 6 mm.[84]

For SP-linked bulk polymer, the alignment of polymer strands and the orientation of SP are vital for mechanochromic activation, which is generally measured by tensile testing. Synthetic SP-centred PCL film was pre-stretched in a water bath at 50 °C to align polymer chains.[63] The pre-stretched specimen produced a significant purple colour under deformation along the pre-stretched direction, whereas the colour change was minor for the specimen without a pre-stretched step. In a more recent study, the alternating copolymer P(SP-*alt*-C$_{10}$) (C$_{10}$ = bisphenol decane linker) was processed into nanofibers by electrospinning.[75] The fibres were either aligned or randomly incorporated into PDMS to prepare mechanochromic composites. The fibre-aligned specimen only presented a pronounced colour change under stretch along the alignment direction but presented indistinguishable colour change under deformation perpendicular to the alignment direction. The randomly aligned-fibre composite displayed colour switching when

stretched along both directions however the blue colour intensity was lower than the fibre-aligned specimen (**Figure 1.15B**). Both studies demonstrated the alignment of polymer chains can efficiently enhance the mechano-response of mechanophore-linked bulk materials from a macroscopic perspective. A quantitative measurement of MC orientation, based on the calculation of anisotropy of fluorescence polarization, was performed on SP-linked PMA elastomers.[85] A comparison of the order parameter between the UV-activated and stretch-activated specimens under similar strain showed that mechanophores in the unstrained sample was randomly oriented and the mechanophores preferentially aligned along the deformation direction under strain. A higher strain resulted in a higher mechanophore orientation. This study provided evidence for the importance of mechanophore orientation to mechanochromic response from a molecular level.

The position of SP in the polymer chain also affects the mechano-activation. For a SP-linked PU elastomer, SP located in hard segment exhibited a higher mechanical activation than the SP located in soft segment with a high content of hard segment systems (40 wt %). However identical levels of activation were observed for both systems with a relatively low hard segment content (22 wt %).[94] This was due to the minor segregation of soft and hard segments in the low hard segment systems but a significant segregation in the high hard segment systems. Despite the importance of SP orientation to the mechano-activation, the less alignment of SP in the hard segment displayed higher fluorescence along the stretching direction, suggesting that a certain mobility of polymer chains is necessary to effectively promote mechanochromism. In terms of the mobility of polymer chains, an earlier study by the Moore group, whereby SP embedded glassy PMMA with a T_g of 127 °C showed that the colour activation was strongly dependent on polymer mobility, as the activation occurred in the temperature range of 90 – 105 °C under a same strain rate (**Figure 1.15C**).[84] When the SP-PMMA was plasticized with methanol, the stretchability was improved from *ca.* 10% to 65% with a decrease breaking stress at 22 °C, and the mechano-activation could be observed upon the polymer yielding. This was due to the improved mobility of the glassy polymer that enabled the mechanical activation at room temperature.

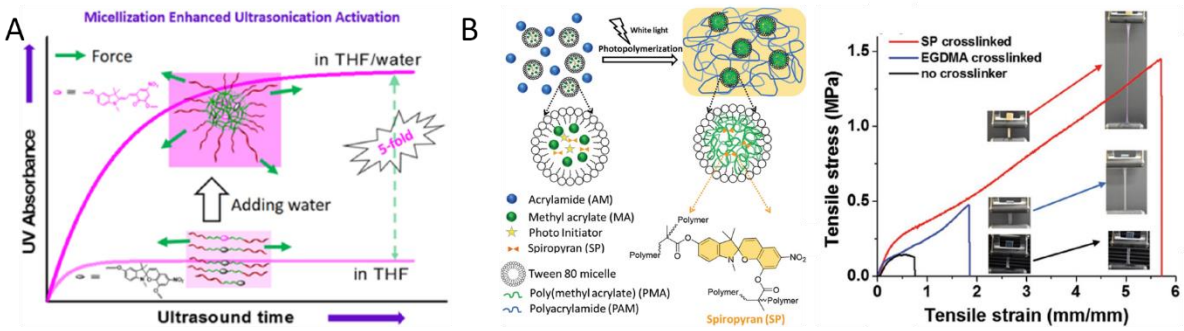

Figure 1.16. Mechano-responses enhanced by micellization. (A) Change in the absorbance at peak wavelength as a function of sonication time for the PNIPAM-P*t*BA-SP-P*t*BA-PNIPAM formed micelles in THF/water and dissolved in THF.[89] (B) Synthesis of poly(AM-*co*-MA/SP) hydrogel via micellar copolymerization, and tensile stress-strain curves of the hydrogels using SP or EGDMA as crosslinkers or without crosslinkers.[82]

When SP was embedded in the centre of an amphiphilic polymer chain (PNIPAM-P*t*BA-SP-P*t*BA-PNIPAM), the block copolymer self-assembled into micelles in aqueous solution.[89] The ultrasound-induced SP-to-MC activation was measured by UV absorbance, and the absorbance of a micellization sample was 4-fold more than that of a dissolved sample (**Figure 1.16A**), suggesting the micellization enhanced the mechano-response of the mechanophore-linked amphiphilic copolymer. This was attributed to the micelles partially swelling under sonication resulting in a larger dielectric constant of the medium around the mechanophore. Another study looked at SP bonded within a core in a bulk material, where SP was incorporated into a hydrogel with SP polymerized with MA in the form of microspheres with polyacrylamide copolymerized in the water phase (**Figure 1.16B**).[82, 116] This design substantially improved the mechanochromic sensitivity of SP-linked materials, as the colour activation occurred at *ca.* 100% strain. A more fascinating property achieved by using SP as crosslinker in this design was the significantly enhanced mechanical properties. The hydrogel with EGDMA as crosslinker fractured at a strain of 180% with 0.47 MPa strength, whereas the hydrogels employing SP as crosslinker could be stretched up to a strain of 570% with a tensile strength of 1.45 MPa. It was believed that covalent bond rupture based on SP-to-MC conversion led to the enhanced toughness. This work provided a strategy for the design of tough mechanophore-linked mechanochromic hydrogels.

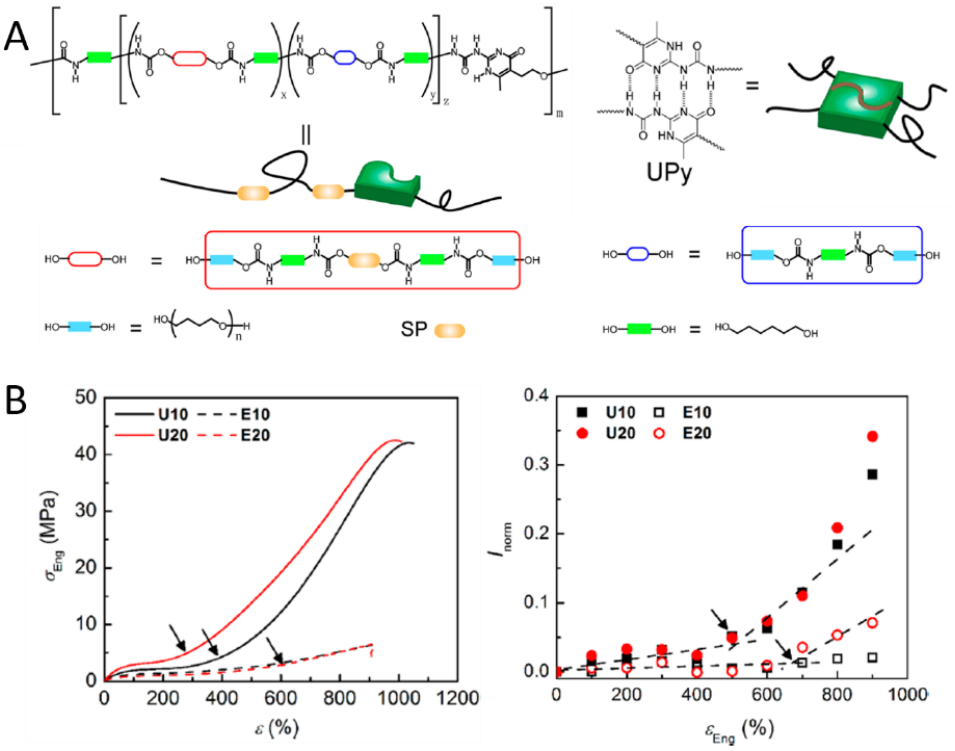

Figure 1.17. Enhanced mechanical properties by introduction of hydrogen bonding. (A) Chemical structure of SP covalently linked PU with UPy motifs integrated along the backbone. Hydrogen bonding is formed due to dimerization of UPy units.[96] (B) The left figure represents stress-strain curves of SP-PU elastomers end-capped with UPy units (U10 and U20) and urethane motifs (E10 and E20). The figure on the right shows the change of normalized fluorescence intensity against tensile strain, and the onset of mechano-activation is determined by the intersection of the two tangent lines.[95]

There are other examples demonstrating that an enhancement of the mechanical properties of mechanochromic materials is beneficial for the force-induced activation. Weng's group focussed on increasing the toughness of SP-linked PU by introducing hydrogen bonding between the polymer chains.[95-97] UPy units were integrated into PU backbone with SP covalently linked in the soft segment.[96] Strong and lateral hydrogen bonding interaction was formed due to the dimerization of UPy units (**Figure 1.17A**), which also facilitated microphase separation of hard and soft domains. The elastomer with UPy motifs could undergo a larger strain (up to 970%) and higher stress (23.7 MPa) without fracture than the sample without UPy motifs incorporated. SAXS data demonstrated that the breakage of hard domains occurred earlier than the mechano-activation of SP, and the force required for dissociation of UPy dimers was lower than

that for the breakage of C-O bond on SP, both of which contributed to a sufficient chain alignment facilitating force-induced activation of SP-PU elastomer. Likewise, the UPy motifs were embedded at the two ends of SP-PU chain to promote chain alignment relying on hydrogen bonding formation.[95] The elastomer with end-capped UPy displayed enhanced mechanical properties leading to an early onset of colour activation strain and a more pronounced colour change than that end-capped with urethane units (**Figure 1.17B**). A physical crosslinked network was achieved by the introduction of UPy motifs into PU backbone, and furthermore a chemical crosslinked network into the system was introduced.[97] The results once again revealed that the onset of mechano-activation located in the strain-hardening region, indicating the importance of regulating the strain-hardening region to the activation of mechanophore-linked materials. Apart from making use of the hydrogen bonding formed by physical interactions, metallosupramolecular interactions were introduced to SP-PU elastomer for stress sensing.[98] A tridentate ligand and SP were covalently linked into PU backbone to afford ligand macromolecules, which could form metal-ligand complexes with metal ions. The metal-ligand complexes aggregated into hard domains to promote chain alignment during stretching. The dynamic complexes also provide a self-healing property for the system.

In another type of system, nanofiller-like POSS units were employed to improve the strength of SP-PU, which relied on aggregation hindering the mobility of hard domains and not by molecular intereactions.[100] POSS is comparable to nanofillers such as clay and its addition can improve the mechanical properties of polymers with advantages of improving compatibility afforded by being covalently linked into polymer systems.[117] Due to the cage-like structure of POSS, its introduction can significantly restrict the mobility of polymer chains, reinforcing the mechanical properties and increasing the thermal stability.[118, 119] Thus it was introduced into SP-linked PU elastomer as chain extenders and crosslinkers.[100] The elastomer conjugated with POSS could be stretched to a strain of 400% at a strength of 8MPa at 70 °C, whereas the specimen without POSS showed a strength of *ca.* 1MPa with a stretchability of 300% at 70 °C, indicating significantly enhanced mechanical properties and thermal stability by the introduction of POSS.

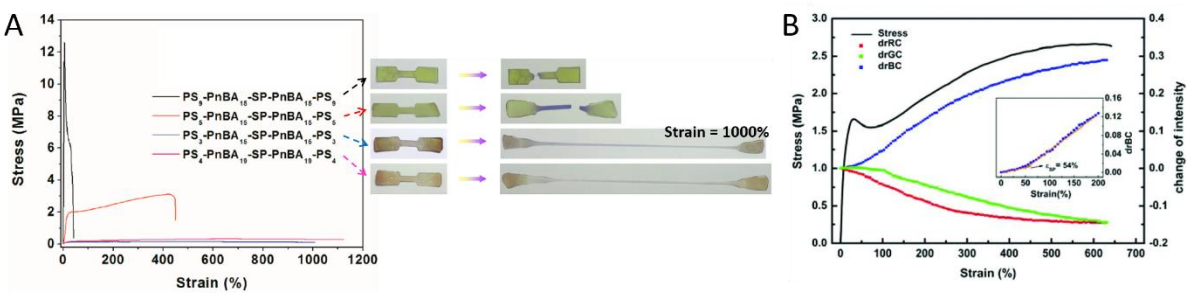

Figure 1.18. Regulable mechanochromic properties by adjusting hard domains. (A) Tensile stress-strain curves of PS-P*n*BA-SP-P*n*BA-PS triblock copolymers varying the ratio of soft/hard blocks, and the corresponding images before and after tensile test.[65] (B) Tensile stress-strain curve of PBA-SP-PS and change of colour intensity as a function of strain. The inset figure indicates the onset of colour activation strain.[66]

The examples above-mentioned have elucidated that the hard domains in the polymer systems play important roles in the mechanochromic activation. The mechano-response of triblock copolymers PS-P*n*BA-SP-P*n*BA-PS has been shown to be PS block length depended.[65] The tensile testing results showed that a high PS hard-block fraction (PS_9-P*n*BA_{15}-SP-P*n*BA_{15}-PS_9) resulted in a more glassy like polymer with a low yield strain of 8% and a high Young's modulus of 240 MPa, leading to an inefficient mechanochromic response until specimen rupture (**Figure 1.18A**). Inefficient force transferred to SP also occurred to the samples with a low hard-block fraction (PS_3-P*n*BA_{15}-SP-P*n*BA_{15}-PS_3 and PS_4-P*n*BA_{19}-SP-P*n*BA_{19}-PS_4) as the specimens were too soft to transfer the applied force. It suggests that a proper microphase separated structure will be useful for the design of mechanophore-linked mechanochromic polymers. Grafted copolymers of PBA-SP-PS with SP located between the incompatible soft and hard domains were reported by Jia and co-workers.[66] This design avoids the possible slip of chain entanglements under loading as the dispersed PS hard domains performed like physical cross-links benefiting stress concentrated at the interface of PS domains, while the soft domains still provided mobility for SP units. A low onset of mechano-activation strain was achieved at 54% strain and excellent mechanical properties with stretchability up to 650% (**Figure 1.18B**). The mechanical and mechanochromic properties were adjustable by varying the composition of soft/hard blocks.

1.5.3 Conditions of Mechanical Testing

The design of SP molecules and polymer architectures have been shown to be important for improved mechanochromic performance. Apart from the structure of the materials themselves, the mechanical testing conditions also influence the mechano-response.

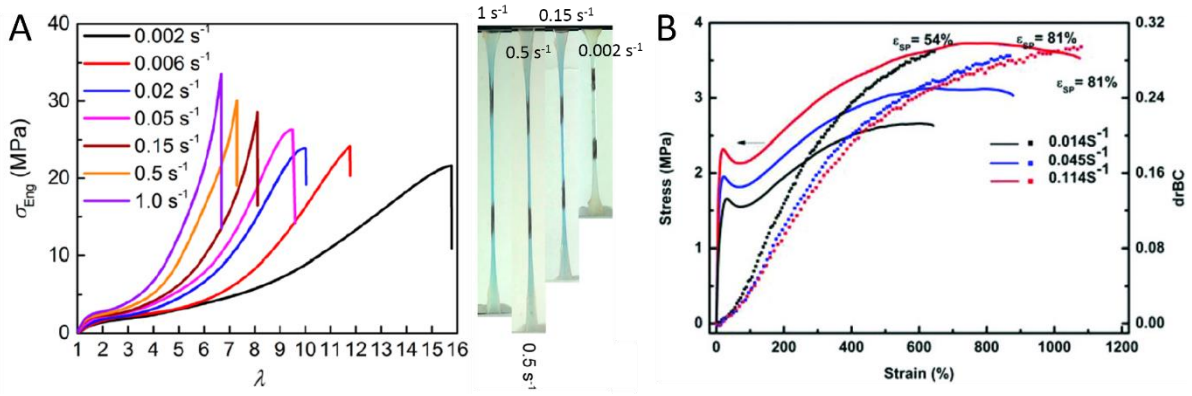

Figure 1.19. Effect of strain rate on mechanochromic properties. (A) Tensile stress-strain curves of dual cross-linked SP-PU elastomers varying strain rates, and optical images of the corresponding specimens stretched to a strain of 600%.[97] (B) Stress-strain curves of PBA-SP-PS polymer at various tensile strain rate, and the corresponding change of blue colour intensity against strain.[66]

Tensile testing of mechanochromic materials are used to quantify their mechanochromic responses. However, the conditions of strain rate used in the testing affect this phenomenon. Higher strain rates usually lead to a higher mechanochromic response. Three different strain rates (0.004, 0.02 and 0.10 s^{-1}) were applied to SP-linked PMA linear polymers.[87] The higher stretch rate resulted in an earlier colour activation and a higher fluorescence intensity under a given strain. It was believed that the higher stress resulted from a higher strain rate facilitated chain alignment and the force transferred to the mechanophores, as the strain-hardening occurred at a relatively low strain for the specimen subjected a high strain rate. In the dual crosslinked SP-PU system, deeper blue colour was also observed in response to a higher strain rate (**Figure 1.19A**), which was consistent to an earlier onset of strain-hardening region with increasing the strain rate.[97]

On the other hand, lower strain rates also influence mechano-response. For the glassy polymer SP-linked PMMA polymer under loading at 90 °C, although a slower strain rate (1.2×10^{-4} s^{-1}) led to the yield at a relatively low stress, the fluorescence intensity at a given

strain value was higher than that of the sample applied with a high strain rate (1.2×10^{-3} - 1.2×10^{-1} s^{-1}).[62] And the trend was observed on both tensile and compression tests. It was attributed to the loading time because a slower strain rate allowed a longer time for the SP-to-MC conversion. When the fluorescence intensity was plotted as a function of loading time, a faster strain rate resulted in a higher fluorescence value at a given loading time. Likewise, a higher tensile strain rate resulting in a less mechanical activation was observed on PBA-SP-PS glassy-like polymer (**Figure 1.19B**).[66] As the mechano-activation for glassy polymers usually occurs after the yielding while that for elastomers it happens at strain-hardening region, the strain rather than the stress plays a more important role in the onset of mechano-activation, whereas the conversion ratio of SP-to-MC more depends on the stress and loading time. In this case, it can explain the opposite trends observed for the effect of strain rate in various polymer systems.

The effect of various loading modes (tension and compression) on mechanochromic performance was also investigated.[62] The SP-PMMA specimens subjected to tension or compression at the same conditions (temperature and strain rate) displayed similar mechanical responses, including the onset of activation strain and higher strain rate leading to higher fluorescence intensity, and only differed at the stress of compression required higher than that of tension. As most of the study in this field use tension to trigger the activation, the mechanism for compression from molecular level, *i.e.* chain alignment and SP orientation, has remained to be investigated.

1.6 Applications

Force-induced colour change materials are interesting as they provide optical changes without the requirement for external monitoring devices.[120] As the fabrication of mechanophore-linked polymers has been well established, the challenge moves to the implementation of these materials for stimuli-responsive applications.

1.6.1 Sensors and Stretchable Electronics

The Craig group has been focusing on applying SP-linked PDMS for stress/strain sensing applications.[68, 101, 102, 113, 114, 121] Balloons and soft robot grippers were prepared by casting and thermal-curing the mixture of di-functional SP and commercial PDMS oligomers

(Ecoflex) in designed moulds.[102] As a proof-of-concept, the balloon started to change colour from a biaxial strain of 70% induced by inflation, laying the foundation for the design of dual-functional soft robot actuated by inflation. The actuation of the prepared robot gripper led to an expansion which was not efficient for an optimized mechanochromic response, but the region with the most intense colour during actuation provided an indication of the area under the risk of failure (**Figure 1.20A**). The soft robot could be also used to detect and trace spatial environment as a confined space would disrupt the inflation and more intense colour was triggered resulted from the external stiff elements.

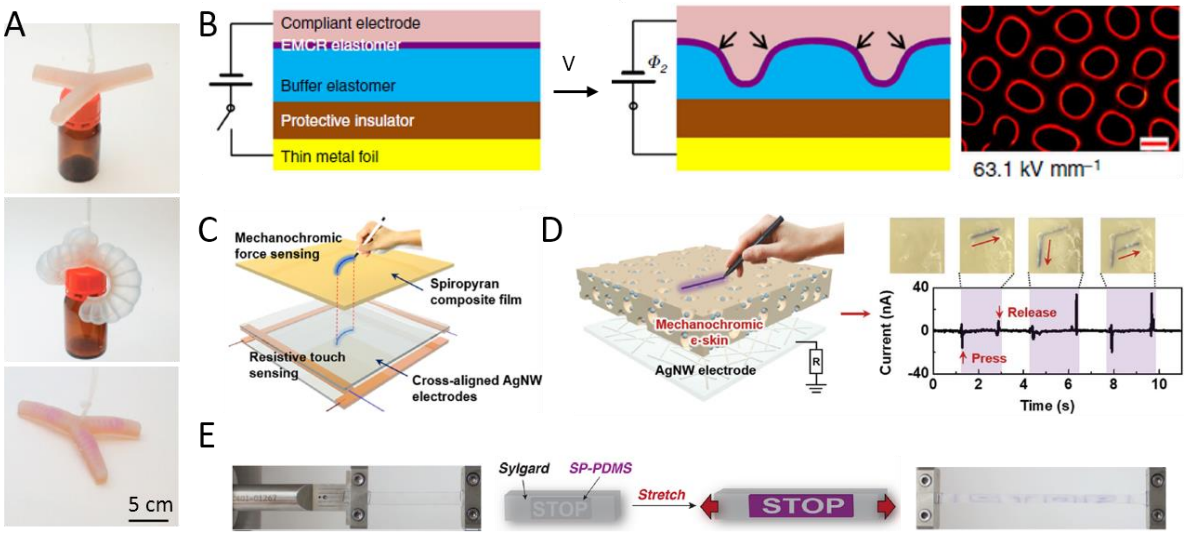

Figure 1.20. Applications using mechanochromic SP-linked PDMS. (A) Images of a three-arm gripper robot before, during and after inflation, with the appearance of purple colour indicating the "at-risk" regions.[102] (B) Laminated structure of an electro-mechano-chemically responsive system, before and after applied with an electric field, and image of fluorescent patterns observed due to the mechano-activation. Scale bar = 250 μm.[101] (C) A pressure-sensitive touch screen with colour change in response to dynamic writing.[113] (D) A dual-mode force sensor with mechanochromic and triboelectric functions using a porous nanoparticle-in-micropore SP-PDMS, enabling spatiotemporal detection of writing force and speed.[114] (E) Metallic nanowires embedded in mechanochromic SP-PDMS for indicating failure.[68]

The devices possessing deformation components can be integrated with mechanochromic polymers for visualization or optical monitoring purposes. The deformation can be directly caused by an external stress or triggered indirectly from

other stimuli, such as electric signals. Mechanochromic SP-PDMS was employed for assembling an electro-mechano-chemically responsive system.[101] The laminate consisted of a buffer elastomer underneath the mechanochromic SP-PDMS elastomer, a protective insulator, a metal foil at the bottom layer and a compliant electrode on the top surface (**Figure 1.20B**). The flat surface of SP-PDMS wrinkled resulting in craters when an electric field was applied. When the deformation around the crater edges was above 6 at a higher electric field above 45 kV mm^{-1}, significant fluorescence could be observed. Different deformed patterns could be achieved by pre-stretching the mechanochromic elastomers or embedding rigid objects.

Metallic nanowires such as silver nanowire (AgNW) have promising properties suitable for displays, wearable electronics and touch sensors due to their excellent flexibility, conductivity and optical transparency.[122, 123] The mechanochromic SP-PDMS elastomer was combined with AgNW electrodes for force-responsive touch screens (**Figure 1.20C**).[113] Cross-aligned AgNW electrodes were prepared by bar-coating technique (Meyer rod-coating) on a polyethylene terephthalate substrate to improve the uniformity, electrical conductivity and transparency of the networks. The SP-PDMS film was then coated on the top surface of prepared AgNW electrodes layer, which was connected to a laptop computer via a four-wire resistive controller board and equipped with a spectroradiometer. The resulted touch screen was highly transparent and flexible, and could quantify the applied force of a stylus writing via analysing the colour generated and trace the location of writing. To further expand the implementation of mechanochromic elastomers into wearable electronics, a hierarchical nanoparticles-in-micropore architecture was adopted to prepare porous mechanochromic SP-PDMS composites to enhance the mechanochromic sensitivity.[114] The porous composites were achieved by evaporation of hydrophilic solvents (water and ethanol) during the thermal curing of SP/PDMS precursor and a subsequent freeze drying, and silica nanoparticles (SNPs) were introduced into the system during the addition of hydrophilic solvents. The pore size could be tuned by controlling the ratio of water to ethanol and SNPs with different size were integrated, both of which impacted the mechanical properties and mechanochromic performance of the composites. The mechanochromic response and stretchability increased with decreasing pore size and increasing SNPs diameter. The resulted composites could be stretched up to a strain of 400% and the colour change was reversible with a stable mechanochromic performance under a strain of 250% for 100

cycles. The mechanochromic sensitivity in terms of applied normal force dramatically dropped with small size pore and large size SNPs, which was ideal for touch-sensitive mechanochromic e-skins applications. The porous composite was combined with the AgNW to assemble a dual-functional mechanochromic and triboelectric force sensor which could detect writing force and speed and acoustic signals (**Figure 1.20D**). The key in the design of multi-functional devices employing these mechanochromic materials is to improve the mechanochromic sensitivity, which includes low activation strain and force.

Another study of combining the mechanochromic SP-PDMS with metallic nanowires was fabrication of mechanochromic stretchable electronics.[68] Eutectic gallium indium alloy was embedded into SP-PDMS elastomer via injection of the conductive liquid metal into the designed PDMS films consisting of microchannels. Stretching the liquid metal devices is accompanied by mechanochromic responses of SP-PDMS at a large strain. As the failure of the wire occurred at 125 – 160% strain and the mechano-activation of the SP-PDMS began at 90% strain, the remarkable colour gave an indication that the wire was under a risk of rupture if it was further stretched (**Figure 1.20E**). This design as a proof of concept provides a direction where the mechanochromic elastomers can be applied, despite that the moulding method restricts their scale-up fabrication.

1.6.2 3D Printing

The development of 3D (three-dimensional) printing in recent years have brought great opportunities to a range of functional materials such as electronics and organs.[124-126] The advantages of precisely controllable shaping and customisation using 3D printing technologies are unique compared to traditional processing methods. Extrusion-based process and vat polymerization process are the two most common 3D printing technologies, with the former building objects by melting and extruding thermoplastic filament onto the building plate, and the latter one building objects by irradiating UV or digital light to photo-polymerizable resins stored in a vat layer by layer. With the growing development of 3D printing, to broaden the options for printable materials is necessary, especially for functional materials which can be used for smart devices.[127, 128] The smart stimuli-responsive polymers undergo change in physical or chemical properties induced by electric field, temperature, light, pH and force have been attempted for 3D printing. So

far, there are only two examples of 3D printed mechanochromic polymers, with both using SP as mechanochromophore.

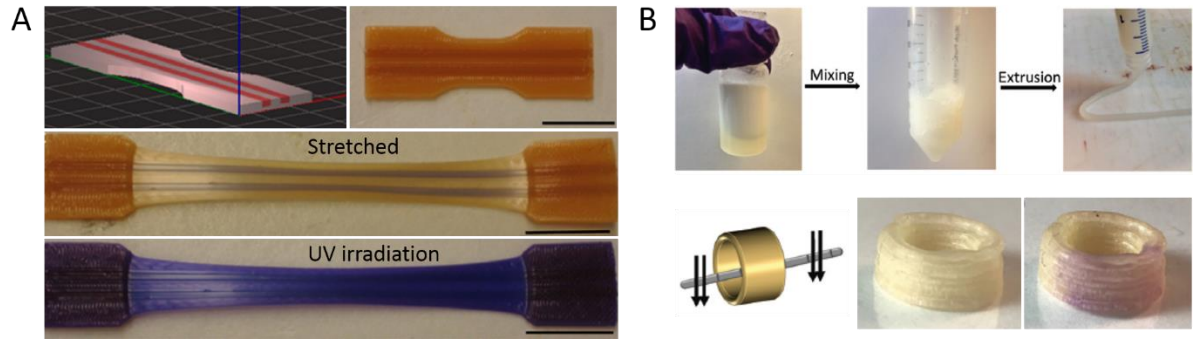

Figure 1.21. 3D printing technique applied to SP-linked mechanochromic polymers. (A) CAD representation of a "dog bone" shaped tensile specimen consisting of a difunctional SP-linked PCL filament responsive to both UV and mechanical force (red strips) embedded in a monofunctional SP-linked filament only responsive to UV, and optical images of the specimen before and after stretched and UV irradiation. Scale bar = 20 mm.[90] (B) So-gel transition is observed under mixing of microbead suspensions with bi-alkene SP, forming uncured silicone ink for extrusion 3D printing (top figure). A schematic illustration of 3D printed cone cylinder and the optical images displaying the colour change of the cone before and after compression (bottom figure).[129]

The mechanochromic SP-linked PCL polymers have been reported to be processed into force sensors by 3D extrusion printing using a fused deposition modelling printer.[90] SP-PCL was blended with commercial PCL filament before being processed into mechanochromic filament (1.55 – 1.85 mm diameter) through melt extrusion at 63 °C. The temperature of the extrusion printing was 110 °C to avoid jamming at lower temperatures. Although the printing temperature was relatively higher than the mixing temperature, neither colour change nor polymer degradation was observed during the printing. Customized specimens containing two different SP-PCL could be printed via dual extrusion technique: one di-functional SP-linked filament responsive to both UV irradiation and mechanical force was embedded as strips in the monofunctional SP-linked filament only showing UV-response (**Figure 1.21A**). Therefore, only the strips displayed colour switch under deformation, whereas the whole sample turned purple under UV irradiation. The unique design achieved by the 3D printing technique not only offers more potential for mechanochromic materials but also expands the options of

functional materials in the 3D printing field. More recently, the Craig group reported a mechanochromic silicone ink for extrusion 3D printing[129] which employed the printable inks prepared by Sangchul *et. al.*[130] SP was incorporated into uncured PDMS (commercially available Dragon Skin™) mixed with PDMS microbeads (a stiffer Sylgard™ 184), and upon mixing, sol-gel transition occurred due to the formation of capillary bridges (**Figure 1.21B**). The resultant uncured silicone ink with suitable yield stress and shear-thinning property could be extruded and printed by a syringe connected to a modified commercially available printer. But the printed samples needed to be post thermo-cured for hours after print, which limit its commercialization. SP sitting in the "bridges" between the microbeads where stress was concentrated at under deformation facilitated the mechano-activation. The advantage of PDMS printable ink over the PCL filament is that the PDMS specimen is shape recoverable. As a proof of concept, the printable mechanochromic silicone elastomer lays a foundation for the printable-functional elastomers.

1.6.3 Latex Materials

Acrylic latexes are widely used in daily life for painting houses, protective coating on appliance and furniture, and adhesives. Water-based acrylic latexes are under rapid development to replace the solvent-based latexes in order to reduce the toxicity to human being's health and the environment. Emulsion polymerization is the approach to solidifying the coated films.[131, 132]

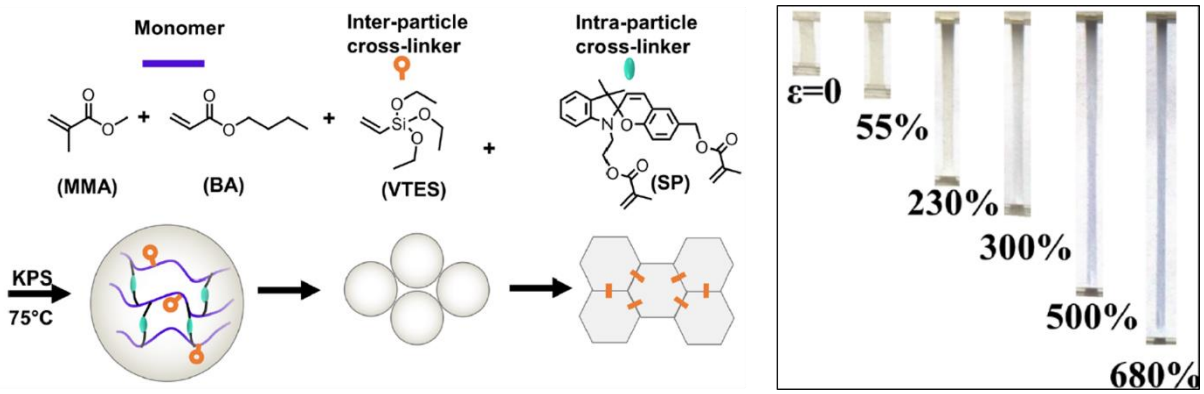

Figure 1.22. Schematic illustration of preparing P(BA-*co*-MMA-*co*-SP-*co*-VTES) latexes via emulsion polymerization, and images of the latex film under stretch at various strains.[133]

Li *et al.* incorporated di-functional SP with methyl acrylate groups into P(BA-*co*-MMA-*co*-SP-*co*-VTES) latexes as crosslinker via emulsion polymerization to prepare mechanochromic latex films (**Figure 1.22**).[133] Siloxane monomer vinyltriethoxysilane (VTEA) was used to form cross-linking between the latex particles via hydrolysis and condensation during the film formation, which provided improved mechanical properties for the latex films. The obtained latex films displayed significant colour change over 300% strain and can be stretched up to 680% strain, demonstrating an efficient mechanochromic performance and excellent mechanical properties. It was the first example of mechanochromic acrylic latex and offers a potential application as force-responsive and self-reporting coatings. However, the practical applications using this mechanochromic acrylic latex remain elusive as the application targets and details of the mechanochromic performance such as repeatability and duration are needed to be further explored.

1.7 Scope of Thesis

1.7.1 Current Challenges and Limitations

Although the fabrications of SP-based mechanochromic materials have been well established, the mechanochromic mechanism regarding to SP geometry has remained unclear, as the difference of SPs with varying attachment positions in their macroscopic mechanochromic properties lacks systematic investigation for understanding the effect of SP geometry on mechano-sensitivity. In addition, although these SP-based polymeric materials display potential for applications as stress/strain sensors with visualization, the employed polymer architectures are mainly focusing on the mechanochromic purpose without considering the mechano-sensitivity, demonstrated by the mechano-activation required for the reported SP-based materials generally requiring large strain or high stress, which limits their practical use. Therefore, reducing the energy for mechano-activation and improving the mechanochromic sensitivity are crucial for practical applications.

1.7.2 Thesis Objectives

The research goals of this thesis are to systematically understand the mechanochromic mechanism from SP molecules level and then develop mechanochromic polymeric materials which are highly sensitive to force by designing advanced polymer architecture. The force efficiency affected by the SP molecule geometry has remained elusive and is essential for the design of SP-linked polymers when choosing the appropriate SP derivatives. To address that, a new tri-functional SP was synthesized and compared with the two most widely studied di-functional SP on their mechanochromic behaviour, by incorporated them into non-polar polymer matrix PDMS (**Chapter 2**) and polar polymer matrix poly (hydroxyethyl acrylate) (PHEA) (**Chapter 3**). These comparisons aim at manipulating the mechano-activation via the design of SP molecule. In addition, a multi-network structure was adopted to integrate the new tri-functional SP to significantly reduce the energy of mechano-activation, aiming at improving the mechano-sensitivity via the design of polymer architecture (**Chapter 4**). **Figure 1.23** represents the structure of this thesis, corresponding to the investigated content mentioned above.

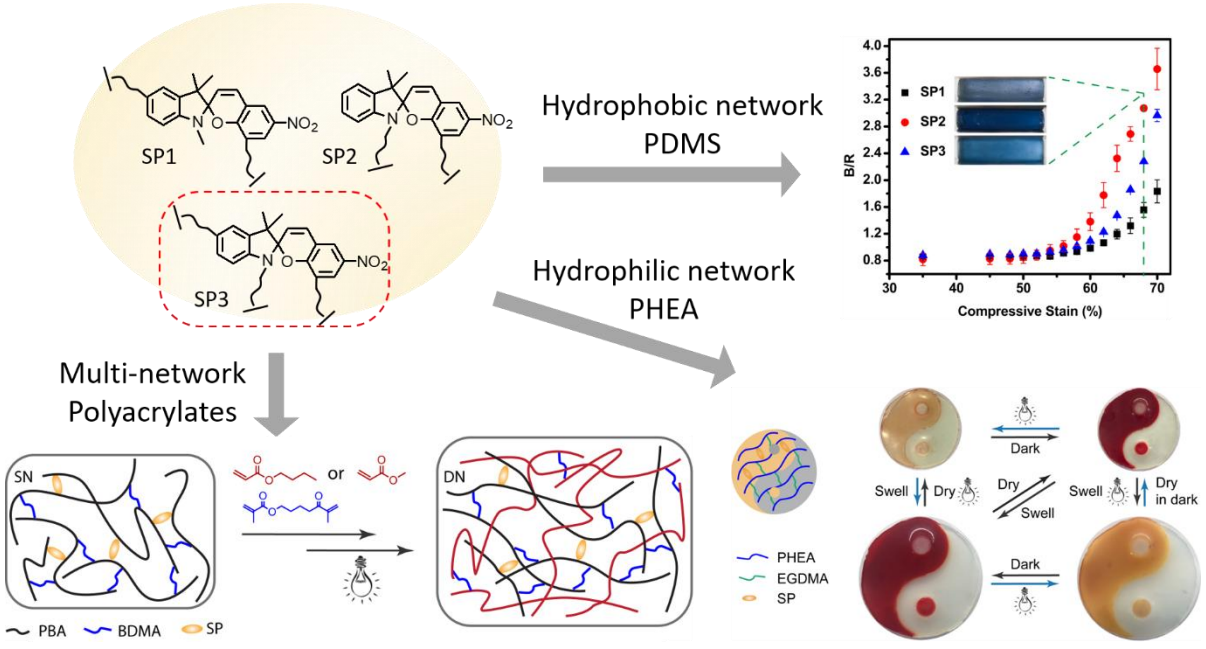

Figure 1.23. Research theme of this thesis: three SPs varying attachment positions and numbers were synthesized and crosslinked into non-polar PDMS and polar PHEA for mechanochromic purpose, to study the effect of SP geometry. A multi-network made of poly acrylates was adopted to covalently link tri-functional SP3 in the pre-stretched first-network, to reduce the energy of mechano-activation.

1.7.3 Thesis Outline

In **Chapter 2**, a new tri-functional SP was synthesized and systematically compared with two widely used di-functional SPs in the same non-polar PDMS matrix on their mechanochromic properties (**Figure 1.24**). A statistical difference at the onset activation stress and strain among the three samples was not observed, however the colour intensity of the three samples under a same strain varies. The phenomenon of blue-shift under loading and after unloading also differed among the three samples which is further investigated by density functional theory calculations. The compression test and density functional theory calculations revealed that both the electronic and geometric effects caused by varying the attachment positions influence the mechanochromic performance, with the geometry playing a more dominant role.

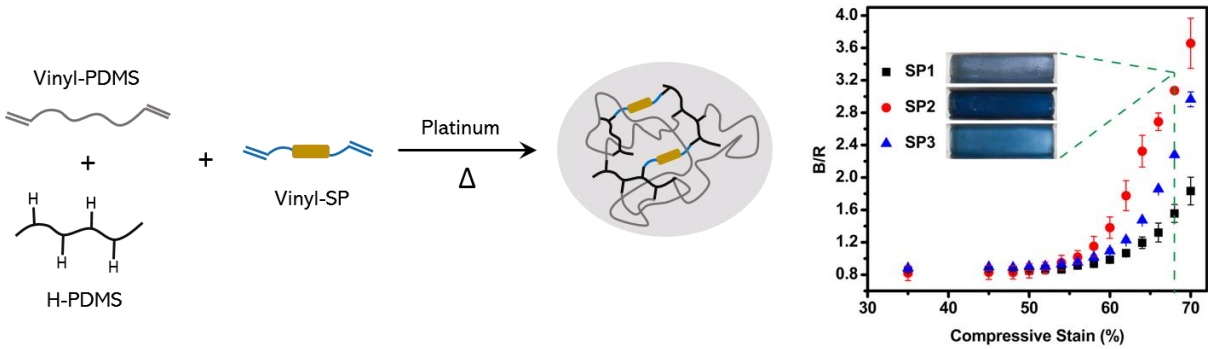

Figure 1.24. Chapter 2: SPs crosslinked into non-polar PDMS and their mechano-responses under compression represented by the plot of blue/red channel intensity as a function of strain and the inset images showing the samples under a strain of 68%.

Since the equilibrium between SP and MC is affected by the polarity of the environment, **Chapter 3** investigated the effect of the attachment positions on mechanochromism and negative photochromism by covalently bonding the three SPs in polar PHEA. The negative photochromism in the dark and mechanical activation by swelling in water were investigated (**Figure 1.25A**). It was found that the tri-substituted SP (SP3) was the least influenced by the polar matrix and showed the fastest mechano-activation during swelling. SP3 also exhibited a significantly slower decolouration rate relative to SP1 and SP2 once dehydrated after swelling. The results demonstrated that the influences from both the polar environment and the mechanochromic nature of spiropyran have an impact on the absorption intensity, rate of change and the decolouration rate of the

materials. By adding more attachment points on SP, the negative photochromism could be efficiently reduced, and the mechano-activation triggered by swelling force could be improved.

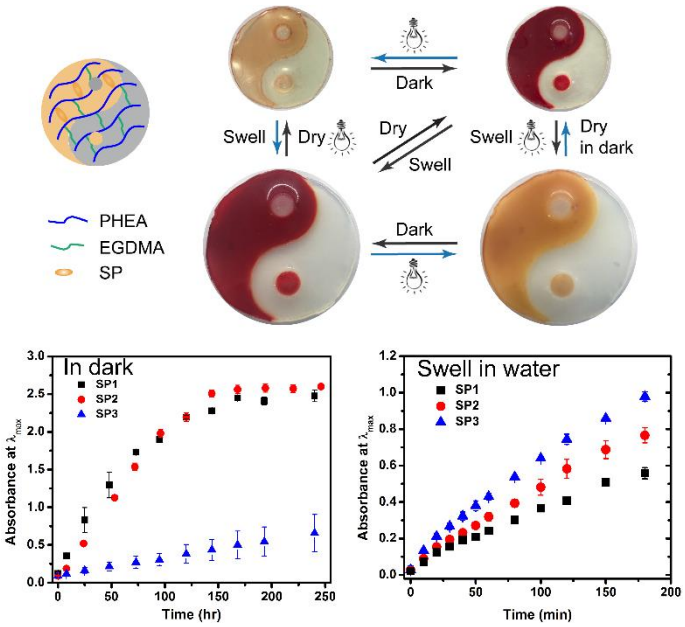

Figure 1.25. Chapter 3: SPs incorporated into polar PHEA and their negative photochromic performances and mechano-responses when swollen in water.

In **Chapter 4**, the tri-substituted SP3 was incorporated into multi-network polyacrylates to reduce the mechano-activation energy adopting advanced polymer architecture. SP was conjugated into the pre-stretched first-network formed by swelling into a monomer solution of the second network which was locked afterwards (**Figure 1.26A**). By repeating the swelling-curing process, a triple-network (TN) can be obtained. The resulted double-network (DN) exhibits remarkable mechanochromic performance whereas no colour change was observed for SP embedded in only one network. A term of colour activation energy (U_A) was used to represent the macroscopic energy of the threshold, taking both stress and strain into consideration. The U_A was further reduced in a third-network formation. The influence of network formation conditions, *i.e.* solvent ratio and type of monomers, were also studied. A comparison of the elastomers prepared in this work to previously reported SP-linked elastomers suggests that the TN in this work achieves the lowest U_A (**Figure 1.26B**).

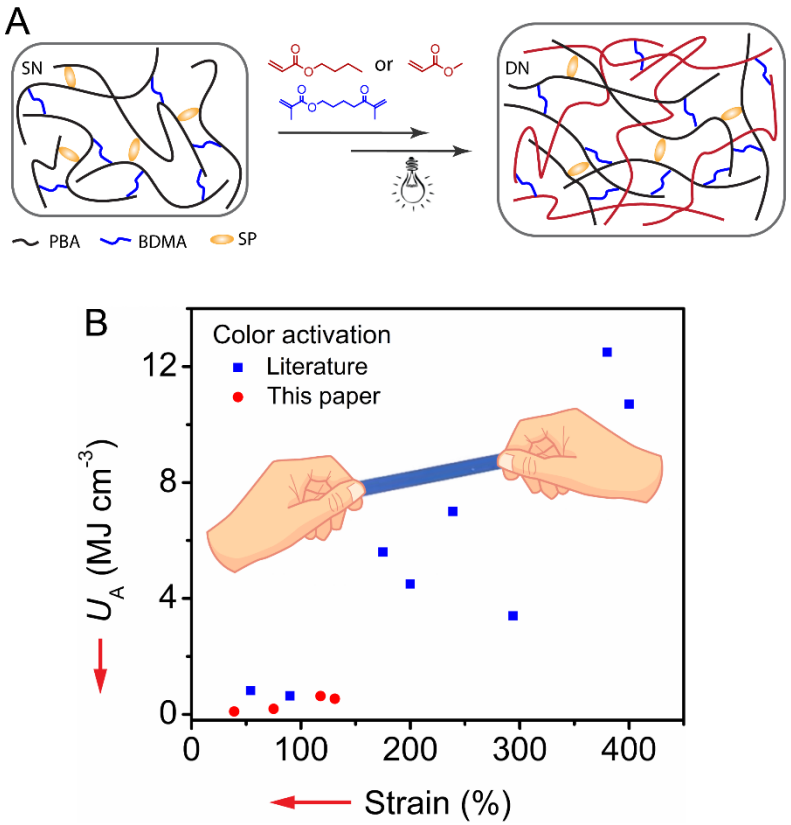

Figure 1.26. Chapter 4: (A) First-network SP-poly(butyl acrylate) was swollen in monomer followed by white light polymerization to prepare DN elastomers. (B) A plot of U_A against strain of SP-linked elastomers presented in this work (red colour) and reported in the literature (blue colour).

Chapter 5 provides an overall conclusion to this thesis and presents some proposed future perspectives in relation to further exploring SP-based mechanochromic materials and their applications.

1.8 References

(1) Beyer, M. K.; Clausen-Schaumann, H. Mechanochemistry: the mechanical activation of covalent bonds. *Chem. Rev.* 2005, 105, 2921-2948.

(2) Kaupp, G. Mechanochemistry: the varied applications of mechanical bond-breaking. *Cryst. Eng. Comm.* 2009, 11, 388-403.

(3) Li, J.; Nagamani, C.; Moore, J. S. Polymer mechanochemistry: from destructive to productive. *Acc. Chem. Res.* 2015, 48, 2181-90.

(4) Wang, J.; Piskun, I.; Craig, S. L. Mechanochemical Strengthening of a Multi-mechanophore Benzocyclobutene Polymer. *ACS Macro Lett.* 2015, 4, 834-837.

(5) Brantley, J. N.; Wiggins, K. M.; Bielawski, C. W. Polymer mechanochemistry: the design and study of mechanophores. *Polym. Int.* 2013, 62, 2-12.

(6) Calvino, C.; Neumann, L.; Weder, C.; Schrettl, S. Approaches to polymeric mechanochromic materials. *J. Polym. Sci., Part A: Polym. Chem.* 2017, 55, 640-652.

(7) Caruso, M. M.; Davis, D. A.; Shen, Q.; Odom, S. A.; Sottos, N. R.; White, S. R.; Moore, J. S. Mechanically-induced chemical changes in polymeric materials. *Chem. Rev.* 2009, 109, 5755-5798.

(8) Barber, R. W.; McFadden, M. E.; Hu, X.; Robb, M. J. Mechanochemically Gated Photoswitching: Expanding the Scope of Polymer Mechanochromism. *Synlett* 2019, 30, A-H.

(9) Klajn, R. Spiropyran-based dynamic materials. *Chem. Soc. Rev.* 2014, 43, 148-84.

(10) Zhang, H.; Gao, F.; Cao, X.; Li, Y.; Xu, Y.; Weng, W.; Boulatov, R. Mechanochromism and Mechanical-Force-Triggered Cross-Linking from a Single Reactive Moiety Incorporated into Polymer Chains. *Angew. Chem. Int. Ed.* 2016, 55, 3092-3096.

(11) Wang, Z.; Ma, Z.; Wang, Y.; Xu, Z.; Luo, Y.; Wei, Y.; Jia, X. A Novel Mechanochromic and Photochromic Polymer Film: When Rhodamine Joins Polyurethane. *Adv. Mater.* 2015, 27, 6469-74.

(12) Wang, T.; Zhang, N.; Dai, J.; Li, Z.; Bai, W.; Bai, R. Novel Reversible Mechanochromic Elastomer with High Sensitivity: Bond Scission and Bending-Induced Multicolour Switching. *ACS Appl. Mater. Interfaces* 2017, 9, 11874-11881.

(13) Guo, K.; Chen, Y. Force-induced cleavage of C–O bond in photochromic naphthopyrans. *Mater. Chem. Phys.* 2013, 137, 1062-1066.

(14) Robb, M. J.; Kim, T. A.; Halmes, A. J.; White, S. R.; Sottos, N. R.; Moore, J. S. Regioisomer-Specific Mechanochromism of Naphthopyran in Polymeric Materials. *J. Am. Chem. Soc.* 2016, 138, 12328-12331.

(15) Imato, K.; Irie, A.; Kosuge, T.; Ohishi, T.; Nishihara, M.; Takahara, A.; Otsuka, H. Mechanophores with a reversible radical system and freezing-induced mechanochemistry in polymer solutions and gels. *Angew. Chem. Int. Ed.* 2015, 54, 6168-6172.

(16) Imato, K.; Kanehara, T.; Ohishi, T.; Nishihara, M.; Yajima, H.; Ito, M.; Takahara, A.; Otsuka, H. Mechanochromic Dynamic Covalent Elastomers: Quantitative Stress Evaluation and Autonomous Recovery. *ACS Macro Lett.* 2015, 4, 1307-1311.

(17) Kosuge, T.; Imato, K.; Goseki, R.; Otsuka, H. Polymer–Inorganic Composites with Dynamic Covalent Mechanochromophore. *Macromolecules* 2016, 49, 5903-5911.

(18) Imato, K.; Otsuka, H. Reorganizable and stimuli-responsive polymers based on dynamic carbon–carbon linkages in diarylbibenzofuranones. *Polymer* 2018, 137, 395-413.

(19) Ishizuki, K.; Oka, H.; Aoki, D.; Goseki, R.; Otsuka, H. Mechanochromic Polymers That Turn Green Upon the Dissociation of Diarylbibenzothiophenonyl: The Missing Piece toward Rainbow Mechanochromism. *Chem. Eur. J.* 2018, 24, 3170-3173.

(20) Ishizuki, K.; Aoki, D.; Goseki, R.; Otsuka, H. Multicolour Mechanochromic Polymer Blends That Can Discriminate between Stretching and Grinding. *ACS Macro Lett.* 2018, 7, 556-560.

(21) Sakai, H.; Sumi, T.; Aoki, D.; Goseki, R.; Otsuka, H. Thermally Stable Radical-Type Mechanochromic Polymers Based on Difluorenylsuccinonitrile. *ACS Macro Lett.* 2018, 7, 1359-1363.

(22) Sumi, T.; Goseki, R.; Otsuka, H. Tetraarylsuccinonitriles as mechanochromophores to generate highly stable luminescent carbon-centered radicals. *Chem. Commun.* 2017, 53, 11885-11888.

(23) Kato, S.; Ishizuki, K.; Aoki, D.; Goseki, R.; Otsuka, H. Freezing-Induced Mechanoluminescence of Polymer Gels. *ACS Macro Lett.* 2018, 7, 1087-1091.

(24) Kato, S.; Aoki, D.; Otsuka, H. Introducing static cross-linking points into dynamic covalent polymer gels that display freezing-induced mechanofluorescence: enhanced force transmission efficiency and stability. *Polym. Chem.* 2019, 10, 2636-2640.

(25) Imato, K.; Nishihara, M.; Kanehara, T.; Amamoto, Y.; Takahara, A.; Otsuka, H. Self-healing of chemical gels cross-linked by diarylbibenzofuranone-based trigger-free dynamic covalent bonds at room temperature. *Angew. Chem. Int. Ed.* 2012, 51, 1138-42.

(26) Imato, K.; Natterodt, J. C.; Sapkota, J.; Goseki, R.; Weder, C.; Takahara, A.; Otsuka, H. Dynamic covalent diarylbibenzofuranone-modified nanocellulose: mechanochromic behaviour and application in self-healing polymer composites. *Polym. Chem.* 2017, 8, 2115-2122.

(27) Chen, Y.; Spiering, A. J.; Karthikeyan, S.; Peters, G. W.; Meijer, E. W.; Sijbesma, R. P. Mechanically induced chemiluminescence from polymers incorporating a 1,2-dioxetane unit in the main chain. *Nat. Chem.* 2012, 4, 559-62.

(28) Ducrot, E.; Chen, Y.; Bulters, M.; Sijbesma, R. P.; Creton, C. Toughening elastomers with sacrificial bonds and watching them break. *Science* 2014, 344, 186-189.

(29) Day, J. H. Thermochromism. *Chem. Rev.* 1963, 63, 65-80.

(30) Fischer, E.; Hirshberg, Y., Formation of coloured forms of spirans by low-temperature irradiation. J. Chem. Soc.: 1952; pp 4522-4524.

(31) Nogami, M.; Abe, Y. Photochromism of spiropyran and diarylethenedoped silica gels prepared by the sol-gel process. *J. Mater. Sci.* 1995, 30, 5789-5792.

(32) Berkovic, G.; Krongauz, V.; Weiss, V. Spiropyrans and spirooxazines for memories and switches. *Chem. Rev.* 2000, 100, 1741-1754.

(33) Such, G.; Evans, R. A.; Yee, L. H.; Davis, T. P. Factors Influencing Photochromism of Spiro-Compounds Within Polymeric Matrices. *J. Macromol. Sci., Polym. Rev.* 2003, 43, 547-579.

(34) Florea, L.; Diamond, D.; Benito-Lopez, F. Photo-Responsive Polymeric Structures Based on Spiropyran. *Macromol. Mater. Eng.* 2012, 297, 1148-1159.

(35) Kortekaas, L.; Browne, W. R. The evolution of spiropyran: fundamentals and progress of an extraordinarily versatile photochrome. *Chem. Soc. Rev.* 2019, 48, 3406-3424.

(36) Potisek, S. L.; Davis, D. A.; Sottos, N. R.; White, S. R.; Moore, J. S. Mechanophore-linked addition polymers. *J. Am. Chem. Soc.* 2007, 129, 13808-13809.

(37) Davis, D. A.; Hamilton, A.; Yang, J.; Cremar, L. D.; Van Gough, D.; Potisek, S. L.; Ong, M. T.; Braun, P. V.; Martinez, T. J.; White, S. R.; Moore, J. S.; Sottos, N. R. Force-induced activation of covalent bonds in mechanoresponsive polymeric materials. *Nature* 2009, 459, 68-72.

(38) Zuo, B.; Wang, M.; Lin, B.-P.; Yang, H. Photomodulated Tricolour-Changing Artificial Flowers. *Chem. Mater.* 2018, 30, 8079-8088.

(39) Dou, Q.; Liow, S. S.; Weng, W.; Loh, X. J. Dual-responsive reversible photo/thermogelling polymers exhibiting high modulus change. *J. Polym. Sci., Part A: Polym. Chem.* 2016, 54, 2837-2844.

(40) Shiraishi, Y.; Miyamoto, R.; Hirai, T. Spiropyran-conjugated thermoresponsive copolymer as a colourimetric thermometer with linear and reversible colour change. *Org. Lett.* 2009, 11, 1571-1574.

(41) Lee, H. I.; Wu, W.; Oh, J. K.; Mueller, L.; Sherwood, G.; Peteanu, L.; Kowalewski, T.; Matyjaszewski, K. Light-induced reversible formation of polymeric micelles. *Angew. Chem. Int. Ed.* 2007, 46, 2453-7.

(42) Liu, C.; Yang, D.; Jin, Q.; Zhang, L.; Liu, M. A Chiroptical Logic Circuit Based on Self-Assembled Soft Materials Containing Amphiphilic Spiropyran. *Adv. Mater.* 2016, 28, 1644-9.

(43) Feng, K.; Xie, N.; Chen, B.; Zhang, L.-P.; Tung, C.-H.; Wu, L.-Z. Reversible Light-Triggered Transition of Amphiphilic Random Copolymers. *Macromolecules* 2012, 45, 5596-5603.

(44) Son, S.; Shin, E.; Kim, B. S. Light-responsive micelles of spiropyran initiated hyperbranched polyglycerol for smart drug delivery. *Biomacromolecules* 2014, 15, 628-634.

(45) He, D.; Arisaka, Y.; Masuda, K.; Yamamoto, M.; Takeda, N. A photoresponsive soft interface reversibly controls wettability and cell adhesion by conformational changes in a spiropyran-conjugated amphiphilic block copolymer. *Acta Biomater.* 2017, 51, 101-111.

(46) Cao, Z.; Bian, Q.; Chen, Y.; Liang, F.; Wang, G. Light-Responsive Janus-Particle-Based Coatings for Cell Capture and Release. *ACS Macro Lett.* 2017, 6, 1124-1128.

(47) ter Schiphorst, J.; Coleman, S.; Stumpel, J. E.; Ben Azouz, A.; Diamond, D.; Schenning, A. P. H. J. Molecular Design of Light-Responsive Hydrogels, For in Situ Generation of Fast and Reversible Valves for Microfluidic Applications. *Chem. Mater.* 2015, 27, 5925-5931.

(48) Delaney, C.; McCluskey, P.; Coleman, S.; Whyte, J.; Kent, N.; Diamond, D. Precision control of flow rate in microfluidic channels using photoresponsive soft polymer actuators. *Lab Chip* 2017, 17, 2013-2021.

(49) Wojtyk, J. T.; Kazmaier, P. M.; Buncel, E. Modulation of the spiropyran− merocyanine reversion via metal-ion selective complexation: trapping of the “transient” cis-merocyanine. *Chem. Mater.* 2001, 13, 2547-2551.

(50) Wu, P. J.; Chen, J. L.; Chen, C. P.; Chan, Y. H. Photoactivated ratiometric copper(II) ion sensing with semiconducting polymer dots. *Chem. Commun.* 2013, 49, 898-900.

(51) Niazov, T.; Shlyahovsky, B.; Willner, I. Photoswitchable electrocatalysis and catalyzed chemiluminescence using photoisomerizable monolayer-functionalized surfaces and Pt nanoparticles. *J. Am. Chem. Soc.* 2007, 129, 6374-6375.

(52) Bronner, C.; Schulze, G.; Franke, K. J.; Pascual, J. I.; Tegeder, P. Switching ability of nitro-spiropyran on Au(111): electronic structure changes as a sensitive probe during a ring-opening reaction. *J. Phys. Condens. Matter.* 2011, 23, 484005.

(53) Sunamoto, J.; Iwamoto, K.; Akutagawa, M.; Nagase, M.; Kondo, H. Rate control by restricting mobility of substrate in specific reaction field. Negative photochromism of water-soluble spiropyran in AOT reversed micelles. *J. Am. Chem. Soc.* 1982, 104, 4904-4907.

(54) Ciardelli, F.; Fabbri, D.; Pieroni, O.; Fissi, A. Photomodulation of polypeptide conformation by sunlight in spiropyran-containing poly(L-glutamic acid). *J. Am. Chem. Soc.* 1989, 111, 3470-3472.

(55) Zhou, J.; Li, Y.; Tang, Y.; Zhao, F.; Song, X.; Li, E. Detailed investigation on a negative photochromic spiropyran. *J. Photochem. Photobiol. A* 1995, 90, 117-123.

(56) Tian, W.; Tian, J. An insight into the solvent effect on photo-, solvato-chromism of spiropyran through the perspective of intermolecular interactions. *Dyes Pigm.* 2014, 105, 66-74.

(57) Kinashi, K.; Nakamura, S.; Imamura, M.; Ishida, K.; Ueda, Y. The mechanism for negative photochromism of spiropyran in silica. *J. Phys. Org. Chem.* 2012, 25, 462-466.

(58) Guo, Z.; Zhu, W.; Xiong, Y.; Tian, H. Multiple Logic Fluorescent Thermometer System Based onN-Isopropylmethacrylamide Copolymer Bearing Dicyanomethylene-4H-pyran Moiety. *Macromolecules* 2009, 42, 1448-1453.

(59) Zhang, Q. M.; Wang, W.; Su, Y.-Q.; Hensen, E. J. M.; Serpe, M. J. Biological Imaging and Sensing with Multiresponsive Microgels. *Chem. Mater.* 2015, 28, 259-265.

(60) ter Schiphorst, J.; van den Broek, M.; de Koning, T.; Murphy, J. N.; Schenning, A. P. H. J.; Esteves, A. C. C. Dual light and temperature responsive cotton fabric functionalized with a surface-grafted spiropyran–NIPAAm-hydrogel. *J. Mater. Chem. A* 2016, 4, 8676-8681.

(61) Hemmer, J. R.; Smith, P. D.; van Horn, M.; Alnemrat, S.; Mason, B. P.; de Alaniz, J. R.; Osswald, S.; Hooper, J. P. High strain-rate response of spiropyran mechanophores in PMMA. *J. Polym. Sci., Part B: Polym. Phys.* 2014, 52, 1347-1356.

(62) Kim, J. W.; Jung, Y.; Coates, G. W.; Silberstein, M. N. Mechanoactivation of Spiropyran Covalently Linked PMMA: Effect of Temperature, Strain Rate, and Deformation Mode. *Macromolecules* 2015, 48, 1335-1342.

(63) O'Bryan, G.; Wong, B. M.; McElhanon, J. R. Stress sensing in polycaprolactone films via an embedded photochromic compound. *ACS Appl. Mater. Interfaces* 2010, 2, 1594-1600.

(64) Gossweiler, G. R.; Hewage, G. B.; Soriano, G.; Wang, Q.; Welshofer, G. W.; Zhao, X.; Craig, S. L. Mechanochemical Activation of Covalent Bonds in Polymers with Full and Repeatable Macroscopic Shape Recovery. *ACS Macro Lett.* 2014, 3, 216-219.

(65) Jiang, S.; Zhang, L.; Xie, T.; Lin, Y.; Zhang, H.; Xu, Y.; Weng, W.; Dai, L. Mechanoresponsive PS-PnBA-PS Triblock Copolymers via Covalently Embedding Mechanophore. *ACS Macro Lett.* 2013, 2, 705-709.

(66) Jia, Y.; Wang, W.-J.; Li, B.-G.; Zhu, S. Design and Synthesis of Mechano-Responsive Colour-Changing Thermoplastic Elastomer Based on Poly(n-Butyl Acrylate)-Spiropyran-Polystyrene Comb-Structured Graft Copolymers. *Macromol. Mater. Eng.* 2018, 303, 1800154.

(67) Barbee, M. H.; Kouznetsova, T.; Barrett, S. L.; Gossweiler, G. R.; Lin, Y.; Rastogi, S. K.; Brittain, W. J.; Craig, S. L. Substituent Effects and Mechanism in a Mechanochemical Reaction. *J. Am. Chem. Soc.* 2018, 140, 12746-12750.

(68) Barbee, M. H.; Mondal, K.; Deng, J. Z.; Bharambe, V.; Neumann, T. V.; Adams, J. J.; Boechler, N.; Dickey, M. D.; Craig, S. L. Mechanochromic Stretchable Electronics. *ACS Appl. Mater. Interfaces* 2018, 10, 29918-29924.

(69) Sommer, M.; Komber, H. Spiropyran main-chain conjugated polymers. *Macromol. Rapid Commun.* 2013, 34, 57-62.

(70) Ng, M.-K.; Yang, J. Synthesis of a Photochromic Conjugated Polymer Incorporating Spirobenzopyran- in the Backbone. *Synthesis* 2006, 2006, 3075-3079.

(71) Li, M.; Zhang, Q.; Zhu, S. Photo-inactive divinyl spiropyran mechanophore cross-linker for real-time stress sensing. *Polymer* 2016, 99, 521-528.

(72) Komber, H.; Müllers, S.; Lombeck, F.; Held, A.; Walter, M.; Sommer, M. Soluble and stable alternating main-chain merocyanine copolymers through quantitative spiropyran–merocyanine conversion. *Polym. Chem.* 2014, 5, 443-453.

(73) Metzler, L.; Reichenbach, T.; Brügner, O.; Komber, H.; Lombeck, F.; Müllers, S.; Hanselmann, R.; Hillebrecht, H.; Walter, M.; Sommer, M. High molecular weight mechanochromic spiropyran main chain copolymers via reproducible microwave-assisted Suzuki polycondensation. *Polym. Chem.* 2015, 6, 3694-3707.

(74) Kempe, F.; Brugner, O.; Buchheit, H.; Momm, S. N.; Riehle, F.; Hameury, S.; Walter, M.; Sommer, M. A Simply Synthesized, Tough Polyarylene with Transient Mechanochromic Response. *Angew. Chem. Int. Ed.* 2018, 57, 997-1000.

(75) Raisch, M.; Genovese, D.; Zaccheroni, N.; Schmidt, S. B.; Focarete, M. L.; Sommer, M.; Gualandi, C. Highly Sensitive, Anisotropic, and Reversible Stress/Strain-Sensors from Mechanochromic Nanofiber Composites. *Adv. Mater.* 2018, 30, 1802813.

(76) Malatesta, V.; Millini, R.; Montanari, L. Key intermediate product of oxidative degradation of photochromic spirooxazines. X-ray crystal structure and electron spin resonance analysis of its 7, 7, 8, 8-tetracyanoquinodimethane ion-radical salt. *J. Am. Chem. Soc.* 1995, 117, 6258-6264.

(77) Malatesta, V.; Renzi, F.; Wis, M. L.; Montanari, L.; Milosa, M.; Scotti, D. Reductive degradation of photochromic spiro-oxazines. Reaction of the merocyanine forms with free radicals. *J. Org. Chem.* 1995, 60, 5446-5448.

(78) Berry, J. F. *Facile Isolation of Functionalized Spiropyran Mechanophores without Recrystallization*; SURVICE Engineering Belcamp: 2018.

(79) Kingsbury, C. M.; May, P. A.; Davis, D. A.; White, S. R.; Moore, J. S.; Sottos, N. R. Shear activation of mechanophore-crosslinked polymers. *J. Mater. Chem.* 2011, 21, 8381.

(80) Degen, C. M.; May, P. A.; Moore, J. S.; White, S. R.; Sottos, N. R. Time-Dependent Mechanochemical Response of SP-Cross-Linked PMMA. *Macromolecules* 2013, 46, 8917-8921.

(81) Celestine, A.-D. N.; Beiermann, B. A.; May, P. A.; Moore, J. S.; Sottos, N. R.; White, S. R. Fracture-induced activation in mechanophore-linked, rubber toughened PMMA. *Polymer* 2014, 55, 4164-4171.

(82) Chen, H.; Yang, F.; Chen, Q.; Zheng, J. A Novel Design of Multi-Mechanoresponsive and Mechanically Strong Hydrogels. *Adv. Mater.* 2017, 29, 1606900.

(83) Li, M.; Liu, W.; Zhu, S. Smart polyolefins feeling the force: Colour changeable poly(ethylene-vinyl acetate) and poly(ethylene-octene) in response to mechanical force. *Polymer* 2017, 112, 219-227.

(84) Beiermann, B. A.; Davis, D. A.; Kramer, S. L. B.; Moore, J. S.; Sottos, N. R.; White, S. R. Environmental effects on mechanochemical activation of spiropyran in linear PMMA. *J. Mater. Chem.* 2011, 21, 8443.

(85) Beiermann, B. A.; Kramer, S. L. B.; Moore, J. S.; White, S. R.; Sottos, N. R. Role of Mechanophore Orientation in Mechanochemical Reactions. *ACS Macro Lett.* 2012, 1, 163-166.

(86) May, P. A.; Munaretto, N. F.; Hamoy, M. B.; Robb, M. J.; Moore, J. S. Is Molecular Weight or Degree of Polymerization a Better Descriptor of Ultrasound-Induced Mechanochemical Transduction? *ACS Macro Lett.* 2016, 5, 177-180.

(87) Beiermann, B. A.; Kramer, S. L. B.; May, P. A.; Moore, J. S.; White, S. R.; Sottos, N. R. The Effect of Polymer Chain Alignment and Relaxation on Force-Induced Chemical Reactions in an Elastomer. *Adv. Funct. Mater.* 2014, 24, 1529-1537.

(88) Grady, M. E.; Beiermann, B. A.; Moore, J. S.; Sottos, N. R. Shockwave loading of mechanochemically active polymer coatings. *ACS Appl. Mater. Interfaces* 2014, 6, 5350-5355.

(89) Wang, L.-J.; Zhou, X.-J.; Zhang, X.-H.; Du, B.-Y. Enhanced Mechanophore Activation within Micelles. *Macromolecules* 2015, 49, 98-104.

(90) Peterson, G. I.; Larsen, M. B.; Ganter, M. A.; Storti, D. W.; Boydston, A. J. 3D-printed mechanochromic materials. *ACS Appl. Mater. Interfaces* 2015, 7, 577-83.

(91) Gossweiler, G. R.; Kouznetsova, T. B.; Craig, S. L. Force-rate characterization of two spiropyran-based molecular force probes. *J. Am. Chem. Soc.* 2015, 137, 6148-6151.

(92) Lee, C. K.; Davis, D. A.; White, S. R.; Moore, J. S.; Sottos, N. R.; Braun, P. V. Force-induced redistribution of a chemical equilibrium. *J. Am. Chem. Soc.* 2010, 132, 16107-16111.

(93) Kim, T. A.; Beiermann, B. A.; White, S. R.; Sottos, N. R. Effect of Mechanical Stress on Spiropyran-Merocyanine Reaction Kinetics in a Thermoplastic Polymer. *ACS Macro Lett.* 2016, 5, 1312-1316.

(94) Lee, C. K.; Beiermann, B. A.; Silberstein, M. N.; Wang, J.; Moore, J. S.; Sottos, N. R.; Braun, P. V. Exploiting Force Sensitive Spiropyrans as Molecular Level Probes. *Macromolecules* 2013, 46, 3746-3752.

(95) Chen, Y.; Zhang, H.; Fang, X.; Lin, Y.; Xu, Y.; Weng, W. Mechanical Activation of Mechanophore Enhanced by Strong Hydrogen Bonding Interactions. *ACS Macro Lett.* 2014, 3, 141-145.

(96) Fang, X.; Zhang, H.; Chen, Y.; Lin, Y.; Xu, Y.; Weng, W. Biomimetic Modular Polymer with Tough and Stress Sensing Properties. *Macromolecules* 2013, 46, 6566-6574.

(97) Zhang, H.; Chen, Y.; Lin, Y.; Fang, X.; Xu, Y.; Ruan, Y.; Weng, W. Spiropyran as a Mechanochromic Probe in Dual Cross-Linked Elastomers. *Macromolecules* 2014, 47, 6783-6790.

(98) Hong, G.; Zhang, H.; Lin, Y.; Chen, Y.; Xu, Y.; Weng, W.; Xia, H. Mechanoresponsive Healable Metallosupramolecular Polymers. *Macromolecules* 2013, 46, 8649-8656.

(99) Zhang, Q.; Wang, Y.; Xing, C.; Cai, Y.; Xi, K.; Jia, X. Light and force dual-responsive waterborne polyurethane in multiple states. *RSC Adv.* 2017, 7, 12682-12689.

(100) Xing, C.; Wang, L.; Xian, L.; Wang, Y.; Zhang, L.; Xi, K.; Zhang, Q.; Jia, X. Enhanced Thermal Ageing Stability of Mechanophore in Polyurethane Network by Introducing Polyhedral Oligomeric Silsesquioxanes (POSS). *Macromol. Chem. Phys.* 2018, 219, 1800042.

(101) Wang, Q.; Gossweiler, G. R.; Craig, S. L.; Zhao, X. Cephalopod-inspired design of electro-mechano-chemically responsive elastomers for on-demand fluorescent patterning. *Nat. Commun.* 2014, 5, 4899.

(102) Gossweiler, G. R.; Brown, C. L.; Hewage, G. B.; Sapiro-Gheiler, E.; Trautman, W. J.; Welshofer, G. W.; Craig, S. L. Mechanochemically Active Soft Robots. *ACS Appl. Mater. Interfaces* 2015, 7, 22431-22435.

(103) Lin, Y.; Barbee, M. H.; Chang, C. C.; Craig, S. L. Regiochemical Effects on Mechanophore Activation in Bulk Materials. *J. Am. Chem. Soc.* 2018, 140, 15969-15975.

(104) Qiu, W.; Gurr, P. A.; da Silva, G.; Qiao, G. G. Insights into the mechanochromism of spiropyran elastomers. *Polym. Chem.* 2019, 10, 1650-1659.

(105) Van De Manakker, F.; Vermonden, T.; Van Nostrum, C. F.; Hennink, W. E. Cyclodextrin-based polymeric materials: synthesis, properties, and pharmaceutical/biomedical applications. *Biomacromolecules* 2009, 10, 3157-3175.

(106) Tan, S.; Ladewig, K.; Fu, Q.; Blencowe, A.; Qiao, G. G. Cyclodextrin-based supramolecular assemblies and hydrogels: recent advances and future perspectives. *Macromol. Rapid Commun.* 2014, 35, 1166-1184.

(107) Wan, S.; Ma, Z.; Chen, C.; Li, F.; Wang, F.; Jia, X.; Yang, W.; Yin, M. A Supramolecule-Triggered Mechanochromic Switch of Cyclodextrin-Jacketed Rhodamine and Spiropyran Derivatives. *Adv. Funct. Mater.* 2016, 26, 353-364.

(108) Shree, S.; Schulz-Senft, M.; Alsleben, N. H.; Mishra, Y. K.; Staubitz, A.; Adelung, R. Light, Force, and Heat: A Multi-Stimuli Composite that Reveals its Violent Past. *ACS Appl. Mater. Interfaces* 2017, 9, 38000-38007.

(109) Kim, G.; Lau, V. M.; Halmes, A. J.; Oelze, M. L.; Moore, J. S.; Li, K. C. High-intensity focused ultrasound-induced mechanochemical transduction in synthetic elastomers. *Proc. Natl. Acad. Sci. U. S. A* 2019, 116, 10214-10222.

(110) Lee, C. K.; Diesendruck, C. E.; Lu, E.; Pickett, A. N.; May, P. A.; Moore, J. S.; Braun, P. V. Solvent Swelling Activation of a Mechanophore in a Polymer Network. *Macromolecules* 2014, 47, 2690-2694.

(111) Li, M.; Lei, L.; Zhang, Q.; Zhu, S. CO2 -Breathing Induced Reversible Activation of Mechanophore within Microgels. *Macromol. Rapid Commun.* 2016, 37, 957-62.

(112) Kim, T. A.; Robb, M. J.; Moore, J. S.; White, S. R.; Sottos, N. R. Mechanical Reactivity of Two Different Spiropyran Mechanophores in Polydimethylsiloxane. *Macromolecules* 2018, 51, 9177-9183.

(113) Cho, S.; Kang, S.; Pandya, A.; Shanker, R.; Khan, Z.; Lee, Y.; Park, J.; Craig, S. L.; Ko, H. Large-Area Cross-Aligned Silver Nanowire Electrodes for Flexible, Transparent, and Force-Sensitive Mechanochromic Touch Screens. *ACS Nano* 2017, 11, 4346-4357.

(114) Park, J.; Lee, Y.; Barbee, M. H.; Cho, S.; Cho, S.; Shanker, R.; Kim, J.; Myoung, J.; Kim, M. P.; Baig, C.; Craig, S. L.; Ko, H. A Hierarchical Nanoparticle-in-Micropore Architecture for Enhanced Mechanosensitivity and Stretchability in Mechanochromic Electronic Skins. *Adv. Mater.* 2019, 31, 1808148.

(115) Sheng, Y.; Leszczynski, J.; Garcia, A. A.; Rosario, R.; Gust, D.; Springer, J. Comprehensive theoretical study of the conversion reactions of spiropyrans: substituent and solvent effects. *J. Phys. Chem. B* 2004, 108, 16233-16243.

(116) Zhang, Y.; Ren, B.; Yang, F.; Cai, Y.; Chen, H.; Wang, T.; Feng, Z.; Tang, J.; Xu, J.; Zheng, J. Micellar-incorporated hydrogels with highly tough, mechanoresponsive, and self-recovery properties for strain-induced colour sensors. *J. Mater. Chem. C* 2018, 6, 11536-11551.

(117) Li, G.; Wang, L.; Ni, H.; Pittman, C. U. Polyhedral oligomeric silsesquioxane (POSS) polymers and copolymers: a review. *J. Inorg. Organomet. Polym.* 2001, 11, 123-154.

(118) Phillips, S. H.; Haddad, T. S.; Tomczak, S. J. Developments in nanoscience: polyhedral oligomeric silsesquioxane (POSS)-polymers. *Curr. Opin. Solid State Mater. Sci.* 2004, 8, 21-29.

(119) Janowski, B.; Pielichowski, K. Thermo(oxidative) stability of novel polyurethane/POSS nanohybrid elastomers. *Thermochim. Acta* 2008, 478, 51-53.

(120) Lee, Y.; Park, J.; Choe, A.; Cho, S.; Kim, J.; Ko, H. Mimicking Human and Biological Skins for Multifunctional Skin Electronics. *Adv. Funct. Mater.* 2019, 1904523.

(121) Xia, Z.; Alphonse, V. D.; Trigg, D. B.; Harrigan, T. P.; Paulson, J. M.; Luong, Q. T.; Lloyd, E. P.; Barbee, M. H.; Craig, S. L. 'Seeing' Strain in Soft Materials. *Molecules* 2019, 24, 542.

(122) Jiu, J.; Suganuma, K. Metallic Nanowires and Their Application. *IEEE Trans. Compon., Packag., Manuf. Technol.* 2016, 6, 1733-1751.

(123) Sofiah, A. G. N.; Samykano, M.; Kadirgama, K.; Mohan, R. V.; Lah, N. A. C. Metallic nanowires: Mechanical properties – Theory and experiment. *Appl. Mater. Today* 2018, 11, 320-337.

(124) Espalin, D.; Muse, D. W.; MacDonald, E.; Wicker, R. B. 3D Printing multifunctionality: structures with electronics. *Int. J. Adv. Manuf. Technol.* 2014, 72, 963-978.

(125) Muth, J. T.; Vogt, D. M.; Truby, R. L.; Menguc, Y.; Kolesky, D. B.; Wood, R. J.; Lewis, J. A. Embedded 3D printing of strain sensors within highly stretchable elastomers. *Adv. Mater.* 2014, 26, 6307-6312.

(126) Schubert, C.; van Langeveld, M. C.; Donoso, L. A. Innovations in 3D printing: a 3D overview from optics to organs. *Br. J. Ophthalmol.* 2014, 98, 159-161.

(127) Nadgorny, M.; Ameli, A. Functional Polymers and Nanocomposites for 3D Printing of Smart Structures and Devices. *ACS Appl. Mater. Interfaces* 2018, 10, 17489-17507.

(128) Shafranek, R. T.; Millik, S. C.; Smith, P. T.; Lee, C.-U.; Boydston, A. J.; Nelson, A. Stimuli-responsive materials in additive manufacturing. *Prog. Polym. Sci.* 2019, 93, 36-67.

(129) Rohde, R. C.; Basu, A.; Okello, L. B.; Barbee, M. H.; Zhang, Y.; Velev, O. D.; Nelson, A.; Craig, S. L. Mechanochromic composite elastomers for additive manufacturing and low strain mechanophore activation. *Polym. Chem.* 2019, 10, 5985-5991.

(130) Roh, S.; Parekh, D. P.; Bharti, B.; Stoyanov, S. D.; Velev, O. D. 3D Printing by Multiphase Silicone/Water Capillary Inks. *Adv. Mater.* 2017, 29, 1701554.

(131) Guo, T.; Chen, X.; Song, M.; Zhang, B. Preparation and properties of core [poly(styrene-n-butyl acrylate)]–shell [poly(styrene–methyl methacrylate–vinyl triethoxide silane)] structured latex particles with self-crosslinking characteristics. *J. Appl. Polym.* 2006, 100, 1824-1830.

(132) Ramos-Fernández, J. M.; Beleña, I.; Romero-Sánchez, M. D.; Fuensanta, M.; Guillem, C.; López-Buendía, Á. M. Study of the film formation and mechanical properties of the latexes obtained by miniemulsion co-polymerization of butyl acrylate, methyl acrylate and 3-methacryloxypropyltrimethoxysilane. *Prog. Org. Coat.* 2012, 75, 86-91.

(133) Li, M.; Liu, W.; Zhang, Q.; Zhu, S. Mechanical Force Sensitive Acrylic Latex Coating. *ACS Appl. Mater. Interfaces* 2017, 9, 15156-15163.

Chapter 2: Insights into the Mechanochromism of Spiropyran Elastomers

2.1 Chapter Perspectives

Despite the intensive studies of SP-based mechanochromic materials, the effect of attachment positions of SP linked to polymers on their mechanochromic properties has remained unclear. In order to improve and manipulate the mechano-responsive efficiency and mechanochromic sensitivity of SP-linked polymers, it is essential to understand how the consequent electronic effect and geometric effect influence the mechanochromic properties when varying the attachment points to the matrix. In this chapter, a new trifunctional SP combining the attachment positions of the two most common difunctional SPs is designed to investigate the effect of attachment position on SP. The three SPs are crosslinked into the same non-polar PDMS matrix, which are subjected to compression and tension to investigate their mechanochromic properties. The three samples show different colour intensities under a given deformation while the onsets of mechano-activation strain are similar. The results indicate that both the electronic and geometric effect influence the mechanochromism, with the latter one playing a more dominant role. Density functional theory (DFT) calculations is also conducted to explain the mechanism of difference varying the attachment points.

2.2 Introduction

Due to the fast mechanical-force responsive transition, from colourless spiropyran to purple merocyanine, covalently linked SP-polymers have been identified as promising candidates for practical reversible colour changing applications. Since the inception of mechanochromic SP-containing polymeric materials, synthetic polymer systems have not diverged significantly. To date, SPs have been covalently incorporated into various polymer networks, such as poly methyl (meth)acrylates, polyurethane, polystyrene, PDMS, poly(ε-caprolactone), poly(ethylene-vinyl acetate), hydrogels and polyarylene.[1-10] The majority of the optical characterizations have been based on tension loading or compression.[11, 12] Kim *et al.* systematically compared the effect of tension and compression on the activation of SP-containing cross-linked PMMA at various temperatures, and found the stress required to activate SP under compression is higher than under tension.[13]

Factors which influence the mechanochromic properties of spiropyran-based materials include the polymeric architecture, the mechanical properties of the matrix and the structure of the spiropyran itself.[13-20] There are several easily functionalized attachment points on the spiropyran rings, where polymers can be covalently attached. The attachment positions can affect the ability of the applied force transmitting to the SP molecule leading to the spiro C-O bond cleavage.[18, 19] The spiropyran molecules comprise of an indoline ring and a chromene ring (**Figure 2.1**), and only when both rings are connected to polymer chains can the external force be transferred to the C-O bond causing it to cleave.[1] Two widely used 6-nitro-SP mechanophores (**Figure 2.1**) with different attachment positions at R_1 and R_3 (SP1), and R_2 and R_3 (SP2) have been prepared and incorporated into various polymer matrices.[12] Single molecule force spectroscopy was utilized to calculate the contour lengths upon ring opening, compared with computational predictions, and concluded that the activation forces for SP1 and SP2 are different.[18] Recently, single molecule force spectroscopy was also used to study the substituent effect and showed strong electron withdrawing groups on the chromene ring helped stabilize the negative charge on the MC resulting in a lower activation energy.[17] Gozzweiler *et al.* reported SP2-PDMS films showed a blue colour under tension and purple upon relaxation, which they hypothesized was a result of MC isomerization.[5] Craig's group designed three SP derivatives without 6-nitro, while varying the

attachment points on the chromene ring at 8-, 7- and 6-positions, to study the regiochemical effects on the mechanochromism.[19]

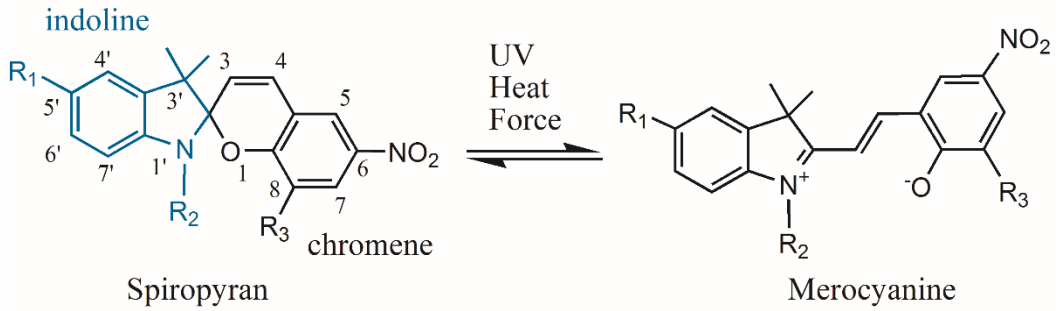

Figure 2.1. Spiropyrans with varying attachment points, for **SP1**: R_1 and R_3; **SP2**: R_2 and R_3; **SP3**: R_1, R_2 and R_3 (this paper). Force, heat and UV light can be the external stimuli to activate the ring-closed SP to ring-open MC.

Varying the attachment positions would cause geometry effect (the isomerization affected by the attachment points' location) and electronic effect (the isomerization affected by the electron donating or withdrawing capacity) differences. It is important to know the dominant effect which influences mechanochromism, in order to guide the design of force-responsive materials. In this study, two previously reported mechanochromic spiropyrans SP1 and SP2, as well as a new SP3 (**Figure 2.1**), which combines the attachment positions of both SP1 and SP2 were prepared. These were tested under compression and tension to investigate whether the geometric effect or electronic effect, caused by varying attachment positions, dominates the mechanochromic responses.

2.3 Experimental Methods

2.3.1 Materials

Dichloromethane (AR, Chem-Supply), diethyl ether (anhydrous, Chem-Supply), 4-dimethylaminopyridine (≥98%, Sigma), ethanol (100%, Chem-Supply), glacial acetic acid (AR, Chem-Supply), hexane (99%, RCI Labscan), hydrobromic acid (48%, AR, Chem-Supply), 2-iodoethanol (99%, Sigma), (4-methoxy)-phenyl hydrazine hydrochloride (99%, ThermoFisher), methanol (AR, Chem-Supply), methyl iodide (99%, Sigma), methyl isopropyl ketone (99%, Sigma), Phenylhydrazine hydrochloride (≥ 99%, Merck),

piperidine (≥99.5%, Sigma), toluene (AR, Chem-Supply), triethylamine (≥99%, Sigma), 4-pentenoic anhydride (98%, Sigma), and o-vanillin (99%, Sigma) were used as received, unless otherwise stated. Tetrahydrofuran (THF, Chem-Supply) was pre-dried over sodium, before being distilled from benzophenone and sodium under an inert atmosphere of nitrogen prior to use. Sylgard® 184 (PDMS) was purchased from Gelest Inc. as a two part system A and B and mixed prior to curing.

2.3.2 Synthesis of Vinyl Functionalized SPs

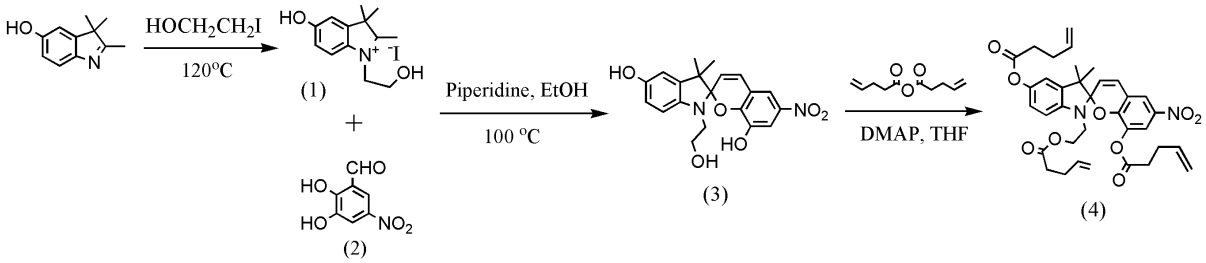

Scheme 2.1. Synthetic route of tri-vinyl SP3.

The di-vinyl spiropyrans SP1 and SP2 were synthesized according to literature procedures.[1, 5] The tri-vinyl spiropyran SP3 was synthesized based on the synthetic strategy of SP1 and SP2.

Tri-vinyl SP: *3',3'-dimethyl-6-nitro-1'-(2-(pent-4-enoyloxy)ethyl)spiro[chromene-2,2'-indoline]-5',8-diyl bis(pent-4-enoate) (SP3)*

Indolium iodide 1 (0.5 g, 1.44 mmol, 1 equiv), 2-hydroxy-3-methoxy-5-nitro-benzaldehyde 2 (0.265 mg, 1.44 mmol, 1 equiv), and piperidine (0.285 mL, 2.88 mmol, 2 equiv) were dissolved in absolute EtOH (15 mL) and heated to reflux. After 2.5 hr, the solution was cooled, filtered and the precipitate rinsed with cold EtOH, to afford tri-functional spiropyran 3 as a black powder. To compound 3 (0.20 g, 0.52 mmol, 1.0 equiv) and 4-dimethylaminopyridine (DMAP) (0.15 g, 1.23 mmol, 2.4 equiv) in THF (10 mL) was added 4-pentenoic anhydride (0.34 mL, 1.88 mmol, 3.6 equiv). After stirring for 7 hr, the crude reaction mixture was passed through a basic alumina column and diluted with DCM (100 mL). The solution was extracted with distilled water (2 × 100 mL), dried over MgSO4, filtered and reduced to dryness in vacuo to afford SP3 as a yellow solid (0.19 g, 0.30 mmol, 58% yield).

All SPs were kept at -20 °C in the absence of light prior to use.

2.3.3 Cylindrical and Film Sample Preparation

The main components of commercial Sylgard™184 in a two-component system A and B, are vinyl terminated polysiloxane, poly (methyl hydrosiloxane-*co*-dimethylsiloxane) copolymer and platinum catalyst. The hydrosilane component reacts with vinyl moieties via hydrosilylation in the presence of platinum catalyst to form covalently linked elastomer networks. Co-reaction of vinyl terminated spiropyrans SP1-3 with Sylgard 184 allows spiropyran mechanophores to be covalently attached into the polymer network.[5, 21]

Two concentrations of SPs in silicone networks were prepared based on varying mole/weight ratios (SP /Sylgard™ base = μmol/g): c1 = 5.0 μmol/g, c2 = 9.4 μmol/g and c3 = 14.1 μmol/g). Vinyl terminated SPs were dissolved in toluene (10 *vol/w*% of Sylgard A), followed by the addition of Sylgard components A and then curing agent B (6:1 ratio respectively). The ratio of base/curing agent was adjusted to 1:6 to reduce viscosity and improve the properties of the cured silicone samples.[22] The mixture was stirred using a glass rod and vortex until homogeneous prior to (i) casting onto a dog-bone shaped Teflon mould or transferring to 3mL polypropylene syringes to prepare (ii) thin films (thickness: 0.4-0.5 mm, width: 0.4 mm, gauge length: 10 mm, other than specifically noted) and (iii) cylindrical elastomers (diameter: 8.5 mm), respectively. All specimens were cured in a vacuum oven at 65°C overnight. The cured cylindrical samples were cut into 8-9 mm height samples for compression testing.

2.3.4 Characterization

Nuclear Magnetic Resonance (NMR) Spectroscopy. 1H NMR spectroscopy was conducted on a Varian Unity 400 MHz spectrometer operating at 400 MHz, using the deuterated solvent as reference and a sample concentration of ~10 mg mL−1.

Mass Spectrometry (MS). Liquid chromatography mass spectrometry (LC-MS) was performed on a high-resolution Agilent 6520 Q-TOF. ESI (Electrospray Ionisation) solutions (~5 ppm) were prepared with HPLC grade acetonitrile and transferred to the electrospray source by an autosampler. For each analysis, 1 μL of sample was injected

into the carrier solvent stream of 70 % acetonitrile in 0.1 % formic acid at a flow rate of 0.3 mL/minute. Recorded m/z data were corrected using a reference mass by a dual-spray electrospray ionisation source and using the factory-defined calibration procedure. Mass spectrometer conditions: drying gas flow rate, 7 L/min; nebulizer pressure, 40 psi; drying gas temperature, 300°C; capillary voltage, 4000 V; skimmer voltage, 65 V; Oct Rf, 750 V; scan range acquired, 100–1000 m/z.

Mechanical Testing and RGB analysis. Compression and tensile tests were performed uniaxially at room temperature on an Instron 5848 Microtester with Bluehill material testing software with a 2kN loading cell. Tensile measurements were performed on dog-bone shaped samples fastened between two grips and tested in triplicate at a strain rate of 1% s^{-1}. Compression testing of cylindrical specimens were performed in triplicate at a strain rate of 1% s^{-1}. Compression test was ended at 70% strain and tensile test was ended at 200% strain. Video recording was performed during testing for colour analysis. RGB values were determined after white balance calibration in Adobe Photoshop™ software. The colour channel ratios were determined as colour channel ratios (Green/Red; Blue/Red and Green/Blue).

UV–visible Spectroscopy (UV-Vis). UV–Vis analysis was performed on a Shimadzu UV–Vis Scanning Spectrophotometer (UV-2101 PC) with a scanning rate of 0.2 nm. Scanning range of wavelength was 750-380 nm.

Absorption Analysis under Load. Test samples were held under various deformation and long loading time, using a purpose-built clamp, which could be adjusted to various compression pressures and was able to be placed in the UV-Vis spectrometer. Standard placement of the mechanochromic and reference sample (PDMS) in line with the beam resulted in the routine analysis of mechanochromic samples under loading. Absorption intensities (Abs) were normalized using equation (2.1):

$$Abs = (I_\varepsilon - I_{\varepsilon=0})/\sqrt{1/(1-\varepsilon)} \quad (2.1)$$

where I_ε is the absorbance value at a given compressive strain ε and $I_{\varepsilon=0}$ is the absorbance value at zero strain. Compressive strain was calculated by $\varepsilon = (l_0 - l)/l_0 \times 100\%$, where l_0 and l are the sample length before and after compression respectively. The factor $\sqrt{1/(1-\varepsilon)}$, normalizes the absorbance caused by diameter change under compression. Since this study focused on comparative compressive response of different SPs but not

kinetics, and the path of the beam passing through the specimens were the same even under the same strain (the diameter of all the specimen were the same), so a ratio of $\sqrt{1/(1-\varepsilon)}$ without exact diameter value was involved here.

2.4 Results and Discussion

In order to study the influence of electronic and geometric effects caused by varying attachment positions on spiropyran, SP3 was prepared which combined all the attachment points present on SP1 and SP2. The series of di- and tri-vinyl functionalized spiropyrans with variable attachment positions (SP1-3) were prepared (**Figure 2.2**). Di-substituted SP1 and SP2 were prepared as previously reported[1, 5] and the new tri-substituted SP3 was prepared in a similar method (**Scheme 2.1**). Thus, condensation of 2-hydroxyethyl-2,3,3-trimethyl-3H-5-hydroxy-indolium iodide (1) with 2,3-dihydroxy-5-nitro-benzaldehyde (2) produced hydroxyl terminated spiropyran (3). Upon isolation, the spiropyran 3 was esterified with 4-pentenoic anhydride to produce vinyl terminated SP3.

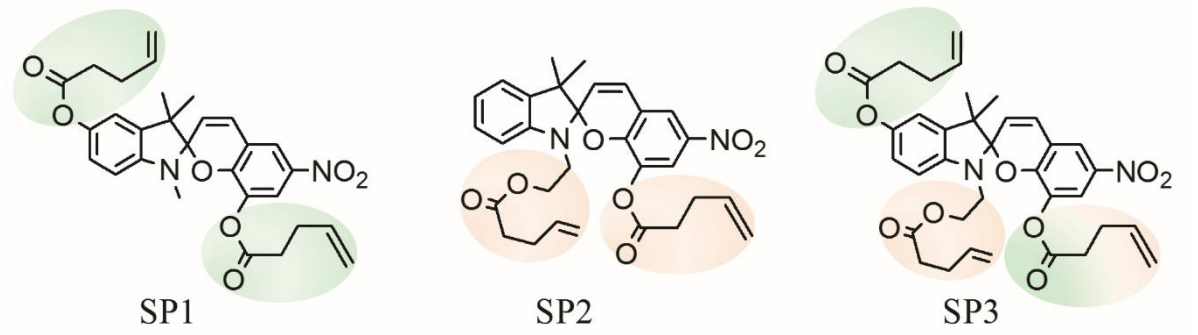

Figure 2.2. Chemical structures of three vinyl terminated SPs (SP1, SP2 and SP3) with different attachment points.

A mixture of Sylgard™ (1.0 g, 6 parts A: 1 part B) and spiropyrans SP1-3 (5-14.1 μmol) were mixed thoroughly and cast in-situ and cured at 65 °C overnight. Thus, pale yellow PDMS crosslinked samples of two "arms" SP1 and SP2, and three "arms" SP3 were prepared. Thus, the attachment points on the chromene ring for all SPs are identical (8-position), with varying attachment positions on the indoline ring for SP1 (5'-position) and SP2 (1' *N* -position), while SP3 has a combination of these (5' and 1' *N*) (**Figure 2.1**). RGB colour analysis and in situ absorption measurement were used to characterize the optical changes. Density functional theory modelling was performed to assist in

understanding the mechanisms responsible for the colour transitions observed in various samples.

2.4.1 Mechanochromic Properties

The mechanical properties of cross-linked PDMS (pure Sylgard) and SP-PDMS samples were investigated, and the effect of incorporation of small amounts of spiropyrans SP1-3 into PDMS were compared (**Figure A2.7**). The stress-strain curves of crosslinked PDMS and all three SP samples were identical within experimental error, demonstrating incorporation of small amounts of SP had negligible effect on the mechanical performance of PDMS bulk samples.

The colour change was observed after the threshold of activation compressive strain. Significant colour changes of samples were observed after release from 70% compression strain (**Figure A2.8**). The RGB colour channel ratios showed a decrease in Green/Blue ratio and an increase in Blue/Red and Green/Red ratios (**Figure A2.9**). The Blue/Red values having the greatest change were used to define the onset of activation points for all samples (**Figure 2.3A**), determined by the crossover point of two tangent lines.[23] Consistent with previous reports,[24] the stress-strain curves rose sharply after the onset of activation, indicating the stress stiffening point is critical for SP activation in elastomers under compression. The threshold activations were at the strain around 60% (**Figure 2.3A**) and under the stress of 4-7 MPa, specifically 58.6 ± 1.0% for SP2, 60.7 ± 0.6 % for SP3 and 61.1 ± 0.8 % for SP1. Noticeably, the ratios of RGB intensity for the three spiropyran systems varied. SP2 showed the greatest change after 70% compressive strain, followed by SP3, and SP1 presented the smallest change among the three systems. In addition, the colour turned darker as concentration increased at a constant strain (**Figure A2.8**). Chromaticity represents a colour quality regardless of the luminance; the chromaticity diagram based on coordinates (*x, y*) is calculated from RGB colour values according to transformation matrix according to standard *CIE1931*.[25] By converting RGB values to chromaticity coordinates, the colour changing paths of SP under compression and relaxation are more visualized (**Figure 2.3B**). Pristine light-yellow SP switched to blue (not obvious for SP1) as compressive strain increased and shifted toward blue-violet colour upon relaxation before returned to light yellow. The variation of SP2 and SP3 is much greater than SP1. The colour difference under pressure and after relaxation could

be caused by different MC isomers,[5] which will be further discussed in the following sections.

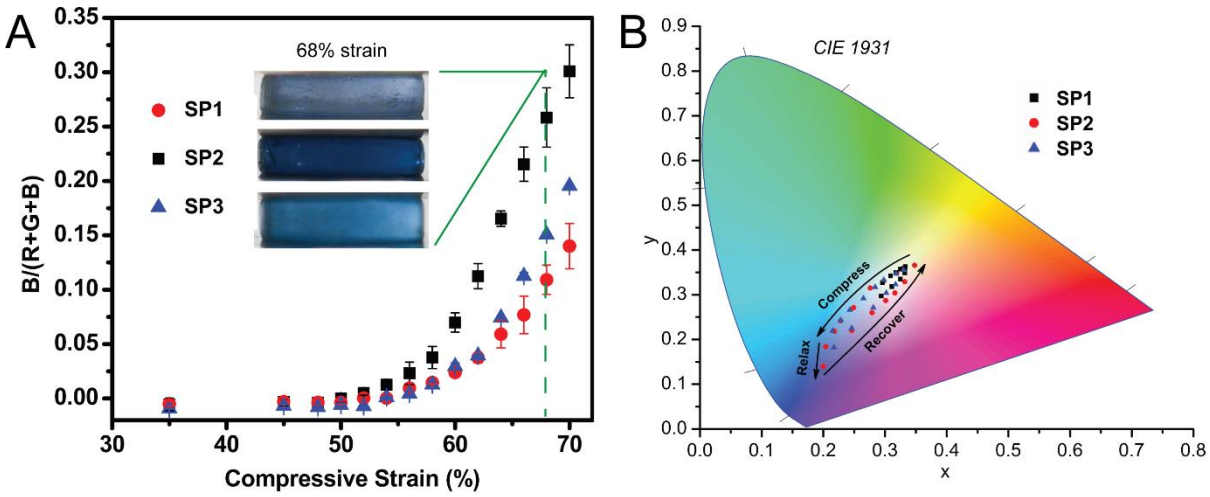

Figure 2.3. (A) Corresponding B/R value (blue channel intensity/red channel intensity) as a function of compressive strain for SP samples (conc. = 5.0 μmol/g), and the inset images of SP samples at 68% strain; (B) Chromaticity diagram (standard CIE 1931) of SP samples showing the colour change directions under compression (strain: 0% to 70%), relaxation and recovery (SP1-3: conc. = 5.0 μmol/g).

Absorption spectra were also utilized to confirm compressive activation of SP-PDMS in addition to RGB analysis from optical images. Before deformation, there was negligible absorption in the visible range for all SP samples, indicating the ring closed spiropyran was the dominant form (**Figure 2.4A-C**). Upon activation, absorption peaks at 500-650 nm appeared, corresponding to ring open merocyanine. The absorption intensity of all SP samples increased as compressive strain increased and reached a relatively steady value after 20-30 min under a constant strain (**Figure A2.10**). This demonstrated that the gradual increase in SP activation to the ring open MC under deformation continued until reaching a plateau after a certain time under a constant strain. This indicates the applied stress in bulk samples requires a certain time to fully equilibrate. The compressive response of three SP systems were compared. At each strain point, absorbance was acquired after 30 min to ensure the conversion between SP and MC achieved equilibrium. Although the absorption intensities of all SPs' were significantly different under large strain, the activation thresholds at 47% strain (SP3), 48% (SP2) and 49% strain (SP1) did not show a statistical difference. The activation thresholds differed from the results of RGB analysis due to different loading rates, as the compression measurements were

finished 70 seconds, while the absorption measurements were given enough time to achieve plateau. This is consistent with the study by Kim which showed the onset of activation strain increased with a faster strain rate.[13] Consistent with the above RGB analysis, the order of the absorption intensity under the strain of 62% is SP2 > SP3 > SP1. These results indicate that SP2-PDMS shows an advantage over SP1 and SP3 in emitting optical signal after the onset of activation. Interestingly, SP3 with an extra attachment point did not show an advantage over SP2, with respect to optical change under large strain, but it remained more active than SP1. A previous study on the simulation of two attachment points on the indoline ring inferred the external force is transferred to the *N* position.[1] In terms of force distribution, it is possible that the applied energy on the SP3 molecule inefficiently transferred to the spiro C-O bond, and is partially distributed on the indoline ring because the two attachment positions are unlikely to be in the same direction against the pulling point on chromene ring under stretching. If so, the extra attachment on SP3 should have less ring opening ability than SP1 and SP2. However, comparing SP1 and SP3, the extra attachment on 1'*N*-position improved the force response; comparing SP2 and SP3, the extra attachment on 5'-position decreased the force response. Thus, the attachment point at the 1'*N*-position having a shorter C-O distance plays a key role in the force activation.

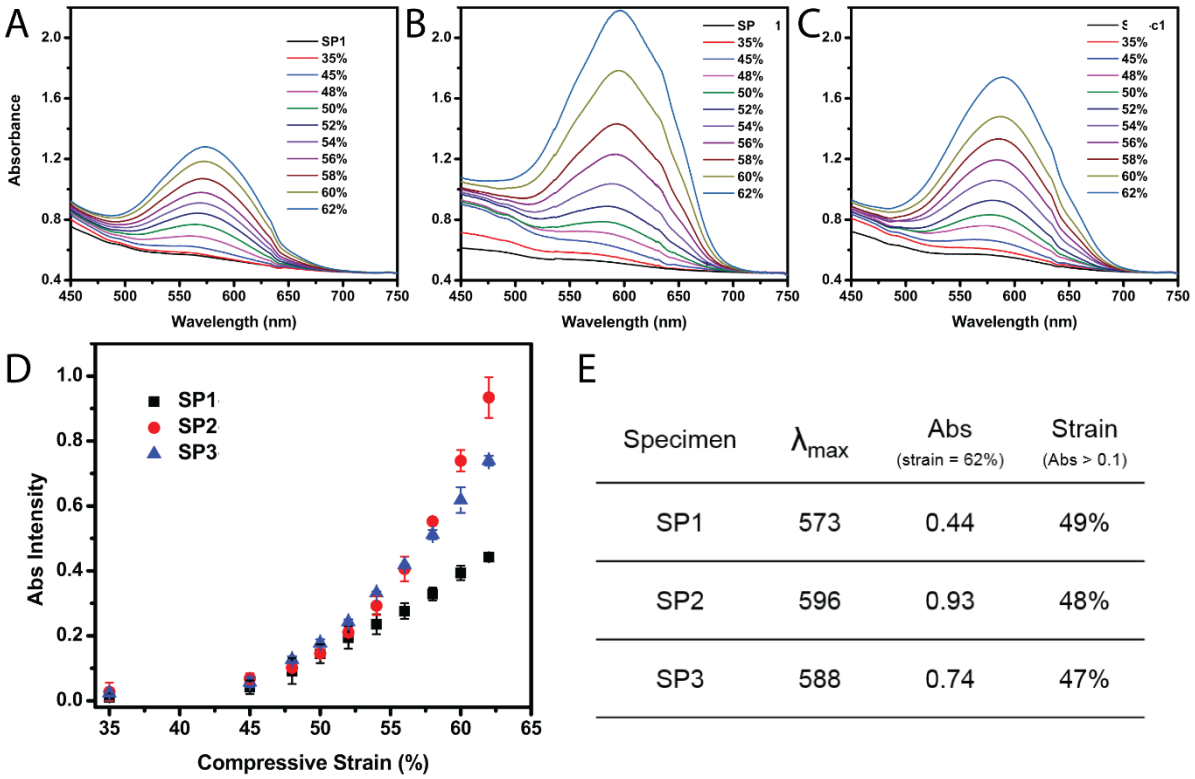

E

Specimen	λ_{max}	Abs (strain = 62%)	Strain (Abs > 0.1)
SP1	573	0.44	49%
SP2	596	0.93	48%
SP3	588	0.74	47%

Figure 2.4. UV-Vis absorption spectra of SP elastomers at concentrations of 5.0 μmol/g, (A) SP1, (B) SP2, (C) SP3 as increasing compressive strain. (D) Plot of absorption intensity vs compressive strain of SP. (E) Parameters from UV-Vis absorption spectra of a-c, where λ_{max} refers to the maximum absorption wavelength at the strain of 62%.

The maximum absorption wavelength (λ_{max}) of SP1, SP2, and SP3 at the compressive strain of 62% are at the wavelengths 573, 596, and 588 nm respectively (**Figure 2.4**), which are assigned to ring-opened MC. As compressive strain increased, the λ_{max} of each SP shifted slightly toward larger wavelengths, but not obvious for SP1. Consistent with the absorption spectra of compression samples, the absorption bands of SP-PDMS under tension performed similarly under stress and after relaxation. The location of absorption bands was more obvious on tensile samples as the deformations were larger. The λ_{max} of SP2 at 598 nm under tension (**Figure 2.5B**), moved to ~573 nm after relaxation. SP3 also exhibited a shift of λ_{max} from 598 nm to 588 nm (**Figure 2.5C**). SP1 did not show a distinguishable shift on the absorption peak under tension and relaxation (**Figure 2.5A**), indicating SP1 may undergo a different isomerization path for loading-relaxation compared with SP2 and SP3. The blue-shift of SP3 again demonstrates the attachment points on the 1'*N*-position is important for mechanochromic SP.

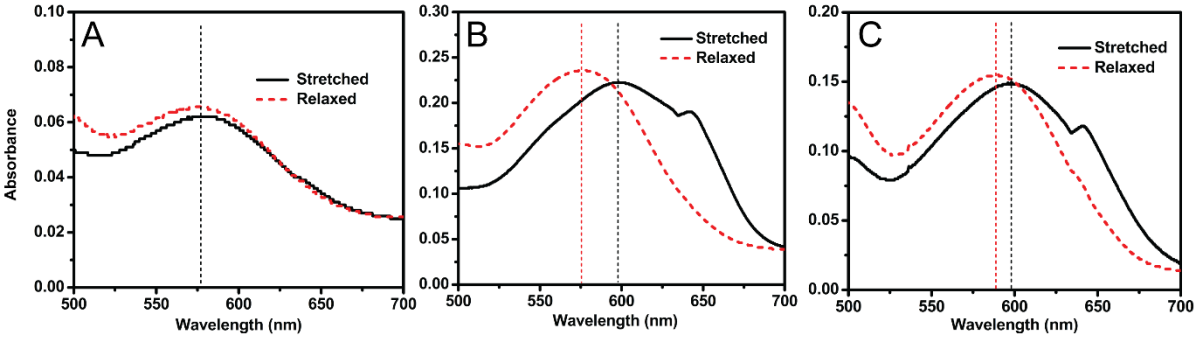

Figure 2.5. UV-Vis spectra of SP1-3 (conc. = 9.4 μmol/g) under tensile strain (≈ 2) and unloading. (A) SP1, width: 5 mm, thickness: 0.8 mm, (B) SP2, width: 4 mm, thickness: 0.8 mm, (C) SP3, width: 4 mm, thickness: 0.8 mm.

2.4.2 Decolouration

The transition between spiropyran and merocyanine in PDMS is reversible, which can also be quantitatively determined by in situ UV-Vis measurement. The absorption intensity of SP decreased rapidly in the dark upon unloading from 62% compressive strain (**Figure 2.6A**), demonstrating MC recovered to ring-closed SP in the bulk state upon relaxation. The absorption ratio (Abs/Abs$_{max}$) of SP1, SP2 and SP3 dropped to 1.3%, 1.3%, and 5.2% at the absorption intensity of 0.0042, 0.0064 and 0.0306 respectively after 40 min stored in the dark. In the absence of visible light, the ring closing is a thermodynamic process.[26] SP2 in PMA was reported to return to colourless after 104 min,[23] which is longer than the observed relaxation time in this PDMS system. The difference is caused by the different glass transition temperature between PMA and PDMS. The time of Abs decreasing to 0.1 was used to compare; the absorbance of SP1 dropped rapidly to 0.1 within 3.5 min and SP2 in 6 min, while it took 14 min for SP3. The decolouration rate to 50% intensity also showed a similar trend. The absorption intensities showed exponential decay, giving straight lines in semi-logarithmic plots (**Figure A2.11**). The decolouration rate (k_d) of polymers SP1-3 were determined from the slope of the log absorbance versus time plots and they were summarized in **Figure 2.6B**. The decolouration rate of SP1 was close to SP2, while SP3 showed a slower decolouration process. It is difficult to comment on the difference between SP1 and SP2 with such close decolouration parameters, given that the Abs of activated SP2-PDMS was much stronger than that of SP1-PDMS. But obviously SP3 with one more attachment position recovered slower than SP1 and SP2. The same trend was observed when the SP-PDMS were under

a constant loading over a long period (**Figure A2.12**). This is a result of more attachment positions on SP3 reducing the mechanophore flexibility. In bulk materials, flexibility is also a key factor for the SP ↔ MC isomerization. This approach of varying attachment positions can lead to a method for controlling mechanophore ring closing process. The slower colour fading process of SP3 is possibly related to the blue-shift under loading and unloading; the less flexibility delays the isomerization process and stabilizes the intermediate isomer longer.

A

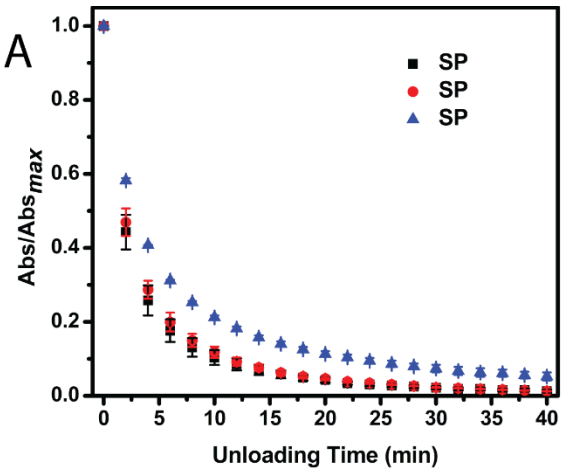

B

Specimen	$T_{1/2}$ (min)	$T_{Abs = 0.1}$ (min)	Abs (Time = 40 min)	k_d
SP1	1.8	3.5	0.0042	0.14
SP2	1.9	6.0	0.0064	0.14
SP3	2.9	14.0	0.031	0.12

Figure 2.6. (A) Plot of absorption intensity/maximum absorption intensity vs relaxation time in darkness after unloading from 62% compressive strain for SP1, SP2 and SP3 (conc. = 9.4 μmol/g). (B) Decolouration parameters from UV-Vis spectra, where $T_{1/2}$ represents relaxation time at Abs/Abs_{max} = 0.5, $T_{Abs < 0.1}$ is the relaxation time at 0.1 absorption intensity, and k_d is the decolouration rate.

2.4.3 Density Functional Theory Calculations

The differences observed between SP1 and SP2 arise from conformational isomerization of the merocyanine forms following ring opening.[5] To explore this further, density functional theory (DFT) calculations were carried out at the M06-2X/6-31G(d)[27] level of theory for SP1 and SP2 models in which the polymer attachment points were replaced by methoxy groups, using the Gaussian 09[29] software package. Energies for the isomers available via ring opening and E/Z isomerization, and their connecting transition states, are shown in **Figure A2.13**. Seven possible merocyanine isomers are predicted to be stable species; the MC-EZZ isomers were found to spontaneously ring close back to SP, and instead a direct transition state is available connecting SP to MC-EEZ (which proceeds

transiently via the unstable EZZ form). Conversely, the MC-ZZZ isomer is predicted to form via a direct ring opening process in SP, although the reverse barrier for ring closing is very small, and this isomer is likely to be transient. For both SP1 and SP2, the EEZ isomer is predicted to be the most stable merocyanine form, which could be the dominant MC form activated by UV in both cases, although other isomers sit within a few kJ/mol. The barrier to form the EEZ isomer from the spiropyran is also similar in both cases.

Table 2.1. Calculated energies for the SP1 and SP2 model compound isomers ordered by change in interatomic distance (ΔD) of the polymer attachment points, O–O on SP1 and C–O on SP2 (shown in red in the inset structures). Wavelength of first excited state is also shown, from TD-DFT calculations.

SP1

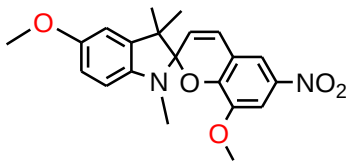

SP2

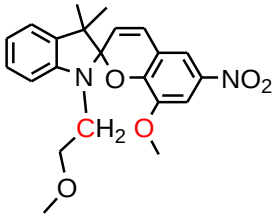

Isomer	Δ O–O (Å)	Relative energy (kJ/mol)	First excited state (nm)	Isomer	Δ C–O (Å)	Relative energy (kJ/mol)	First excited state (nm)
SP1	0.0	0.0	299	SP2	0.0	0.0	290
ZZZ	1.3	77.0	456	ZZZ	-0.3	91.3	456
EZE	4.5	117.6	489	ZZE	1.4	108.4	501
ZZE	5.4	96.5	509	EEZ	2.1	74.2	455
ZEZ	5.6	80.3	456	ZEE	2.2	81.2	464
EEE	5.6	73.4	466	ZEZ	3.1	79.5	452
EEZ	5.8	70.6	455	EZE	4.0	121.4	484
ZEE	6.3	80.8	464	EEE	4.1	77.0	463

To better understand the effects of conformational isomerization on SP1 and SP2 upon ring opening under force, their merocyanine isomers have been arranged in order of increasing distance between polymer attachment positions being pulled in the opposite directions along the molecules (shown in **Table 2.1**). We define this change in

interatomic distance as ΔD, which for SP1 is an O–O separation and for SP2 is a C–O separation. Importantly, from Table 1 we see that ΔD required for deformation to ring open SP2 is far less than that for SP1. For instance, to reach the most stable EEZ MC isomer, the attachments need only be separated by a further 2 Å from their starting geometry in SP2, compared to 5.6 Å in SP1.

This trend revealed above is consistent with the literature.[18, 20] Although Kim *et al.* claimed that there was only a minimal effect on the mechanochromic response between SP1 and SP2 in PDMS bulk materials which is in contrast to the calculation results,[20] the difference of colour intensity under a constant deformation is significant from our study (**Figure 2.3** and **Figure 2.4**). We believed that this is related to the ΔD difference between SP1 and SP2. Although the activation deformation threshold did not show statistic difference in the bulk polymer, but the stronger colour intensity of SP2 than SP1 under a same strain demonstrated higher ring opening occurs in SP2 systems. The easier bond cleavage should be attributed to a shorter ΔD. Lin *et al.* came up with an opposite hypothesis, the larger change in the pulling points length, the more force response will be produced.[19] That hypothesis could not explain our observation that SP1 showed less response under force than SP2, but the largest ΔD of SP1 is greater that of SP2.

The calculation also showed less deformation is required for SP2 than SP1 to reach the higher-energy MC isomers ZZE and EZE. Due to their energies, these forms are likely to be shorter-lived isomers, and may explain the shift in absorption peak during relaxation found for SP2. Interestingly, the position of the first excited state in ZZE and EZE is blue-shifted by around 40 nm relative to the other lower-energy isomers. Thus, we hypothesize that ZZE at a much shorter ΔD than EZE could be the blue state for SP2-PDMS under force; after relaxation, ZZE isomerizes to the shorter ΔD isomer ZZZ giving purple colour before it reverts to ring closed SP2 (**Figure 2.7**). For SP1, the majority of ring open merocyanine may stay at the short ΔD isomer ZZZ under a same strain and upon relaxation, resulting in an indistinguishable blue-purple shift, as the long wavelength isomers EZE and ZZE require much more ΔD. Kim *et al.* claimed that the λ_{max} was also detected on SP1 at the tension strain of 2.3.[20] As the DFT calculation results indicate the ΔD of SP1 is longer than SP2, it is possible to observe a λ_{max} shift of SP1 when the deformation is large enough. However, in our study no obvious λ_{max} shift was observed for SP1 up to 200% tensile strain, although SP2 and SP3 showed an obvious shift (**Figure**

2.5). Thus, under a relatively short deformation and after relaxation, the majority of MC species from SP1 remain in the ZZZ confirmation, while SP2 transitions through an intermediate confirmation (ZZE) of MC (**Figure 2.7**). SP3 is believed to have an intermediate isomer under loading similar to SP2, since it has the same 1'*N*-attachment position.

In order to better understand the influence of either geometric changes to the attachment points, relative to electronic effects associated with varying functionalities on the SPs, SP3 was prepared. SP3 combines the same attachment positions of both SP1 and SP2 and was designed to study the effect of geometry on force responses. In terms of the electronic effect, SP1 is similar to SP3 with identical vinyl ester functionality and very minor electronic effects due to the alkyl and methyl functionalities on 1'*N* position. SP3 differs from SP2, as it has an additional slight electron donating vinyl ester functionality at position 5'. Electronic effect causing UV response was studied previously by Balmond, showing the addition of methoxy group (electron donating group) on 5'-position on the indoline ring reduced UV response.[28] If the electronic effect is the influencing factor here, the order of mechanochromic change might be expected to follow in the order of intensity: SP2 > SP1 ≈ SP3 as there is no electron donating chain on 5'-position. If the geometric effect due to the attachment positions is the key factor, with ΔD dominating the ring opening process, the optical response should be SP2 ≈ SP3 > SP1 as there were attachment chains on 1'*N* -position for SP2 and SP3. According to the above results the optical change is in the order of SP2 > SP3 > SP1, with SP3 behaving more similarly to SP2 (blue-shift). Preliminary calculations on a SP3 model showed similar C-O ΔD, in agreement with the experimental observation. Due to the increase of isomer possibility, the simulation of SP3 model was not further carried out and direct comparison between SP1 and SP2 models provides the best explanation. Both the electronic and geometric effects influence the mechanochromic properties, however the geometric effect caused by varying the attachment positions is the dominant factor. The assumption is consistent with Lin's study concluding that the geometric effect probably dominates the mechanochromic behavior.[19] This again implies that the attachment points on the 1'*N*-position is more active than the 5'-position for mechanochromism.

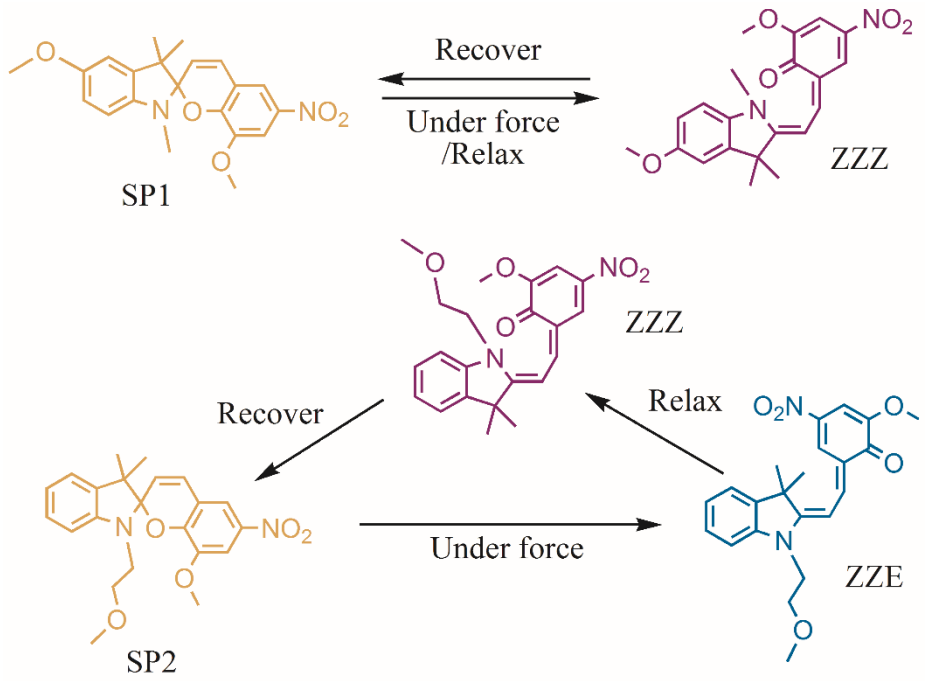

Figure 2.7. Hypothesized paths for merocyanine (MC) isomers of SP1 and SP2 model compounds under force and relaxation.

2.5 Conclusion

In summary, we investigated the effect of the attachment positions on the mechanochromism of three spiropyrans in crosslinked PDMS network to find out how the geometric or electronic effect influences the optical change. Varying the attachment points on the indoline ring did not cause a statistical difference at the onset activation stress and strain, however SP2 showed a higher absorption intensity than SP1 under 62-70% compressive strain. SP3 which combined the attachment points of SP1 and SP2 showed higher absorption intensity than SP1 but lower than SP2. SP2 and SP3 showed an obvious blue-shift under loading and after unloading, while the shift was not observed for SP1. The results indicate that both electronic and geometric effects influence the mechanochromic properties, with the geometric effect being the more dominant factor. The DFT calculation showed the pulling points distance ΔD of the MC isomers differed between SP1 and SP2, and this ΔD is believed to affect the mechanochromic response and the blue-purple shift. Restricted by the mobility with an extra attachment point in the matrix, SP3 showed a slower ring closing rate than SP1 and SP2 after relaxation and under a long-term loading. This comparison study provides more understanding of the

mechanochromic properties of spiropyran, which could be useful for the design where spiropyran is employed as a force-responsive chromophore.

2.6 References

(1) Davis, D. A.; Hamilton, A.; Yang, J.; Cremar, L. D.; Van Gough, D.; Potisek, S. L.; Ong, M. T.; Braun, P. V.; Martinez, T. J.; White, S. R.; Moore, J. S.; Sottos, N. R. Force-induced activation of covalent bonds in mechanoresponsive polymeric materials. *Nature* 2009, 459, 68-72.

(2) Lee, C. K.; Diesendruck, C. E.; Lu, E.; Pickett, A. N.; May, P. A.; Moore, J. S.; Braun, P. V. Solvent Swelling Activation of a Mechanophore in a Polymer Network. *Macromolecules* 2014, 47, 2690-2694.

(3) Lee, C. K.; Davis, D. A.; White, S. R.; Moore, J. S.; Sottos, N. R.; Braun, P. V. Force-induced redistribution of a chemical equilibrium. *J. Am. Chem. Soc.* 2010, 132, 16107-16111.

(4) Grady, M. E.; Beiermann, B. A.; Moore, J. S.; Sottos, N. R. Shockwave loading of mechanochemically active polymer coatings. *ACS Appl. Mater. Interfaces* 2014, 6, 5350-5355.

(5) Gossweiler, G. R.; Hewage, G. B.; Soriano, G.; Wang, Q.; Welshofer, G. W.; Zhao, X.; Craig, S. L. Mechanochemical Activation of Covalent Bonds in Polymers with Full and Repeatable Macroscopic Shape Recovery. *ACS Macro Lett.* 2014, 3, 216-219.

(6) O'Bryan, G.; Wong, B. M.; McElhanon, J. R. Stress sensing in polycaprolactone films via an embedded photochromic compound. *ACS Appl. Mater. Interfaces* 2010, 2, 1594-1600.

(7) Li, M.; Liu, W.; Zhu, S. Smart polyolefins feeling the force: Colour changeable poly(ethylene-vinyl acetate) and poly(ethylene-octene) in response to mechanical force. *Polymer* 2017, 112, 219-227.

(8) Chen, H.; Yang, F.; Chen, Q.; Zheng, J. A Novel Design of Multi-Mechanoresponsive and Mechanically Strong Hydrogels. *Adv. Mater.* 2017, 29, 1606900.

(9) Raisch, M.; Genovese, D.; Zaccheroni, N.; Schmidt, S. B.; Focarete, M. L.; Sommer, M.; Gualandi, C. Highly Sensitive, Anisotropic, and Reversible Stress/Strain-Sensors from Mechanochromic Nanofiber Composites. *Adv. Mater.* 2018, 30, 1802813.

(10) Kempe, F.; Brugner, O.; Buchheit, H.; Momm, S. N.; Riehle, F.; Hameury, S.; Walter, M.; Sommer, M. A Simply Synthesized, Tough Polyarylene with Transient Mechanochromic Response. *Angew. Chem. Int. Ed.* 2018, 57, 997-1000.

(11) Zhang, H.; Gao, F.; Cao, X.; Li, Y.; Xu, Y.; Weng, W.; Boulatov, R. Mechanochromism and Mechanical-Force-Triggered Cross-Linking from a Single Reactive Moiety Incorporated into Polymer Chains. *Angew. Chem. Int. Ed.* 2016, 55, 3092-3096.

(12) Li, M.; Zhang, Q.; Zhou, Y.-N.; Zhu, S. Let spiropyran help polymers feel force! *Prog. Polym. Sci.* 2018, 79, 26-39.

(13) Kim, J. W.; Jung, Y.; Coates, G. W.; Silberstein, M. N. Mechanoactivation of Spiropyran Covalently Linked PMMA: Effect of Temperature, Strain Rate, and Deformation Mode. *Macromolecules* 2015, 48, 1335-1342.

(14) Chen, Y.; Zhang, H.; Fang, X.; Lin, Y.; Xu, Y.; Weng, W. Mechanical Activation of Mechanophore Enhanced by Strong Hydrogen Bonding Interactions. *ACS Macro Lett.* 2014, 3, 141-145.

(15) Jiang, S.; Zhang, L.; Xie, T.; Lin, Y.; Zhang, H.; Xu, Y.; Weng, W.; Dai, L. Mechanoresponsive PS-PnBA-PS Triblock Copolymers via Covalently Embedding Mechanophore. *ACS Macro Lett.* 2013, 2, 705-709.

(16) Zhang, H.; Chen, Y.; Lin, Y.; Fang, X.; Xu, Y.; Ruan, Y.; Weng, W. Spiropyran as a Mechanochromic Probe in Dual Cross-Linked Elastomers. *Macromolecules* 2014, 47, 6783-6790.

(17) Barbee, M. H.; Kouznetsova, T.; Barrett, S. L.; Gossweiler, G. R.; Lin, Y.; Rastogi, S. K.; Brittain, W. J.; Craig, S. L. Substituent Effects and Mechanism in a Mechanochemical Reaction. *J. Am. Chem. Soc.* 2018, 140, 12746-12750.

(18) Gossweiler, G. R.; Kouznetsova, T. B.; Craig, S. L. Force-rate characterization of two spiropyran-based molecular force probes. *J. Am. Chem. Soc.* 2015, 137, 6148-6151.

(19) Lin, Y.; Barbee, M. H.; Chang, C. C.; Craig, S. L. Regiochemical Effects on Mechanophore Activation in Bulk Materials. *J. Am. Chem. Soc.* 2018, 140, 15969-15975.

(20) Kim, T. A.; Robb, M. J.; Moore, J. S.; White, S. R.; Sottos, N. R. Mechanical Reactivity of Two Different Spiropyran Mechanophores in Polydimethylsiloxane. *Macromolecules* 2018, 51, 9177-9183.

(21) Johnston, I. D.; McCluskey, D. K.; Tan, C. K. L.; Tracey, M. C. Mechanical characterization of bulk Sylgard 184 for microfluidics and microengineering. *Journal of Micromechanics and Microengineering* 2014, 24, 035017.

(22) Jiang, K.; Thomas, P. C.; Forry, S. P.; DeVoe, D. L.; Raghavan, S. R. Microfluidic synthesis of monodisperse PDMS microbeads as discrete oxygen sensors. *Soft Matter* 2012, 8, 923-926.

(23) Li, M.; Zhang, Q.; Zhu, S. Photo-inactive divinyl spiropyran mechanophore cross-linker for real-time stress sensing. *Polymer* 2016, 99, 521-528.

(24) Hong, G.; Zhang, H.; Lin, Y.; Chen, Y.; Xu, Y.; Weng, W.; Xia, H. Mechanoresponsive Healable Metallosupramolecular Polymers. *Macromolecules* 2013, 46, 8649-8656.

(25) Zuo, B.; Wang, M.; Lin, B.-P.; Yang, H. Photomodulated Tricolour-Changing Artificial Flowers. *Chem. Mater.* 2018, 30, 8079-8088.

(26) Tian, W.; Tian, J. An insight into the solvent effect on photo-, solvato-chromism of spiropyran through the perspective of intermolecular interactions. *Dyes Pigm.* 2014, 105, 66-74.

(27) Zhao, Y.; Truhlar, D. G. The M06 suite of density functionals for main group thermochemistry, thermochemical kinetics, noncovalent interactions, excited states, and transition elements: two new functionals and systematic testing of four M06-class functionals and 12 other functionals. *Theoretical Chemistry Accounts* 2007, 120, 215-241.

(28) Balmond, E. I.; Tautges, B. K.; Faulkner, A. L.; Or, V. W.; Hodur, B. M.; Shaw, J. T.; Louie, A. Y. Comparative Evaluation of Substituent Effect on the Photochromic Properties of Spiropyrans and Spirooxazines. *J. Org. Chem.* 2016, 81, 8744-8758.

(29) Gaussian 09, Revision E.01. http://gaussian.com/g09citation/

Chapter 3: Colour-switchable Polar Polymeric Materials

3.1 Chapter Perspectives

Spiropyrans have been commonly incorporated into non-polar polymers rather than polar polymers for mechanochromic purposes since a polar environment can stabilize the more polar isomer merocyanine (MC) in the absence of visible light, which is referred as negative photochromism. In this chapter, with the aim to broaden the polymer options for SP-linked mechanochromic materials and understanding the effect of SP attachment positions in polar polymer matrices on their mechanochromic properties, difunctional and tri-functional SPs are incorporated into polar poly(hydroxyethyl acrylate) via free radical polymerisation initiated by white light, which expands the investigation from Chapter 2. Here we have demonstrated the effect of attachment positions and numbers on their mechanochromic properties by swelling in water and negative photochromism when stored in the dark. It will be shown that the force of swelling in water is sufficient to induce the ring-opening reaction of SP, and that the tri-substituted SP (SP3) is less influenced by the polar matrix but shows the fastest colour activation during swelling. This indicates that the colour intensity can be manipulated by varying the number of attachment positions. The results demonstrate that influences from both the polar environment and the mechanochromic nature of SP have an impact on the absorption intensity, rate of change, and the decolouration rate of the materials.

3.2 Introduction

SP based mechanochromic materials can be obtained by covalent [1-6] and non-covalent bonding to the matrix.[7] The concern for non-covalently bonded systems is that SP has the potential to leach from the matrix, especially in the presence of solvents and this limits their practical application. For SP covalently bonded systems, a diverse range of polymers have been utilized, including poly methyl (meth)acrylates,[8] polystyrene,[9] poly(ε-caprolactone),[2, 10] and polydimethylsiloxane.[3] These non-polar polymers are designed to stabilize the non-polar ring-closed SP before being subjected to external stimuli.

A polar environment will affect the SP ↔ MC equilibrium due to the difference in polarity between SP and MC,[11] and the energy barrier of the isomerization, with a lower ground state energy of the MC in a polar environment.[12-14]. This phenomenon has been defined as negative photochromism.[15] For SP linked hydrophilic polymer systems, the effect from the polar environment results in coloured and more polar MC being the dominant form in the absence of visible light. As an example, it has been reported that SP conjugated with PEG as a soft segment in PU changed colour without an applied force when kept in the dark.[16] To avoid the effect from the polar environment for mechanochromism, SP has been protected in a non-polar environment within micelles in hydrogel systems, to ensure the SP remains in the colourless form prior to colour triggering by an external force.[17] Manipulating the colour switching of SP in hydrophilic matrices is important for applications such as for optical data storage.[11, 18] Efforts have been made to control the influence from polar environments, by adding electron withdrawing or electron donating groups to the SP molecule, or by using polar polymers with different functionalities, varying local electrostatic effects.[19] Additionally, the interaction between the polar components and MC not only affects the equilibrium of SP ↔ MC, but also causes maximum absorbance wavelength (λ_{max}) shift.[13, 20] The polar effect can be induced from either a solvent or a polymer matrix.[11, 21] The negative photochromism cannot be neglected when hydrophilic polymers are employed in SP systems.[22] Although incorporation of SP into hydrophilic polymers for mechanochromism has barely been studied, the broad range of potential applications of hydrophilic polymers in coatings, food packaging, membranes and biomedical devices necessitates development of a range of polymer options for SP contained mechanochromic materials.

The forces induced by swelling of mechanochromic SP polymers in organic solvent and CO_2 are sufficient to activate SP to its coloured MC form. Moore's group reported that crosslinked SP-PMMA can be activated by swelling in organic solvents.[23] It was found that the swelling rate was important to the colour change behaviour, given that too slow a swelling rate could not trigger the ring-opening reaction, while too fast a swelling rate would cause sample damage. Microgels of 2-(diethylamino)ethyl-methacrylate (PDEA) with conjugated SP were developed by Zhu's group, which showed a colour switching from pale yellow to pink due to the deformation caused by absorbing CO_2.[24] This implies that the efficient activation by swelling is attributed to the three-dimensional deformation, rather than uniaxial strain. Water is a widely used and non-toxic solvent, but cannot swell non-polar polymers to induce colour change due to the high polarity.[23] To date, water has not been used to swell hydrophilic polymers containing SP for mechanochromism. For the potential applications as mentioned earlier, it is important to see how the mechanical activation of SP to MC will behave differently in a hydrophilic polymer due to its interaction with such a polar environment.

As mechanochromic SPs have yet been crosslinked in pure swellable hydrophilic polymers, it is necessary to know the factors affecting the equilibrium between SP and MC, and how the mechanical swelling affects the chromism in a polar environment. Here, we incorporated a series of spiropyrans, which have been shown mechanochromic properties in PDMS in **Chapter 2**, into hydrophilic poly(hydroxyethyl acrylate) (PHEA), which act as a reversible sensor, switching colour in response to the presence and absence of visible light and water. Herein the effect of a polar matrix on the colour forming properties of these materials in the dark as well as the mechanochromic behaviour when swollen in water are investigated, with the presentation of a fully reversible switchable cyclic mechanochromic and negative photochromic materials.

3.3 Experimental Methods

3.3.1 Materials

Hydroxyethyl acrylate (HEA, 96%, Sigma) and ethylene glycol dimethacrylate (EGDMA, 98%, Sigma) were passed through basic aluminium oxide to remove the inhibitor monomethyl ether hydroquinone before use. Tetrahydrofuran (THF, Chem-Supply) was

pre-dried over sodium, before being distilled from benzophenone and sodium under an inert atmosphere of nitrogen prior to use. 4-Dimethylaminopyridine (DMAP, ≥98%, Sigma), phenylbis(2,4,6-trimethylbenzoyl)phosphine oxide (BAPOs, 97%, Sigma), methacrylic anhydride (94%, Sigma) were used as received. 3',3'-dimethyl-6-nitro-1'-(2-hydroxyethyl)spiro[chromene-2,2'-indoline]-5',8-diol was synthesized according to our previous work.[25] 1',3',3'-trimethyl-6-nitrospiro[chromene-2,2'-indoline]-5',8-diol, and 1'-(2-hydroxyethyl)-3',3'-dimethyl-6-nitrospiro[chromene-2,2'-indolin]-8-ol were synthesized according to literature procedures.[1, 3]

3.3.2 Synthesis of Tri-methacrylate SP3

3',3'-dimethyl-6-nitro-1'-(2-hydroxyethyl)spiro[chromene-2,2'-indoline]-5',8-diol (0.20g, 0.52 mmol, 1.0 equiv) and DMAP (0.15 g, 1.23 mmol, 2.4 equiv) dissolved in THF (10 mL) was added methacrylic anhydride (0.28 mL, 1.87 mmol, 3.6 equiv). After stirring for 24 hr under Argon at room temperature, removed the solvent. The crude product was dissolved in minimal DCM, which was passed through basic alumina with DCM to obtain product SP3 (0.20g, 0.34 mmol, 64% yield).

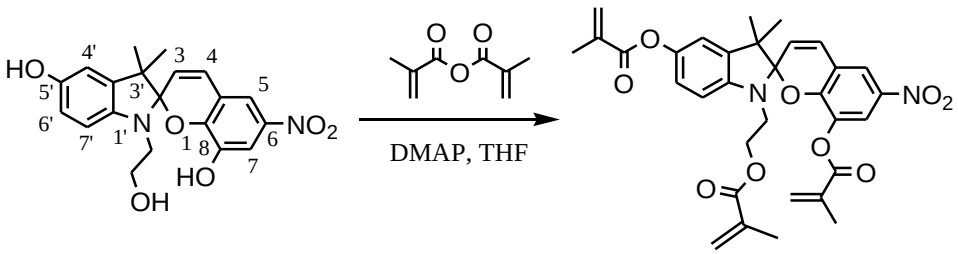

Scheme 3.1. Synthesis of tri-methacrylate SP3.

3.3.3 Preparation of SP Crosslinked PHEA Film Samples

For 1 mol % crosslinker density, HEA (0.4g, 1 equiv), SP3 (2.0 mg, 0.001 equiv), EGDMA (6.0 μL, 0.009 equiv), and photo initiator BAPOs (5.8 mg, 0.004 equiv) were mixed thoroughly in a vial. The mixture was injected into a glass mold (width: 1.6 cm, length: 5.0 cm, thickness: around 0.5 mm) with a silicone spacer sandwiched by two glass sheets and exposed to white light (4W cool white light, 350 lumens) for 2 hr to polymerization. For 2.5% EGDMA crosslinked SP3-PHEA films, 15.1 μL EGDMA was added; for 5% EGDMA crosslinked SP3-PHEA films, 30.2 μL EGDMA was added; for 7.5% EGDMA crosslinked

SP3-PHEA films, 45.2 µL EGDMA was added; for 10% EGDMA crosslinked SP3-PHEA films, 60.3 µL EGDMA was added. Regarding SP1-PHEA and SP2-PHEA, 0.1 mol % mechanophores and 0.95 mol % EGDMA were added respectively. To quantify the conversion ratio, crosslinked films were soaked in methanol for 2 days, which was changed regularly with fresh solvent, to remove the unreacted species, followed by drying under vacuum at ambient temperature until constant mass. The unreacted species for the samples were quantified to be less than 3 wt %; UV-Vis analysis of the extracted methanol solution, showed no detectable signals at 500-600 nm, confirming the mechanophores were conjugated in the polymer network.

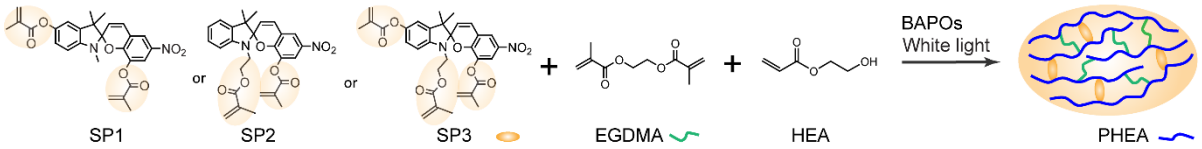

Scheme 3.2. Synthesis of SP-PHEA bulk materials via free radical polymerization under white light.

3.3.4 Characterization

^{1}H NMR spectroscopy was conducted on a Varian Unity 400 MHz spectrometer operating at 400 MHz, using deuterated chloroform ($CDCl_3$) as solvent and reference peak. UV–Vis spectrum was recorded on a Shimadzu UV–Vis Scanning Spectrophotometer (UV-2101 PC) with a fast scanning rate of 0.5 nm interval over a range of wavelengths 750-380 nm.

Swelling activation. Polymeric rectangular samples were cut to 7.5 mm × 20 mm. The samples were immersed in excess deionized water in vials fully covered with foil to avoid any light. Mass and dimensions were recorded during the swelling process. The ratio of size change ΔV was defined as $\Delta V=(V-V_0)/V_0$, where V and V_0 was calculated by *width* × *length* × *thickness*; the ratio of mass change Δm was determined by $\Delta m=(m-m_0)/m_0$.[23] Absorbance measurements were utilized to quantify the ring opening process from SP to MC.

MC reverting to SP under white light irradiation. Two decolouration processes were compared: swollen (hydrated) films or dehydrated films from the swollen state were exposed to white light. For measurement of the hydrated films, the coloured samples activated by water swelling were exposed to white light until a constant absorption value

was observed. For measurement of the dehydrated films, the coloured swollen films were dehydrated under vacuum at room temperature until a constant mass, then irradiated with white light to force MC to return to SP until a stable absorbance was achieved.

Colouration-decolouration cycles. Two methods of colouration-decolouration cycles were conducted corresponding to the two decolouration processes. Coloured swollen hydrated films were kept in water and placed under white light to force the MC ring close to SP until the stabilized absorbance was recorded; then the samples were covered with foil to block exposure to light, while recording the absorbance until it plateaued. The white light stimulated process was repeated 10 times. For the dehydrated films, the colour saturated swollen films were dried in the dark under vacuum at ambient temperature until a constant mass, and the absorbance was recorded; the dehydrated films were exposed to white light until a constant absorbance was observed, before being swollen in water again during which the mass and absorbance were recorded. The dehydration-hydration process was repeated 10 times.

3.4 Results and Discussion

Methacrylated SPs were synthesized according to our previous work.[25] A series of spiropyrans with hydroxyl groups were treated with methacrylic anhydride to afford the methacrylate-SP (**Scheme 3.1**), which was polymerized with monomer HEA and co-crosslinker EGDMA via free radical polymerization under white light (**Scheme 3.2**). Thermal and UV polymerization techniques which are typical approaches to obtaining SP polymeric materials lead to incomplete ring-closed mechanophores, with the former approach requiring post bleaching with visible light, whereas the latter approach is affected by the formation of MC in situ, resulting in incomplete polymerization. Thus, using white light and BAPOs as an initiator avoided these issues and ensured the ring-closed form being dominant species.[17, 26] The obtained samples were used to study the effect of the polar environments on the colouration in the dark (negative photochromism) and activation by swelling in water (mechanochromism) (**Scheme 3.3**).

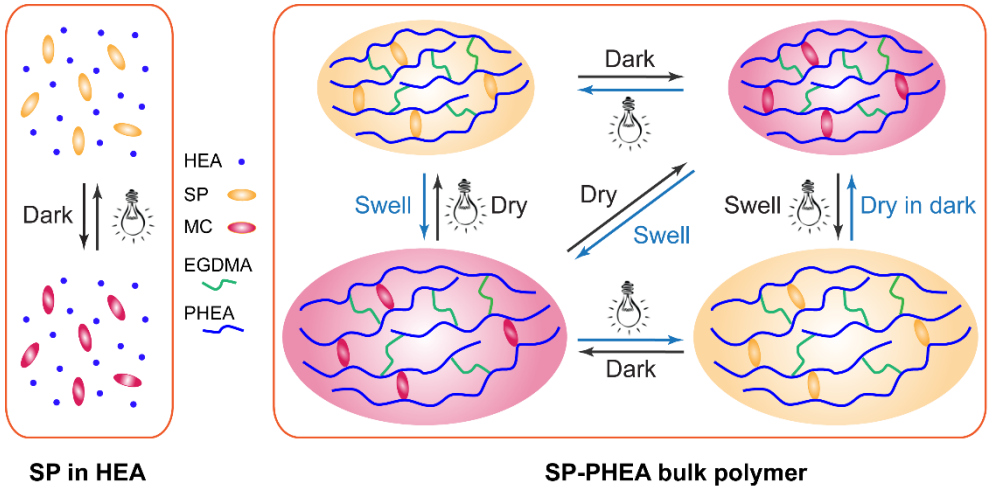

Scheme 3.3. Solutions of SP dissolved in HEA were used to study the thermodynamic equilibrium of free SP in a polar solvent, and SP-PHEA films were used to study their negative photochromic and mechanochromic properties in the solid state. The colour reversibility is due to the isomerization between ring-closed SP and ring-open MC.

3.4.1 Effect of Polarity on SP Colouration in Solution and Bulk Polymer

The negative photochromism of different SPs in polar solvent were evaluated by dissolving SP in HEA. Samples of SP in HEA at 0.1 μmol % were prepared under ambient conditions and exposed to white light for 1 min to convert any MC to ring-closed SP, prior to being stored in the dark. The UV-Vis absorption peaks at around 550 nm attributed to ring-open MC were negligible in all the samples after white light bleaching (**Figure A3.4A**), demonstrating the majority of mechanophores were in the ring closed form. The samples were kept in the dark under ambient conditions and measured for absorption regularly until they reached a plateau. The colour change was reversible by exposed to the white light and kept in the dark (**Figure A3.4B**).

Figure 1 shows the saturated absorbance of the SP1-3 in HEA solution in the dark. The absorption intensity of SP3 was significantly lower than SP1 and SP2 (**Figure 3.1**). This suggests that the interaction of SP1-3 with polar HEA differs (affecting the equilibrium between SP and MC) due to the different polarities of these three SPs. According to Tian *et al*, for the thermal competition between SP and MC in the absence of light, the energy for ring opening is mainly determined by MC conformational change.[13] In this case, the variation in the functionality position and number of SP1-3 may affect the equilibrium between SP and MC, resulting in different energies for stabilizing MC, leading to

differences in absorption intensity. SP3 having all the different attachment positions has the least unstable coloured MC isomers. Additionally, a slight red shift of maximum absorption wavelength (λ_{max}) was observed from SP1 to SP3 (**Figure 3.1A**). It has been reported that red shift occurs with decreasing solvent polarity for a specific SP.[18] Since the solvent was constant here, the λ_{max} shift in these three SP solutions was a result of the polarity difference of the chromophores. Both absorption intensity and λ_{max} differences revealed that the three SP had different extents of interaction with polar HEA.

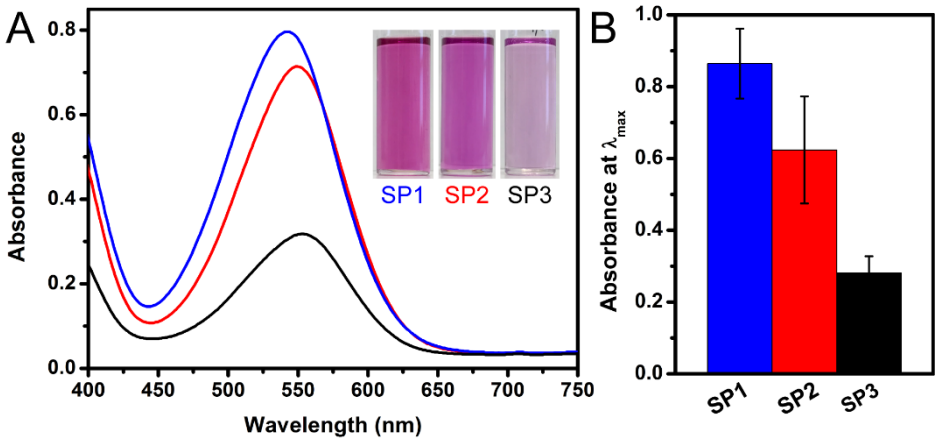

Figure 3.1. (A) Absorbance spectra of SP1-3 dissolved in HEA after absorption plateaued in darkness and the corresponding images, and (B) the absorption intensity at the maximum wavelength of 542nm, 549nm and 553nm respectively.

Next the negative photochromism of SP crosslinked in PHEA polymer was investigated. The prepared SP-PHEA films were pale yellow (**Figure 3.2B**) and characterized by UV-Vis spectroscopy showing no absorption peak in the visible range (**Figure A3.5**), indicating the ring-closed SP was the dominant form. The films gradually turned red in the absence of light, with λ_{max} at 537 nm, 544 nm and 549 nm for SP1, SP2 and SP3 respectively, indicating SP converted to ring-open MC. Over 10 days in the dark, the absorption of SP1 and SP2 films plateaued, while SP3 having a much lower absorbance still showed an increasing linear trend (**Figure 3.2A**). The overall absorption intensity curves of SP1 and SP2 showed non-linear increase. The saturated absorbance of SP3 was obtained after one month in the dark, with the absorbance of 1.35 ± 0.05. Since the absorption equilibrating time of SP3 was much longer than SP1 and SP2, the initial linear colour change was used to determine the colouration rates. To show the colour change more vividly, a "Yin-Yang" shaped SP1-PHEA/PHEA film was prepared by a three-step curing polymerization process (**Figure A3.6**). In a dark environment overnight, the SP1-

PHEA segments changed colour (the inserted pictures in **Figure 3.2A**), while the pale yellow PHEA segments remained unchanged.

The slopes of linearly fitted curves (**Figure A3.7**) were defined as the colouration rate in the absence of light, k_c, while $t_{1/2}$ was defined as the time to reach an absorbance at half maximum $Abs_{1/2}$ and are shown in **Table 3.1**. The colouration rate k_c of SP1&2 was an order of magnitude higher than SP3, and $t_{1/2}$ of SP3 was longer than SP1&2 by an order of magnitude. The much slower colouration speed of SP3 demonstrated that the majority of chromophores were still in the ring closed spiropyran form over a long period in the dark. The trend of absorption intensity is consistent with that observed for SP molecule dissolved in HEA solution, yet changed on a much longer time scale. The flexibility of SP in the crosslinked network was reduced compared to free SP molecules in solution, leading to a slower thermal ring-opening process. The λ_{max} of bulk samples showed the same trend as the solution samples, with SP3 having a higher λ_{max} followed by SP2 then SP1. SP2 and SP1 showed similar colouration rates and maximum absorbance behaviour in the dark, indicating the attachment number of SP in the polymer chains affects the thermal SP ↔ MC equilibrium. SP3 which exhibited a slower colouration speed and lower saturated absorbance is attributed to less flexibility (more conjugating positions) and polarity difference. The maximum absorbance of SP3 is around half that of SP1&2, which indicates that more than half of the SP3 mechanophore was still in ring-closed state. The incorporation of one more attachment point on SP effectively reduces the negative photochromism.

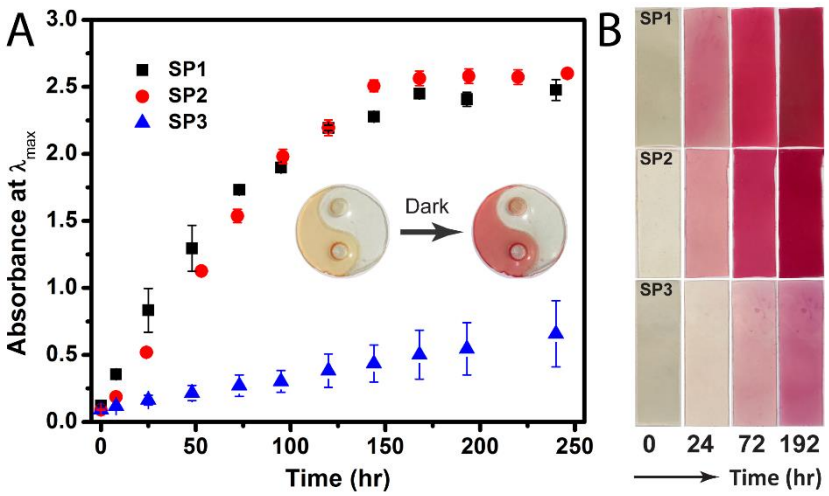

Figure 3.2. (A) Plot of absorbance at λ_{max} versus time in the dark for SP1-3 with 1 mol % crosslinkers (inserted pictures of SP1-PHEA/PHEA film in "Yin-Yang" symbol shape before and after being stored in the dark overnight, diameter: ~ 5 cm), and (B) images showing the colour change of SP1-3 relative to time.

Table 3.1. Data calculated from Figure 2: Wavelength at maximum absorbance λ_{max}, colouration rate k_c, absorbance at half $Abs_{1/2}$ and the corresponding time $t_{1/2}$ for SP1-3 contained PHEA samples kept in the dark.

Sample	λ_{max}	$k_c \times 10^{-2}$ (R^2)	$Abs_{1/2}$	$t_{1/2}$
SP1	537	2.6 (0.999)	1.2	41.5
SP2	544	2.0 (0.998)	1.3	57.4
SP3	549	0.23 (0.998)	0.68	246

3.4.2 Colour Activation by Swelling in Water

To investigate the colour activation by swelling in water, SP-PHEA films with 1 mol % crosslinker were immersed in water and subsequently swelled. Absorbance, sample size and mass change were measured as shown in **Figure 3.3A-C**. All samples became reddish pink as the size increased (**Figure 3.3D**, representative pictures not in scale), indicating spiropyrans were activated to ring-open MC. The inserted pictures in **Figure 3.3B** also showed the colour change of an SP3-PHEA/PHEA film in "Yin-Yang" shape after swelling in water for 1.5 hr; the four components of the symbol stuck well together even after swelling in water. The swelling ratios calculated by volume and mass expansion. These were identical for each of the samples although it was shown that the mass change

calculation was more accurate (**Figure 3.3C**). To investigate how the dark environment affects the colouration during swelling, a control sample, a mono functionalized SP was also synthesized, which remained pendant (non-crosslinked) in the polymer network with 1 mol % EGDMA as crosslinker (**Figure A3.8A**). The control SP-PHEA specimen did not show a colour change within 4 hours in water, although the swelling ratio was the same as the other SP samples (**Figure A3.8B-E**). This confirms that the SP1-3 ring-opening process within 4 hours was caused by the swelling force rather than the solvatochromism/negative photochromism from the hydrophilic environment. After the swelling ceased the absorbance continued to increase gradually over 40 hr. This differs from the swelling in organic solvents for SP in non-polar polymers as reported by Moore's group.[23] Here they observed an increase in absorbance at the same rate as the swelling. As with SP/non-polar samples mechanical force partially induces SP to MC colour change,[27] however for our SP/polar samples the additional polar effect due to the polymer and water, continued to facilitate further ring opening of the SP to MC. A comparison of the time scale for colour equilibrium of swelling in water with dry samples in the dark, the swelling force activating the mechanophore speeds up the colour change.

The polar effect induced by the hydrophilic environment was also observed for the control sample which was not affected by swelling. After 4 hr, the absorption peak at 519 nm began to appear on the control sample demonstrating the isomerization to ring-open MC; the absorption plateaued after 4 days (**Figure A3.8C**), a longer period than the mechanochromic SP1-3 samples (2 days). The study of non-polar polymer swelling in organic solvent by Moore *et al* assumed that an early plateauing of the fluorescence in THF was due to solvatochromism,[23] however here the swelling process of the control SP in polar PHEA demonstrated that the polar effect slowed down the colouration process, compared to colouration of a dry sample kept in the dark (**Figure A3.8E**). This shows that the swelling force can accelerate the mechano-active SP ring-opening reaction. Additionally, Stretching can also induce ring-opening reaction of SP1-3 PHEA, however the activation ratio was too low to be measured until samples fracture. It's believed that the higher ratio of ring-opening triggered by swelling than that induced by stretching is due to the multi-direction expansion of swelling.

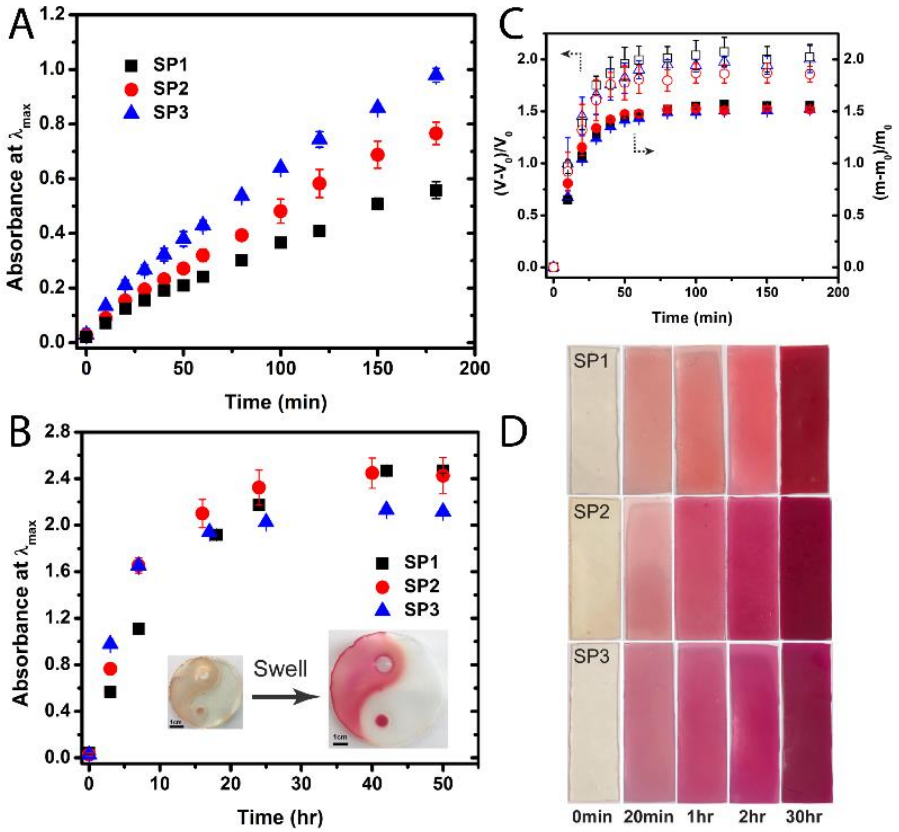

Figure 3.3. Absorbance as a function of the swelling time in water for SP1-3 samples with 1 mol % crosslinker (λ_{max} of SP1 at 522 nm, SP2 at 532 nm and SP3 at 540 nm): (A) over 3hr and (B) over 50 hr (pictures of a SP3-PHEA/PHEA film in "Yin-Yang" shape before and after swelling in water for 1.5 hr as inserted, scale bar: 1 cm); (C) volume and mass change ratio of the three samples versus the immersing time in water; (D) the representative images showing the colour change relative to the swelling time (images are not to scale).

Table 3.2. Summary of λ_{max}, k_c within 200 min, $Abs_{1/2}$ and $t_{1/2}$ for SP1-3 contained PHEA samples swelling in water.

Sample	λ_{max}	$k_c \times 10^{-3}$ (R^2)	$Abs_{1/2}$	$t_{1/2}$ (hr)
SP1	522	3.0 (0.996)	1.2	7.1
SP2	532	4.2 (0.997)	1.2	5.4
SP3	540	5.5 (0.993)	1.1	3.4

Differences in activation rate by swelling were observed for SP1-3, with SP3 > SP2 > SP1 (**Figure 3.3A** & **Table 3.2**). The faster swelling activation rate of SP3 film is influenced by the multi-axial deformation due to the increased crosslinking points in the polymer network. SP1 and SP2 differed in activation rate due to their attachment positions; the attachment points on *N*-position is more advantageous than on 5' position in force activation due to the bond cleavage distance, which is consistent with our previous study.[25] After two days immersed in water, the absorbance of SP1-3 samples plateaued, indicating an equilibrium of SP ↔ MC toward MC was reached. SP1 and SP2 showed the identical absorbance within statistical error, slightly higher than SP3. This is due to SP1&2 being more influenced by the polar environment, as discussed earlier.

3.4.3 Decolouration Studies

The coloured films can revert to light yellow by exposure to white light leading to ring closure of MC to SP.[12, 19] The decolouration of coloured SP1-3 films in swollen and corresponding dehydrated states were investigated by measuring the absorbance over time under white light. The colour fading time (t_f) was determined by the intersection of the two tangent lines in both wet and dry conditions (**Figure 3.4**). The swollen films were shown to bleach within 1-2 min, while all the dehydrated films took significantly longer time to decolour, in 30-110 min. This demonstrates that the stability of MC is poorer in the wet swollen state than the dry state. In this case, water acts as a plasticiser in the swollen films [28], leading to an increase in free volume and flexibility, which facilitates the MC ring closure process. The difference of SP1-3 decolouration in the swollen state was minor with t_f summarized in **Table 3.3**.

It was noted that a large difference in the fading time t_f of SP1-3 polymer films was observed in the dehydrated state (**Figure 3.4B**), with the order of SP1 < SP2 < SP3. The colour fading times t_f were 30 min, 62 min and 108 min for SP1-3 respectively. The decolouration rates (k_f) were determined by fitting the initial linear range (the first tangent line) (**Figure A3.9**), resulting in 0.033, 0.016 and 0.0082 for SP1-3 respectively (**Table 3.3**). SP1 was shown to have a faster bleaching rate and is attributed to the attachment point at 5'-position speeding up the ring closure under visible light as previously reported.[29] The slow decolouration speed observed for SP3 is believed to be

due to a higher number of cross-linkable points which reduces the flexibility of conformational isomerization of the mechanophore.

Noticeably, λ_{max} of the corresponding dehydrated films shifted towards longer wavelength compared to that of the swollen films, with $\Delta\ \lambda_{max}$ of 17, 16 and 12 nm for SP1-3 respectively (**Figure A3.10**). This reflects the change in polarity due to the polar (water) environment. The polarity decreases with the removal of water, resulting in an increase of λ_{max} after dehydration. The λ_{max} of dehydrated SP1-3 PHEA samples was close to that of coloured films in the dark (**Figure 3.2** and **Table 3.1**), and is slightly longer due to the exposure to moisture.[28, 30] Utilizing the differences SP causes on λ_{max} shift in dissimilar environments, there is the potential for solvent sensors which respond to changes in the polarity.

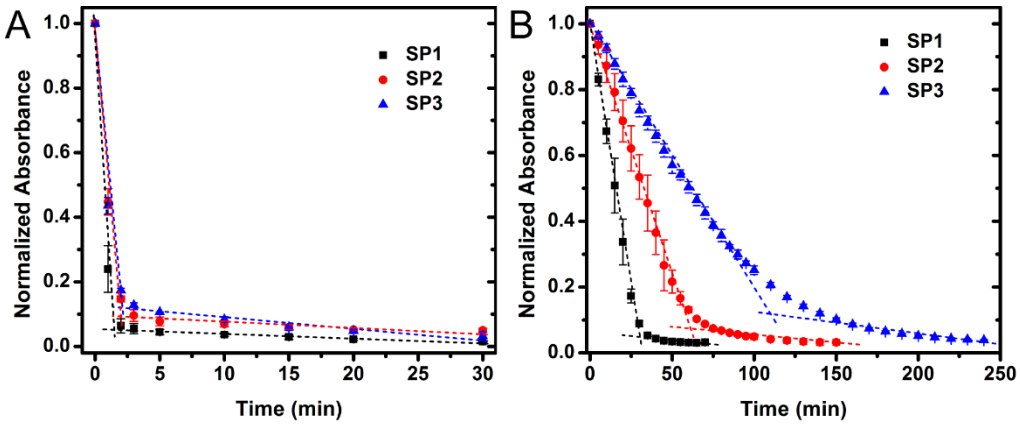

Figure 3.4. Decrease of absorbance at λ_{max} of SP1-3 PHEA (1 mol % crosslinkers) swollen films under white light irradiation in (A) swollen and (B) corresponding dehydrated states. Colour fading time t_f is defined as the intersection of two tangent lines (dot lines).

Table 3.3. Summary of λ_{max}, colour fading time t_f and decolouration rate k_f of SP1-3 samples in swollen and dehydrated states under white light, and the shift of λ_{max} from swollen to dehydrated state.

Sample	Swollen state			Dehydrated state			$\Delta\ \lambda_{max}$
	λ_{max}	t_f (min)	$k_f \times 10^{-1}$	λ_{max}	t_f	$k_f \times 10^{-2}$	(nm)
SP1	522	1.5	- 5.3	539	30	- 3.3	17
SP2	532	2.0	- 4.5	548	62	- 1.6	16
SP3	540	2.1	- 4.4	552	108	- 0.82	12

3.4.4 Colour Switchability

Colour switchability is essential when a sensor is required to be reused to track usage history. By turning white light on and off, the coloured SP films switch between pale yellow and red colour due to the isomerization between SP and MC. Based on the two decolouration conditions mentioned above, two cyclic tests were conducted, a) irradiating with white light then left in the dark while the sample was in the swollen state and b) swelling the sample in water, drying in the dark and then irradiating with white light as shown in **Figure 3.5**. The absorbance was normalized based on the maximum value of the swollen state for a direct comparison of the two different switching modes.

For the tests irradiating white light on swollen films (**Figure 3.5A**), all samples showed colour switchability over ten cycles. Upon white light irradiation, the ring-closed SP was the dominant form, and the MC signal after ten cycles stabilized at around 10% of original bleached value. The intensity of the sample due to MC, kept in the dark after swelling and white light irradiation was found to drop with increasing ring open-closure repetitions, with the absorbance of MC decreasing to 45-60% of the original intensity for SP1-3. This cyclic fatigue is due to the photodegradation of MC when irradiated by white light.[31-33] No significant difference in the absorption signal among SPs was observed (**Figure 3.5A**), which is expected since **Figure 3.4A** showed all three SPs had a similar rate of ring closure when exposed to white light. For the tests irradiating white light onto dehydrated films after swelling, similar trends of MC signal at bleached and coloured states were recorded, with the degree of fatigue mainly dependant on the number of ring open-closure cycles. However, SP1 showed faster fatigue than SP2&3 after ten cycles especially in the dehydrated sample cycles (**Figure 3.5B**), although the time for SP1 ring closure was shorter than SP2&3 (**Figure 3.4B**).

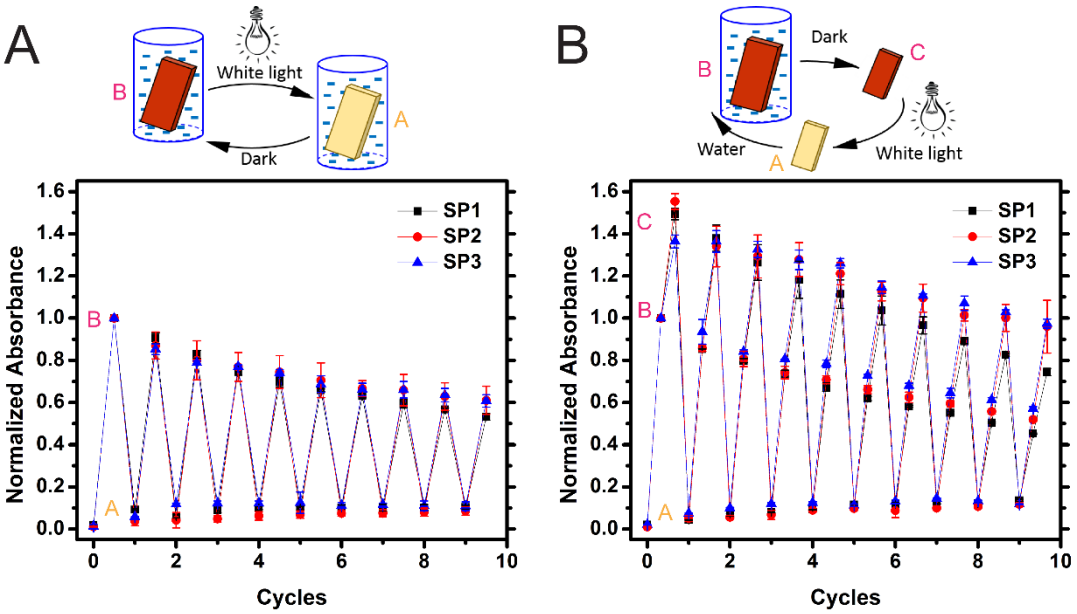

Figure 3.5. (A) Scheme of cyclic absorbance measurements between SP and MC by white light irradiation and subsequent storage in the dark for recovery, and the absorption plot of the SP1-3 films (1 mol % crosslinkers) in water; (B) scheme of cyclic absorbance measurements between SP and MC by swelling in water, dehydration in the dark at ambient conditions and white light irradiation, and the absorption plot of the SP1-3 films. The absorbance is normalized based on the maximum value in the swollen state.

3.4.5 Effect of Cross-link Density on Colour Activation in Water

It has been reported that swelling activation of SP non-polar polymer in organic solvent is cross-link density dependant.[23] Here, a series of SP3-PHEA with 1-10% crosslinker density were prepared, varying EGDMA content with a constant concentration of SP3, to study the effect of cross-link density on colour activation in a polar polymer environment. The absorbance with time immersed in water and the corresponding mass change were recorded and shown in **Figure 3.6**. All samples achieved maximum absorbance and mass after 50 and 2 hr respectively. The swelling ratio reduced with increasing cross-linking density, and consequently the absorption signal of MC also decreased. Although the SP chromophore would slowly form MC without swelling, here the crosslinking density can be used to control the rate of colour activation of SP3. This can be attributed to the reduced water content in the polymer network, causing a difference in the polarity of the matrix and free volume of the polymer chains. Interestingly, the absorption intensity in

this instance due to the degree of crosslinking it does not follow the linear dependence reported for SP/non-polar polymer systems in organic solvent.[23]

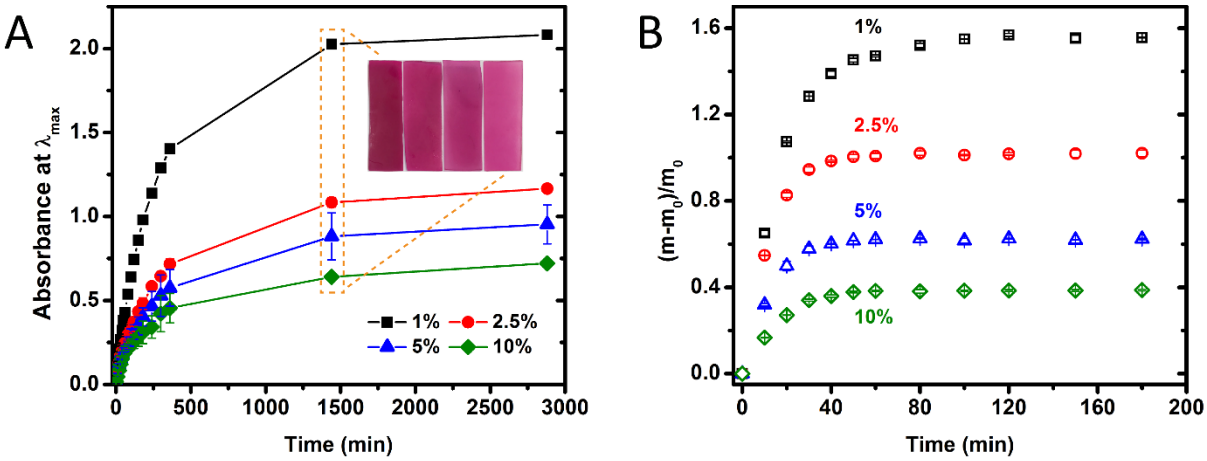

Figure 3.6. (A) Influence of crosslinking density on absorption intensity as a function of the swelling time for SP3-PHEA films (1 mol %, 2.5%, 5% and 10%), and the inset images of different crosslinked films swelling over 1 day; (B) swelling ratio of the SP3-PHEA films at different crosslinking density.

3.5 Conclusion

We have prepared three spiropyran molecules with two and three acrylate attachment positions which were subsequently covalently crosslinked with polar HEA monomer via white light induced polymerization. The effect of the polar environment on SP colouration (negative photochromism) was studied in HEA solution and crosslinked PHEA bulk materials, with the latter having a much longer activation time. SP-PHEA polymer films showed activation by swelling in water, due to mechanochromism, which was confirmed by incorporating a single functional SP into PHEA matrix which resulted in no colour change during swelling. De-swelling in the dark could not reverse the coloured MC to colourless SP due to the polar matrix. Under swollen conditions, the colour reversibility can be achieved by exposure to visible light or stored in the dark, which was the same for dry bulk samples. It was determined that the tri-functional SP3 was least affected by negative photochromism, resulting in the lowest absorption intensity when stored in the dark, however it displayed the fastest colour activation by swelling. SP3 also exhibited a significantly slower decolouration rate relative to SP1 and SP2 once dehydrated after swelling. The colour switchability was dependent on the number of cycles, with 45-60%

absorption intensity remaining in the MC form after 10 cycles. The cross-linking density affected the rate and degree of SP ring-opening, with the absorption results showing that the lowest cross-linking density presented the highest absorption intensity. These results demonstrated that SP3 in PHEA has a greater resistance to the polar environment in switching to coloured MC, and that the absorption can be regulated by controlling the degree of cross-linking. The switchable colour triggering by swelling in water and light offer opportunities to tailor polar hydrophilic swellable films with colour changing properties suitable for biomedical applications such as biosensors or optical storage devices.

3.6 References

(1) Davis, D. A.; Hamilton, A.; Yang, J.; Cremar, L. D.; Van Gough, D.; Potisek, S. L.; Ong, M. T.; Braun, P. V.; Martinez, T. J.; White, S. R.; Moore, J. S.; Sottos, N. R. Force-induced activation of covalent bonds in mechanoresponsive polymeric materials. *Nature* 2009, 459, 68-72.

(2) O'Bryan, G.; Wong, B. M.; McElhanon, J. R. Stress sensing in polycaprolactone films via an embedded photochromic compound. *ACS Appl. Mater. Interfaces* 2010, 2, 1594-1600.

(3) Gossweiler, G. R.; Hewage, G. B.; Soriano, G.; Wang, Q.; Welshofer, G. W.; Zhao, X.; Craig, S. L. Mechanochemical Activation of Covalent Bonds in Polymers with Full and Repeatable Macroscopic Shape Recovery. *ACS Macro Lett.* 2014, 3, 216-219.

(4) Zhang, H.; Chen, Y.; Lin, Y.; Fang, X.; Xu, Y.; Ruan, Y.; Weng, W. Spiropyran as a Mechanochromic Probe in Dual Cross-Linked Elastomers. *Macromolecules* 2014, 47, 6783-6790.

(5) Li, M.; Liu, W.; Zhang, Q.; Zhu, S. Mechanical Force Sensitive Acrylic Latex Coating. *ACS Appl. Mater. Interfaces* 2017, 9, 15156-15163.

(6) Kempe, F.; Brugner, O.; Buchheit, H.; Momm, S. N.; Riehle, F.; Hameury, S.; Walter, M.; Sommer, M. A Simply Synthesized, Tough Polyarylene with Transient Mechanochromic Response. *Angew. Chem. Int. Ed.* 2018, 57, 997-1000.

(7) Shree, S.; Schulz-Senft, M.; Alsleben, N. H.; Mishra, Y. K.; Staubitz, A.; Adelung, R. Light, Force, and Heat: A Multi-Stimuli Composite that Reveals its Violent Past. *ACS Appl. Mater. Interfaces* 2017, 9, 38000-38007.

(8) Beiermann, B. A.; Davis, D. A.; Kramer, S. L. B.; Moore, J. S.; Sottos, N. R.; White, S. R. Environmental effects on mechanochemical activation of spiropyran in linear PMMA. *J. Mater. Chem.* 2011, 21, 8443.

(9) Grady, M. E.; Beiermann, B. A.; Moore, J. S.; Sottos, N. R. Shockwave loading of mechanochemically active polymer coatings. *ACS Appl. Mater. Interfaces* 2014, 6, 5350-5355.

(10) Peterson, G. I.; Larsen, M. B.; Ganter, M. A.; Storti, D. W.; Boydston, A. J. 3D-printed mechanochromic materials. *ACS Appl. Mater. Interfaces* 2015, 7, 577-583.

(11) Such, G.; Evans, R. A.; Yee, L. H.; Davis, T. P. Factors Influencing Photochromism of Spiro-Compounds Within Polymeric Matrices. *J. Macromol. Sci., Polym. Rev.* 2003, 43, 547-579.

(12) Zhou, J.; Li, Y.; Tang, Y.; Zhao, F.; Song, X.; Li, E. Detailed investigation on a negative photochromic spiropyran. *J. Photochem. Photobiol., A* 1995, 90, 117-123.

(13) Tian, W.; Tian, J. An insight into the solvent effect on photo-, solvato-chromism of spiropyran through the perspective of intermolecular interactions. *Dyes Pigm.* 2014, 105, 66-74.

(14) Shiraishi, Y.; Itoh, M.; Hirai, T. Thermal isomerization of spiropyran to merocyanine in aqueous media and its application to colourimetric temperature indication. *Phys. Chem. Chem. Phys.* 2010, 12, 13737-13745.

(15) Sunamoto, J.; Iwamoto, K.; Akutagawa, M.; Nagase, M.; Kondo, H. Rate control by restricting mobility of substrate in specific reaction field. Negative photochromism of water-soluble spiropyran in AOT reversed micelles. *J. Am. Chem. Soc.* 1982, 104, 4904-4907.

(16) Kim, T. A.; Beiermann, B. A.; White, S. R.; Sottos, N. R. Effect of Mechanical Stress on Spiropyran-Merocyanine Reaction Kinetics in a Thermoplastic Polymer. *ACS Macro Lett.* 2016, 5, 1312-1316.

(17) Chen, H.; Yang, F.; Chen, Q.; Zheng, J. A Novel Design of Multi-Mechanoresponsive and Mechanically Strong Hydrogels. *Adv. Mater.* 2017, 29, 1606900.

(18) Abdollahi, A.; Alinejad, Z.; Mahdavian, A. R. Facile and fast photosensing of polarity by stimuli-responsive materials based on spiropyran for reusable sensors: a physico-chemical study on the interactions. *J. Mater. Chem. C* 2017, 5, 6588-6600.

(19) Feeney, M. J.; Thomas, S. W. Tuning the Negative Photochromism of Water-Soluble Spiropyran Polymers. *Macromolecules* 2018, 51, 8027-8037.

(20) Marini, A.; Munoz-Losa, A.; Biancardi, A.; Mennucci, B. What is solvatochromism? *J. Phys. Chem. B* 2010, 114, 17128-17135.

(21) Julia-Lopez, A.; Hernando, J.; Ruiz-Molina, D.; Gonzalez-Monje, P.; Sedo, J.; Roscini, C. Temperature-Controlled Switchable Photochromism in Solid Materials. *Angew. Chem. Int. Ed.* 2016, 55, 15044-15048.

(22) Schaudel, B.; Guermeur, C.; Sanchez, C.; Nakatani, K.; Delaire, J. A. Spirooxazine-and spiropyran-doped hybrid organic–inorganic matrices with very fast photochromic responses. *J. Mater. Chem.* 1997, 7, 61-65.

(23) Lee, C. K.; Diesendruck, C. E.; Lu, E.; Pickett, A. N.; May, P. A.; Moore, J. S.; Braun, P. V. Solvent Swelling Activation of a Mechanophore in a Polymer Network. *Macromolecules* 2014, 47, 2690-2694.

(24) Li, M.; Lei, L.; Zhang, Q.; Zhu, S. CO2 -Breathing Induced Reversible Activation of Mechanophore within Microgels. *Macromol. Rapid Commun.* 2016, 37, 957-662.

(25) Qiu, W.; Gurr, P. A.; da Silva, G.; Qiao, G. G. Insights into the mechanochromism of spiropyran elastomers. *Polym. Chem.* 2019, 10, 1650-1659.

(26) Ziółkowski, B.; Florea, L.; Theobald, J.; Benito-Lopez, F.; Diamond, D. Self-protonating spiropyran-co-NIPAM-co-acrylic acid hydrogel photoactuators. *Soft Matter* 2013, 9, 8754-8760.

(27) Fang, X.; Zhang, H.; Chen, Y.; Lin, Y.; Xu, Y.; Weng, W. Biomimetic Modular Polymer with Tough and Stress Sensing Properties. *Macromolecules* 2013, 46, 6566-6574.

(28) Ellis, T.; Karasz, F. Interaction of epoxy resins with water: the depression of glass transition temperature. *Polymer* 1984, 25, 664-669.

(29) Balmond, E. I.; Tautges, B. K.; Faulkner, A. L.; Or, V. W.; Hodur, B. M.; Shaw, J. T.; Louie, A. Y. Comparative Evaluation of Substituent Effect on the Photochromic Properties of Spiropyrans and Spirooxazines. *J. Org. Chem.* 2016, 81, 8744-8758.

(30) Kemal, E.; Adesanya, K. O.; Deb, S. Phosphate based 2-hydroxyethyl methacrylate hydrogels for biomedical applications. *J. Mater. Chem.* 2011, 21, 2237-2245.

(31) Malatesta, V.; Renzi, F.; Wis, M. L.; Montanari, L.; Milosa, M.; Scotti, D. Reductive degradation of photochromic spiro-oxazines. Reaction of the merocyanine forms with free radicals. *J. Org. Chem.* 1995, 60, 5446-5448.

(32) Demadrille, R.; Rabourdin, A.; Campredon, M.; Giusti, G. Spectroscopic characterisation and photodegradation studies of photochromic spiro[fluorene-9,3′-[3′H]-naphtho[2,1-b]pyrans]. *J. Photochem. Photobiol. A* 2004, 168, 143-152.

(33) Radu, A.; Byrne, R.; Alhashimy, N.; Fusaro, M.; Scarmagnani, S.; Diamond, D. Spiropyran-based reversible, light-modulated sensing with reduced photofatigue. *J. Photochem. Photobiol. A* 2009, 206, 109-115.

Chapter 4: Sensitive Mechanochromic Elastomers with Low Activation Energy

4.1 Chapter Perspectives

Improving the mechano-response of mechanophore-linked polymers is essential for their practical applications such as sensors and packaging. Other than modifying the SP molecule, another effective approach to improving the mechano-response is designing polymer architecture that can facilitate the force transmitted to SP and polymer chain alignment. In this chapter, a multi-network strategy is adopted to integrate our new designed trifunctional SP in a pre-stretched first network of polyacrylates to lower the colour activation threshold. The onset of colour activation strain is demonstrated to be tunable by adjusting the network components. A new term U_A is used to represent the macroscopic energy required for the colour activation. Through a comparison of U_A presented in this work with previously reported elastomers, the lowest colour activation energy so far is achieved. In addition, the comparison between mechanical and UV light activations shows that the double-network systems remarkably improved the conversion ratio of SP to MC by stretching.

4.2 Introduction

Mechanochromic compounds which are triggered because of a chemical structure change, fall into two main categories, either based on isomerization or radical formation mechanisms.[1, 2] Isomerisation-based mechanophores include spiropyran, spirothiopyran, rhodamine and naphthopyran, which all contain a spiro-junction that undergoes ring-opening under force, to give a resonance structure with a change in colour.[3-6] Mechanophores based on radical formation are less reported, with diarylbibenzofuranone being one such example.[7, 8] Among the developed mechanophores, spiropyran (SP) is one of the most studied and undergoes a ring-opening reaction to form a purple coloured merocyanine (MC) structure. SP has been incorporated into a variety of polymers, including polyacrylates, polyurethane, and PDMS.[9-12] In these examples, most are in the form of linear polymers or simple networks, relying on the intrinsic elasticity of the materials to transfer an applied force to the mechanophores. Examples which aimed to utilize increased intermolecular forces through hydrogen bonding and led to improved strength of the polymer networks, were achieved with the introduction of ureidopyrimidinone moieties along a PU backbone.[13, 14] However, these modified SP-PUs still required a large onset of activation strains (400–500%) for colour activation. A low activation strain and stress are essential to make such mechanochromic elastomers useful in practical applications. Relying on simple polymer structures has been a major challenge in achieving low strain/stress activation. Additionally, the ratio of colourless SP converting to ring-opened MC induced by force has been reported significantly lower than that activated by UV light, indicating a low efficiency of SP as a mechanophore.[10, 15] Improving the equilibrium towards the coloured ring-opened MC isomer when triggered by force needs to be improved, given that the synthesis of cross-linkable SP molecules is not facile. Therefore, more advanced polymer architectures may provide new pathways to improve the mechanochromic sensitivity (low strain/stress) and efficiency of SP transforming to MC.

Double-network (DN) hydrogels have been well known for their distinct mechanical properties which in spite of their large water content, exhibit tough and extendible properties.[16, 17] As chain alignment and SP orientation are crucial to the mechanical activation of SP to MC, [18] pre-stretching the polymer chain with the mechanophores linked will be a strategy to reduce the threshold of activation. To achieve this, the first-

network needs to be rigid and brittle in order to dissipate mechanical energy, while the second-network is required to be ductile allowing for a large deformation. This contrasting nature of the first and second networks results in the fascinating mechanical properties exhibited by DN hydrogels. However, this principle was initially limited to hydrogels for over a decade since their invention, and was not translated to solvent-free elastomers due to the low swelling capability of neutral polymers.[19] In 2014, the Creton group successfully applied the DN principles to develop multi-network polyacrylate elastomers, which exhibited excellent mechanical properties.[20] When the first-network polyacrylate was swollen in acrylate monomers followed by polymerization of the second-network, a pre-stretched first-network was formed. A triple-network obtained by one more swelling-curing step further achieved a higher strength and an earlier stress hardening region.[20] This multi-network elastomer is ideal for incorporation of mechanophores. We propose that the spiropyran covalently linked in the first network of multi-network elastomer may result in an even better and lower activation threshold with improved efficiency.

Herein, we synthesized double- and triple-network polyacrylates with tri-functional SP crosslinked in the first-network and investigated their mechanochromic performance. For a better representation of the activation threshold, the activation energy of colour change (U_A) considering both stress and strain was used, which was calculated by using area underneath the onset of colour change on stress-strain curve. The influences of SP concentration, solvent volume in preparation of first-network, and types of monomer in the second-network were examined. A comparison of SP activation by stretching and UV irradiation was also conducted to investigate any advantages of employing a DN architecture for SP mechanical activation. Cyclic tensile tests were performed to study the mechanochromic reversibility. Through a comparison of U_A, we found that the newly designed elastomers adopting multi-network structure showed the lowest activation energy for SP-linked elastomers ever reported.

4.3 Experimental Methods

4.3.1 Materials

Butyl acrylate (BA, 99%, Sigma), methyl acrylate (MA, 99%, Sigma) and 1,4-butanediol dimethacrylate (BDMA, 95%, Sigma) were passed through basic aluminium oxide to remove the inhibitor monomethyl ether hydroquinone prior to use. Phenylbis(2,4,6-trimethylbenzoyl)phosphine oxide (BAPOs, 97%, Sigma) was used as received. Toluene (AR grade) and petroleum ether (bp. 40 – 60 ^{o}C, AR grade) were used as received. Tri-methacrylate spiropyran was synthesized according to our previous work.[21, 22]

4.3.2 Bulk Sample Preparation

Preparation of first-network. The concentration of crosslinkers (based on total methyl acrylate groups of SP and BDMA) were fixed at 3.5 mol % relative to monomer BA. As an example, for sample $BA_{0.5}$ (0.5 mol % SP), SP (10.3 mg, 0.0174 mmol, 0.005 equiv), BDMA (7.71 μL, 0.0349 mmol, 0.01 equiv), photo initiator BAPOs (5.83 mg, 0.0140 mmol, 0.004 equiv), BA (0.5 mL, 3.49 mmol, 1 equiv), and toluene (0.5 mL) were mixed thoroughly in a vial under argon. The homogeneous solution was injected into a glass mould (width:1.6 cm, length 5-5.5 cm, thickness: 0.4-0.5mm) with a silicone spacer sandwiched by two glass sheets, which was subsequently exposed to white light (4W cool white light, 350 lumens) for 2 hr for polymerization. Once cured, the samples were removed from the mould and soaked in a solution of petroleum ether (50 vol %) and toluene (50 vol %) for two days, with regular changing of the solvent, to remove any unreacted species. The swollen samples were then dried *in vacuo* to a constant mass. Samples $BA_{0.83}$ and $BA_{1.17}$ (0.83 mol % and 1.17 mol % of SP), were prepared in the same method varying the recipes accordingly. For the samples prepared with 40% and 60% toluene, the concentrations of SP were fixed at 0.83 mol % and the volume ratios of BA to toluene were changed to 6:4 and 4:6, respectively. Single networks (SN) were prepared at SP concentration of 0.8 wt % relative to butyl acrylate. This SP weight content was comparable to that in SP-$PBA_{DN\text{-}0.83}$ prepared with 50% toluene. Two SNs were prepared, in the presence of toluene (BA_T) and without toluene (BA_0).

Preparation of double-network. The dried first-network samples were swollen in excess volume of solution containing monomer BA (1 equiv), crosslinker BDMA (0.02 mol % equiv) and photo initiator BAPOs (0.4 mol % equiv) to a constant mass, which typically took 5 – 6 hr. The swollen samples were removed from the solution, sandwiched between two glass sheets and sealed within petri dishes to avoid oxygen and evaporation. They were then exposed to white light for 2 hr to effect polymerization affording double-network specimens. The specimens were soaked in mixed solvent of petroleum ether and toluene for two days, with regular changing of the solvent, to remove any unreacted species. The swollen samples were dried under vacuum until a constant mass. These DN elastomers were denoted by BABA, specifically $BA_{0.5}BA$, $BA_{0.83}BA$, $BA_{1.17}BA$ for different SP concentration in the first-network. For a different polyacrylate as a second-network, a $BA_{0.83}$ was swollen in a solution of monomer MA (1 equiv), crosslinker BDMA (0.02 mol % equiv) and photo initiator BAPOs (0.4 mol % equiv) to a constant mass; and then repeated as before. This sample was denoted by $BA_{0.83}MA$.

Preparation of triple-network. Triple-network samples were obtained by repeating the swelling and curing process with $BA_{0.83}BA$ and $BA_{0.83}MA$. The specimens were labelled as $BA_{0.83}BABA$ and $BA_{0.83}MAMA$, respectively.

4.3.3 Characterization

Tensile tests were performed uniaxially at room temperature on an Instron 5944 Microtester with Bluehill material testing software using a 2 kN loading cell. Dog-bone shaped specimens (gauge length: 15 mm, gauge width: 4 mm, total length: 50 mm) were used for tensile measurements cut from the obtained films using a cutting die. Tensile measurements were performed on the specimens fastened between two grips and tested in duplicate or triplicate at a strain rate of 0.5 mm s^{-1} (**Figure A4.1**). Video recording was performed during testing for colour analysis. The colour change was quantified by RGB analysis. RGB values were determined after white balance calibration in Adobe Photoshop™ software. The blue colour channel ratio was determined as: rBc = Blue/(Red + Green + Blue), and the same calculation method was used for red and green colour channel ratios, rRc and rGc, respectively. The onset strain of colour activation was determined as the intersection of two tangent lines on the curves of rBc against tensile strain. Differential scanning calorimetry (DSC) measurements were carried out on a

Perkin Elmer DSC 8500 with a heating rate of 10 °C min^{-1}. T_g values were determined by the midpoint of the transition range (**Figure A4.2**). Absorbance spectra were obtained on a Shimadzu UV−Vis Scanning Spectrophotometer (UV-2101 PC) with a fast scanning rate of 1 nm intervals.

The pre-stretched ratios of the first-network in the final elastomers, $\lambda_{prestretch}$, were calculated by the equation of h_{DN}/h_{SN} (h_{TN}/h_{SN}), where $h_{SN,}$ h_{DN} and h_{TN} represents the thickness of the single (first), double and triple-network respectively. The swollen ratios of the first-network in the double-network or triple-network $\lambda_{swollen}$ were calculated as either m_{DN}/m_{SN} or m_{TN}/m_{SN} respectively, where m_{SN}, m_{DN} *and* m_{TN} represent the mass of the single (first), double and triple-network.

4.4 Results and Discussion

A trifunctional SP was employed in this work due to its increased chain-aligning ability under swelling, afforded by more cross-linkable points on the molecule.[22, 23] SP was incorporated into single network (SN) via free radical polymerization initiated by white light. The SP-based SN was using butyl acrylate (BA) as a monomer and toluene as a solvent. Unreacted BA and toluene were removed prior to fabrication of the second-network. The SN was then swollen in acrylate monomers (BA or MA) followed by photo polymerization to form double-network (DN) (**Scheme 4.1**); here the first-network was pre-stretched by swelling and locked by the second-network formation, which facilitated chain alignment and orientation of SP mechanophores. A triple-network (TN) was obtained by a repeated swelling-curing process with a DN.

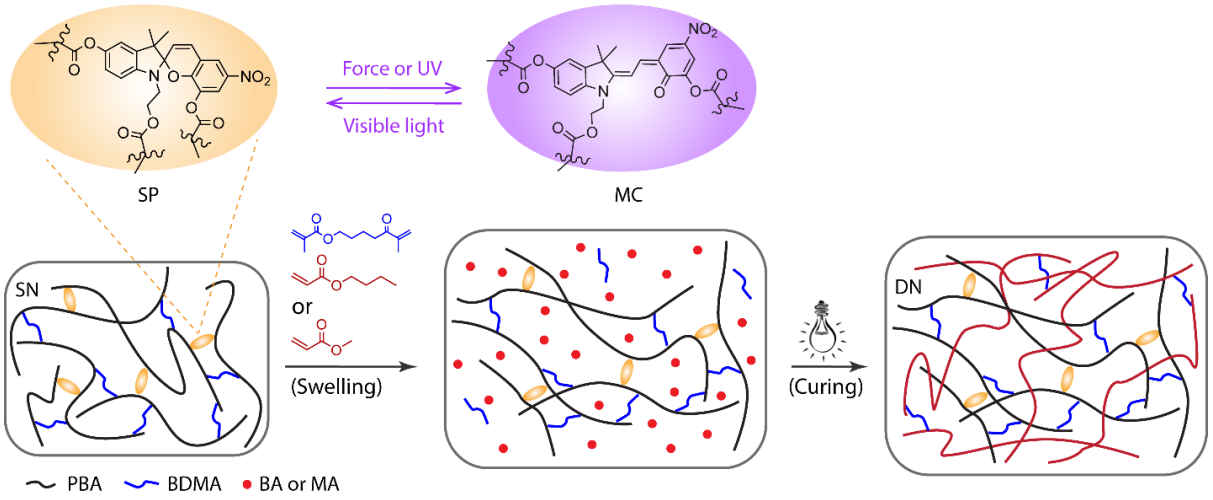

Scheme 4.1. First-network SP-poly(butyl acrylate) was swollen in a solution of acrylate monomer and co-crosslinker, followed by white light polymerization to afford DN elastomers. SP converts to MC under external stimuli, either by force or UV irradiation, and the process is reversible upon relaxation or exposure to visible light.

DN hydrogels with good mechanical properties typically consist of a rigid first-network and a ductile second-network.[16, 24] Here, for elastomers, we adopt this approach and use double-network polyacrylates achieved with a high cross-link density in the first-network and a low cross-link density in the second-network. For the preparation, the pre-stretched first network was formed by swelling in the monomer solution followed by polymerization of the second network. As such, a series of SP based DN elastomers were prepared by varying the SP concentration, toluene volume in the first-network and the type of acrylate used in the second-network (denoted by BABA or BAMA), to study the factors which influence their mechanochromic behaviour. Two SNs, with toluene solvent (BA_T) and without toluene (BA_0), and two TN ($BA_{0.83}$BABA and $BA_{0.83}$MAMA) were also prepared for a comparison with the DNs. The compositions of the elastomers, pre-stretched and swollen ratio of the first-network are summarized in **Table A4.1**. The mechanical properties and mechanochromic performance of the elastomers are summarized in **Table 4.1**.

Table 4.1. Mechanical properties of the prepared elastomers: T_g, ultimate strength σ_{break}, strain at break ε_{break}, onset of colour activation strain ε_{MC}, onset of colour activation stress σ_{MC} and colour activation energy U_A

Sample	T_g (°C)	σ_{break} (MPa)	ε_{break} (%)	ε_{MC} (%)	σ_{MC} (MPa)	U_A (MJ m^{-3})
BA_0	-44.6 ± 0.47	0.57 ± 0.07	86 ± 6	/	/	/
BA_T	-44.9 ± 0.10	0.24 ± 0.02	143 ± 17	/	/	/
$BA_{0.5}BA$	-46.9 ± 0.15	7.95 ± 0.18	347 ± 11	158 ± 1.1	1.39 ± 0.17	0.63 ± 0.08
$BA_{0.83}BA$	-46.4 ± 0.30	7.57 ± 1.14	335 ± 39	159 ± 1.6	1.40 ± 0.05	0.71 ± 0.06
$BA_{1.17}BA$	-46.6 ± 0.25	7.25 ± 0.62	328 ± 25	156 ± 2.8	1.40 ± 0.21	0.60 ± 0.03
$BA_{0.83(40)}BA$	-46.7 ± 0.46	8.04 ± 0.81	278 ± 14	131 ± 3.7	1.30 ± 0.18	0.54 ± 0.07
$BA_{0.83(60)}BA$	-47.5 ± 0.20	6.04 ± 0.30	397 ± 27	189 ± 12.5	1.38 ± 0.18	0.71 ± 0.13
$BA_{0.83}MA$	10.5 ± 1.49	8.55 ± 0.31	471 ± 64	118 ± 4.4	1.11 ± 0.03	0.63 ± 0.04
$BA_{0.83}BABA$	-47.9 ± 0.23	/	/	75 ± 3.8	0.81 ± 0.14	0.19 ± 0.03
$BA_{0.83}MAMA$	-8.9 ± 0.71	/	/	39 ± 1.4	0.72 ± 0.02	0.10 ± 0.02

4.4.1 Mechanochromic Properties of SN vs DN

Poly(butylacrylate) is an elastomer with a low glass transition temperature (T_g), thus it behaves as an elastic polymer at room temperature. The T_g measured for the prepared samples from DSC are summarized in **Table 4.1**. Interestingly, although the mechanical properties of the DNs were better than SNs, the T_g for the DNs were lower than SNs (comparing the BA series). This is attributed to the swelling-curing process endowing the DN with more free volume for the polymer chains. A further decreased T_g was detected for TN (more significant for $BA_{0.83}MA$ and $BA_{0.83}MAMA$), suggesting that a greater free volume was achieved by TN structure.

SN samples BA_T and BA_0, and DN sample $BA_{0.83}BA$ with similar SP weight contents, were compared for their elasticity and mechanochromic performance. The ultimate tensile strength (σ_{break}) and stretchability (ε_{break}) of BA_T and BA_0 were determined to be 0.24 ± 0.02 MPa at 143 ± 17% and 0.57 ± 0.07 MPa at 86 ± 6%, respectively, which were much weaker than those of the $BA_{0.83}BA$ with 7.57 ± 1.14 MPa at 335 ± 39% (**Table 4.1** and **Figure 4.1A**). Neither of the SNs exhibited a strain-hardening characteristic on the stress-strain curves. As expected, BA_T was weaker than BA_0 but with larger elongation,

indicating a looser network was formed in the presence of solvent. The stress-strain curve of DN presented two regions, including a softening region due to the uncoiling of polymer chains and a hardening region due to stretching of the bonds.[25] The DN $BA_{0.83}BA$ exhibited a significant colour change from light yellow to blue during tensile testing, whereas the SNs did not show any colour change prior to fracture (**Figure 4.1C**). It demonstrated that the SN samples BA_T and BA_0 crosslinked via white light polymerization are soft and brittle, with the applied force unable to transform SP into its coloured ring-opened counterpart. In contrast by performing a subsequent swelling-curing process to build a second-network, the mechanical properties are greatly improved enabling a sufficient mechanical activation of SP thus inducing a significant colour change prior to breaking. The improved elasticity of $BA_{0.83}BA$ is due to the first-network acting as a filler which can dissipate energy and enhance the elasticity.[26] The colour change was analysed based on RGB value, and the ratio of colour channel intensities were calculated. The change of blue colour ratio (rBc) was more significant than rRc and rGc (**Figure A4.3**), thus rBc was used to analyse the colour activation. The onset of colour activation strain (ε_{MC}) for $BA_{0.83}BA$ occurred at ~ 159 ± 1.6%, at the early stage of the hardening region (**Figure 4.1B**). This is consistent with the phenomena observed in SP-PDMS and PU reported previously.[11, 27] The ε_{MC} of $BA_{0.83}BA$ was significantly lower than the reported simple structure elastomers, such as 259% for SP-PMA and 400% for SP-PU.[14, 28] The reason for this is due to SP being in the first-network which was pre-stretched by the second-network thus shortening the deformation for chain alignment and mechanophore orientation. The onset of colour activation stress (σ_{MC}) then can be determined from the stress-strain curve at the position of ε_{MC}. For a better description of the colour activation threshold, the term of colour activation energy (U_A) was introduced and it is determined by the area underneath the σ_{MC}-ε_{MC} on the stress-strain curve (**Figure 4.1B**). It represents the amount of energy per unit volume that the elastomer needs to absorb for inducing the colour change. The calculated U_A for $BA_{0.83}BA$ is 0.71 ± 0.06 MJ m^{-3}, and the U_A of all the samples are summarized in **Table 4.1**.

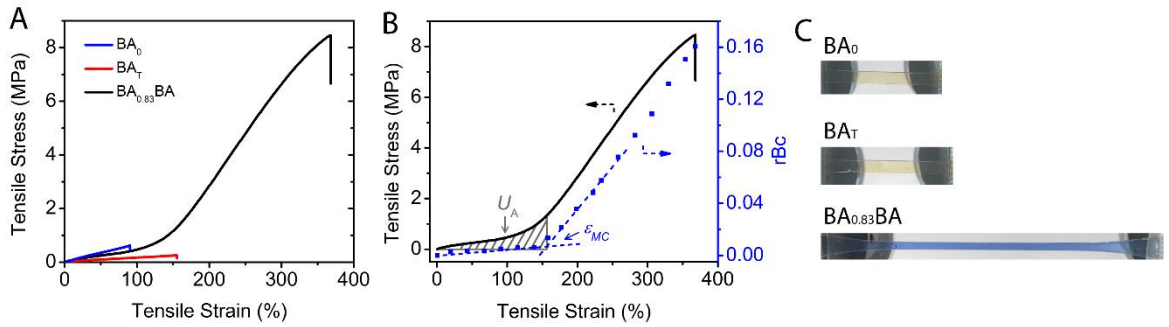

Figure 4.1. (A) Tensile stress-strain curves of SNs prepared in the presence/absence of toluene (BA_T and BA_0) and DN ($BA_{0.83}BA$). (B) A plot of rBc as a function of tensile strain for $BA_{0.83}BA$ with ε_{MC} determined by the intersection of two tangent lines. The colour activation energy U_A is calculated by integration of the area underneath the onset of colour change on stress-strain curve. (C) Images of the two SNs and DN $BA_{0.83}BA$ under tension prior to fracture.

4.4.2 Effect of SP Concentration

The concentration of SP in the first-network was varied to study its effect on the U_A. The cross-link density was fixed at a constant value by varying the proportion of co-crosslinker BDMA. DNs with SP concentrations of 0.5, 0.83 and 1.17 mol % relative to BA were prepared and denoted by $BA_{0.5}BA$, $BA_{0.83}BA$ and $BA_{1.17}BA$, respectively. The stress-strain curves of the three samples are shown in **Figure 4.2A**, with similar ε_{break} at ca. 340% and σ_{break} at 7.2–7.9 MPa (**Table 4.1**), indicating that the mechanical properties of the three samples were almost identical. It demonstrated that the elasticity of DN is dependent on the crosslinking density, and the variation of the low SP concentration had insignificant effect on the mechanical properties. The T_g for the three samples were the same within standard error. The curves of rBc against the strain showed that the ε_{MC} was $158 \pm 1.1\%$, $159 \pm 1.6\%$ and $156 \pm 2.8\%$ for $BA_{0.5}BA$, $BA_{0.83}BA$ and $BA_{1.17}BA$, respectively (**Figure 4.2B**), which were at the strain-hardening regions. The minor differences of ε_{MC} for the DNs with various SP concentrations revealed that ε_{MC} was reliant on the onset of stress-hardening. With increasing tensile strain, rBc exhibited a linear growth, indicating that more and more SP converted to ring-open MC. The higher SP concentration, the greater slope was observed, indicating a faster colour deepening rate. Thus, at a certain strain above ε_{MC}, $BA_{1.17}BA$ presented the highest rBc. The images of the three samples under a strain around 330% exhibited a blue colour with $BA_{1.17}BA$ showing the deepest

colour (**Figure 4.2C**). The U_A calculated for $BA_{0.5}BA$, $BA_{0.83}BA$ and $BA_{1.17}BA$ are 0.63 ± 0.08, 0.71 ± 0.06 and 0.60 ± 0.03 MJ m^{-3} (**Table 4.1**).

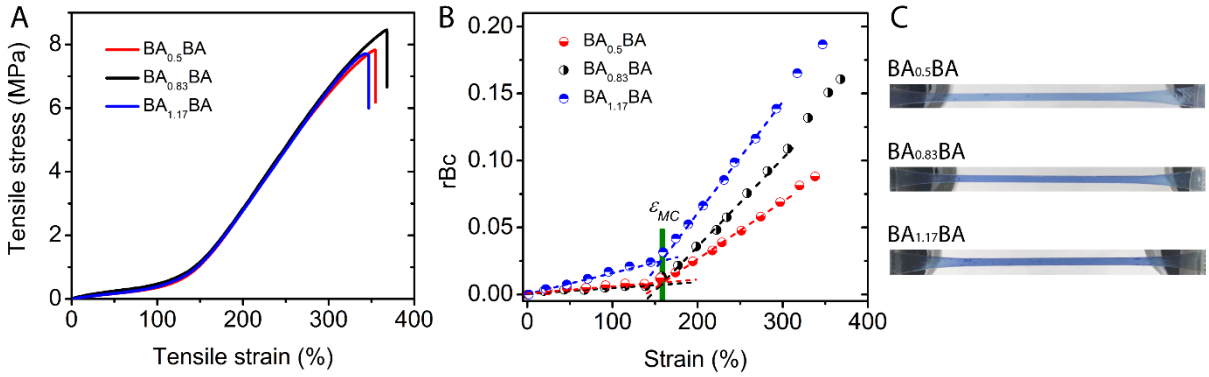

Figure 4.2. (A) Tensile stress-strain curves of DN samples with SP concentration of 0.5, 0.83, 1.17 mol % in the first-network. (B) Colour change plots of rBc against strain for the three samples, and the onset strain of colour activation ε_{MC} determined by the intersection of the two tangent lines. (C) Images of the three samples under tensile at a strain of 338%, 330% and 332%, respectively.

4.4.3 Effect of Toluene Volume

The first-network acted as a filler to improve the elasticity of the subsequent DN, which could be affected by the pre-stretched ratio and swelling ability of the first-network.[26] By varying the toluene volume in the first-network, the pre-stretched ratio ($\lambda_{prestretch}$) and swelling ratio ($\lambda_{swollen}$) can be tuned. Three DN samples of BABA with toluene volume at 40, 50 and 60 vol % were prepared. The $\lambda_{swollen}$ determined by mass ratio for the three samples were 3.84 ± 0.42, 4.57 ± 0.03 and 5.34 ± 0.10, respectively (**Table A4.1**), demonstrating that an increase of the solvent volume would lead to an increase of $\lambda_{swollen}$ indicating a looser SN after solvent removal. The T_g was slightly reduced with increasing toluene volume, which was attributed to the increased $\lambda_{swollen}$ resulting in more free volume. The tensile stress-strain curves showed that the decrease of solvent volume caused a relatively early strain-hardening region, but at the expense of ε_{break} (**Figure 4.3A**). The rBc-strain curves shown in Figure 3B displayed that the ε_{MC} differed for the three samples due to the differences of onset of strain hardening region, with ε_{MC} at 131 ± 3.7%, 159 ± 1.6% and 189 ± 12.5% for 40%, 50% and 60% toluene volume. Accordingly, the U_A of the three samples are 0.54 ± 0.07, 0.71 ± 0.06 and 0.71 ± 0.013 MJ m^{-3} (**Table**

4.1), with the U_A of $BA_{0.83(40)}BA$ significantly lower than the other two samples. It revealed that the colour activation of the DN system was tunable by adjusting the solvent volume when prepare the first-network.

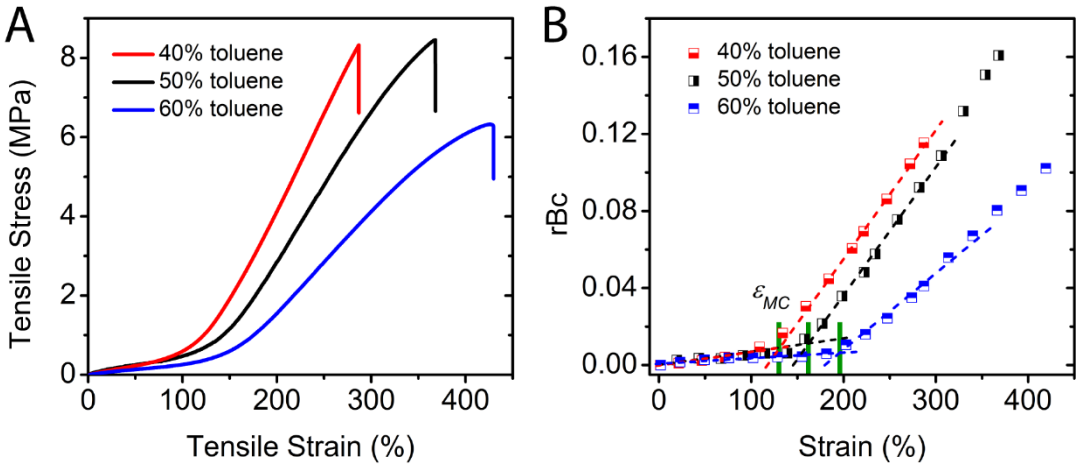

Figure 4.3. (A) Tensile stress-strain curves of DN samples prepared with various toluene volume in the first-network, 40%, 50% and 60%, respectively, and SP concentration of 0.83 mol %. (B) Colour change curves of rBc against strain for the three samples, and the onset of colour activation strain ε_{MC} indicated by green lines.

4.4.4 Cyclic Loading-unloading Tests

Cyclic tensile testing was performed on a dog-bone shaped sample of $BA_{0.83}BA$ under a maximum strain of 250% (above ε_{MC}) with a strain rate of 0.5 mm s^{-1} until rupture. A significant hysteresis loop was observed for the first cycle, and the dissipated energy was determined to be ca. 1.65 MJ m^{-3} (**Figure 4.4A**). The dissipated energy decreased remarkably after the first loading-unloading cycle and continued to drop slightly in the subsequent cycles (inset figure in **Figure 4.4A**). The residue of strain for the 1st cycle was ca. 45% and increased to 62% after 8 times of stretching. The maximum stress of the specimen gradually dropped in the following cycles. The images of the specimen under 250% strain for the cycle of 1, 3, 5 and 7 showed that the blue colour visually weakened, and it can also be seen from the quantitative analysis of rBc, which decreased continuously with increasing loading-unloading cycles (**Figure 4.4B**). As MC reverted to SP under room light, the decline of rBc was not surprising. An additional step-cyclic test was conducted with MC returning to SP forced by room light for each cycle. The sample was repeatedly stretched to a certain strain before further elongated. The plot of

normalized absorbance intensity versus cycles suggested that the intensity dropped significantly with repeating the same elongation (dashed lines in **Figure 4.4C**). This irreversibility of colour activation is attributed to the mechanical hysteresis and the bond breakage occurring in the first-network under a certain strain,[20, 29] which could result in the SPs located in those fragments losing their mechanochromic function once the ring-closing reaction occurs. This differs to the observation reported by Weng *et al.*, where SP in PU showed no loss of colour intensity after multiple cyclic stretching.[14] Besides, the sample further stretched to a larger deformation displayed a pronounced absorbance intensity again, meaning that more bonds were stretched.

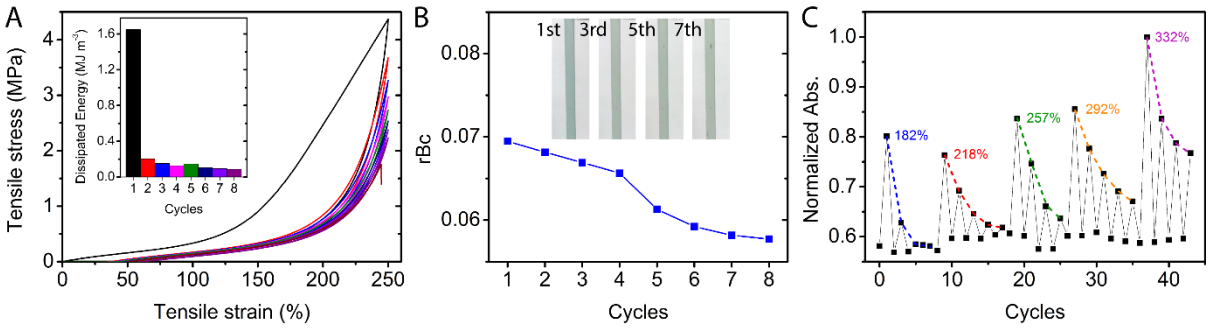

Figure 4.4. Cyclic tensile test on a specimen of $BA_{0.83}BA$ until rupture. (A) Loading-unloading curves obtained at a strain rate of 0.5mm s^{-1} and the dissipated energy for each cycle in the inset figure. (B) The rBc value as a function of loading-unloading cycles and the inset images of the sample under a strain of 250% for the 1st, 3rd, 5th, and 7th cycle, without MC returning to SP upon relaxation for each cycle. (C) A plot of normalized absorbance intensity against loading-unloading cycles, with MC recovering to SP under exposure to room light for 30-40 min for each cycle. The sample was subjected to a specific strain for 4-5 times before increasing the elongation, and the numbers show the value of strain corresponding to each dashed line.

4.4.5 Different Acrylate Monomers for the Second-network

The elasticity of elastomers is usually related to their T_g. Different polyacrylates exhibit various mechanical properties usually due to the difference in their T_g. Here, since the colour activation of SP is elasticity dependent, a higher T_g monomer, methyl acrylate (MA) was also employed to prepare a second-network. The $\lambda_{swollen}$ of the first-network in MA was 5.80 ± 0.29, which was higher than that in BA with 4.57 ± 0.03 (**Table A4.1**). This is

most likely due to the viscosity of MA lower than BA. The T_g determined by DSC for $BA_{0.83}BA$ and $BA_{0.83}MA$ were -46.4 °C and 10.5 °C, respectively (**Table 4.1**). This suggests that the T_g in the DN systems were mainly determined by the material of the second-network, since its proportion is dominant in the DN. Both samples were in the rubber state at room temperature, endowing them stretchable. The tensile stress-strain curves were similar for the two specimens. The ε_{MC} for $BA_{0.83}BA$ at 159 ± 1.6% was significantly higher than that for $BA_{0.83}MA$ at 118 ± 4.4% (**Figure 4.5**) due to an earlier strain-hardening for $BA_{0.83}MA$. The stress at ε_{MC} was 1.4 MPa for $BA_{0.83}BA$ and 1.1 MPa for $BA_{0.83}MA$, and thus, the U_A of the two samples were 0.71 ± 0.06 and 0.63 ± 0.04 MJ m^{-3}, respectively. The ε_{break} for $BA_{0.83}MA$ (471 ± 64%) is higher than that for $BA_{0.83}BA$ (335 ± 39%). The improvement of extensibility for $BA_{0.83}MA$ was likely due to a bigger contrast between the first- and second-network and a higher $\lambda_{swollen}$, according to the design principles of DN hydrogels.[29] Noticeably, the first-network was the same for both DN systems, meaning that the final SP weight content in $BA_{0.83}MA$ was lower than that in $BA_{0.83}BA$ due to a higher $\lambda_{swollen}$ value for $BA_{0.83}MA$; but the rBc of $BA_{0.83}MA$ prior to rupture was higher than that of $BA_{0.83}BA$.

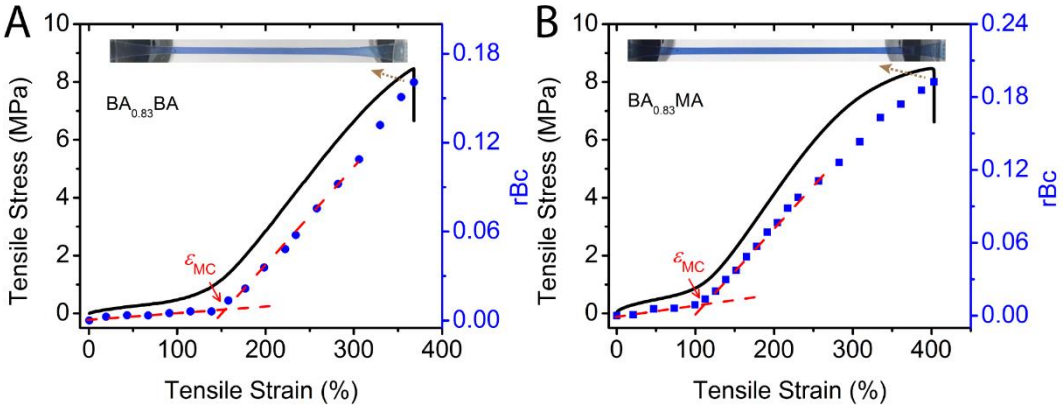

Figure 4.5. Tensile stress-strain curves and colour change plot of rBc against strain for (A) $BA_{0.83}BA$ and (B) $BA_{0.83}MA$. The onset of colour activations ε_{MC} are indicated by the arrows. Inset pictures showed a blue colour when the samples were under stretching prior to fracture.

4.4.6 Mechanical Activation vs UV Light Activation

The activation ratio of SP to MC induced by force has been reported much lower than that by UV light, i.e. around 30% intensity for PU bearing SP, indicating a low efficiency of SP

as mechanochromophore in polymers.[10, 15] Here, the samples of $BA_{0.83}BA$ and $BA_{0.83}MA$ exposed to UV light were compared to those subjected to stretching to study the influence of DN structure on SP mechanical activating efficiency. The bulk samples were exposed to UV light (20 W, 365 nm) with absorption measurements performed every minute until the relative absorption intensity plateaued. Since intensity of light irradiation could affect the photo stationary state, the results obtained here were analysed based on this specific experimental condition. The absorption peak at 580 nm attributing to MC reached a plateau after 20–30 min UV irradiation for both samples, to an absorbance intensity of 1.75 ± 0.003 and 1.27 ± 0.07 for $BA_{0.83}BA$ and $BA_{0.83}MA$, respectively (**Figure 4.6**). The absorbance intensity for the stretched samples after fracture were 1.15 ± 0.03 and 1.76 ± 0.06 for $BA_{0.83}BA$ and $BA_{0.83}MA$. The fraction of absorbance intensity by mechanical activation to that by UV activation was defined as $R_{F/UV}$, which was determined to be 66% for $BA_{0.83}BA$ and 138% for $BA_{0.83}MA$, and both were higher than that of the simple structure polymers bearing SP as mentioned earlier. The $R_{F/UV}>1$ for $BA_{0.83}MA$ highlighted that for this sample UV activation was weaker than mechanical activation, which was attributed to the higher pre-stretched ratio of $BA_{0.83}MA$ than $BA_{0.83}BA$. To the best of our knowledge, this is the first time that mechanochromic activation has been shown to be stronger than photochromic activation for SP-based mechanochromic polymeric materials. It's believed that the extensibility, toughness and pre-stretched first-network of $BA_{0.83}MA$ contribute to the high ratio of SP to MC conversion. The high conversion proportion triggered by force proved that the DN structure elastomer bearing SP in the pre-stretched network is an effective strategy for enhancing polymer chain alignment to increase mechanical activation of the mechanophores.

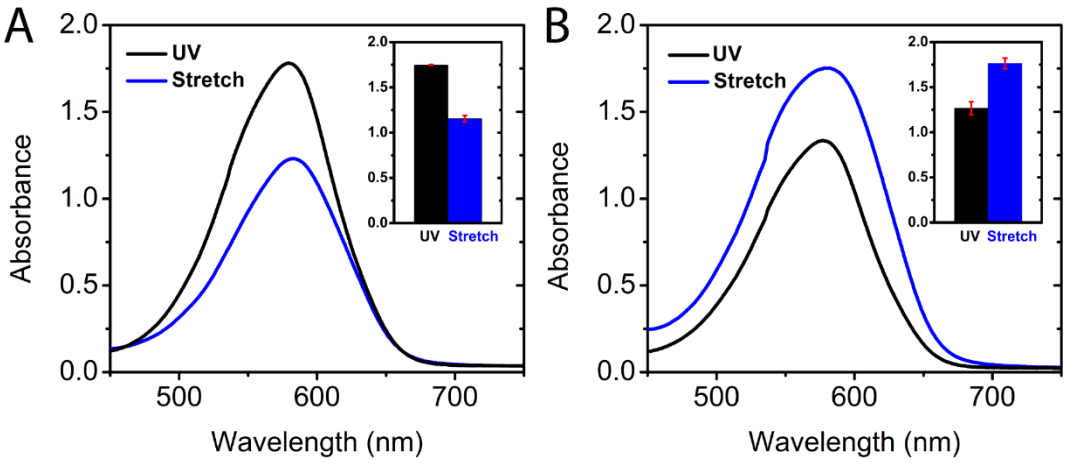

Figure 4.6. Absorbance spectra of (A) $BA_{0.83}BA$ and (B) $BA_{0.83}MA$ activated by UV light until plateaued and by stretching upon fracture. The inset figures presented the absorbance intensity at the peak wavelength at 580 nm.

4.4.7 Triple-network and Necking Phenomenon

Necking phenomena for DN gels occur as a thinning zone on the sample and further grows with elongation.[30, 31] Necking phenomenon was not observed on triple-network elastomers[10] until a quadruple-network polyacrylate which was obtained through three times of swelling-curing process.[26] However in this study, necking phenomenon has been observed on triple-network samples at a strain around 220% (**Figure 4.7**). Necking phenomena observed for DN hydrogels have been reported to be dependent on the structure of the first-network, i.e. cross-link density and extensibility.[30, 32] In this case, although the cross-link density here was comparable to the reported PEA triple-network elastomer, which did not show necking,[26] the differences of monomer and polymerization conditions (white light initiated here) led to a dissimilar first-network, resulting in the necking phenomenon. The strain-hardening for $BA_{0.83}BABA$ occurred at ca. 60%, resulting in a ε_{MC} at 75% (**Figure 4.7B**). The ε_{MC} for $BA_{0.83}MAMA$ sat at 39 ± 1.4% (**Figure 4.7D**), lower than that of $BA_{0.83}BABA$ due to an earlier onset of strain-hardening. The lower ε_{MC} of TN than that of DN was due to a further pre-stretching of the first-network. It led to the U_A of $BA_{0.83}MAMA$ was 0.10 ± 0.02 MJ m^{-3}, lower than that of 0.19 ± 0.03 MJ m^{-3} for $BA_{0.83}BABA$. The colour intensity of $BA_{0.83}MAMA$ was also higher than that of $BA_{0.83}BABA$ before the occurrence of necking. Upon further stretching after ε_{MC}, the stress remained almost constant whereas the strain kept increasing, suggesting the occurrence

of necking. The specimen displayed two regions, necked and unnecked regions (**Figure 4.7A&C**). With increasing the strain, the necked domain further elongated whereas the unnecked region gradually shortened, like "eaten" by the necked region. When the sample fracture occurred before the necked area occupied the whole gauge section, a deeper colour was observed on the necked area than the unnecked domain (inset images **Figure 4.7A&C**). This could be explained by the internal fracture of the first-network leading to the necking,[32] and SPs were activated with the first-network expansion prior to fracture. When the sample fracture happened with the necked area expanding to nearly the whole gauge section, the purple colour was distributed along the gauge section. The shape of the DN samples can nearly fully recover upon rupture. However, the colour activation was irreversible on the necking region, due to the rupture of first-network. This uneven distribution of force/deformation on the materials upon necking would be interesting if the necking position can be controlled. According to this study and previously reported work,[30] the necking phenomena generally appear near the end of the gauge section. Further research work needs to be performed on this necking phenomenon on mechanochromic materials.

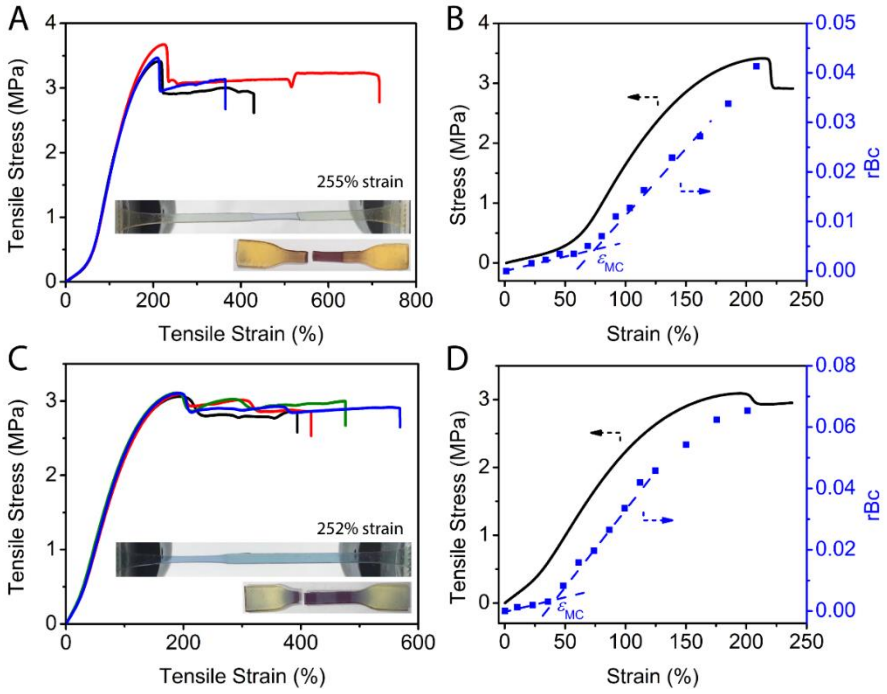

Figure 4.7. Stress-strain curves for (A) $BA_{0.83}BABA$ and (B) $BA_{0.83}MAMA$. The inset images show the samples under necking and after rupture. A stress-strain curve and a plot of rBc against strain for (C) $BA_{0.83}BABA$ and (D) $BA_{0.83}MAMA$ before the onset of necking phenomenon, with ε_{MC} determined by two tangent lines.

4.4.8 Comparison of Mechanical Activation

To evaluate the sensitivity of mechanochromic activation, the U_A of SP-linked multi-network elastomers presented in this paper are compared to the elastomers reported in the literature. It's worth noting that the mechanical testing conditions of these works are different, e.g. strain rate, which may affect their mechanochromic properties. Here we only compare the SP-elastomers with activation thresholds which are clearly reported and those characterized by RGB color intensity analysis. The plot of onset of colour activation stress-strain and the calculated U_A are shown in **Figure 4.8**, and the corresponding plot of U_A against strain is shown in **Figure A4.4**. Overall, the U_A of triple-network elastomer in this work is the lowest. SN of PMA bearing SP require much larger strain and higher stress (entries 1 & 2) than the DN and TN in this work, resulting in a U_A difference in an order of magnitude. The graft copolymer PS-SP-PBA displayed an ideally low strain and stress for mechanochromic activation (entry 7), however the synthesis is tedious. Commercial PDMS (Sylgard 184) provides a facile preparation approach with an ideally low U_A, but still the TN elastomers in this work offer a lower U_A. Thus, the multi-network elastomers are excellent candidates for SP mechanochromic materials, combining the advantages of a low activation energy and a facile preparation process.

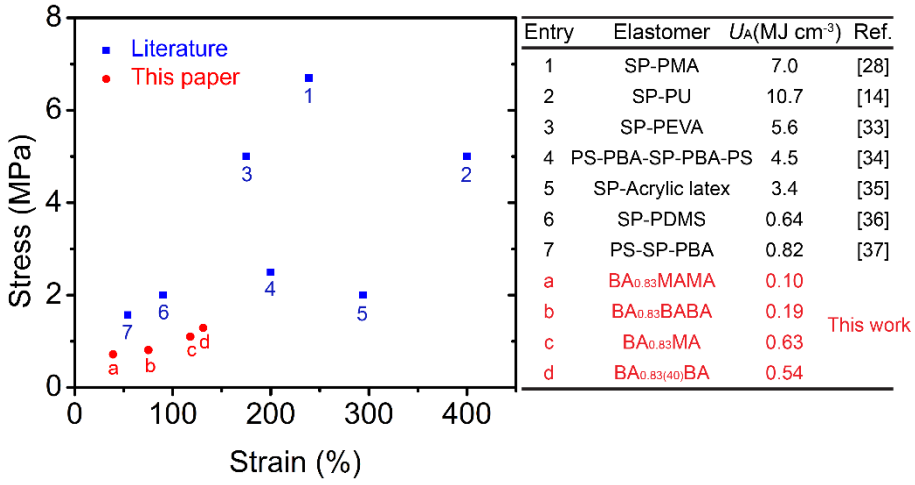

Entry	Elastomer	U_A(MJ cm^{-3})	Ref.
1	SP-PMA	7.0	[28]
2	SP-PU	10.7	[14]
3	SP-PEVA	5.6	[33]
4	PS-PBA-SP-PBA-PS	4.5	[34]
5	SP-Acrylic latex	3.4	[35]
6	SP-PDMS	0.64	[36]
7	PS-SP-PBA	0.82	[37]
a	$BA_{0.83}MAMA$	0.10	This work
b	$BA_{0.83}BABA$	0.19	
c	$BA_{0.83}MA$	0.63	
d	$BA_{0.83(40)}BA$	0.54	

Figure 4.8. A plot of onset of tensile stress-strain for mechanical activation of SP-linked elastomers presented in this work (a-d) and reported in the literature (1-7).[14, 28, 33-37] The U_A values in the literature were calculated from reported data using methods described in this work.

4.5 Conclusion

In this chapter, we have adopted double-network polyacrylates to allow SP to be pre-stretched in the first-network for improving mechanochromic sensitivity. The results showed that the mechanochromic activation was reliant on the strain-hardening region, while the variation of SP concentration had negligible effect on the onset strain of colour activation, but a higher SP content resulted in a deeper blue colour intensity. A reduced toluene volume allowed an early appearance of onset of colour activation strain but at a cost of ultimate elongation. A change in acrylate monomer for the second-network showed that $BA_{0.83}MA$ displayed an advantage over $BA_{0.83}BA$ at the mechanochromic performance, with a lower U_A and a greater blue colour intensity prior to fracture. The cyclic tension test suggested that there was a significant hysteresis loop in the first loading, and the blue colour intensity gradually dropped with increasing cycle numbers. Through a comparison between SP activation by stretching and UV irradiation, it was found that the mechanical activation of SP to MC was improved remarkably compared to those reported simple structure polymers bearing mechano-active SP. A triple-network elastomer could further reduce the U_A, and exhibited a necking phenomenon, which could be utilized for colour switchable applications required to indicate large deformations at a low stress. The comparison of U_A between this work and the reported elastomers shows that the TN has the lowest U_A, i.e. the most sensitive mechanochromic elastomer made so far. The highly sensitive mechanochromic elastomer making use of the benefits from a multi-network structure provides potential for the fabrication of new sensors based on colour response materials. This study offers an approach for SP employed for force/deformation-sensing elastomers with low colour activation energies and excellent mechanical properties.

4.6 References

(1) Calvino, C.; Neumann, L.; Weder, C.; Schrettl, S. Approaches to polymeric mechanochromic materials. *J. Polym. Sci., Part A: Polym. Chem.* **2017,** 55, 640-652.

(2) Barber, R. W.; McFadden, M. E.; Hu, X.; Robb, M. J. Mechanochemically Gated Photoswitching: Expanding the Scope of Polymer Mechanochromism. *Synlett* **2019,** 30, A-H.

(3) Davis, D. A.; Hamilton, A.; Yang, J.; Cremar, L. D.; Van Gough, D.; Potisek, S. L.; Ong, M. T.; Braun, P. V.; Martinez, T. J.; White, S. R.; Moore, J. S.; Sottos, N. R. Force-induced activation of covalent bonds in mechanoresponsive polymeric materials. *Nature* **2009,** 459, 68-72.

(4) Zhang, H.; Gao, F.; Cao, X.; Li, Y.; Xu, Y.; Weng, W.; Boulatov, R. Mechanochromism and Mechanical-Force-Triggered Cross-Linking from a Single Reactive Moiety Incorporated into Polymer Chains. *Angew. Chem. Int. Ed.* **2016,** 55, 3092-3096.

(5) Wang, T.; Zhang, N.; Dai, J.; Li, Z.; Bai, W.; Bai, R. Novel Reversible Mechanochromic Elastomer with High Sensitivity: Bond Scission and Bending-Induced Multicolor Switching. *ACS Appl. Mater. Interfaces* **2017,** 9, 11874-11881.

(6) Robb, M. J.; Kim, T. A.; Halmes, A. J.; White, S. R.; Sottos, N. R.; Moore, J. S. Regioisomer-Specific Mechanochromism of Naphthopyran in Polymeric Materials. *J. Am. Chem. Soc.* **2016,** 138, 12328-12331.

(7) Imato, K.; Irie, A.; Kosuge, T.; Ohishi, T.; Nishihara, M.; Takahara, A.; Otsuka, H. Mechanophores with a reversible radical system and freezing-induced mechanochemistry in polymer solutions and gels. *Angew. Chem. Int. Ed.* **2015,** 54, 6168-6172.

(8) Kosuge, T.; Imato, K.; Goseki, R.; Otsuka, H. Polymer–Inorganic Composites with Dynamic Covalent Mechanochromophore. *Macromolecules* **2016,** 49, 5903-5911.

(9) Beiermann, B. A.; Kramer, S. L. B.; May, P. A.; Moore, J. S.; White, S. R.; Sottos, N. R. The Effect of Polymer Chain Alignment and Relaxation on Force-Induced Chemical Reactions in an Elastomer. *Adv. Funct. Mater.* **2014,** 24, 1529-1537.

(10) Lee, C. K.; Davis, D. A.; White, S. R.; Moore, J. S.; Sottos, N. R.; Braun, P. V. Force-induced redistribution of a chemical equilibrium. *J. Am. Chem. Soc.* **2010,** 132, 16107-16111.

(11) Gossweiler, G. R.; Hewage, G. B.; Soriano, G.; Wang, Q.; Welshofer, G. W.; Zhao, X.; Craig, S. L. Mechanochemical Activation of Covalent Bonds in Polymers with Full and Repeatable Macroscopic Shape Recovery. *ACS Macro Lett.* **2014,** 3, 216-219.

(12) Li, M.; Zhang, Q.; Zhou, Y.-N.; Zhu, S. Let spiropyran help polymers feel force! *Prog. Polym. Sci.* **2018,** 79, 26-39.

(13) Fang, X.; Zhang, H.; Chen, Y.; Lin, Y.; Xu, Y.; Weng, W. Biomimetic Modular Polymer with Tough and Stress Sensing Properties. *Macromolecules* **2013,** 46, 6566-6574.

(14) Zhang, H.; Chen, Y.; Lin, Y.; Fang, X.; Xu, Y.; Ruan, Y.; Weng, W. Spiropyran as a Mechanochromic Probe in Dual Cross-Linked Elastomers. *Macromolecules* **2014,** 47, 6783-6790.

(15) Chen, Y.; Zhang, H.; Fang, X.; Lin, Y.; Xu, Y.; Weng, W. Mechanical Activation of Mechanophore Enhanced by Strong Hydrogen Bonding Interactions. *ACS Macro Lett.* **2014,** 3, 141-145.

(16) Gong, J. P.; Katsuyama, Y.; Kurokawa, T.; Osada, Y. Double-Network Hydrogels with Extremely High Mechanical Strength. *Adv. Mater.* **2003,** 15, 1155-1158.

(17) Chen, Q.; Chen, H.; Zhu, L.; Zheng, J. Fundamentals of double network hydrogels. *J. Mater. Chem. B* **2015,** 3, 3654-3676.

(18) Beiermann, B. A.; Kramer, S. L. B.; Moore, J. S.; White, S. R.; Sottos, N. R. Role of Mechanophore Orientation in Mechanochemical Reactions. *ACS Macro Lett.* **2012,** 1, 163-166.

(19) Gong, J. P. Materials both tough and soft. *Science* **2014,** 344, 161-162.

(20) Ducrot, E.; Chen, Y.; Bulters, M.; Sijbesma, R. P.; Creton, C. Toughening elastomers with sacrificial bonds and watching them break. *Science* **2014,** 344, 186-189.

(21) Qiu, W.; Gurr, P. A.; da Silva, G.; Qiao, G. G. Insights into the mechanochromism of spiropyran elastomers. *Polym. Chem.* **2019,** 10, 1650-1659.

(22) Qiu, W.; Gurr, P. A.; Qiao, G. G. Color-Switchable Polar Polymeric Materials. *ACS Appl. Mater. Interfaces* **2019,** 11, 29268-29275.

(23) Wang, L.-J.; Yang, K.-X.; Zhou, Q.; Yang, H.-Y.; He, J.-Q.; Zhang, X.-Y. Rhodamine Mechanophore Functionalized Mechanochromic Double Network Hydrogels with High Sensitivity to Stress. *Chin. J. Polym. Sci.* **2020**, 28, 24-36.

(24) Haque, M. A.; Kurokawa, T.; Gong, J. P. Super tough double network hydrogels and their application as biomaterials. *Polymer* **2012,** 53, 1805-1822.

(25) Ma, Y.; Feng, X.; Rogers, J. A.; Huang, Y.; Zhang, Y. Design and application of 'J-shaped' stress-strain behavior in stretchable electronics: a review. *Lab Chip* **2017,** 17, 1689-1704.

(26) Millereau, P.; Ducrot, E.; Clough, J. M.; Wiseman, M. E.; Brown, H. R.; Sijbesma, R. P.; Creton, C. Mechanics of elastomeric molecular composites. *Proc. Natl. Acad. Sci. U. S. A* **2018,** 115, 9110-9115.

(27) Hong, G.; Zhang, H.; Lin, Y.; Chen, Y.; Xu, Y.; Weng, W.; Xia, H. Mechanoresponsive Healable Metallosupramolecular Polymers. *Macromolecules* **2013,** 46, 8649-8656.

(28) Li, M.; Zhang, Q.; Zhu, S. Photo-inactive divinyl spiropyran mechanophore cross-linker for real-time stress sensing. *Polymer* **2016,** 99, 521-528.

(29) Webber, R. E.; Creton, C.; Brown, H. R.; Gong, J. P. Large strain hysteresis and mullins effect of tough double-network hydrogels. *Macromolecules* **2007,** 40, 2919-2927.

(30) Na, Y.-H.; Tanaka, Y.; Kawauchi, Y.; Furukawa, H.; Sumiyoshi, T.; Gong, J. P.; Osada, Y. Necking phenomenon of double-network gels. *Macromolecules* **2006,** 39, 4641-4645.

(31) Nakajima, T.; Kurokawa, T.; Ahmed, S.; Wu, W.-l.; Gong, J. P. Characterization of internal fracture process of double network hydrogels under uniaxial elongation. *Soft Matter* **2013,** 9, 1955-1966.

(32) Matsuda, T.; Nakajima, T.; Fukuda, Y.; Hong, W.; Sakai, T.; Kurokawa, T.; Chung, U.-i.; Gong, J. P. Yielding Criteria of Double Network Hydrogels. *Macromolecules* **2016,** 49, 1865-1872.

(33) Li, M.; Liu, W.; Zhu, S. Smart polyolefins feeling the force: Color changeable poly(ethylene-vinyl acetate) and poly(ethylene-octene) in response to mechanical force. *Polymer* **2017,** 112, 219-227.

(34) Jiang, S.; Zhang, L.; Xie, T.; Lin, Y.; Zhang, H.; Xu, Y.; Weng, W.; Dai, L. Mechanoresponsive PS-PnBA-PS Triblock Copolymers via Covalently Embedding Mechanophore. *ACS Macro Lett.* **2013,** 2, 705-709.

(35) Li, M.; Liu, W.; Zhang, Q.; Zhu, S. Mechanical Force Sensitive Acrylic Latex Coating. *ACS Appl. Mater. Interfaces* **2017,** 9, 15156-15163.

(36) Lin, Y.; Barbee, M. H.; Chang, C. C.; Craig, S. L. Regiochemical Effects on Mechanophore Activation in Bulk Materials. *J. Am. Chem. Soc.* **2018,** 140, 15969-15975.

(37) Jia, Y.; Wang, W.-J.; Li, B.-G.; Zhu, S. Design and Synthesis of Mechano-Responsive Color-Changing Thermoplastic Elastomer Based on Poly(n-Butyl Acrylate)-Spiropyran-Polystyrene Comb-Structured Graft Copolymers. *Macromol. Mater. Eng.* **2018,** 303, 1800154.

Chapter 5: Conclusion and future perspectives

5.1 Conclusions

To fill the research gaps of lacking understanding the mechanochromic properties when varying the SP attachment to polymer matrices and overcoming the high mechano-activation energy in the mechanophore-linked mechanochromic materials, this thesis has presented the investigation and development of spiropyran-linked polymers that could manipulate and improve mechano-activity and sensitivity via the design of the SP mechanochromophore and the polymer architecture. A new tri-functional SP3 was designed and synthesized to be compared with the two most commonly used di-functional SP1 & SP2 on their mechanochromic properties. The first experimental section (**Chapter 2**) reported the mechanochromic performance of the three SPs crosslinked into non-polar PDMS, while the second part (**Chapter 3**) presented their differences in mechanochromic properties and negative photochromism when crosslinked in polar polymer matrix PHEA. The last experimental section (**Chapter 4**) demonstrated the significant improvement of the mechano-sensitivity by adopting a multi-network to integrate the tri-substituted SP into the pre-stretched first network.

In **Chapter 2**, the three SPs varying attachment positions and numbers were covalently linked into PDMS to investigate how the geometric or electronic effect influences the mechanochromic properties. The onset activation stress and strain were almost identical for the three samples but SP2 displayed a higher absorption intensity than SP1 when the compressive strain was over 70%, while SP3 combining the attachment points of SP1 and SP2 showed a higher absorption intensity than SP1 but lower than SP2. SP2 and SP3 having attachment at 1'-position showed blue-shift under loading and unloading whereas the shift was not observed for SP1. The results indicate that both electronic and geometric effects influence the mechanochromic properties, with the geometric effect being the more dominant factor. With the assistance of DFT calculation, it is believed that the pulling points distance ΔD affects the mechanochromic response and the blue-purple shift.

In **Chapter 3**, the three SP molecules were crosslinked into polar PHEA via free radical polymerization initiated by white light. The effect of the polar environment resulting in

negative photochromism was studied in solution and in bulk, with the latter version presenting a much longer equilibrium time. The colouration of the SP-PHEA samples could be activated by the swelling force in water due to the mechanochromic properties, which was elucidated by the control sample. The results showed that the three-arm SP3 in both solution and bulk was least affected by negative photochromism, resulting in the lowest absorption intensity when stored in the dark, and its bulk sample displayed the fastest colour activation during swelling. SP3 also exhibited a significantly slower decolouration rate relative to SP1 and SP2 once dehydrated after swelling due to the more cross-linkable points. The colouration was reversable by exposure to visible light and 45-60% colour intensity was remained after 10 cycles. The colour intensity was tunable by varying the cross-link density of SP-PHEA samples, despite the influence of the polar environment. These results demonstrated that SP3 has a greater resistance to the polar environment in switching to coloured MC, and that the absorption can be regulated by controlling the degree of cross-linking.

In **Chapter 4**, double-network polyacrylates were adopted to incorporate the tri-functional SP in the pre-stretched first-network. It illustrated that the mechanochromic activation relied on the strain-hardening region, while the variation of SP concentration had negligible effect on the onset strain of colour activation, but a higher SP content resulted in a deeper blue colour intensity. A reduced toluene volume allowed an early appearance of onset of colour activation strain but at a cost of ultimate elongation. A change in acrylate monomer for the second-network showed that $BA_{0.83}MA$ displayed an advantage over $BA_{0.83}BA$ at the mechanochromic performance, with a lower U_A and a greater blue colour intensity prior to fracture. Through a comparison between SP activation by stretching and UV irradiation, it was found that the mechanical activation of SP to MC was improved remarkably compared to those reported simple structure polymers bearing mechano-active SP. The U_A was further reduced by a formation of triple network and the TN displayed the lowest U_A compared to the previously reported SP-linked elastomers, indicating a significant improvement of the mechano-sensitivity by employing the multi-network structure.

Taken together, these studies provide insights into the properties of mechanochromic SP-linked polymers and strategies of manipulating and improving the mechano-sensitivity,

which will be useful when SP is employed for mechanochromic stress/strain sensing applications.

5.2 Future Perspectives

The attachment positions on SP have shown to be important to their covalently linked materials for mechanochromic properties in Chapter 2 and 3, which can be expanded to extra attachments to polymer matrix to further adjust the mechano-sensitivity. The structure of dendrimer-like star polymers with the mechanophore in the core is believed to promote the mechano-response, as it was applied to the dynamic bond cleavage type mechanochromophore DABBF but in the form of powder.[1, 2] If the structure can be applied to the ring-opening type mechanochromophore SP and bulk materials will be more versatile. It is worth to study how the dendrimer-like star structure will affect the force-induced equilibrium between SP and MC. To achieve that, branched SP can be synthesized by modification of di-hydroxyl SP or tri-hydroxyl SP with 3-Chloro-1,2-propanediol to afford 4 or 6 arm SP, which can be extended to more arms by repeating the modification step (**Figure 5.1**). The resultant hyper-branched SP with hydroxyl functionalities can be covalently linked into PU as a core crosslinker via step growth polymerization; or modified to other functional groups for building block polymers consisting soft and hard blocks. Tensile test can be used to investigate the mechano-responses. Using this design and following on from Chapter 3, the effect of arm number on the mechano-activation triggered by swelling force should also be studied.

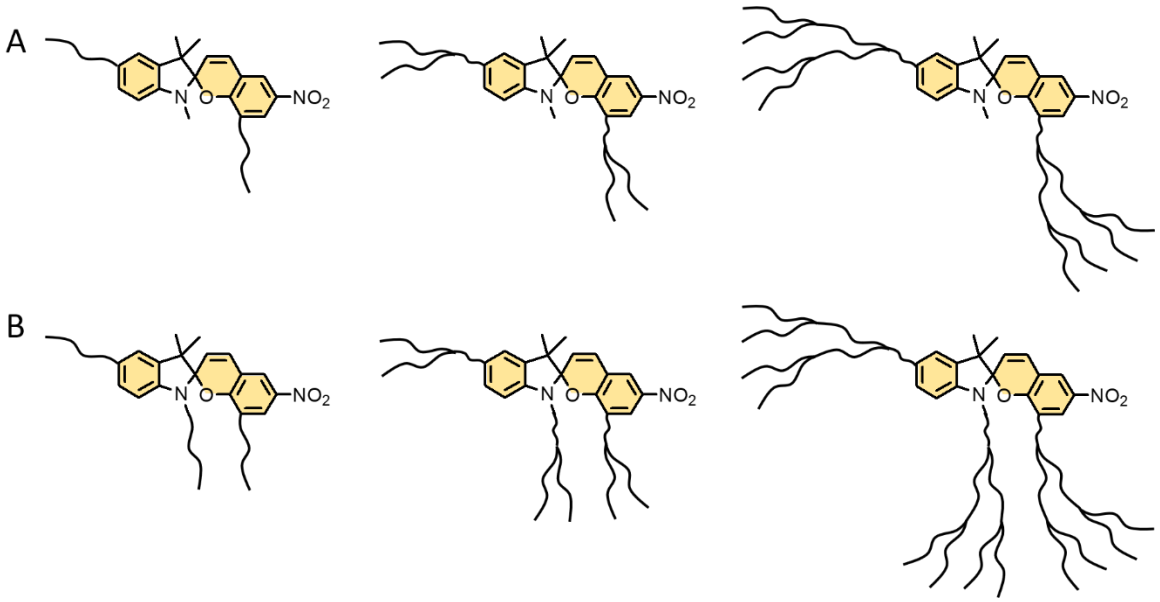

Figure 5.1. Illustrations of SP-cored branched structures with various numbers of arms via functionalization of (A) di- and (B) tri-substituted SPs and attached to polymers chains.

The enhancement of mechano-sensitivity via varying the polymer architecture has been showed efficient and following on from the triple-network structure in Chapter 4, a fourth network can be built from the triple-network to further reduce the mechano-activation energy. To achieve that, it is necessary to avoid the necking phenomenon by varying the first-network composition, i.e. monomer type, cross-link density and crosslinker length, and the thickness of the films. With these highly sensitive mechanochromic polymers, 3D printing technologies can be employed to design novel structures when preparing the first network, such as a ring structure which can be activated by the force of expanding. The vat polymerization of 3D printing technologies has not been reported to print mechanochromic polymers although it is a widely used 3D printing approach. There is a highly achievable opportunity to fabricate 3D structured mechanochromic polymers making use of the vat polymerization 3D printing technology. To achieve that, the white light induced free radical polymerization employed in Chapter 3 can be used in digital light processing (DLP) for printing the SP-based mechanochromic polymers, by replacing the UV light source with white light in the current DLP printer in Polymer Science Group (**Figure 5.2**). Printing conditions and novel structures can be explored to fabricate some "smart" devices, combining the advantages of the mechanochromic polymers and 3D printing techniques.

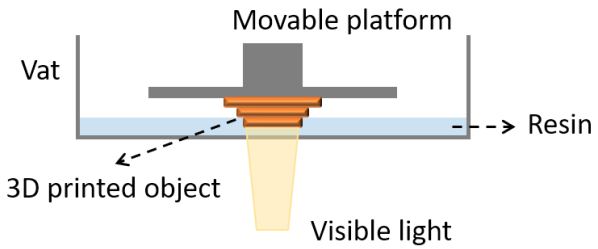

Figure 5.2. An illustrated representation of DLP 3D printing technique that can be used for printing SP-based polymers using acrylates as photocurable resin when replace the light source with visible light.

Advancing the structural strategies of modifying SP mechanochromophores and polymer architectures, a new type of mechanochromic SP-based polymers triggered by an indirect shearing force due to thermo-response can be developed. Dendronized polymers have been shown thermo-responsiveness and shearing thinning due to intermolecular bonding interactions.[3, 4] If these two properties are combined to develop a dendronized polymer which exhibits shearing force induced by a phase transition due to a temperature change, SP can be bonded in such a system to show mechanochromic activity triggered via regulating temperature. This study will not only broaden a new polymer architecture to this field, but also expand the triggering source for the mechanochromic materials.

5.3 References

(1) Oka, H.; Imato, K.; Sato, T.; Ohishi, T.; Goseki, R.; Otsuka, H. Enhancing Mechanochemical Activation in the Bulk State by Designing Polymer Architectures. *ACS Macro Lett.* 2016, 5, 1124-1127.

(2) Imato, K.; Otsuka, H. Reorganizable and stimuli-responsive polymers based on dynamic carbon–carbon linkages in diarylbibenzofuranones. *Polymer* 2018, 137, 395-413.

(3) Liu, L.; Li, W.; Yan, J.; Zhang, A. Thermoresponsive dendronized polymeric sensors. *J. Polym. Sci., Part A: Polym. Chem.* 2014, 52, 1706-1713.

(4) Costanzo, S.; Scherz, L. F.; Schweizer, T.; Kröger, M.; Floudas, G.; Schlüter, A. D.; Vlassopoulos, D. Rheology and Packing of Dendronized Polymers. *Macromolecules* 2016, 49, 7054-7068.

Appendix

Chapter 2 Appendix

Synthesis of di-vinyl spiropyran SP1: *1',3',3'-trimethyl-6-nitrospiro[chromene-2,2'-indoline]-5',8-diyl bis(pent-4-enoate)*

1',3',3'-trimethyl-6-nitrospiro[chromene-2,2'-indoline]-5',8-diol[1] (0.20 g, 0.56 mmol, 1.0 equiv) and 4-dimethylaminopyridine (DMAP) (0.12 g, 1.02 mmol, 1.8 equiv) in THF (5 mL) were treated with 4-pentenoic anhydride (0.27 mL, 1.47 mmol, 2.6 equiv). After stirring for 7 hr, the crude reaction mixture was passed through a basic alumina column and rinsed with DCM (100 mL). The solution was extracted with distilled water (2 × 100 mL), dried over $MgSO_4$, filtered and reduced to dryness *in vacuo* to afford SP1 as a dark yellow solid (0.17g, 0.33mmol, 59% yield). ^{1}H NMR (400 MHz, $CDCl_3$): δ 7.94 (d, 1H), 7.82 (d, 1H), 6.99 (d, 1H), 6.85 – 6.80 (ddd, 2H), 6.49 (d, 1H), 5.92 -5.89 (m, 2H), 5.66 – 5.59 (m, 1H), 5.16 – 5.06 (m, 2H), 4.96 – 4.92 (m, 2H), 2.65 (s, 3H),2.62 – 2.51 (m, 2H), 2.21 (m, 2H), 1.96 (m, 2H), 1.25 (s, 3H), 1.21 (s, 3H). MS (ESI): [M + H^+] calculated for $C_{29}H_{30}N_2O_7$, calculated for, 518.2; found, 519.20117.

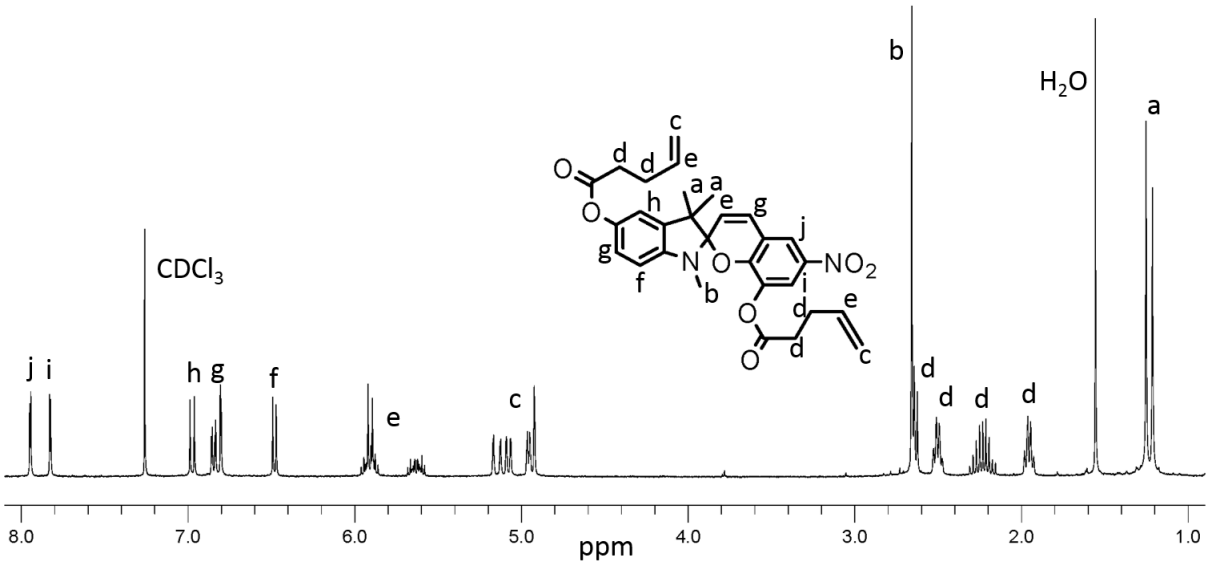

Figure A2.1. ^{1}H NMR spectrum of SP1 (400 MHz, $CDCl_3$).

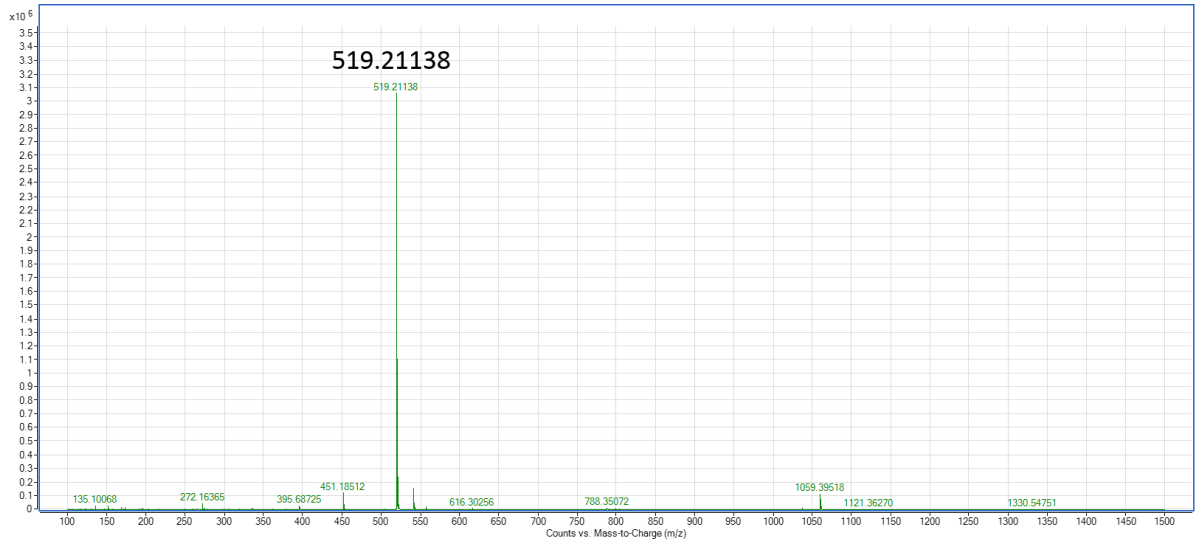

Figure A2.2. Mass spectrum of SP1.

Synthesis of di-vinyl spiropyran SP2: *3',3'-dimethyl-6-nitro-1'-(2-(pent-4 enoyloxy)ethyl)spiro[chromene-2,2'-indolin]-8-yl pent-4-enoate*

1'-(2-Hydroxyethyl)-3',3'-dimethyl-6-nitrospiro[chromene-2,2'-indolin]-8-ol[2] (0.20 g, 0.54 mmol, 1.0 equiv) and 4-dimethylaminopyridine (DMAP) (0.12 g, 1.02 mmol, 1.8 equiv) in 5 mL THF was added 4-pentenoic anhydride (0.26 mL, 1.45 mmol, 2.6 equiv). After stirring for 7 hr, the crude reaction mixture was passed through a plug of basic alumina and eluted from the column with DCM. The solution was extracted with distilled water (2 × 100 mL), dried over $MgSO_4$, filtered and reduced to dryness *in vacuo* to afford SP2 as a yellow solid (0.17g, 0.32mmol, 59% yield). ^{1}H NMR (400 MHz, $CDCl_3$): δ 7.95 (d, 1H), 7.82 (d, 1H) , 7.16 (t, 1H) , 7.06 (d, 1H) , 6.95 (d, 1H) , 6.86 (t, 1H) , 6.65 (d, 1H) , 5.96 (d, 1H) , 5.81 – 5.71 (m, 1H) , 5.59 – 5.49 (m, 1H) , 5.03 – 4.86 (m, 4H), 4.27 – 4.11 (m, 2H), 3.33 (t, 2H), 2.38 – 2.24 (m, 4H), 2.24 – 2.09 (m, 2H), 1.88 – 1.82 (m, 2H), 1.26 (s, 3H), 1.18 (s, 3H). MS (ESI): [M + H^+] calculated for $C_{30}H_{32}N_2O_7$, calculated for, 532.2; found, 533.21592.

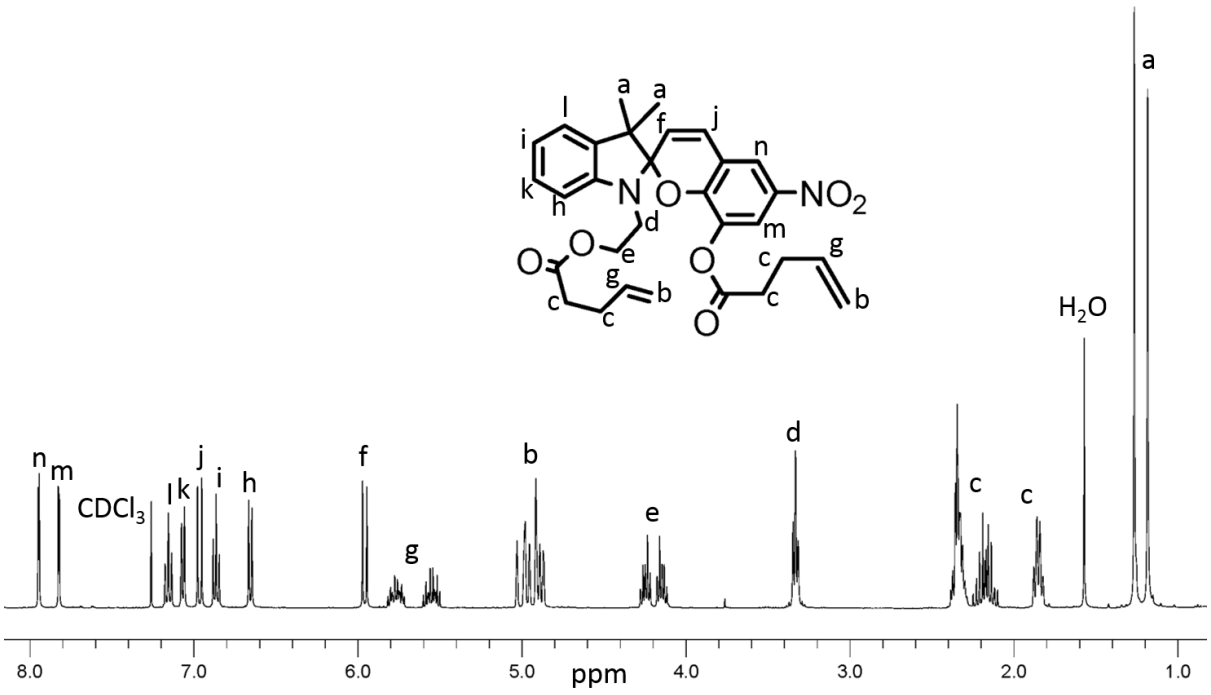

Figure A2.3. ^{1}H NMR spectrum of SP2 (400 MHz, $CDCl_3$).

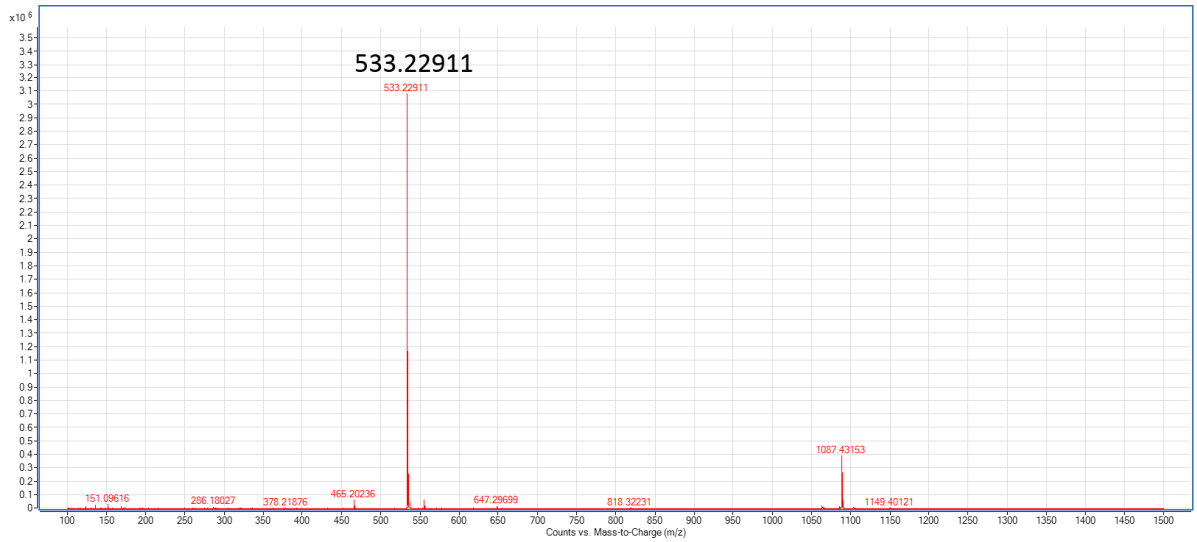

Figure A2.4. Mass spectrum of SP2.

Tri-vinyl spiropyran SP3: 1H NMR (400 MHz, CDCl3): δ 7.94 (d, 1H), 7.83 (d, 1H), 6.98 (d, 1H), 6.85 – 6.80 (ddd, 2H), 6.62 (d, 1H), 5.95 – 5.84 (m, 2H), 5.83 – 5.70 (m, 1H), 5.17 – 4.90 (m, 6H), 4.26 – 4.18 (m, 1H), 4.16 – 4.07 (m, 1H), 3.30 (t, 2H), 2.64 (t, 2H), 2.50 (m, 2H), 2.39 – 2.13 (m, 6H), 1.96 (m, 2H), 1.24 (s, 1H), 1.19 (s, 1H). MS (ESI): [M + H+] calculated for C35H38N2O9, calculated for, 630.2; found, 631.26077.

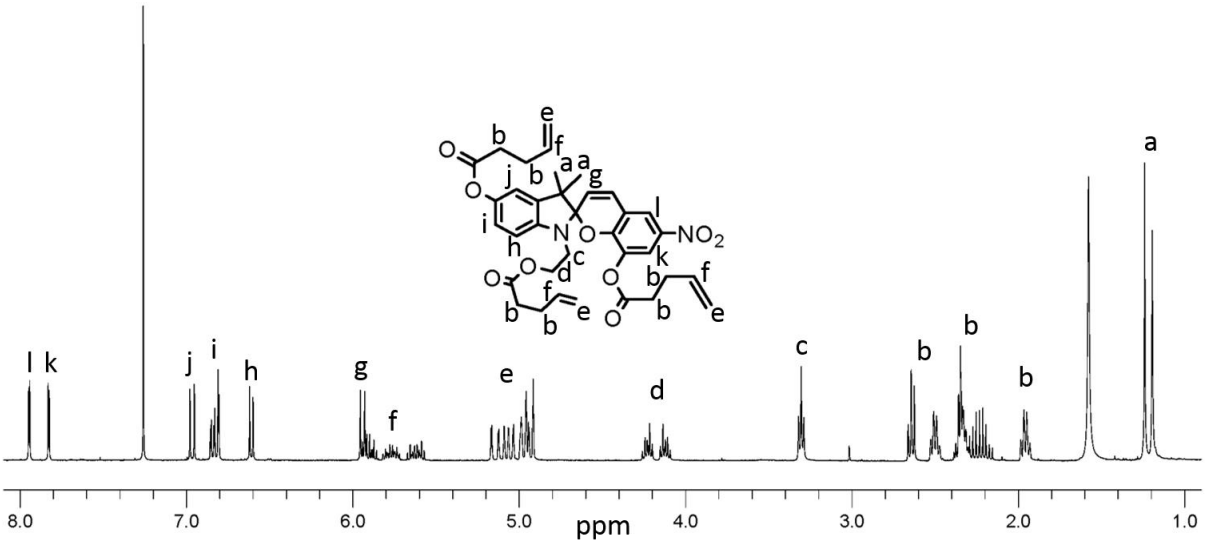

Figure A2.5. ^{1}H NMR spectrum of SP3 (400 MHz, $CDCl_3$).

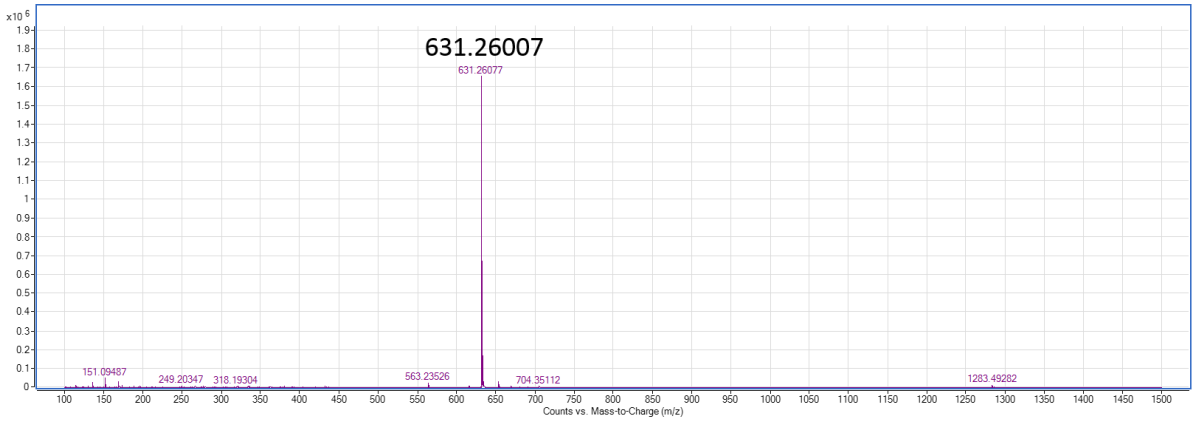

Figure A2.6. Mass spectrum of SP3.

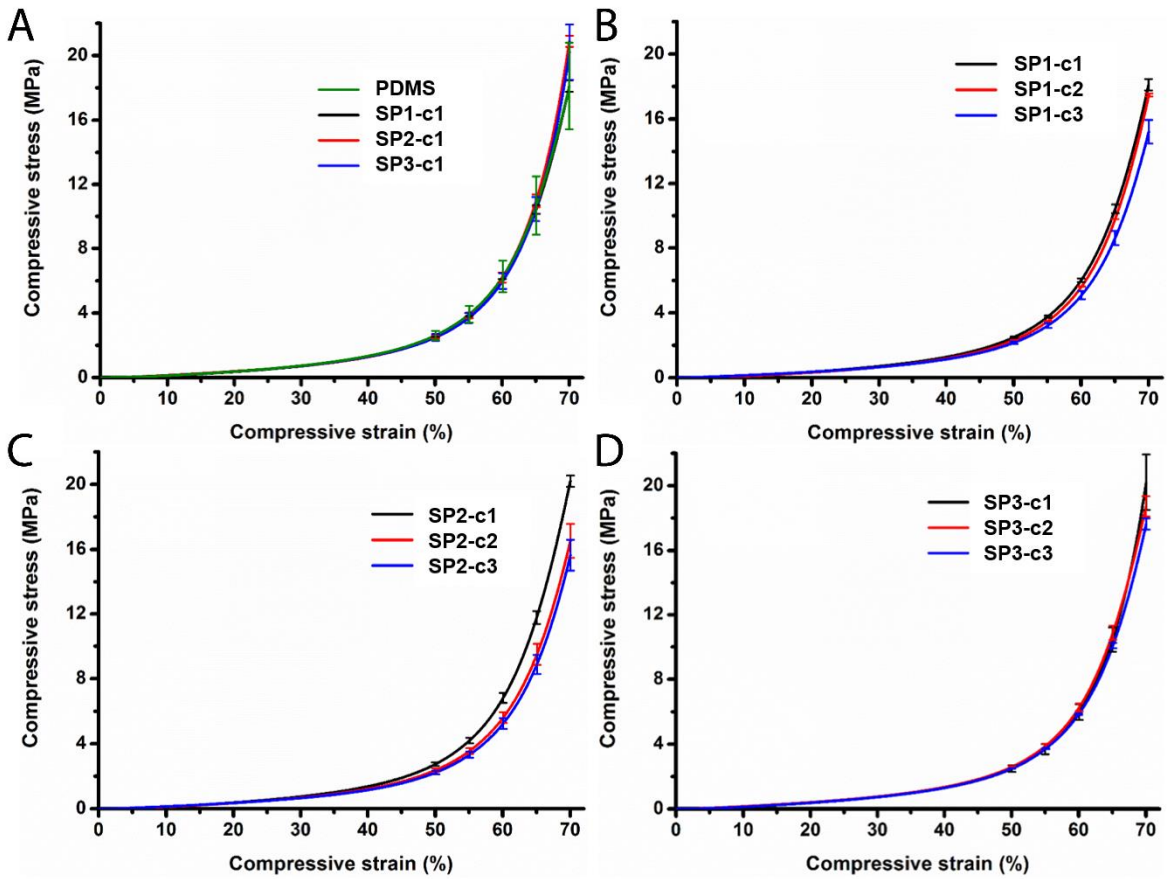

Figure A2.7. Compressive stress-strain curves of (A) PDMS and SP-c1, (B) SP1-c(1-3), (C) SP2-c(1-3), (D) SP3- c(1-3) at concentration of 5.0, 9.4 and 14.1 μmol/g.

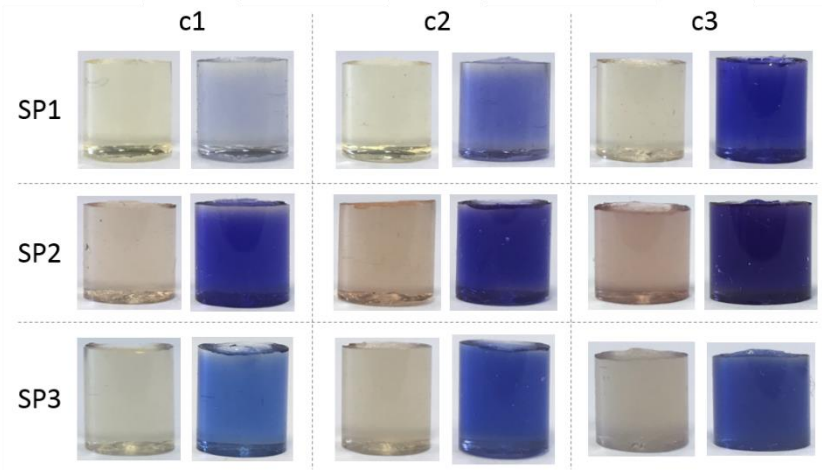

Figure A2.8. Optical images of SP-PDMS with different SP concentration before and after compression at a strain of 70%.

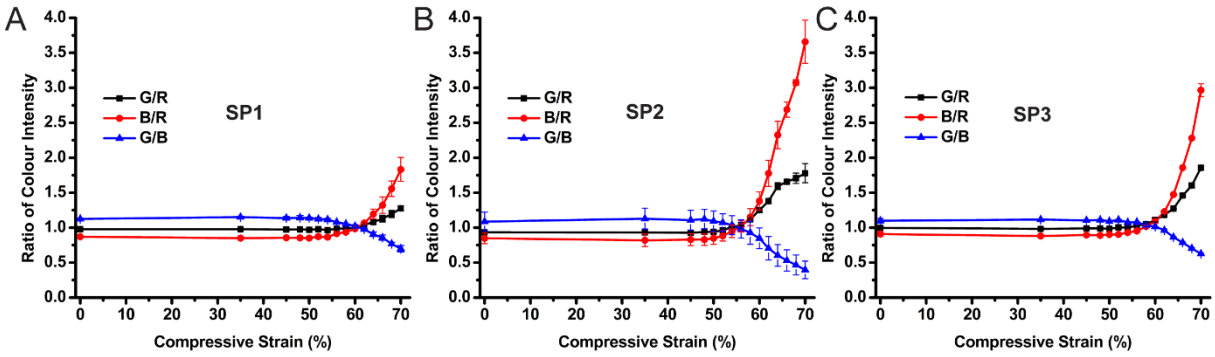

Figure A2.9. Ratio of RGB colour channel intensities as a function of compressive strain, (a) SP1, (b) SP2, and (c) SP3, at the concentration of c1.

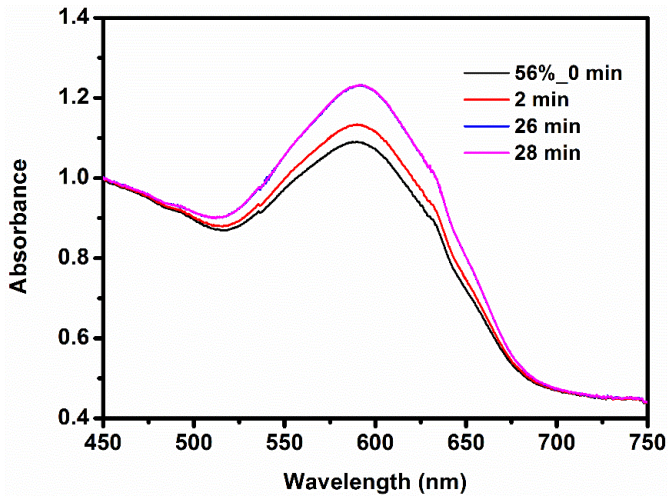

Figure A2.10. Absorption spectra of SP2-c1 under 56% compressive strain at different time.

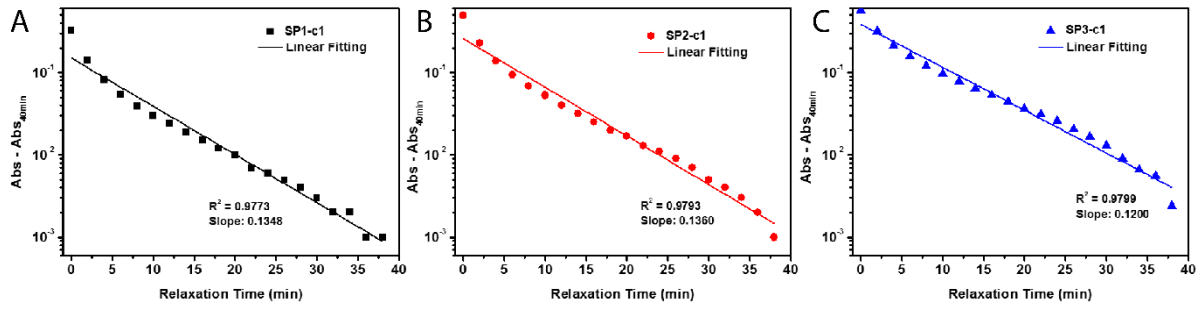

Figure A2.11. Plot of absorption intensity vs relaxation time for (A) SP1-c1, (B) SP2-c1, (C) SP3-c1, and their linear fitting curves.

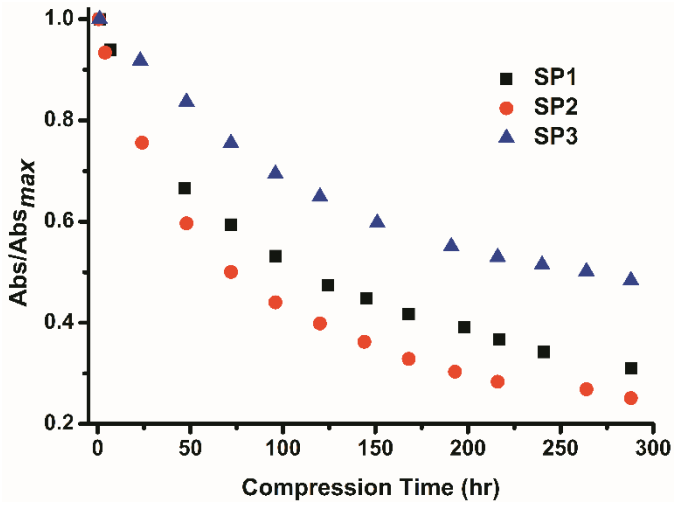

Figure A2.12. Plot of absorption intensity/maximum absorption intensity vs compression time at a strain of 62% in darkness for SP-c1.

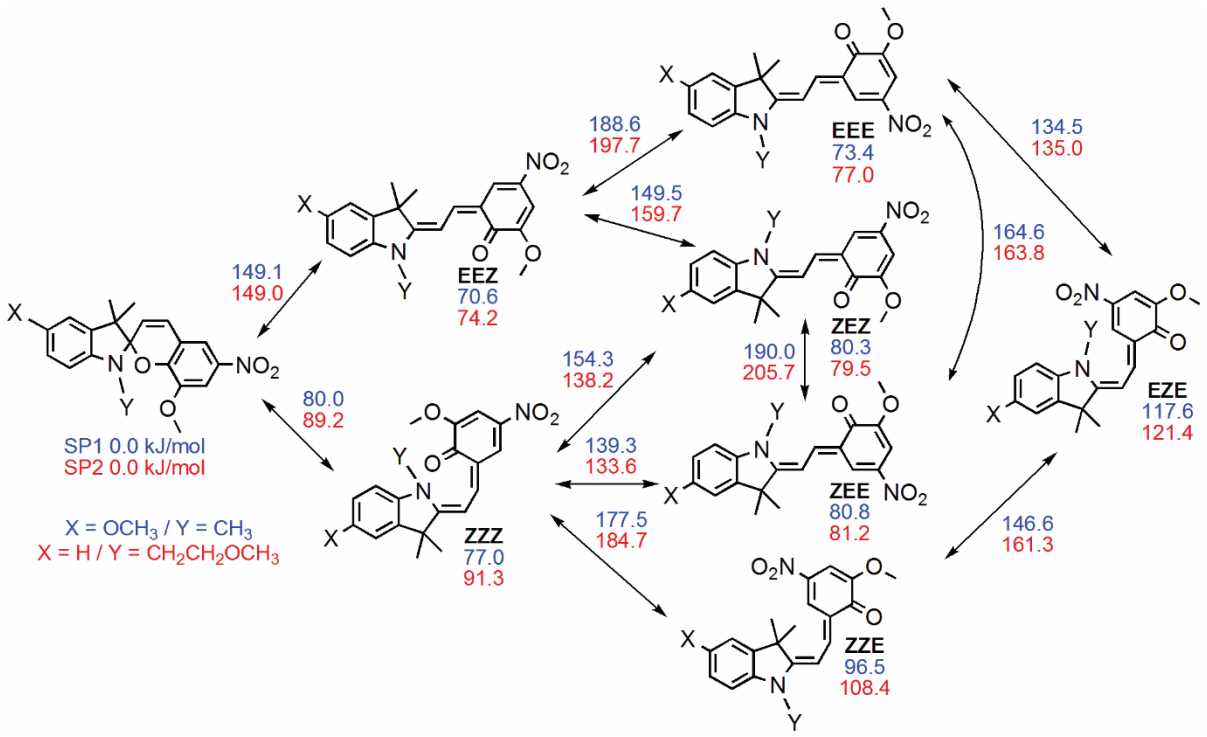

Figure A2.13. Calculated energies for merocyanine (MC) isomers of SP1 (blue) and SP2 (red) model compounds, with connecting transition state energies. Energies are 0 K enthalpies at the M06-2X/6-31G(d) level of theory.

Chapter 3 Appendix

Tri-methacrylate SP3: ^{1}H NMR (400 HZ, $CDCl_3$): δ 7.96 (d, 1H), 7.92 (d, 1H), 6.98-6.96 (d, 1H), 6.87-6.85 (dd, 1H), 6.80 (d, 1H), 6.60-6.58 (d, 1H), 6.32 (s, 1H), 6.07 (s, 1H), 5.93 (m, 2H), 5.74 (s, 1H), 5.57 (s, 1H), 5.51 (s, 1H), 4.25 (m, 2H), 3.35 (m, 2H), 2.07 (s, 3H), 1.92 (s, 3H), 1.70 (s, 3H), 1.23 (s, 3H), 1.19 (s, 3H).

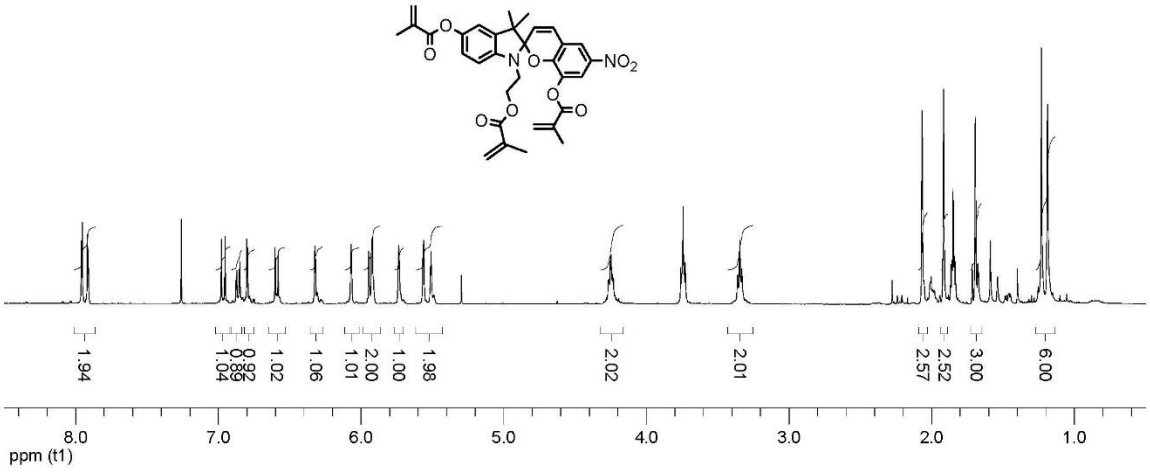

Figure A3.1. ^{1}H NMR spectrum of SP3.

1',3',3'-trimethyl-6-nitrospiro[chromene-2,2'-indoline]-5',8-diyl bis(2-methylacrylate) (di-methacrylate spiropyran **SP1**), and 3',3'-dimethyl-6-nitro-1'-(2-(methacryloyloxy)ethyl)spiro[chromene-2,2'-indoline]-8-yl (2-methylacrylate) (di-methacrylate spiropyran **SP2**) were synthesized via the same method from the hydroxyl versions. **SP1**: ^{1}H NMR (400 MHz, $CDCl_3$): δ 7.96 (d, 1H), 7.92 (d, 1H), 6.98 (d, 1H), 6.86 (dd, 1H), 6.79 (d, 1H), 6.45 (d, 1H), 6.32 (s, 1H), 5.91 (d, 1H), 5.89 (s, 1H), 5.74 (s, 1H), 5.51 (s, 1H), 2.64 (s, 3H), 2.07 (s, 3H), 1.69 (m, 3H), 1.24 (s, 3H), 1.21 (s, 3H). **SP2**: ^{1}H NMR (400 MHz, $CDCl_3$): δ 7.95 (d, 1H), 7.90 (d, 1H), 7.12 (m, 1H), 7.00 (d, 1H), 6.96 (d, 1H), 6.83 (m, 1H), 6.63 (m, 1H), 6.07 (s, 1H), 5.93 (d, 1H), 5.87 (s, 1H), 5.56 (s, 1H), 5.38 (s, 1H), 4.24 (m, 2H), 3.36 (m, 2H), 1.92 (s, 3H), 1.61 (s, 3H), 1.24 (s, 3H), 1.17 (s, 3H).

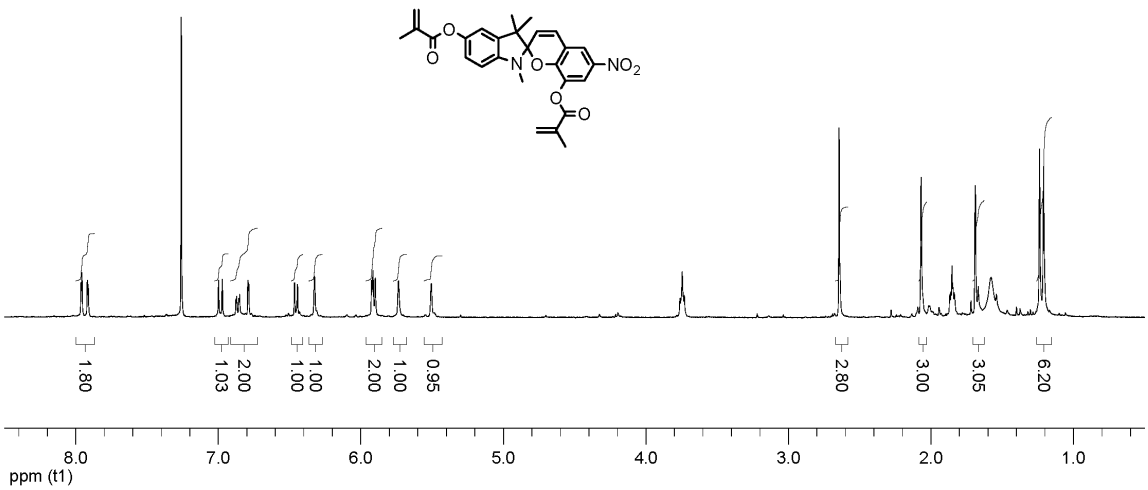

Figure A3.2. ^{1}H NMR spectrum of SP1.

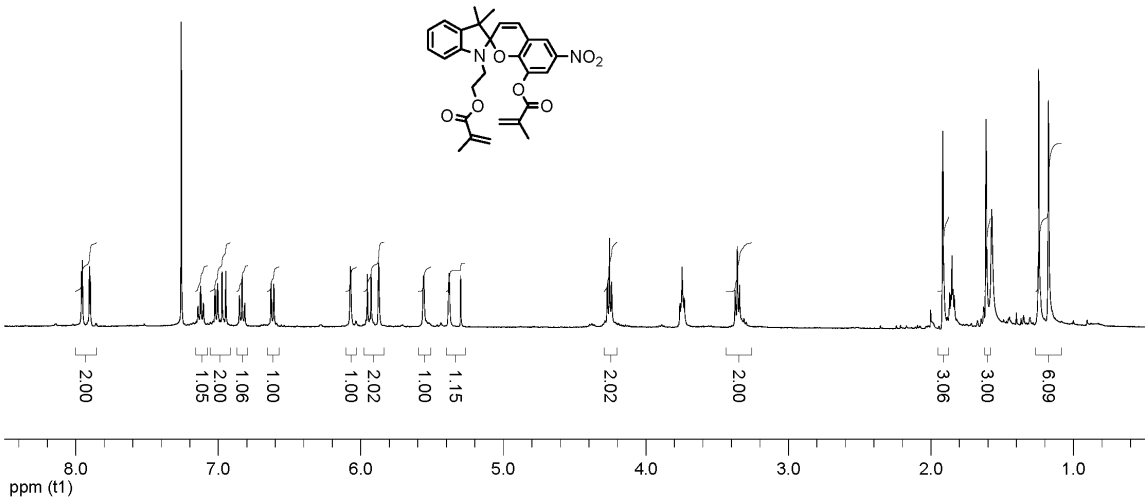

Figure A3.3. ^{1}H NMR spectrum of SP2.

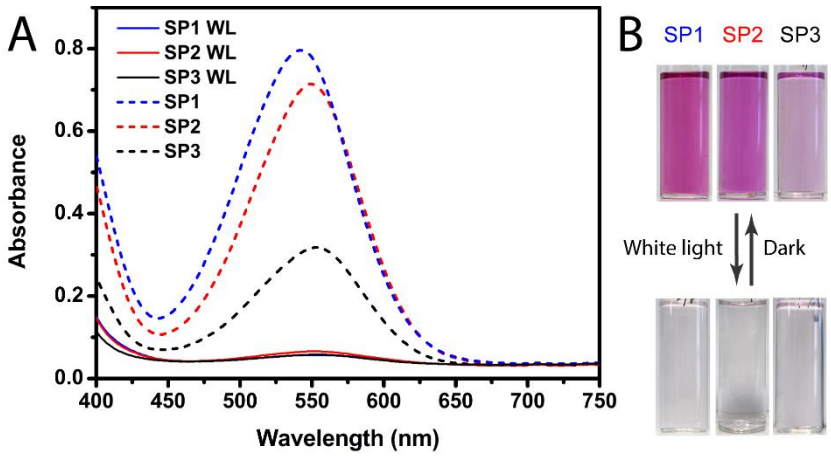

Figure A3.4. (a) Absorbance spectra of SP in HEA before (solid lines) and after being kept in the dark until plateaued (dashed lines), (b) images showing the reversibility of SP1-3 in HEA in the presence of white light and in the dark.

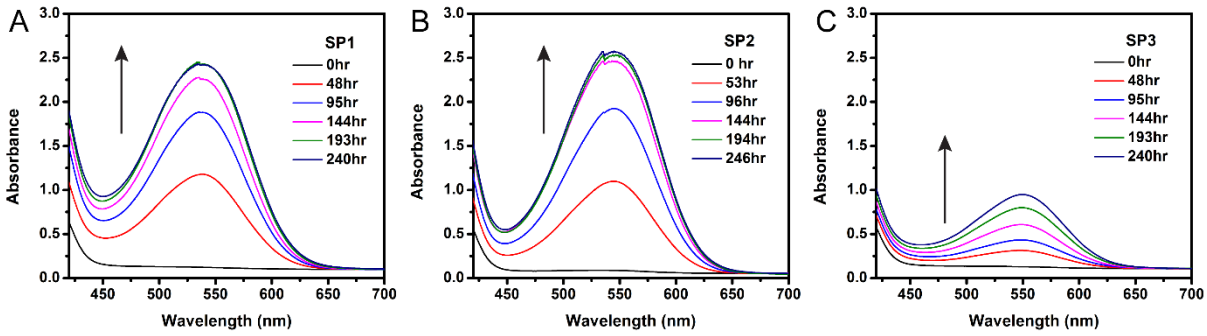

Figure A3.5. Absorbance spectra of SP(1-3)-PHEA films in the dark over 10 days.

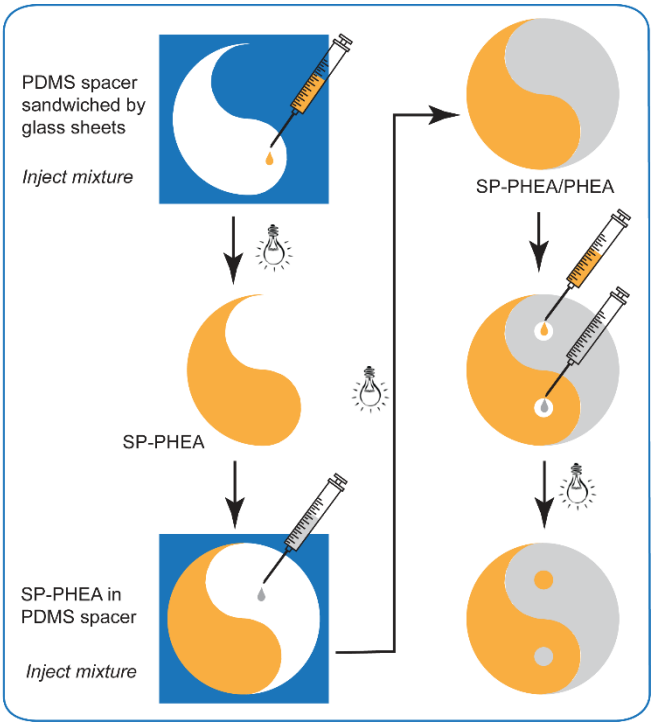

Figure A3.6. Preparation processes for "Yin-Yang" sample using SP-PHEA/PHEA.

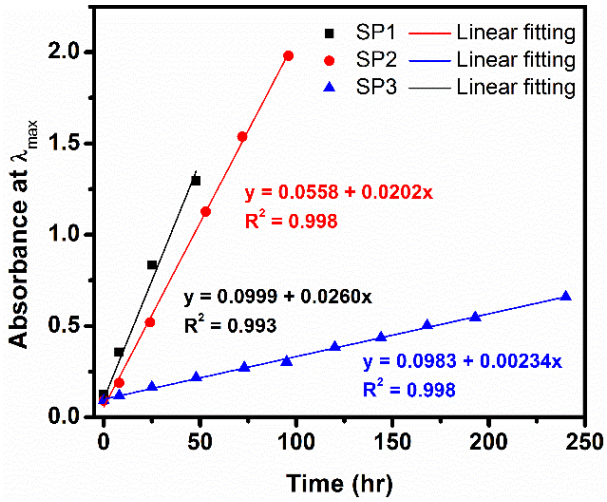

Figure A3.7. Linear fitting curves of absorption plots for SP1-3 films against the time stored in the dark.

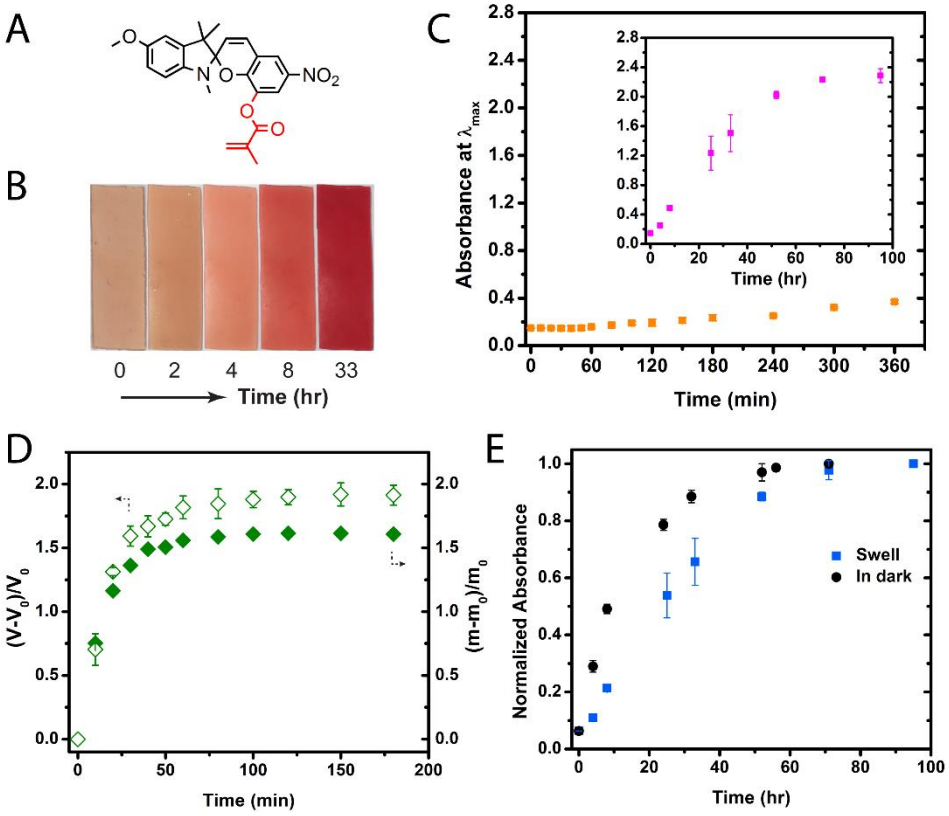

Figure A3.8. (A) Chemical structure of the control SP, (B) images of the control SP-PHEA films swollen in water with increasing time (images are not to scale), (C) plot of absorbance versus swelling time in water, (D) volume and mass change ratio, and (E) comparison of normalized absorbance plots of control SP-PHEA samples kept in the dark and swelling in water.

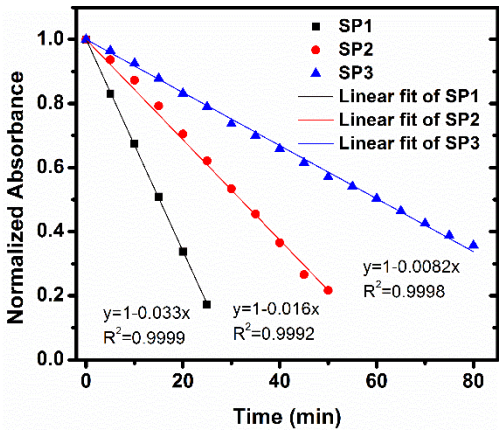

Figure A3.9. Linear fitting of absorption plots (linear range) for SP1-3 dehydrated films as a function of white light irradiation time, with slopes indicating the decolouration speed k_f.

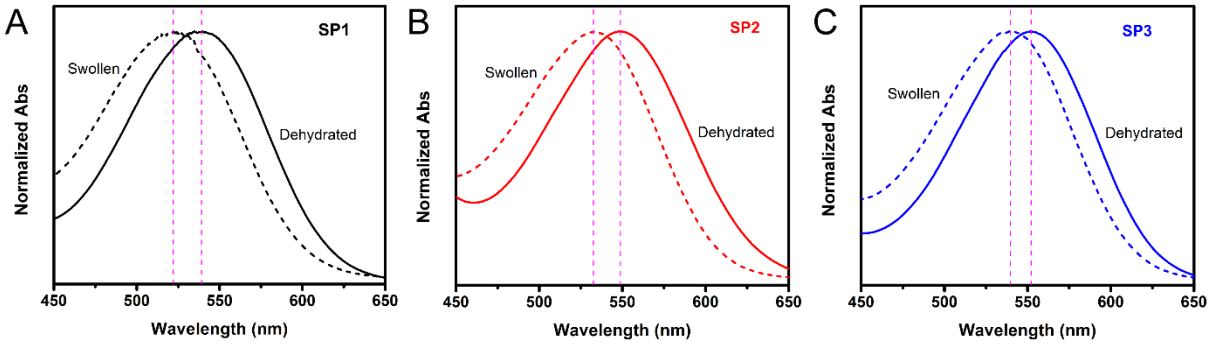

Figure A3.10. Changes in absorption spectra for SP1-3 (a-c) PHEA films under swollen and dehydrated state.

Chapter 4 Appendix

Table A4.1. Compositions of double and triple-network SP-polyacrylates; 1st-network pre-stretched ratio $\lambda_{prestretch}$ and swollen ratio $\lambda_{swollen}$

Sample	First network	$\lambda_{prestretch}$	$\lambda_{swollen}$
$BA_{0.5}BA$	SP 0.5 mol % (50% toluene)	1.77 ± 0.01	4.53 ± 0.17
$BA_{0.83}BA$	SP 0.83 mol % (50% toluene)	1.72 ± 0.02	4.57 ± 0.03
$BA_{1.17}BA$	SP 1.17 mol % (50% toluene)	1.73 ± 0.05	4.42 ± 0.10
$BA_{0.83(40)}BA$	SP 0.83 mol % (40% toluene)	1.64 ± 0.06	3.84 ± 0.42
$BA_{0.83(60)}BA$	SP 0.83 mol % (60% toluene)	1.81 ± 0.04	5.34 ± 0.10
$BA_{0.83}MA$	SP 0.83 mol % (50% toluene)	1.91 ± 0.04	5.80 ± 0.29
$BA_{0.83}BABA$	SP 0.83 mol % (50% toluene)	2.77 ± 0.17	13.2 ± 0.02
$BA_{0.83}MAMA$	SP 0.83 mol % (50% toluene)	3.16 ± 0.05	25.3 ± 1.60

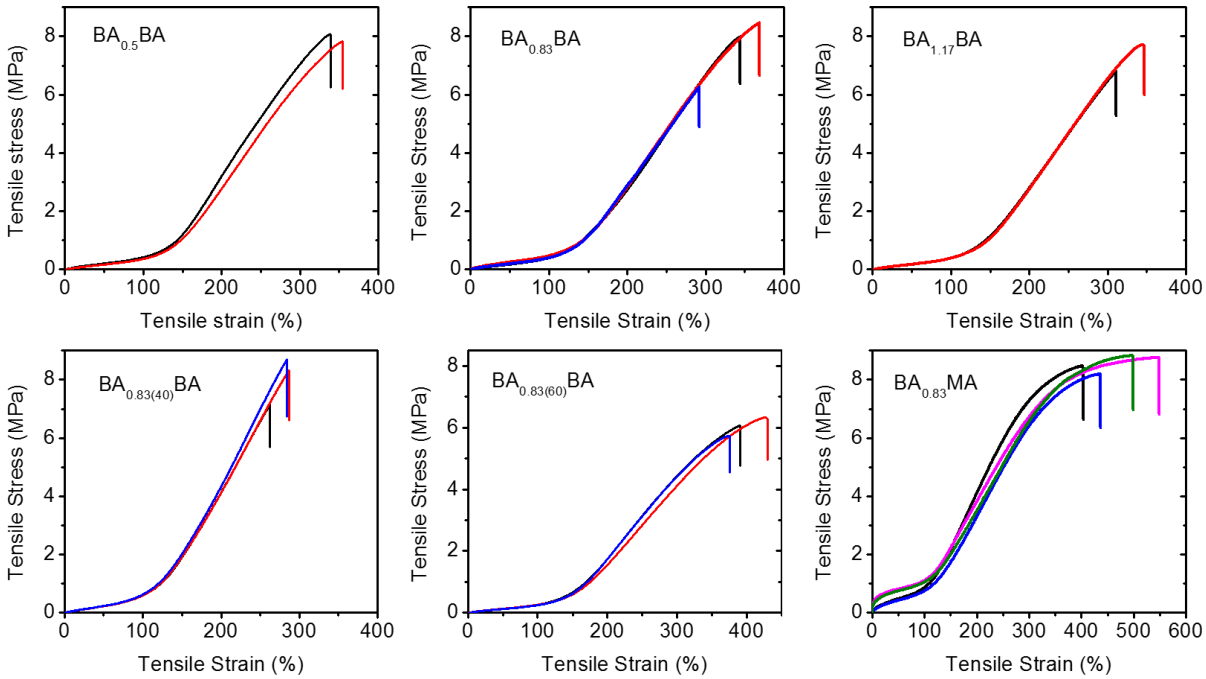

Figure A4.1. Tensile stress-strain curves of DN samples.

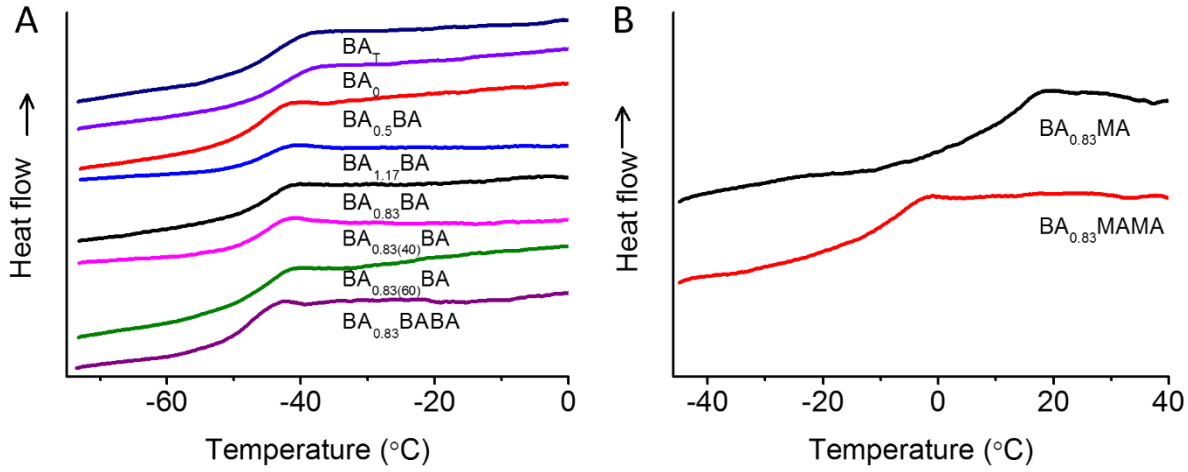

Figure A4.2. DSC curves presenting glass transition temperature for all the elastomers bearing spiropyran, with (A) butyl acrylate for all the networks, and (B) butyl acrylate for the first-network and methyl acrylate as the second- and third-network. *T*g is determined by the midpoint of the transition range.

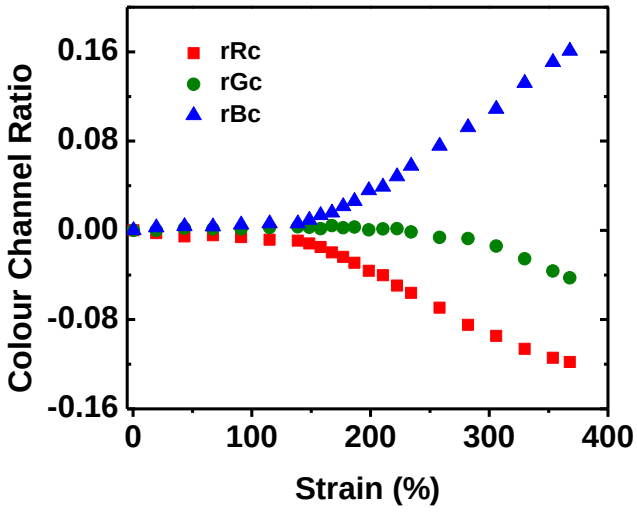

Figure A4.3. Plots of the ratio of RGB colour channel intensities as a function of tensile strain for DN sample $BA_{0.83}BA$.

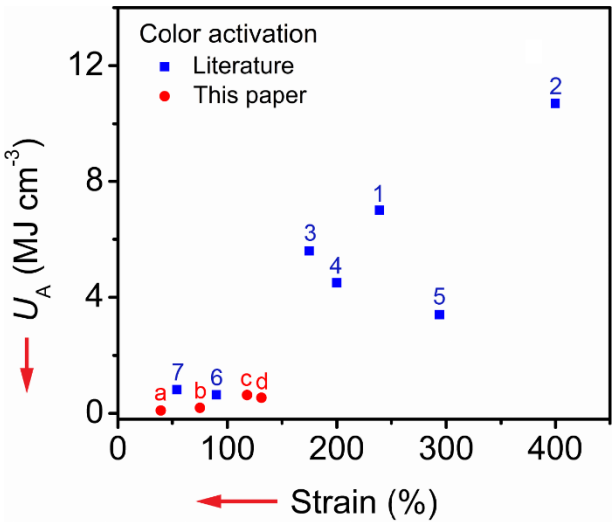

Figure A4.4. A plot of U_A against strain of SP-linked elastomers presented in this work (a-d) and reported in the literature (1-7).

References

(1) Davis, D. A.; Hamilton, A.; Yang, J.; Cremar, L. D.; Van Gough, D.; Potisek, S. L.; Ong, M. T.; Braun, P. V.; Martinez, T. J.; White, S. R.; Moore, J. S.; Sottos, N. R. Force-induced activation of covalent bonds in mechanoresponsive polymeric materials. *Nature* 2009, 459, 68-72.

(2) Gossweiler, G. R.; Hewage, G. B.; Soriano, G.; Wang, Q.; Welshofer, G. W.; Zhao, X.; Craig, S. L. Mechanochemical Activation of Covalent Bonds in Polymers with Full and Repeatable Macroscopic Shape Recovery. *ACS Macro Lett.* 2014, 3, 216-219.

Polymer Chemistry

PAPER

View Article Online
View Journal | View Issue

Cite this: *Polym. Chem.*, 2019, **10**, 1650

Insights into the mechanochromism of spiropyran elastomers†

Wenlian Qiu, Paul A. Gurr, Gabriel da Silva and Greg G. Qiao *

Received 7th January 2019,
Accepted 15th February 2019

DOI: 10.1039/c9py00017h

rsc.li/polymers

Colourless polymeric samples comprising mechanochromic spiropyrans (SPs) rapidly appear coloured under external pressure, due to their transition from ring-closed SP to ring-open merocyanine (MC). Here, we design a new spiropyran with three attachment points which was systematically compared with two widely used spiropyrans having two attachment positions in the same PDMS matrix on their mechanochromic properties, to determine whether the geometric effect or electronic effect dominates the force-responses. The attachment positions on the chromene ring on the three spiropyrans are identical, with varying attachment positions on the indoline ring. RGB colour analysis and *in situ* absorption measurements were used to characterize the optical changes and density functional theory calculations were used to better understand the isomerization process. The results demonstrated that by changing the attachment positions of SPs, both the electronic and geometric effects influenced mechanochromism with geometry playing a more dominant role.

1. Introduction

Mechanochromic materials are a class of stimuli responsive materials that show changes in optical properties under an external force. These have been shown to have potential applications as force sensors,[1–5] such as to display the impact of a ball on a tennis court, or as failure detection devices of polymeric materials such as those used in medical devices.[6] Mechanochromic materials have been reported to include inorganic fluorescent compounds,[7] photonic gels,[8] polymer films,[9] dye-polymer blends[10] and covalently linked chromophore polymers.[2–4,11] As early as 1926, spiropyrans (SPs) (Fig. 1) were reported to exhibit thermochromism[12] and have been widely investigated for their photochromic properties.[13,14] However, it was not until 2007 that spiropyran-linked PMA was shown to exhibit mechano-responsive properties in solution under ultrasound, and mechanochromism in bulk polymers in 2009.[11,15] Due to their fast mechanical-force responsive transition, from colourless spiropyran (SP) to purple merocyanine (MC), covalently linked spiropyran-polymers have been identified as promising candidates for practical reversible colour changing applications. Since the inception of mechanochromic SP-containing polymeric materials, synthetic polymer systems have not diverged significantly. To date, SPs have been covalently incorporated into various polymer networks, such as poly methyl (meth)acrylates, polyurethane, polystyrene, polydimethylsiloxane (PDMS), poly(ε-caprolactone), poly(ethylene-vinyl acetate), hydrogels and polyarylene.[15–24] The majority of the optical characterization studies have been based on tension loading or compression.[25,26] Kim *et al.* systematically compared the effect of tension and compression on the activation of SP-containing cross-linked PMMA at various temperatures, and found the stress required to activate SP under compression is higher than that under tension.[27]

Factors which influence the mechanochromic properties of spiropyran based materials include the polymeric architecture, the mechanical properties of the matrix and the structure of

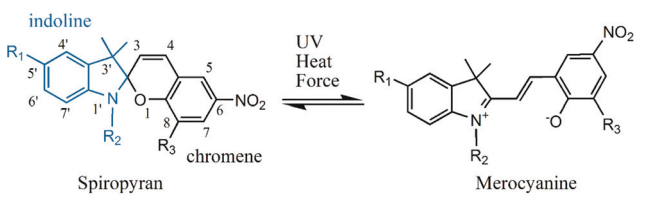

Fig. 1 Spiropyrans with varying attachment points, for **SP1**: R_1 and R_3; **SP2**: R_2 and R_3; **SP3**: R_1, R_2 and R_3 (this paper). Force, heat and UV light can be the external stimuli to activate the ring-closed SP to ring-open MC.

Department of Chemical Engineering, The University of Melbourne, VIC 3010, Australia. E-mail: gregghq@unimelb.edu.au

†Electronic supplementary information (ESI) available: NMR spectra and Mass spectra of SPs, compressive stress–strain curves of PDMS and SP-PDMS, RGB colour channel intensity ratios against strain curves, optical images of SP-PDMS, absorption spectra under a constant strain, plot of absorption intensity *vs.* relaxation time for SP, plot of absorption intensity ratio *vs.* compression time at 62% strain for SP over a long period, and calculated energies for merocyanine isomers. See DOI: 10.1039/c9py00017h

the spiropyran itself.[27–34] There are several easily functionalized attachment points on the spiropyran rings, where polymers can be covalently attached. The attachment positions can affect the ability of the applied force transmitted to the SP molecule leading to the spiro C–O bond cleavage.[32,33] The spiropyran molecules comprise an indoline ring and a chromene ring (Fig. 1), and only when both rings are connected to polymer chains can the external force be transferred to the C–O bond causing it to cleave.[15] Two widely used 6-nitro-SP mechanophores (Fig. 1) with different attachment positions at R_1 and R_3 (**SP1**), and R_2 and R_3 (**SP2**) have been prepared and incorporated into various polymer matrices.[26] Single molecule force spectroscopy was utilized to calculate the contour lengths upon ring opening, compared with computational predictions, and concluded that the activation forces for **SP1** and **SP2** are different.[32] Recently, single molecule force spectroscopy was also used to study the substituent effect and showed strong electron withdrawing groups on the chromene ring helped stabilize the negative charge on the MC resulting in a lower activation energy.[31] Gossweiler *et al.* reported that **SP2**-PDMS films showed a blue colour under tension and purple upon relaxation, which they hypothesized was a result of MC isomerization.[19] Craig's group designed three SP derivatives without 6-nitro, while varying the attachment points on the chromene ring at 8-, 7- and 6-positions, to study the regiochemical effects on the mechanochromism.[33]

Varying the attachment positions would cause geometry effect (the isomerization affected by the attachment points' location) and electronic effect (the isomerization affected by the electron donating or withdrawing capacity) differences. It is important to know the dominant effect which influences mechanochromism, in order to guide the design of force-responsive materials. In this study, two previously reported mechanochromic spiropyrans **SP1** and **SP2**, as well as a new **SP3** (Fig. 1), which combines the attachment positions of both **SP1** and **SP2**, were prepared. These were tested under compression and tension to investigate whether the geometric effect or electronic effect, caused by varying attachment positions, dominates the mechanochromic responses.

2. Experimental

2.1. Materials

Dichloromethane (AR, Chem-Supply), diethyl ether (anhydrous, Chem-Supply), 4-dimethylaminopyridine (≥98%, Sigma), ethanol (100%, Chem-Supply), glacial acetic acid (AR, Chem-Supply), hexane (99%, RCI Labscan), hydrobromic acid (48%, AR, Chem-Supply), 2-iodoethanol (99%, Sigma), (4-methoxy)-phenyl hydrazine hydrochloride (99%, ThermoFisher), methanol (AR, Chem-Supply), methyl iodide (99%, Sigma), methyl isopropyl ketone (99%, Sigma), phenylhydrazine hydrochloride (≥99%, Merck), piperidine (≥99.5%, Sigma), toluene (AR, Chem-Supply), triethylamine (≥99%, Sigma), 4-pentenoic anhydride (98%, Sigma), and *o*-vanillin (99%, Sigma) were used as received, unless otherwise stated. Tetrahydrofuran (THF, Chem-Supply) was pre-dried over sodium, before being distilled from benzophenone and sodium under an inert atmosphere of nitrogen prior to use. Sylgard® 184 (PDMS) was purchased from Gelest Inc. as a two part system A and B and mixed prior to curing.

2.2. Synthesis of vinyl functionalized spiropyrans (SP1–3)

The di-vinyl spiropyrans **SP1** and **SP2** were synthesized according to literature procedures.[15,19] The tri-vinyl spiropyran **SP3** was synthesized based on the synthesis strategy of **SP1** and **SP2**.

Synthesis of di-vinyl spiropyran: 1′,3′,3′-trimethyl-6-nitrospiro[chromene-2,2′-indoline]-5′,8-diyl bis(pent-4-enoate) (SP1). 1′,3′,3′-Trimethyl-6-nitrospiro[chromene-2,2′-indoline]-5′,8-diol[15] (0.20 g, 0.56 mmol, 1.0 equiv.) and 4-dimethylaminopyridine (DMAP) (0.12 g, 1.02 mmol, 1.8 equiv.) in THF (5 mL) were treated with 4-pentenoic anhydride (0.27 mL, 1.47 mmol, 2.6 equiv.). After stirring for 7 h, the crude reaction mixture was passed through a basic alumina column and rinsed with DCM (100 mL). The solution was extracted with distilled water (2 × 100 mL), dried over $MgSO_4$, filtered and reduced to dryness *in vacuo* to afford **SP1** as a dark yellow solid (0.17 g, 0.33 mmol, 59% yield). ^{1}H NMR (400 MHz, $CDCl_3$): δ 7.94 (d, 1H), 7.82 (d, 1H), 6.99 (d, 1H), 6.85–6.80 (ddd, 2H), 6.49 (d, 1H), 5.92–5.89 (m, 2H), 5.66–5.59 (m, 1H), 5.16–5.06 (m, 2H), 4.96–4.92 (m, 2H), 2.65 (s, 3H), 2.62–2.51 (m, 2H), 2.21 (m, 2H), 1.96 (m, 2H), 1.25 (s, 3H), 1.21 (s, 3H). MS (ESI): $[M + H^+]$ calculated for $C_{29}H_{30}N_2O_7$, calculated for, 518.2; found, 519.20117.

Synthesis of di-vinyl spiropyran: 3′,3′-dimethyl-6-nitro-1′-(2-(pent-4 enoyloxy)ethyl)spiro[chromene-2,2′-indolin]-8-yl pent-4-enoate (SP2). To 1′-(2-hydroxyethyl)-3′,3′-dimethyl-6-nitrospiro[chromene-2,2′-indolin]-8-ol[19] (0.20 g, 0.54 mmol, 1.0 equiv.) and 4-dimethylaminopyridine (DMAP) (0.12 g, 1.02 mmol, 1.8 equiv.) in 5 mL THF was added 4-pentenoic anhydride (0.26 mL, 1.45 mmol, 2.6 equiv.). After stirring for 7 h, the crude reaction mixture was passed through a plug of basic alumina and eluted from the column with DCM. The solution was extracted with distilled water (2 × 100 mL), dried over $MgSO_4$, filtered and reduced to dryness *in vacuo* to afford **SP2** as a yellow solid (0.17 g, 0.32 mmol, 59% yield). ^{1}H NMR (400 MHz, $CDCl_3$): δ 7.95 (d, 1H), 7.82 (d, 1H), 7.16 (t, 1H), 7.06 (d, 1H), 6.95 (d, 1H), 6.86 (t, 1H), 6.65 (d, 1H), 5.96 (d, 1H), 5.81–5.71 (m, 1H), 5.59–5.49 (m, 1H), 5.03–4.86 (m, 4H), 4.27–4.11 (m, 2H), 3.33 (t, 2H), 2.38–2.24 (m, 4H), 2.24–2.09 (m, 2H), 1.88–1.82 (m, 2H), 1.26 (s, 3H), 1.18 (s, 3H). MS (ESI): $[M + H^+]$ calculated for $C_{30}H_{32}N_2O_7$, calculated for, 532.2; found, 533.21592.

Synthesis of tri-vinyl spiropyran: 3′,3′-dimethyl-6-nitro-1′-(2-(pent-4-enoyloxy)ethyl)spiro[chromene-2,2′-indoline]-5′,8-diyl bis(pent-4-enoate) (SP3). Indolium iodide **1** (0.5 g, 1.44 mmol, 1 equiv.), 2-hydroxy-3-methoxy-5-nitro-benzaldehyde **2** (0.265 mg, 1.44 mmol, 1 equiv.), and piperidine (0.285 mL, 2.88 mmol, 2 equiv.) were dissolved in absolute EtOH (15 mL) and heated to reflux. After 2.5 h, the solution was cooled, filtered and the precipitate rinsed with cold EtOH, to afford tri-

functional spiropyran **3** as a black powder. To compound **3** (0.20 g, 0.52 mmol, 1.0 equiv.) and 4-dimethylaminopyridine (DMAP) (0.15 g, 1.23 mmol, 2.4 equiv.) in THF (10 mL) was added 4-pentenoic anhydride (0.34 mL, 1.88 mmol, 3.6 equiv.). After stirring for 7 h, the crude reaction mixture was passed through a basic alumina column and diluted with DCM (100 mL). The solution was extracted with distilled water (2 × 100 mL), dried over $MgSO_4$, filtered and reduced to dryness *in vacuo* to afford **SP3** as a yellow solid (0.19 g, 0.30 mmol, 58% yield). ^{1}H NMR (400 MHz, $CDCl_3$): δ 7.94 (d, 1H), 7.83 (d, 1H), 6.98 (d, 1H), 6.85–6.80 (ddd, 2H), 6.62 (d, 1H), 5.95–5.84 (m, 2H), 5.83–5.70 (m, 1H), 5.17–4.90 (m, 6H), 4.26–4.18 (m, 1H), 4.16–4.07 (m, 1H), 3.30 (t, 2H), 2.64 (t, 2H), 2.50 (m, 2H), 2.39–2.13 (m, 6H), 1.96 (m, 2H), 1.24 (s, 1H), 1.19 (s, 1H). MS (ESI): [M + H^+] calculated for $C_{35}H_{38}N_2O_9$, calculated for, 630.2; found, 631.26077.

All SPs were kept at −20 °C in the absence of light prior to use.

Cylindrical and film sample preparation. The main components of commercial Sylgard™184 in a two-component system A and B are vinyl terminated polysiloxane, the poly (methyl hydrosiloxane-*co*-dimethylsiloxane) copolymer and a platinum catalyst. The hydrosilane component reacts with vinyl moieties *via* hydrosilylation in the presence of the platinum catalyst to form covalently linked elastomer networks. The co-reaction of vinyl terminated spiropyrans **SP1–3** with Sylgard 184 allows spiropyran mechanophores to be covalently attached to the polymer network.[19,35]

Three concentrations of SPs in silicone networks were prepared based on varying mole/weight ratios (SP/Sylgard™ base = μmol g^{-1}: *c*1 = 5.0 μmol g^{-1}, *c*2 = 9.4 μmol g^{-1} and *c*3 = 14.1 μmol g^{-1}). Vinyl terminated SPs were dissolved in toluene (10 vol/wt% of Sylgard A), followed by the addition of the Sylgard component A and then the curing agent B (6 : 1 ratio respectively). The ratio of the base/curing agent was adjusted to 1 : 6 to reduce viscosity and improve the properties of the cured silicone samples.[36] The mixture was stirred using a glass rod and vortexed until homogeneous prior to (i) casting onto a dog-bone shaped Teflon mould or transferring to 3 mL polypropylene syringes to prepare (ii) thin films (thickness: 0.4–0.5 mm, width: 0.4 mm, gauge length: 10 mm, other than specifically noted) and (iii) cylindrical elastomers (diameter: 8.5 mm), respectively. All specimens were cured in a vacuum oven at 65 °C overnight. The cured cylindrical samples were cut into 8–9 mm height samples for compression testing.

2.3. Characterization

Nuclear magnetic resonance (NMR) spectroscopy. ^{1}H NMR spectroscopy was conducted on a Varian Unity 400 MHz spectrometer operating at 400 MHz, using the deuterated solvent as the reference and a sample concentration of ~10 mg mL^{-1}.

Mass spectrometry (MS). Liquid chromatography mass spectrometry (LC-MS) was performed on a high-resolution Agilent 6520 Q-TOF. ESI (Electrospray Ionisation) solutions (~5 ppm) were prepared with HPLC grade acetonitrile and transferred to the electrospray source by using an autosampler. For each analysis, 1 μL of sample was injected into the carrier solvent stream of 70% acetonitrile in 0.1% formic acid at a flow rate of 0.3 mL per minute. Recorded *m*/*z* data were corrected using a reference mass by a dual-spray electrospray ionisation source and using the factory-defined calibration procedure. Mass spectrometer conditions: drying gas flow rate, 7 L min^{-1}; nebulizer pressure, 40 psi; drying gas temperature, 300 °C; capillary voltage, 4000 V; skimmer voltage, 65 V; Oct Rf, 750 V; scan range acquired, 100–1000 *m*/*z*.

Mechanical tests and RGB analysis. Compression and tensile tests were performed uniaxially at room temperature on an Instron 5848 Microtester with Bluehill material testing software with a 2 kN loading cell. Tensile measurements were performed on dog-bone shaped samples fastened between two grips and tested in triplicate at a strain rate of 1% s^{-1}. Compression testing of cylindrical specimens was performed in triplicate at a strain rate of 1% s^{-1}. The compression test was ended at 70% strain and the tensile test was ended at 200% strain. Video recording was performed during testing for colour analysis. RGB values were determined after white balance calibration in Adobe Photoshop™ software. The colour channel ratios were determined as green/red, blue/red and green/blue.

UV–visible spectroscopy (UV-Vis). UV–Vis analysis was performed on a Shimadzu UV–Vis Scanning Spectrophotometer (UV-2101 PC) with a scanning rate of 0.2 nm. The scanning range of the wavelength was 750–380 nm.

Absorption analysis under load. Test samples were held under various deformation and long loading time, using a purpose-built clamp, which could be adjusted to various compression pressures and was able to be placed in the UV-Vis spectrometer. The standard placement of the mechanochromic and reference samples (PDMS) in line with the beam resulted in the routine analysis of mechanochromic samples under loading. Absorption intensities (Abs) were normalized using eqn (1):

$$\mathrm{Abs} = (I_\varepsilon - I_{\varepsilon=0})/\sqrt{1/(1-\varepsilon)} \quad (1)$$

where I_ε is the absorbance value at a given compressive strain ε and $I_{\varepsilon=0}$ is the absorbance value at zero strain. Compressive strain was calculated by $\varepsilon = (l_0 - l)/l_0 \times 100\%$, where l_0 and l are the sample length before and after compression respectively. The factor $\sqrt{1/(1-\varepsilon)}$ normalizes the absorbance caused by diameter change under compression. Since this study focused on the comparative compressive response of different SPs but not kinetics, and the path of the beam passing through the specimens was the same even under the same strain (the diameter of all the specimens was the same), so a ratio of $\sqrt{1/(1-\varepsilon)}$ without the exact diameter value was involved here.

3. Results and discussion

In order to study the influence of electronic and geometric effects caused by varying attachment positions on spiropyran,

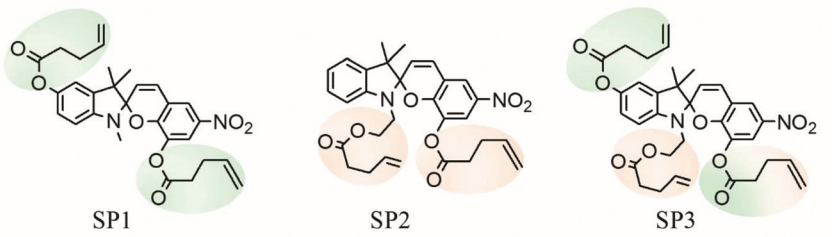

Fig. 2 Chemical structures of three vinyl terminated SPs (**SP1**, **SP2** and **SP3**) with different attachment points.

SP3 was prepared which combined all of the attachment points present on **SP1** and **SP2**. The series of di- and tri-vinyl functionalized spiropyrans with variable attachment positions (**SP1–3**) were prepared (Fig. 2). Di-substituted **SP1** and **SP2** were prepared as previously reported[15,19] and the new tri-substituted **SP3** was prepared by a similar method (Scheme 1). Thus, the condensation of 2-hydroxyethyl-2,3,3-trimethyl-3*H*-5-hydroxy-indolium iodide (**1**) with 2,3-dihydroxy-5-nitro-benzaldehyde (**2**) produced hydroxyl terminated spiropyran (**3**). Upon isolation, the spiropyran **3** was esterified with 4-pentenoic anhydride to produce vinyl terminated **SP3**.

The cross-linked SP-PDMS samples were prepared from **SP1–3** according to a previous publication.[19] A mixture of Sylgard™ (1.0 g, 6 parts A : 1 part B) and spiropyrans **SP1–3** (5–14.1 μmol) were mixed thoroughly and cast *in situ* and cured at 65 °C overnight. Thus, pale yellow PDMS crosslinked samples of two "arms" **SP1** and **SP2**, and three "arms" **SP3** were prepared. Thus, the attachment points on the chromene ring for all SPs are identical (8-position), with varying attachment positions on the indoline ring for **SP1** (5′-position) and **SP2** (1′*N*-position), while **SP3** has a combination of these (5′ and 1′*N*) (Fig. 1). RGB colour analysis and *in situ* absorption measurement were used to characterize the optical changes. Density functional theory modelling was performed to assist in understanding the mechanisms responsible for the colour transitions observed in various samples.

3.1. Mechanochromic properties

The mechanical properties of cross-linked PDMS (pure Sylgard) and SP-PDMS samples were investigated, and the effect of the incorporation of small amounts of spiropyrans **SP1–3** into PDMS was compared (Fig. S7†). The stress–strain curves of crosslinked PDMS and all three SP samples were identical within experimental error, demonstrating the incorporation of small amounts of SP had negligible effect on the mechanical performance of PDMS bulk samples.

The colour change was observed after the threshold of activation compressive strain. Significant colour changes of samples were observed after release from 70% compression strain (Fig. S9†). The RGB colour channel ratios showed a decrease in the green/blue ratio and an increase in blue/red and green/red ratios (Fig. S8†). The blue/red values having the greatest change were used to define the onset of activation points for all samples (Fig. 3a), determined by the crossover point of two tangent lines.[37] Consistent with previous reports,[38] the stress–strain curves rose sharply after the onset of activation, indicating that the stress stiffening point is critical for SP activation in elastomers under compression. The threshold activations were at the strain around 60% (Fig. 3a) and under the stress of 4–7 MPa, specifically 58.6 ± 1.0% for **SP2**, 60.7 ± 0.6% for **SP3** and 61.1 ± 0.8% for **SP1**. Notably, the ratios of RGB intensity for the three spiropyran systems varied. **SP2** showed the greatest change after 70% compressive strain, followed by **SP3**, and **SP1** presented the smallest change among the three systems. In addition, the colour turned darker as the concentration increased at a constant strain (Fig. S9†). Chromaticity represents a colour quality regardless of the luminance; the chromaticity diagram based on coordinates (x, y) is calculated from RGB colour values according to the transformation matrix according to standard CIE1931.[39] By converting RGB values to chromaticity coordinates, the colour changing paths of SP under compression and relaxation are more visualized (Fig. 3b). Pristine light-yellow SP switched to blue (not obvious for **SP1**) as compressive strain increased and shifted toward the blue-violet colour upon relaxation before returning to light yellow. The variation of **SP2** and **SP3** is much

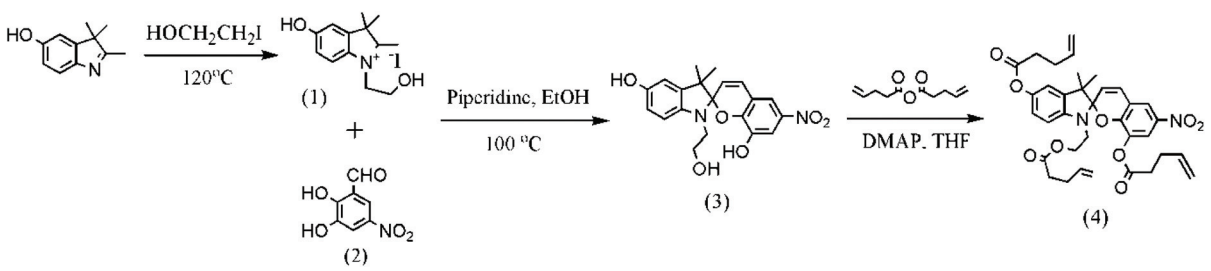

Scheme 1 Synthesis route of tri-vinyl **SP3** (**4**).

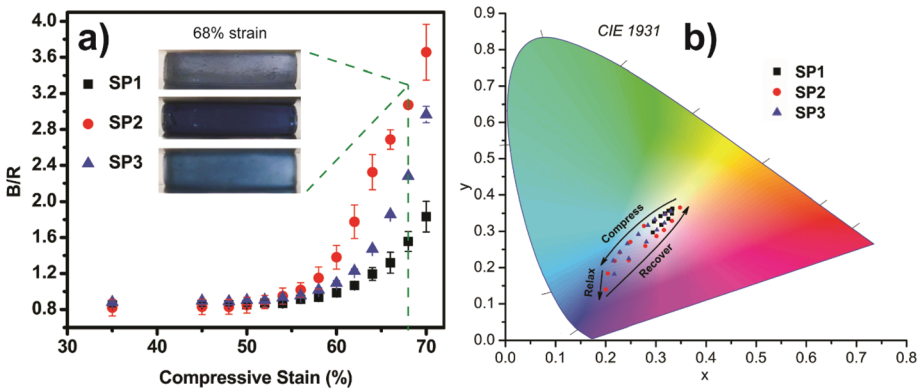

Fig. 3 (a) Corresponding B/R values (blue channel intensity/red channel intensity) as a function of compressive strain for SP samples (conc. = 5.0 μmol g^{-1}), and the inset images of SP samples at 68% strain; (b) chromaticity diagram (standard CIE 1931) of SP samples showing the colour change directions under compression (strain: 0% to 70%), relaxation and recovery (**SP1–3**: conc. = 5.0 μmol g^{-1}).

greater than that of **SP1**. The colour difference under pressure and after relaxation could be caused by different MC isomers,[19] which will be further discussed in the following sections.

Absorption spectra were also utilized to confirm the compressive activation of SP-PDMS (Fig. 4) in addition to RGB analysis from optical images (Fig. 3). Before deformation, there was negligible absorption in the visible range for all SP samples, indicating that the ring-closed spiropyran was the dominant form (Fig. 4a–c). Upon activation, absorption peaks at 500–650 nm appeared, corresponding to ring-open merocyanine. The absorption intensity of all SP samples increased as

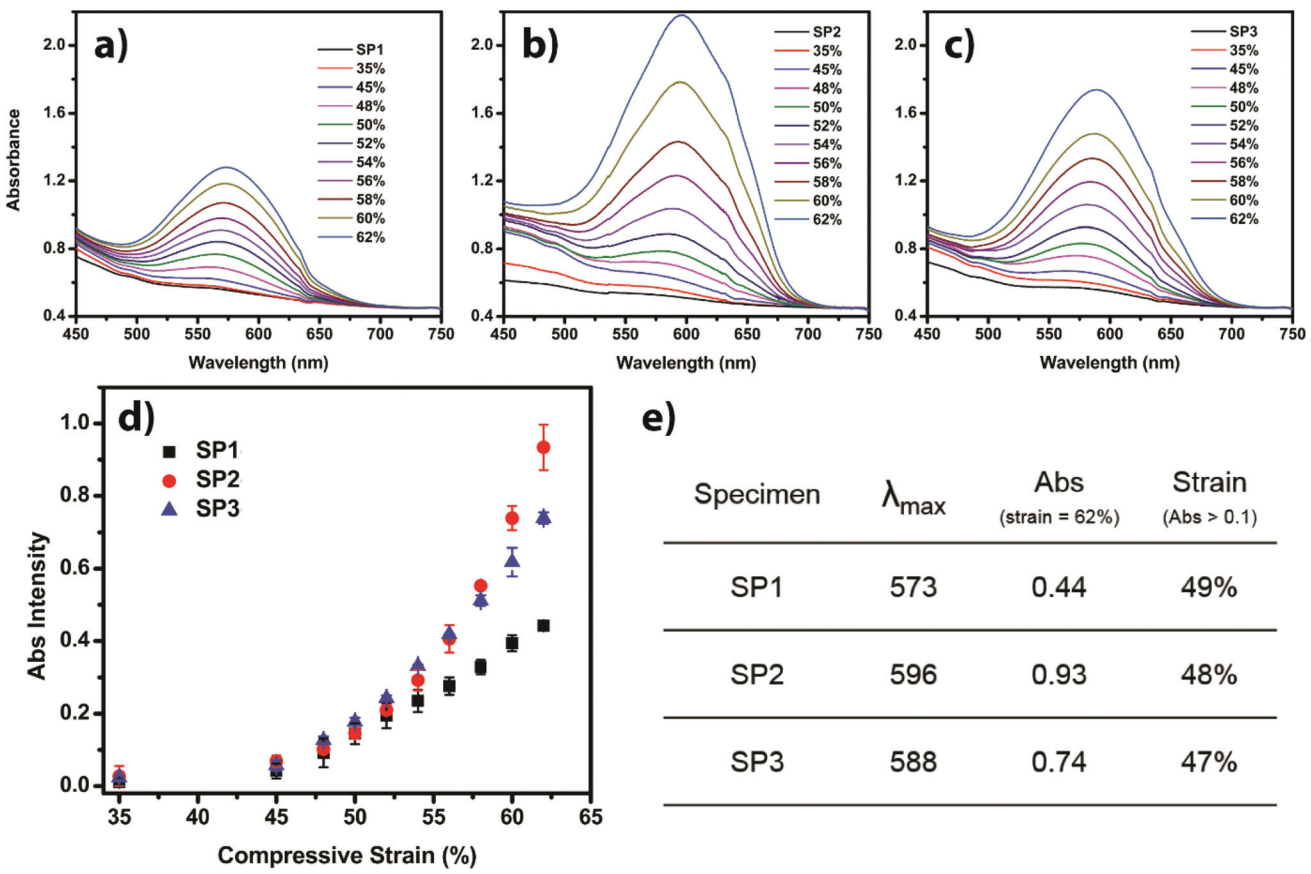

Specimen	λ_{max}	Abs (strain = 62%)	Strain (Abs > 0.1)
SP1	573	0.44	49%
SP2	596	0.93	48%
SP3	588	0.74	47%

Fig. 4 UV-Vis absorption spectra of SP elastomers at a concentration of 5.0 μmol g^{-1}, (a) **SP1**, (b) **SP2**, (c) **SP3** with increasing compressive strain. (d) Plot of absorption intensity *vs.* compressive strain. (e) Parameters from UV-Vis absorption spectra of a–c, where λ_{max} refers to the maximum absorption wavelength at the strain of 62%.

compressive strain increased and reached a relatively steady value after 20–30 min under a constant strain (Fig. S10†). This demonstrated that the gradual increase in SP activation to the ring-open MC under deformation continued until reaching a plateau after a certain time under a constant strain. This indicates the applied stress in bulk samples requires a certain time to fully equilibrate. The compressive response of the three SP systems was compared. At each strain point, absorbance was acquired after 30 min to ensure the conversion between SP and MC achieved equilibrium. Although the absorption intensities of all SP's were significantly different under a large strain, the activation thresholds at 47% strain (**SP3**), 48% (**SP2**) and 49% strain (**SP1**) did not show a statistical difference. The activation thresholds differed from the results of RGB analysis due to different loading rates, as the compression measurements were completed in 70 seconds, while the absorption measurements were given enough time to reach a plateau. This is consistent with the study by Kim which showed that the onset of activation strain increased with a faster strain rate.[27] Consistent with the above RGB analysis, the order of the absorption intensity under the strain of 62% is **SP2** > **SP3** > **SP1**. These results indicate that **SP2**-PDMS shows an advantage over **SP1** and **SP3** in emitting the optical signal after the onset of activation. Interestingly, **SP3** with an extra attachment point did not show an advantage over **SP2**, with respect to optical change under a large strain, but it remained more active than **SP1**. A previous study on the simulation of two attachment points on the indoline ring inferred that the external force is transferred to the *N* position.[15] In terms of force distribution, it is possible that the applied energy on the **SP3** molecule inefficiently transferred to the spiro C–O bond, and is partially distributed on the indoline ring because the two attachment positions are unlikely to be in the same direction against the pulling point on the chromene ring under stretching. If so, the extra attachment on **SP3** should have less ring opening ability than **SP1** and **SP2**. However, comparing **SP1** and **SP3**, the extra attachment at the 1′ *N*-position improved the force response; comparing **SP2** and **SP3**, the extra attachment at the 5′-position decreased the force response. Thus, the attachment point at the 1′*N*-position having a shorter C–O distance plays a key role in force activation.

The maximum absorption wavelength (λ_{max}) of **SP1**, **SP2**, and **SP3** at the compressive strain of 62% is 573, 596, and 588 nm respectively (Fig. 4a–c), which are assigned to ring-opened MC. As compressive strain increased, the λ_{max} of each SP shifted slightly toward larger wavelengths, but not obvious for **SP1**. Consistent with the absorption spectra of compression samples, the absorption bands of SP-PDMS under tension performed similarly under stress and after relaxation. The location of absorption bands was more obvious on tensile samples as the deformations were larger. The λ_{max} of **SP2** at 598 nm under tension (Fig. 5b), moved to ~573 nm after relaxation. **SP3** also exhibited a shift of λ_{max} from 598 nm to 588 nm (Fig. 5c). **SP1** did not show a distinguishable shift on the absorption peak under tension and relaxation (Fig. 5a), indicating **SP1** may undergo a different isomerization path for loading-relaxation compared with **SP2** and **SP3**. The blue-shift of **SP3** again demonstrates that the attachment points at the 1′ *N*-position are important for mechanochromic SP.

3.2 Decolouration

The transition between spiropyran and merocyanine in PDMS is reversible, which can also be quantitatively determined by *in situ* UV-Vis measurement. The absorption intensity of SP decreased rapidly in the dark upon unloading from 62% compressive strain (Fig. 6a), demonstrating MC recovered to ring-closed SP in the bulk state upon relaxation. The absorption ratio (Abs/Abs_{max}) of **SP1**, **SP2** and **SP3** dropped to 1.3%, 1.3%, and 5.2% at the absorption intensity of 0.0042, 0.0064 and 0.0306 respectively after storing for 40 min in the dark. In the absence of visible light, the ring closing is a thermal dynamic process.[40] **SP2** in PMA was reported to return to colourless after 104 min,[37] which is longer than the observed relaxation time in this PDMS system. The difference is caused by the different glass transition temperature between PMA and PDMS. The time of Abs decreasing to 0.1 was used as comparison; the absorbance of **SP1** dropped rapidly to 0.1 within 3.5 min and **SP2** in 6 min, while it took 14 min for **SP3**. The decolouration rate to 50% intensity also showed a similar trend. The absorption intensities showed exponential decay, giving straight lines in semi-logarithmic plots (Fig. S11†). The

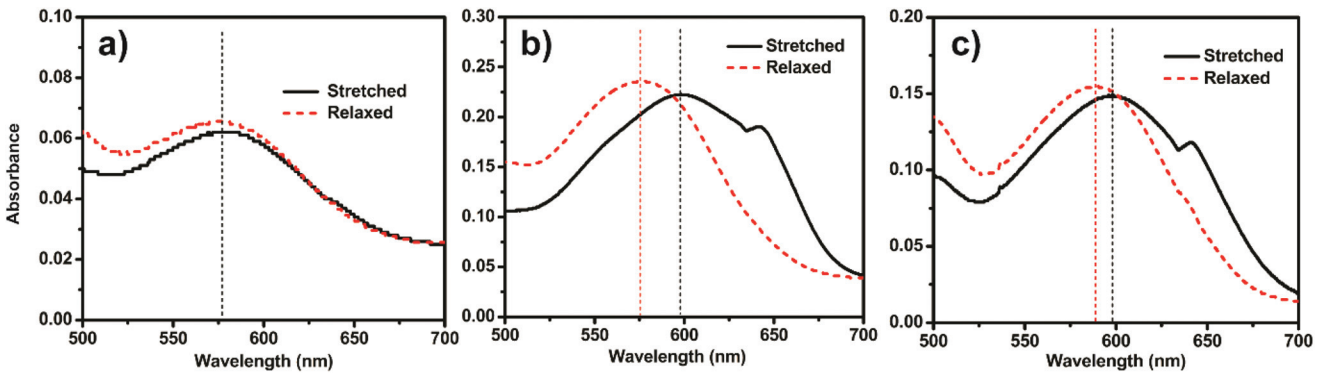

Fig. 5 UV-Vis spectra of **SP1–3** (conc. = 9.4 μmol g^{-1}) under tensile strain (≈2) and unloading. (a) **SP1**, width: 5 mm, thickness: 0.8 mm, (b) **SP2**, width: 4 mm, thickness: 0.8 mm, (c) **SP3**, width: 4 mm, thickness: 0.8 mm.

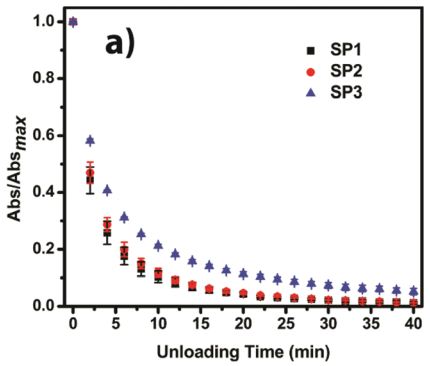

b)

Specimen	$T_{1/2}$ (min)	$T_{Abs = 0.1}$ (min)	Abs (Time = 40 min)	k_d
SP1	1.8	3.5	0.0042	0.14
SP2	1.9	6.0	0.0064	0.14
SP3	2.9	14.0	0.031	0.12

Fig. 6 (a) Plot of absorption intensity/maximum absorption intensity *vs.* relaxation time in darkness after unloading from 62% compressive strain for **SP1**, **SP2** and **SP3** (conc. = 9.4 μmol g^{-1}). (b) Decolouration parameters from UV-Vis spectra, where $T_{1/2}$ represents relaxation time at Abs/Abs$_{max}$ = 0.5, $T_{Abs < 0.1}$ is the relaxation time at 0.1 absorption intensity, and k_d is the decolouration rate.

decolouration rate (k_d) of polymers **SP1–3** were determined from the slope of the log absorbance *versus* time plots (Fig. S11†) and they were summarized in Fig. 6b. The decolouration rate of **SP1** was close to **SP2**, while **SP3** showed a slower decolouration process. It is difficult to comment on the difference between **SP1** and **SP2** with such close decolouration parameters, given that the Abs of activated **SP2**-PDMS was much stronger than that of **SP1**-PDMS. But obviously **SP3** with one more attachment position recovered slower than **SP1** and **SP2**. The same trend was observed when the SP-PDMS was under a constant loading over a long period (Fig. S12†). This is a result of more attachment positions on **SP3** reducing the mechanophore flexibility. In bulk materials, flexibility is also a key factor for the SP ↔ MC isomerization. This approach of varying attachment positions can lead to a method for controlling the mechanophore ring closing process. The slower colour fading process of **SP3** is possibly related to the blue-shift under loading and unloading (Fig. 5); the less flexibility delays the isomerization process and stabilizes the intermediate isomer longer.

3.3 Density functional theory calculations

The differences observed between **SP1** and **SP2** arise from conformational isomerization of the merocyanine forms following ring opening.[19] To explore this further, density functional theory (DFT) calculations were carried out at the M06-2X/6-31G (d)[41] level of theory for **SP1** and **SP2** models in which the polymer attachment points were replaced by methoxy groups, using the Gaussian 09[43] software package. Energies for the isomers available *via* ring opening and *E*/*Z* isomerization, and their connecting transition states, are shown in Fig. S13.† Seven possible merocyanine isomers are predicted to be stable species; the MC-EZZ isomers were found to spontaneously revert to ring-closed SP, and instead a direct transition state is available connecting SP to MC-EEZ (which proceeds transiently *via* the unstable EZZ form). Conversely, the MC-ZZZ isomer is predicted to form *via* a direct ring opening process in SP, although the reverse barrier for ring closing is very small, and this isomer is likely to be transient. For both **SP1** and **SP2**, the EEZ isomer is predicted to be the most stable merocyanine form, which could be the dominant MC form activated by UV in both cases, although other isomers sit within a few kJ mol^{-1}. The barrier to form the EEZ isomer from the spiropyran is also similar in both cases.

To better understand the effects of conformational isomerization on **SP1** and **SP2** upon ring opening under force, their merocyanine isomers have been arranged in order of increasing distance between polymer attachment positions being pulled in the opposite directions along the molecules (shown in Table 1). We define this change in interatomic distance as Δ*D*, which for **SP1** is an O–O separation and for **SP2** is a C–O separation. Importantly, from Table 1 we see that Δ*D* required for the deformation to ring-open **SP2** is far less than that for **SP1**. For instance, to reach the most stable EEZ MC isomer, the attachments need only be separated by a further 2 Å from their starting geometry in **SP2**, compared to 5.6 Å in **SP1**.

This trend revealed above is consistent with the literature.[32,34] Although Kim *et al.* claimed that there was only a minimal effect on the mechanochromic response between **SP1** and **SP2** in PDMS bulk materials which is in contrast to the calculation results,[34] the difference of colour intensity under a constant deformation is significant from our study (Fig. 3 and 4). We believed that this is related to the Δ*D* difference between **SP1** and **SP2**. Although the activation deformation threshold did not show statistic difference in the bulk polymer, but the stronger colour intensity of **SP2** than **SP1** under a same strain demonstrated higher ring opening occurs in **SP2** systems. The easier bond cleavage should be attributed to a shorter Δ*D*. Lin *et al.* came up with an opposite hypothesis, the larger the change in the pulling point length, the more force response will be produced.[33] That hypothesis could not explain our observation that **SP1** showed less response under force than **SP2**, but the largest Δ*D* of **SP1** is greater than that of **SP2**.

The calculation also showed less deformation is required for **SP2** than **SP1** to reach the higher-energy MC isomers ZZE and EZE. Due to their energies, these forms are likely to be short-lived isomers, and may explain the shift in the absorp-

Table 1 Calculated energies for the **SP1** and **SP2** model compound isomers ordered by change in the interatomic distance (ΔD) of the polymer attachment points, ΔO–O on **SP1** and ΔC–O on **SP2** (shown in red in the inset structures). The wavelength of the first excited state is also shown, from TD-DFT calculations

SP1

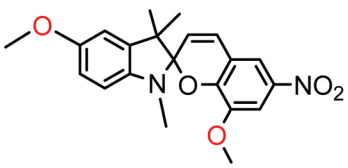

Isomer	ΔO–O (Å)	Relative energy (kJ mol^{-1})	First excited state (nm)
SP1	0.0	0.0	299
ZZZ	1.3	77.0	456
EZE	4.5	117.6	489
ZZE	5.4	96.5	509
ZEZ	5.6	80.3	456
EEE	5.6	73.4	466
EEZ	5.8	70.6	455
ZEE	6.3	80.8	464

SP2

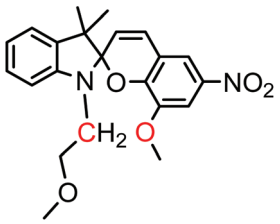

Isomer	ΔC–O (Å)	Relative energy (kJ mol^{-1})	First excited state (nm)
SP2	0.0	0.0	290
ZZZ	−0.3	91.3	456
ZZE	1.4	108.4	501
EEZ	2.1	74.2	455
ZEE	2.2	81.2	464
ZEZ	3.1	79.5	452
EZE	4.0	121.4	484
EEE	4.1	77.0	463

tion peak during relaxation found for **SP2**. Interestingly, the position of the first excited state in ZZE and EZE is blue-shifted by around 40 nm relative to the other lower-energy isomers. Thus, we hypothesize that ZZE at a much shorter ΔD than EZE could be the blue state for **SP2**-PDMS under force; after relaxation, ZZE isomerizes to the shorter ΔD isomer ZZZ giving a purple colour before it reverts to ring-closed **SP2** (Fig. 7). For **SP1**, the majority of ring-open merocyanine may stay at the short ΔD isomer ZZZ under the same strain and upon relaxation, resulting in an indistinguishable blue-purple shift, as the long wavelength isomers EZE and ZZE require much more ΔD. Kim *et al.* claimed that the λ_{max} was also detected on **SP1** at the tension strain of 2.3.[34] As the DFT calculation results indicate the ΔD of **SP1** is longer than **SP2**, it is possible to observe a λ_{max} shift of **SP1** when the deformation is large enough. However, in our study no obvious λ_{max} shift was observed for **SP1** up to 200% tensile strain, although **SP2** and **SP3** showed an obvious shift (Fig. 5). Thus, under a relatively short deformation and after relaxation, the majority of MC species from **SP1** remain in the ZZZ confirmation, while **SP2** transitions through an intermediate confirmation (ZZE) of MC (Fig. 7). **SP3** is believed to have an intermediate isomer under a loading similar to **SP2**, since it has the same 1′*N*-attachment position.

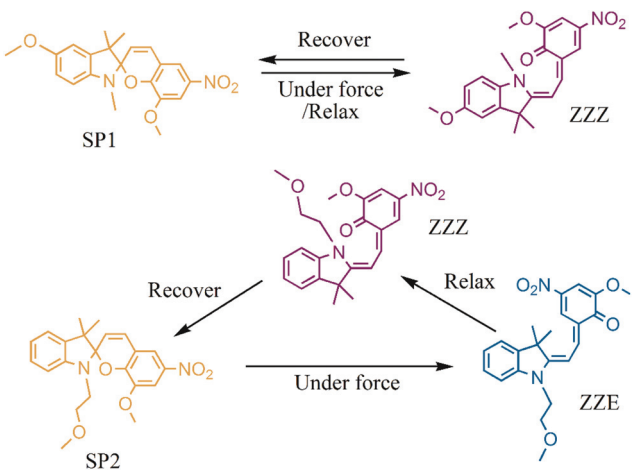

Fig. 7 Hypothesized paths for merocyanine (MC) isomers of **SP1** and **SP2** model compounds under force and relaxation.

In order to better understand the influence of either geometric changes on the attachment points, relative to electronic effects associated with varying functionalities on the SPs, **SP3** was prepared. **SP3** combines the same attachment positions of both **SP1** and **SP2** and was designed to study the effect of geometry on force responses. In terms of the electronic effect, **SP1** is similar to **SP3** with identical vinyl ester functionality and very minor electronic effects due to the alkyl and methyl functionalities at the 1′*N* position. **SP3** differs from **SP2**, as it has an additional slight electron donating vinyl ester functionality at position 5′. The electronic effect causing UV response was studied previously by Balmond, showing that the addition of a methoxy group (electron donating group) at the 5′-position on the indoline ring reduced UV response.[42] If the electronic effect is the influencing factor here, the order of mechanochromic change might be expected to follow in the order of intensity: **SP2** > **SP1** ≈ **SP3** as there is no electron donating chain at the 5′-position. If the geometric effect due to the attachment positions is the key factor, with ΔD dominating the ring opening process, the optical response should be **SP2** ≈ **SP3** > **SP1** as there were attachment chains at the 1′*N*-position for

SP2 and **SP3**. According to the above results the optical change is in the order of **SP2** > **SP3** > **SP1** (Fig. 3 and 4), with **SP3** behaving more similarly to **SP2** (blue-shift). Preliminary calculations on a **SP3** model showed similar C–O ΔD, in agreement with the experimental observation. Due to the increase of isomer possibility, the simulation of **SP3** model was not further carried out and direct comparison between **SP1** and **SP2** models provides the best explanation. Both the electronic and geometric effects influence the mechanochromic properties, however the geometric effect caused by varying the attachment positions is the dominant factor. The assumption is consistent with Lin's study concluding that the geometric effect probably dominates the mechanochromic behavior.[33] This again implies that the attachment points at the 1′*N*-position are more active than those at the 5′-position for mechanochromism.

4. Conclusions

In summary, we investigated the effect of the attachment positions on the mechanochromism of three spiropyrans in a crosslinked PDMS network to find out how the geometric or electronic effect influences the optical change. Varying the attachment points on the indoline ring did not cause a statistical difference at the onset activation stress and strain, however **SP2** showed a higher absorption intensity than **SP1** under 62–70% compressive strain. **SP3** which combined the attachment points of **SP1** and **SP2** showed a higher absorption intensity than **SP1** but lower than that of **SP2**. **SP2** and **SP3** showed an obvious blue-shift under loading and after unloading, while the shift was not observed for **SP1**. The results indicate that both electronic and geometric effects influence the mechanochromic properties, with the geometric effect being the more dominant factor. The DFT calculation showed the pulling point distance ΔD of the MC isomers differed between **SP1** and **SP2**, and this ΔD is believed to affect the mechanochromic response and the blue-purple shift. Restricted by the mobility with an extra attachment point in the matrix, **SP3** showed a slower ring closing rate than **SP1** and **SP2** after relaxation and under a long-term loading. This comparison study provides more understanding of the mechanochromic properties of spiropyran, which could be useful for the design where spiropyran is employed as a force-responsive chromophore.

Conflicts of interest

The authors declare no competing financial interest.

Acknowledgements

This research was funded partially by the Australian Government through the Australian Research Council. IH120100053 "Unlocking the Food Value Chain: Australian industry transformation for ASEAN markets." W. Qiu is thankful to the University of Melbourne for providing the Melbourne International Research Scholarship. G. da Silva is supported by the Australian Research Council through the Future Fellowship program (FT130101304).

References

1 Q. Wang, G. R. Gossweiler, S. L. Craig and X. Zhao, Cephalopod-inspired design of electro-mechano-chemically responsive elastomers for on-demand fluorescent patterning, *Nat. Commun.*, 2014, **5**, 4899.
2 T. Kosuge, K. Imato, R. Goseki and H. Otsuka, Polymer–Inorganic Composites with Dynamic Covalent Mechanochromophore, *Macromolecules*, 2016, **49**, 5903–5911.
3 T. Wang, N. Zhang, J. Dai, Z. Li, W. Bai and R. Bai, Novel Reversible Mechanochromic Elastomer with High Sensitivity: Bond Scission and Bending-Induced Multicolor Switching, *ACS Appl. Mater. Interfaces*, 2017, **9**, 11874–11881.
4 M. J. Robb, T. A. Kim, A. J. Halmes, S. R. White, N. R. Sottos and J. S. Moore, Regioisomer-Specific Mechanochromism of Naphthopyran in Polymeric Materials, *J. Am. Chem. Soc.*, 2016, **138**, 12328–12331.
5 N. Bruns, K. Pustelny, L. M. Bergeron, T. A. Whitehead and D. S. Clark, Mechanical nanosensor based on FRET within a thermosome: damage-reporting polymeric materials, *Angew. Chem., Int. Ed.*, 2009, **48**, 5666–5669.
6 M. Ferrara and M. Bengisu, *Materials that change color: smart materials, intelligent design*, Springer, New York, 2014, pp. 47–52.
7 X. Zhang, Z. Chi, J. Zhang, H. Li, B. Xu, X. Li, S. Liu, Y. Zhang and J. Xu, Piezofluorochromic properties and mechanism of an aggregation-induced emission enhancement compound containing N-hexyl-phenothiazine and anthracene moieties, *J. Phys. Chem. B*, 2011, **115**, 7606–7611.
8 X. Jia, J. Wang, K. Wang and J. Zhu, Highly sensitive mechanochromic photonic hydrogels with fast reversibility and mechanical stability, *Langmuir*, 2015, **31**, 8732–8737.
9 J. Wang, X. Zhao, E. B. Berda, C. Chen, K. Wang, S. Chen, B. Zou, B. Liu, Q. Zhou and F. Li, The elastic properties and piezochromism of polyimide films under high pressure, *Polymer*, 2016, **90**, 1–8.
10 F. Donati, A. Pucci, C. Cappelli, B. Mennucci and G. Ruggeri, Modulation of the optical response of polyethylene films containing luminescent perylene chromophores, *J. Phys. Chem. B*, 2008, **112**, 3668–3679.
11 S. L. Potisek, D. A. Davis, N. R. Sottos, S. R. White and J. S. Moore, Mechanophore-linked addition polymers, *J. Am. Chem. Soc.*, 2007, **129**, 13808–13809.
12 J. H. Day, Thermochromism, *Chem. Rev.*, 1963, **63**, 65–80.
13 R. Klajn, Spiropyran-based dynamic materials, *Chem. Soc. Rev.*, 2014, **43**, 148–184.
14 E. Fischer and Y. Hirshberg, Formation of coloured forms of spirans by low-temperature irradiation, *J. Chem. Soc.*, 1952, 4522–4524.

15 D. A. Davis, A. Hamilton, J. Yang, L. D. Cremar, D. Van Gough, S. L. Potisek, M. T. Ong, P. V. Braun, T. J. Martinez, S. R. White, J. S. Moore and N. R. Sottos, Force-induced activation of covalent bonds in mechanoresponsive polymeric materials, *Nature*, 2009, **459**, 68–72.

16 C. K. Lee, C. E. Diesendruck, E. Lu, A. N. Pickett, P. A. May, J. S. Moore and P. V. Braun, Solvent Swelling Activation of a Mechanophore in a Polymer Network, *Macromolecules*, 2014, **47**, 2690–2694.

17 C. K. Lee, D. A. Davis, S. R. White, J. S. Moore, N. R. Sottos and P. V. Braun, Force-induced redistribution of a chemical equilibrium, *J. Am. Chem. Soc.*, 2010, **132**, 16107–16111.

18 M. E. Grady, B. A. Beiermann, J. S. Moore and N. R. Sottos, Shockwave loading of mechanochemically active polymer coatings, *ACS Appl. Mater. Interfaces*, 2014, **6**, 5350–5355.

19 G. R. Gossweiler, G. B. Hewage, G. Soriano, Q. Wang, G. W. Welshofer, X. Zhao and S. L. Craig, Mechanochemical Activation of Covalent Bonds in Polymers with Full and Repeatable Macroscopic Shape Recovery, *ACS Macro Lett.*, 2014, **3**, 216–219.

20 G. O'Bryan, B. M. Wong and J. R. McElhanon, Stress sensing in polycaprolactone films via an embedded photochromic compound, *ACS Appl. Mater. Interfaces*, 2010, **2**, 1594–1600.

21 M. Li, W. Liu and S. Zhu, Smart polyolefins feeling the force: Color changeable poly(ethylene-vinyl acetate) and poly(ethylene-octene) in response to mechanical force, *Polymer*, 2017, **112**, 219–227.

22 H. Chen, F. Yang, Q. Chen and J. Zheng, A Novel Design of Multi-Mechanoresponsive and Mechanically Strong Hydrogels, *Adv. Mater.*, 2017, **29**, 1606900.

23 M. Raisch, D. Genovese, N. Zaccheroni, S. B. Schmidt, M. L. Focarete, M. Sommer and C. Gualandi, Highly Sensitive, Anisotropic, and Reversible Stress/Strain-Sensors from Mechanochromic Nanofiber Composites, *Adv. Mater.*, 2018, **30**, e1802813.

24 F. Kempe, O. Brugner, H. Buchheit, S. N. Momm, F. Riehle, S. Hameury, M. Walter and M. Sommer, A Simply Synthesized, Tough Polyarylene with Transient Mechanochromic Response, *Angew. Chem., Int. Ed.*, 2018, **57**, 997–1000.

25 H. Zhang, F. Gao, X. Cao, Y. Li, Y. Xu, W. Weng and R. Boulatov, Mechanochromism and Mechanical-Force-Triggered Cross-Linking from a Single Reactive Moiety Incorporated into Polymer Chains, *Angew. Chem., Int. Ed.*, 2016, **55**, 3040–3044.

26 M. Li, Q. Zhang, Y.-N. Zhou and S. Zhu, Let spiropyran help polymers feel force!, *Prog. Polym. Sci.*, 2018, **79**, 26–39.

27 J. W. Kim, Y. Jung, G. W. Coates and M. N. Silberstein, Mechanoactivation of Spiropyran Covalently Linked PMMA: Effect of Temperature, Strain Rate, and Deformation Mode, *Macromolecules*, 2015, **48**, 1335–1342.

28 Y. Chen, H. Zhang, X. Fang, Y. Lin, Y. Xu and W. Weng, Mechanical Activation of Mechanophore Enhanced by Strong Hydrogen Bonding Interactions, *ACS Macro Lett.*, 2014, **3**, 141–145.

29 S. Jiang, L. Zhang, T. Xie, Y. Lin, H. Zhang, Y. Xu, W. Weng and L. Dai, Mechanoresponsive PS-PnBA-PS Triblock Copolymers via Covalently Embedding Mechanophore, *ACS Macro Lett.*, 2013, **2**, 705–709.

30 H. Zhang, Y. Chen, Y. Lin, X. Fang, Y. Xu, Y. Ruan and W. Weng, Spiropyran as a Mechanochromic Probe in Dual Cross-Linked Elastomers, *Macromolecules*, 2014, **47**, 6783–6790.

31 M. H. Barbee, T. Kouznetsova, S. L. Barrett, G. R. Gossweiler, Y. Lin, S. K. Rastogi, W. J. Brittain and S. L. Craig, Substituent Effects and Mechanism in a Mechanochemical Reaction, *J. Am. Chem. Soc.*, 2018, **140**, 12746–12750.

32 G. R. Gossweiler, T. B. Kouznetsova and S. L. Craig, Force-rate characterization of two spiropyran-based molecular force probes, *J. Am. Chem. Soc.*, 2015, **137**, 6148–6151.

33 Y. Lin, M. H. Barbee, C. C. Chang and S. L. Craig, Regiochemical Effects on Mechanophore Activation in Bulk Materials, *J. Am. Chem. Soc.*, 2018, **140**, 15969–15975.

34 T. A. Kim, M. J. Robb, J. S. Moore, S. R. White and N. R. Sottos, Mechanical Reactivity of Two Different Spiropyran Mechanophores in Polydimethylsiloxane, *Macromolecules*, 2018, **51**, 9177–9183.

35 I. D. Johnston, D. K. McCluskey, C. K. L. Tan and M. C. Tracey, Mechanical characterization of bulk Sylgard 184 for microfluidics and microengineering, *J. Micromech. Microeng.*, 2014, **24**, 035017.

36 K. Jiang, P. C. Thomas, S. P. Forry, D. L. DeVoe and S. R. Raghavan, Microfluidic synthesis of monodisperse PDMS microbeads as discrete oxygen sensors, *Soft Matter*, 2012, **8**, 923–926.

37 M. Li, Q. Zhang and S. Zhu, Photo-inactive divinyl spiropyran mechanophore cross-linker for real-time stress sensing, *Polymer*, 2016, **99**, 521–528.

38 G. Hong, H. Zhang, Y. Lin, Y. Chen, Y. Xu, W. Weng and H. Xia, Mechanoresponsive Healable Metallosupramolecular Polymers, *Macromolecules*, 2013, **46**, 8649–8656.

39 B. Zuo, M. Wang, B.-P. Lin and H. Yang, Photomodulated Tricolor-Changing Artificial Flowers, *Chem. Mater.*, 2018, **30**, 8079–8088.

40 W. Tian and J. Tian, An insight into the solvent effect on photo-, solvato-chromism of spiropyran through the perspective of intermolecular interactions, *Dyes Pigm.*, 2014, **105**, 66–74.

41 Y. Zhao and D. G. Truhlar, The M06 suite of density functionals for main group thermochemistrythermochemical kinetics, noncovalent interactions, excited states, and transition elements: two new functionals and systematic testing of four M06-class functionals and 12 other functionals, *Theor. Chem. Acc.*, 2007, **120**, 215–241.

42 E. I. Balmond, B. K. Tautges, A. L. Faulkner, V. W. Or, B. M. Hodur, J. T. Shaw and A. Y. Louie, Comparative Evaluation of Substituent Effect on the Photochromic Properties of Spiropyrans and Spirooxazines, *J. Org. Chem.*, 2016, **81**, 8744–8758.

43 *Gaussian 09, Revision E.01*. http://gaussian.com/g09citation/.

ACS APPLIED MATERIALS & INTERFACES

Research Article

Cite This: ACS Appl. Mater. Interfaces 2019, 11, 29268−29275

www.acsami.org

Color-Switchable Polar Polymeric Materials

Wenlian Qiu, Paul A. Gurr, and Greg G. Qiao*

Department of Chemical Engineering, The University of Melbourne, Parkville, Victoria 3010, Australia

Supporting Information

ABSTRACT: Spiropyran is an important mechanophore, which has rarely been incorporated as a cross-linker in polar polymer matrices, limiting its applications in innovative mechanochromic devices. Here, three spiropyrans with two- or three-attachment positions were synthesized and covalently bonded in polar poly(hydroxyethyl acrylate) (PHEA), to achieve color-switchable materials, triggered by light and when swollen in water. The negative photochromism in the dark and mechanical activation by swelling in water were investigated. Measurements of negative photochromism were conducted in solution and cross-linked PHEA bulk polymers, with both showing color reversibility when stored in the dark or on exposure to visible light. The force of swelling in water was sufficient to induce the ring-opening reaction of spiropyran. It was found that tri-substituted spiropyran (SP3) was less influenced by the polar matrix but showed the fastest color activation during swelling. SP3 also showed accelerated ring opening to the colored state during the swelling process. Bleaching rates and color switchability were investigated under swollen and dehydrated conditions. The effect of cross-link density on the swelling activation was explored to better understand the interaction between the mechanophore and the polar environment. The results demonstrated that influences from both the polar environment and the mechanochromic nature of spiropyran had an impact on the absorption intensity, rate of change, and the decoloration rate of the materials. This study provides the opportunity to manipulate the properties of spiropyrans to afford materials with a range of color-switching properties under different stimuli.

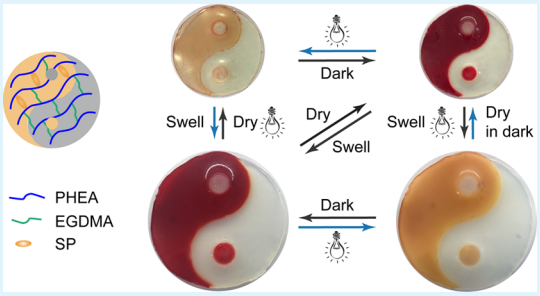

KEYWORDS: *spiropyran, mechanochromism, negative photochromism, color-switching, water-swelling, polar polymer*

INTRODUCTION

Smart materials responsive to external stimuli, such as light, temperature, pH, and force, have attracted a lot of attention because of their potential applications in packaging, ophthalmic lens, textiles, chemical diagnostics, force sensors, and pressure-sensitive coatings.[1−5] Mechanochromic polymeric materials, which change color under an applied force, have been well studied.[6−10] Spiropyran (SP) is one of the most promising mechanophores, which is colorless and undergoes a 6-π electrocyclic ring-opening reaction to form colored merocyanine (MC) under external force.[11,12] SP-based mechanochromic materials can be obtained by covalent[11−16] and noncovalent bonding to the matrix.[17] The concern for noncovalently bonded systems is that SP has the potential to leach from the matrix, especially in the presence of solvents and this limits their practical applications. For SP covalently bonded systems, a diverse range of polymers have been utilized, including poly methyl(meth)acrylate (PMMA),[18] polystyrene,[19] poly(ε-caprolactone),[13,20] and polydimethylsiloxane.[14] These nonpolar polymers are designed to stabilize the nonpolar ring-closed SP before being subjected to external stimuli.

A polar environment will affect the SP ↔ MC equilibrium because of the difference in polarity between SP and MC,[21] and the energy barrier of the isomerization, will have a lower ground-state energy for MC in a polar environment.[22−24] This phenomenon has been defined as negative photochromism.[25]

For SP-linked hydrophilic polymer systems, the effect from the polar environment results in colored and more polar MC being the dominant form in the absence of visible light. As an example, it has been reported that SP conjugated with poly(ethylene glycol) as a soft segment in PU changed color without an applied force when kept in the dark.[26] To avoid the effect from the polar environment for mechanochromism, SP has been protected in a nonpolar environment within micelles in hydrogel systems, to ensure that the SP remains in the colorless form prior to color-triggering by an external force.[27] Manipulating the color-switching of SP in hydrophilic matrices is important for applications such as optical data storage.[21,28] Efforts have been made to control the influence from polar environments, by adding electron-withdrawing or electron-donating groups to the SP molecule, or by using polar polymers with different functionalities, varying the local electrostatic effects.[29] Additionally, the interaction between the polar components and MC not only affects the equilibrium of SP ↔ MC, but also causes maximum absorbance wavelength (λ_{max}) shift.[23,30] The polar effect can be induced from either a solvent or a polymer matrix.[21,31] The negative photochromism cannot be neglected when hydrophilic polymers are employed in SP systems.[32] Although incorpo-

Received: May 23, 2019
Accepted: July 23, 2019
Published: July 23, 2019

DOI: 10.1021/acsami.9b09023
ACS Appl. Mater. Interfaces 2019, 11, 29268−29275

ration of SP into hydrophilic polymers for mechanochromism has barely been studied, the broad range of potential applications of hydrophilic polymers in coatings, food packaging, membranes, and biomedical devices necessitates development of a range of polymer options for SP-contained mechanochromic materials.

The forces induced by swelling of mechanochromic SP polymers in organic solvents and CO_2 are sufficient to activate SP to its colored MC form. Moore's group reported that cross-linked SP−PMMA can be activated by swelling in organic solvents.[33] It was found that the swelling rate was important to the color change behavior, given that too slow a swelling rate could not trigger the ring-opening reaction, whereas too fast a swelling rate would cause sample damage. Microgels of 2-(diethylamino)ethyl-methacrylate with conjugated SP were developed by Zhu's group, which showed a color-switching from pale yellow to pink because of the deformation caused by absorbing CO_2.[34] This implies that the efficient activation by swelling is attributed to the three-dimensional deformation, rather than uniaxial strain. Water is a widely used and nontoxic solvent, but cannot swell nonpolar polymers to induce color change because of the high polarity.[33] To date, water has not been used to swell hydrophilic polymers containing SP for mechanochromism. For the potential applications as mentioned earlier, it is important to see how the mechanical activation of SP to MC will behave differently in a hydrophilic polymer because of its interaction with such a polar environment.

As mechanochromic SPs have yet been cross-linked in pure swellable hydrophilic polymers, it is necessary to understand the factors affecting the equilibrium of SP to MC, and how the mechanical swelling affects the chromism in a polar environment. In this article, we incorporated a series of spiropyrans into hydrophilic poly(hydroxyethyl acrylate) (PHEA), which act as a reversible sensor, switching color in response to the presence and absence of visible light and water. Herein, the effects of a polar matrix on the color-forming properties of these materials in the dark as well as the mechanochromic behavior when swollen in water are investigated, with the presentation of a fully reversible switchable cyclic mechanochromic and negative photochromic materials.

EXPERIMENTAL METHODS

Materials. Hydroxyethyl acrylate (HEA, 96%, Sigma) and ethylene glycol dimethacrylate (EGDMA, 98%, Sigma) were passed through basic aluminum oxide to remove the inhibitor monomethyl ether hydroquinone before use. Tetrahydrofuran (THF, Chem-Supply) was pre-dried over sodium, before being distilled from benzophenone and sodium under an inert atmosphere of nitrogen prior to use. 4-Dimethylaminopyridine (DMAP, ≥98%, Sigma), phenylbis(2,4,6-trimethylbenzoyl)phosphine oxide (BAPOs, 97%, Sigma), and methacrylic anhydride (94%, Sigma) were used as received. 3′,3′-dimethyl-6-nitro-1′-(2-hydroxyethyl)spiro[chromene-2,2′-indoline]-5′,8-diol was synthesized according to our previous work.[35] 1′,3′,3′-trimethyl-6-nitrospiro[chromene-2,2′-indoline]-5′,8-diol and 1′-(2-hydroxyethyl)-3′,3′-dimethyl-6-nitrospiro[chromene-2,2′-indolin]-8-ol were synthesized according to literature procedures.[11,14]

Synthesis of Tri-methacrylate Spiropyran. 3′,3′-Dimethyl-6-nitro-1′-(2-(methacryloyloxy)ethyl)spiro[chromene-2,2′-indoline]-5′,8-diyl bis(2-methylacrylate) 3′,3′-dimethyl-6-nitro-1′-(2-hydroxyethyl)-spiro[chromene-2,2′-indoline]-5′,8-diol (0.20 g, 0.52 mmol, 1.0 equiv) and DMAP (0.15 g, 1.23 mmol, 2.4 equiv) dissolved in THF (10 mL) was added to methacrylic anhydride (0.28 mL, 1.87 mmol, 3.6 equiv). After stirring for 24 h under argon at room temperature, the solvent was removed. The crude product was dissolved in minimal DCM, which was passed through basic alumina with DCM to obtain the product tri-methacrylate spiropyran (SP3) (0.20 g, 0.34 mmol, 64% yield). ^{1}H NMR (400 HZ, $CDCl_3$): δ 7.96 (d, 1H), 7.92 (d, 1H), 6.98−6.96 (d, 1H), 6.87−6.85 (dd, 1H), 6.80 (d, 1H), 6.60−6.58 (d, 1H), 6.32 (s, 1H), 6.07 (s, 1H), 5.93 (m, 2H), 5.74 (s, 1H), 5.57 (s, 1H), 5.51 (s, 1H), 4.25 (m, 2H), 3.35 (m, 2H), 2.07 (s, 3H), 1.92 (s, 3H), 1.70 (s, 3H), 1.23 (s, 3H), 1.19 (s, 3H).

1′,3′,3′-Trimethyl-6-nitrospiro[chromene-2,2′-indoline]-5′,8-diyl bis(2-methylacrylate)(di-methacrylate spiropyran SP1), and 3′,3′-dimethyl-6-nitro-1′-(2-(methacryloyloxy)ethyl)spiro[chromene-2,2′-indoline]-8-yl(2-methylacrylate)(di-methacrylate spiropyran SP2) were synthesized via the same method from the hydroxyl versions. SP1: ^{1}H NMR (400 MHz, $CDCl_3$): δ 7.96 (d, 1H), 7.92 (d, 1H), 6.98 (d, 1H), 6.86 (dd, 1H), 6.79 (d, 1H), 6.45 (d, 1H), 6.32 (s, 1H), 5.91 (d, 1H), 5.89 (s, 1H), 5.74 (s, 1H), 5.51 (s, 1H), 2.64 (s, 3H), 2.07 (s, 3H), 1.69 (m, 3H), 1.24 (s, 3H), 1.21 (s, 3H). SP2: ^{1}H NMR (400 MHz, $CDCl_3$): δ 7.95 (d, 1H), 7.90 (d, 1H), 7.12 (m, 1H), 7.00 (d, 1H), 6.96 (d, 1H), 6.83 (m, 1H), 6.63 (m, 1H), 6.07 (s, 1H), 5.93 (d, 1H), 5.87 (s, 1H), 5.56 (s, 1H), 5.38 (s, 1H), 4.24 (m, 2H), 3.36 (m, 2H), 1.92 (s, 3H), 1.61 (s, 3H), 1.24 (s, 3H), 1.17 (s, 3H).

Preparation of SP Cross-linked PHEA Film Samples. For 1 mol % cross-linker density, HEA (0.4 g, 1 equiv), SP3 (2.0 mg, 0.001 equiv), EGDMA (6.0 μL, 0.009 equiv), and photoinitiator BAPOs (5.8 mg, 0.004 equiv) were mixed thoroughly in a vial. The mixture was injected into a glass mold (width: 1.6 cm, length: 5.0 cm, thickness: around 0.5 mm) with a silicone spacer sandwiched by two glass sheets, and exposed to white light (4 W cool white light, 350 lumens) for 2 h to polymerization. For 2.5% EGDMA cross-linked SP3−PHEA films, 15.1 μL of EGDMA was added; for 5% EGDMA cross-linked SP3−PHEA films, 30.2 μL of EGDMA was added; for 7.5% EGDMA cross-linked SP3−PHEA films, 45.2 μL of EGDMA was added; for 10% EGDMA cross-linked SP3−PHEA films, 60.3 μL of EGDMA was added. Regarding SP1−PHEA and SP2−PHEA, 0.1 mol % mechanophores and 0.95 mol % EGDMA were added, respectively. To quantify the conversion ratio, cross-linked films were soaked in methanol for 2 days, which was changed regularly with fresh solvent, to remove the unreacted species, followed by drying under vacuum at ambient temperature until constant mass. The unreacted species for the samples were quantified to be less than 3 wt %; UV−vis analysis of the extracted methanol solution showed no detectable signals at 500−600 nm, confirming that the mechanophores were conjugated in the polymer network.

Characterization. ^{1}H NMR spectroscopy was conducted on a Varian Unity 400 MHz spectrometer operating at 400 MHz, using deuterated chloroform ($CDCl_3$) as the solvent and reference peak. The UV−vis spectrum was recorded on a Shimadzu UV−vis scanning spectrophotometer (UV-2101 PC) with a fast scanning rate of 0.5 nm interval over a range of wavelengths of 750−380 nm.

Swelling Activation. Polymeric rectangular samples were cut to 7.5 mm × 20 mm. The samples were immersed in excess deionized water in vials fully covered with foil to avoid any light. Mass and dimensions were recorded during the swelling process. The ratio of size change ΔV was defined as $\Delta V = (V - V_0)/V_0$, where V and V_0 were calculated by width × length × thickness; the ratio of mass change Δm was determined by $\Delta m = (m - m_0)/m_0$.[33] Absorbance measurements were utilized to quantify the ring-opening process from SP to MC.

MC Reverting to SP Under White Light Irradiation. Two decoloration processes were compared: swollen (hydrated) films or dehydrated films from the swollen state were exposed to white light. For measurement of the hydrated films, the colored samples activated by water-swelling were exposed to white light until a constant absorption value was observed. For measurement of the dehydrated films, the colored swollen films were dehydrated under vacuum at room temperature until a constant mass, then irradiated with white light to force MC to return to SP until a stable absorbance was achieved.

Coloration−Decoloration Cycles. Two methods of coloration−decoloration cycles were conducted corresponding to the two

DOI: 10.1021/acsami.9b09023
ACS Appl. Mater. Interfaces 2019, 11, 29268−29275

decoloration processes. Colored swollen hydrated films were kept in water and placed under white light to force the MC ring close to SP until the stabilized absorbance was recorded; then, the samples were covered with foil to block exposure to light, while recording the absorbance until it plateaued. The white light-stimulated process was repeated 10 times. For the dehydrated films, the color saturated swollen films were dried in the dark under vacuum at ambient temperature until a constant mass, and the absorbance was recorded; the dehydrated films were exposed to white light until a constant absorbance was observed, before being swollen in water again during which the mass and absorbance were recorded. The dehydration–hydration process was repeated 10 times.

RESULTS AND DISCUSSION

Methacrylated SPs were synthesized according to our previous work.[35] A series of spiropyrans with hydroxyl groups were treated with methacrylic anhydride to afford the methacrylate–SP (Scheme 1), which was polymerized with monomer HEA

Scheme 1. Synthesis of Tri-methacrylate SP3

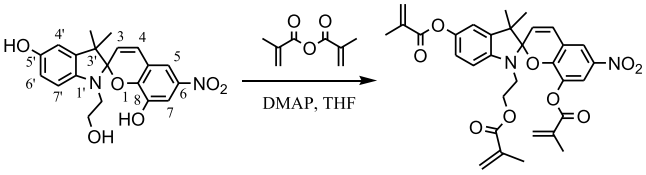

and co-crosslinker EGDMA via free radical polymerization under white light (Scheme 2). Thermal and UV polymerization techniques, which are typical approaches to obtaining SP polymeric materials, lead to incomplete ring-closed mechanophores, with the former approach requiring post bleaching with visible light, whereas the latter approach is affected by the formation of MC in situ, resulting in incomplete polymerization. Thus, using white light and BAPOs as an initiator avoided these issues and ensured the ring-closed form is the dominant species.[27,36] The obtained samples were used to study the effect of the polar environments on the coloration in the dark (negative photochromism) and activation by swelling in water (mechanochromism) (Scheme 3).

Effect of Polarity on SP Coloration in Solution and Bulk Polymer. The negative photochromism of different SPs in the polar solvent were evaluated by dissolving SP in HEA. Samples of SP in HEA at 0.1 μmol % were prepared under ambient conditions and exposed to white light for 1 min to convert any MC to ring-closed SP, prior to being stored in the dark. The UV–vis absorption peaks at around 550 nm attributed to ring-open MC were negligible in all the samples after white light bleaching (Figure S1), demonstrating the majority of mechanophores were in the ring closed form. The samples were kept in the dark under ambient conditions and measured for absorption regularly until they reached a plateau. The color change was reversible by exposing to the white light and keeping in the dark (Figure S1).

Scheme 3. Solutions of SP Dissolved in HEA Were Used to Study the Thermodynamic Equilibrium of Free SP in a Polar Solvent, and SP–PHEA Films Were Used to Study Their Negative Photochromic and Mechanochromic Properties in the Solid State[a]

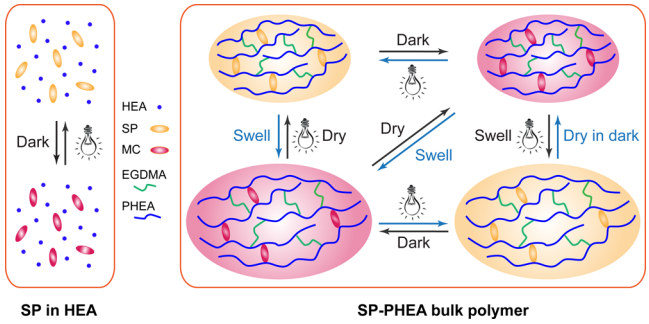

[a]The color reversibility is due to the isomerization between ring-closed SP and ring-open MC.

Figure 1 shows the saturated absorbance of the SP1–3 in HEA solution in the dark. The absorption intensity of SP3 was

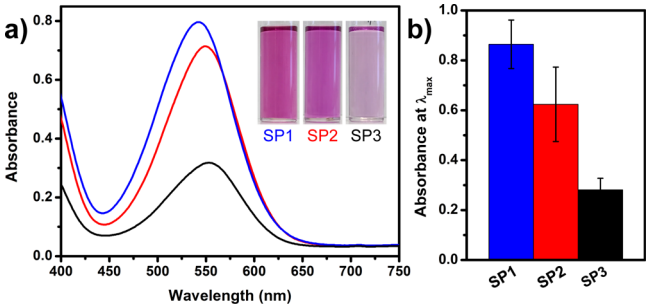

Figure 1. (a) Absorbance spectra of SP1–3 dissolved in HEA after absorption plateaued in darkness and the corresponding images, and (b) absorption intensity at the maximum wavelength of 542, 549, and 553 nm, respectively.

significantly lower than those of SP1 and SP2 (Figure 1b). This suggests that the interaction of SP1–3 with polar HEA differs (affecting the equilibrium between SP and MC) because of the different polarities of these three SPs. According to Tian and Tian, for the thermal competition between SP and MC in the absence of light, the energy for ring opening is mainly determined by MC conformational change.[23] In this case, the variation in the functionality position and number of SP1–3 may affect the equilibrium between SP and MC, resulting in different energies for stabilizing MC, leading to differences in absorption intensity. SP3 having all the different attachment positions has the least unstable colored MC isomers. Additionally, a slight red shift of the maximum absorption wavelength (λ_{max}) was observed from SP1 to SP3 (Figure 1a). It has been reported that the red shift occurs with decreasing solvent polarity for a specific SP.[28] As the solvent was constant,

Scheme 2. Synthesis of SP–PHEA Bulk Materials via Free Radical Polymerization Under White Light

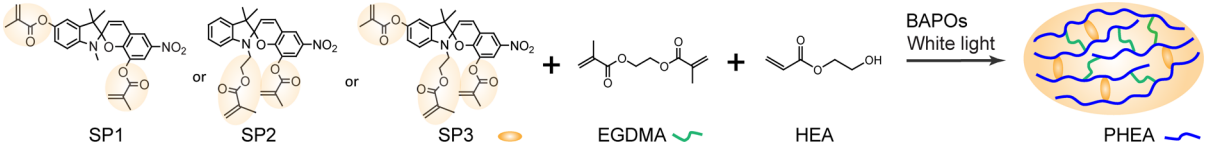

DOI: 10.1021/acsami.9b09023
ACS Appl. Mater. Interfaces 2019, 11, 29268–29275

the λ_{max} shift in these three SP solutions was a result of the polarity difference of the chromophores. Both absorption intensity and λ_{max} differences revealed that the three SPs had different extents of interaction with polar HEA.

Next, the negative photochromism of SP cross-linked with the PHEA polymer was investigated. The prepared SP−PHEA films were pale yellow (Figure 2b) and characterized by UV−

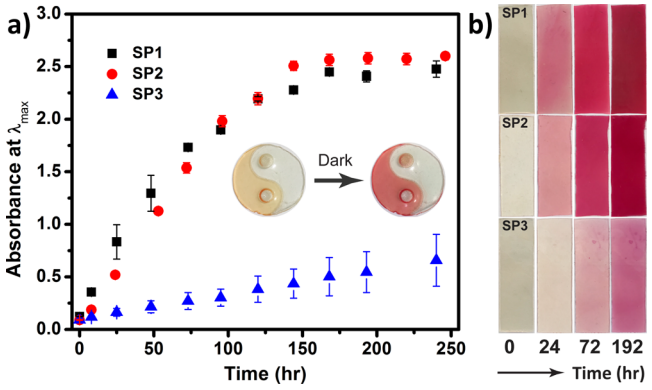

Figure 2. (a) Plot of absorbance at λ_{max} vs time in the dark for SP1−3 with 1 mol % cross-linkers (inset pictures of SP1−PHEA/PHEA film in the "Yin-Yang" symbol shape before and after being stored in the dark overnight, diameter: ∼5 cm), and (b) images showing the color change of SP1−3 relative to time.

vis spectroscopy, showing no absorption peak in the visible range (Figure S2), indicating that the ring-closed SP was the dominant form. The films gradually turned red in the absence of light, with λ_{max} at 537, 544, and 549 nm for SP1, SP2, and SP3, respectively, indicating that SP converted to ring-open MC. Over 10 days in the dark, the absorption of SP1 and SP2 films plateaued, whereas SP3 having a much lower absorbance still showed an increasing linear trend (Figure 2a). The overall absorption intensity curves of SP1 and SP2 showed a nonlinear increase. The saturated absorbance of SP3 was obtained after 1 month in the dark, with the absorbance of 1.35 ± 0.05. As the absorption equilibrating time of SP3 was much longer than that of SP1 and SP2, the initial linear color change was used to determine the coloration rates. To show the color change more vividly, a "Yin-Yang" shaped SP1−PHEA/PHEA film was prepared by a three-step curing polymerization process (Figure S7). In a dark environment overnight, the SP1−PHEA segments changed color (the inset pictures in Figure 2a), whereas the pale yellow PHEA segments remained unchanged.

The slopes of linearly fitted curves (Figure S3) were defined as the coloration rate in the absence of light, k_c, whereas $t_{1/2}$ was defined as the time to reach an absorbance at half-maximum $Abs_{1/2}$ and are shown in Table 1. The coloration rate k_c of SP1&2 was an order of magnitude higher than that of SP3, and $t_{1/2}$ of SP3 was longer than those of SP1&2 by an order of magnitude. The much slower coloration speed of SP3 demonstrated that the majority of chromophores were still in the ring-closed spiropyran form over a long period in the dark. The trend of absorption intensity is consistent with that observed for SP dissolved in HEA solution, yet changed on a much longer time scale. The flexibility of SP in the cross-linked network was reduced compared to free SP molecules in solution, leading to a slower thermal ring-opening process. The λ_{max} of bulk samples showed the same trend as the solution samples, with SP3 having a higher λ_{max} followed by SP2, then SP1. SP2 and SP1 showed similar coloration rates and maximum absorbance behavior in the dark, indicating that the attachment number of SP in the polymer chains affects the thermal SP ↔ MC equilibrium. SP3, which exhibited a slower coloration speed and lower saturated absorbance, is attributed to less flexibility (more conjugating positions) and polarity difference. The maximum absorbance of SP3 was around half that of SP1&2, which indicates that more than half of the SP3 mechanophores were still in the ring-closed state. The incorporation of one more attachment point on SP effectively reduced the negative photochromism.

Table 1. Data Calculated from Figure 2[a]

sample	λ_{max} (nm)	$k_c \times 10^{-2}$ (R^2)	$Abs_{1/2}$	$t_{1/2}$ (h)
SP1	537	2.6 (0.999)	1.2	41.5
SP2	544	2.0 (0.998)	1.3	57.4
SP3	549	0.23 (0.998)	0.68	246

[a]Wavelength at maximum absorbance λ_{max}, coloration rate k_c, absorbance at half $Abs_{1/2}$ and the corresponding time $t_{1/2}$ for SP1−3-contained PHEA samples kept in the dark.

Color Activation by Swelling in Water. To investigate the color activation by swelling in water, SP−PHEA films with 1 mol % cross-linker were immersed in water and subsequently swelled. Absorbance, sample size, and mass change were measured as shown in Figure 3a−c. All samples became

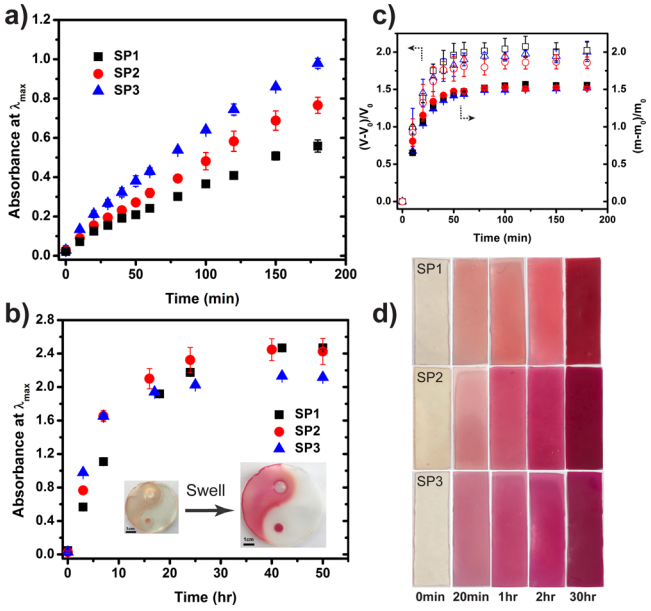

Figure 3. Absorbance as a function of the swelling time in water for SP1−3 samples with 1 mol % cross-linker (λ_{max} of SP1 at 522 nm, SP2 at 532 nm, and SP3 at 540 nm): (a) over 3 h and (b) over 50 h (pictures of an SP3−PHEA/PHEA film in "Yin-Yang" shape before and after swelling in water for 1.5 h as in the inset, scale bar: 1 cm); (c) volume and mass change ratio of the three samples versus the immersion time in water; (d) representative images showing the color change relative to the swelling time (images are not to scale).

reddish-pink as the size increased (Figure 3d, representative pictures not in scale), indicating that spiropyrans were activated to ring-open MC. The inset pictures in Figure 3b also show the color change of an SP3−PHEA/PHEA film in "Yin-Yang" shape after swelling in water for 1.5 h; the four components of the symbol stuck well together even after

DOI: 10.1021/acsami.9b09023
ACS Appl. Mater. Interfaces 2019, 11, 29268−29275

swelling in water. The swelling ratios were calculated by volume and mass expansion. These were identical for each of the samples although it was shown that the mass change calculation was more accurate (Figure 3c). To investigate how the dark environment affects the coloration during swelling, a control sample, a mono functionalized SP, was also synthesized, which remained pendant (non-crosslinked) in the polymer network with 1 mol % EGDMA as cross-linker (Figure S4a). The control SP−PHEA specimen did not show a color change within 4 h in water, although the swelling ratio was the same as the other SP samples (Figure S4b−e). This confirms that the SP1−3 ring-opening process within 4 h was caused by the swelling force rather than the solvatochromism/negative photochromism from the hydrophilic environment. After the swelling ceased, the absorbance continued to increase gradually over 40 h (Figure 3). This differs from the swelling in organic solvents for SP in nonpolar polymers as reported by Moore's group.[33] Here, they observed an increase in absorbance at the same rate as the swelling. As with SP/nonpolar samples, mechanical force partially induces SP to MC color change;[37] however, for our SP/polar samples the additional polar effect because of the polymer and water continued to facilitate further ring opening of the SP to MC. On a comparison of the time scale for color equilibrium of swelling in water to dry samples in the dark, the swelling force activating the mechanophore speeded up the color change as the equilibrium time for SP1&2 by swelling was 40 h, and when kept in the dark was around 170 h. The polar effect induced by the hydrophilic environment was also observed for the control sample, which was not affected by swelling. After 4 h, the absorption peak at 519 nm began to appear on the control sample, demonstrating the isomerization to ring-open MC; the absorption plateaued after 4 days (Figure S4c), a longer period than the mechanochromic SP1−3 samples (2 days). The study of nonpolar polymer swelling in the organic solvent by Moore et al. assumed that an early plateauing of the fluorescence in THF was due to solvatochromism;[33] however, here, the swelling process of the control SP in polar PHEA demonstrated that the polar effect slowed down the coloration process, compared to coloration of a dry sample kept in the dark (Figure S4e). This shows that the swelling force can accelerate the mechano-active SP ring-opening reaction. Additionally, stretching can also induce the ring-opening reaction of SP1−3 PHEA; however, the activation ratio was too low to be measured prior to sample fracture. It is believed that the higher ratio of ring-opening triggered by swelling than that induced by stretching is due to the multidirectional expansion of swelling.

Differences in activation rate by swelling were observed for SP1−3, with SP3 > SP2 > SP1 (Figure 3a and Table 2). The faster swelling activation rate of SP3 film is influenced by the multiaxial deformation because of the increased cross-linking points in the polymer network. SP1 and SP2 differed in activation rate because of their attachment positions; the attachment points on the *N*-position is more advantageous than on the 5′-position in force activation because of the bond cleavage distance, which is consistent with our previous study.[35] After 2 days of being immersed in water, the absorbance of SP1−3 samples plateaued, indicating that an equilibrium of SP ↔ MC toward MC was reached. SP1 and SP2 showed the identical absorbance within statistical error, slightly higher than SP3. This is due to SP1&2 being more influenced by the polar environment, as discussed earlier.

Table 2. Summary of λ_{max}, k_c within 200 min, $Abs_{1/2}$ and $t_{1/2}$ for SP1−3-Contained PHEA Samples Swelling in Water

sample	λ_{max}	$k_c \times 10^{-3}$ (R^2)	$Abs_{1/2}$	$t_{1/2}$ (h)
SP1	522	3.0 (0.996)	1.2	7.1
SP2	532	4.2 (0.997)	1.2	5.4
SP3	540	5.5 (0.993)	1.1	3.4

Decoloration Studies. The colored films can revert to light yellow by exposure to white light, leading to ring closure of MC to SP.[22,29] The decoloration of colored SP1−3 films in swollen and corresponding dehydrated states was investigated by measuring the absorbance over time under white light. The color fading time (t_f) was determined by the intersection of the two tangent lines in both wet and dry conditions (Figure 4a,b). The swollen films were shown to bleach within 1−2 min, whereas all the dehydrated films took a significantly longer time to decolor, in 30−110 min. This demonstrates that the stability of MC is poorer in the wet swollen state than in the dry state. In this case, water acts as a plasticizer in the swollen films,[38] leading to an increase in free volume and flexibility, which facilitates the MC ring closure process. The difference of SP1−3 decoloration in the swollen state was minor with t_f summarized in Table 3.

It was noted that a large difference in the fading time t_f of SP1−3 polymer films was observed in the dehydrated state (Figure 4b), with the order of SP1 < SP2 < SP3. The color fading times t_f were 30, 62, and 108 min for SP1−3, respectively. The decoloration rates (k_f) were determined by fitting the initial linear range (the first tangent line), resulting in f = 0.033, 0.016, and 0.0082 for SP1−3, respectively (Table 3). SP1 was shown to have a faster bleaching rate, which is attributed to the attachment point at the 5′-position speeding up the ring closure under visible light as previously reported.[39] The slow decoloration speed observed for SP3 is believed to be due to a higher number of cross-linkable points, which reduces the flexibility of conformational isomerization of the mechanophore.

Noticeably, λ_{max} of the corresponding dehydrated films shifted toward a longer wavelength compared to that of the swollen films, with $\Delta\lambda_{max}$ of 17, 16, and 12 nm for SP1−3, respectively (Figure S6). This reflects the change in polarity due to the polar (water) environment. The polarity decreases with the removal of water, resulting in an increase of λ_{max} after dehydration. The λ_{max} of dehydrated SP1−3 PHEA samples was close to that of colored films in the dark (Figure 2 and Table 1), and is slightly longer because of the exposure to moisture.[38,40] Utilizing the differences on λ_{max} shift in dissimilar environments, there is the potential for solvent sensors, which respond to changes in the polarity.

Color Switchability. Color switchability is essential when a sensor is required to be reused to track the usage history. By turning white light on and off, the colored SP films switch between pale yellow and red color because of the isomerization between SP and MC. On the basis of the two decoloration conditions mentioned above, two cyclic tests were conducted, (a) irradiating with white light and then left in the dark while the sample was in the swollen state and (b) swelling the sample in water, drying in the dark, and then irradiating with white light as shown in Figure 5. The absorbance was normalized based on the maximum value of the swollen state for a direct comparison of the two different switching modes.

DOI: 10.1021/acsami.9b09023
ACS Appl. Mater. Interfaces 2019, 11, 29268−29275

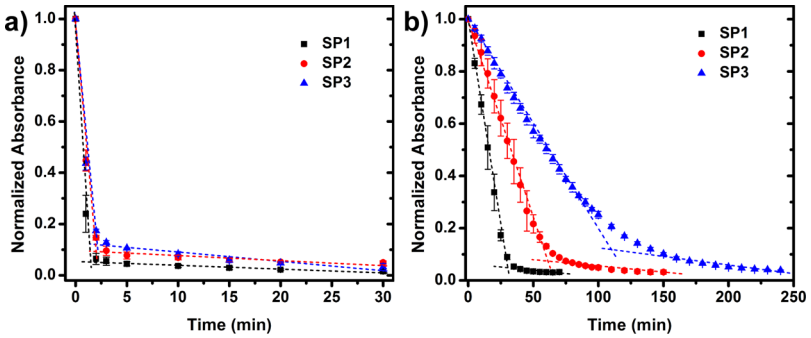

Figure 4. Decrease of absorbance at λ_{max} of SP1−3 PHEA (1 mol % cross-linkers) swollen films under white light irradiation in (a) swollen and (b) corresponding dehydrated states. Color fading time t_f is defined as the intersection of two tangent lines (dashed lines).

Table 3. Summary of λ_{max}, Color Fading Time t_f, and Decoloration Rate k_f of SP1−3 Samples in Swollen and Dehydrated States Under White Light, and the Shift of λ_{max} from the Swollen to the Dehydrated State

	swollen state			dehydrated state			
sample	λ_{max} (nm)	t_f (min)	$k_f \times 10^{-1}$	λ_{max} (nm)	t_f (min)	$k_f \times 10^{-2}$	$\Delta\lambda_{max}$ (nm)
SP1	522	1.5	−5.3	539	30	−3.3	17
SP2	532	2.0	−4.5	548	62	−1.6	16
SP3	540	2.1	−4.4	552	108	−0.82	12

For the tests irradiating white light on swollen films (Figure 5a), all samples showed color switchability for over 10 cycles. Upon white light irradiation, the ring-closed SP was the dominant form, and the MC signal after 10 cycles stabilized at around 10% of the original bleached value. The color intensity of the sample resulting from MC, kept in the dark after swelling was found to drop with increasing ring open-closure repetitions, with the absorbance of MC decreasing to 45−60% of the original intensity for SP1−3. This cyclic fatigue is due to the photodegradation of MC when irradiated by white light.[41−43] No significant difference in the absorption signal among SPs was observed (Figure 5a), which is expected as Figure 4a shows that all three SPs had a similar rate of ring closure when exposed to white light. For the tests irradiating white light onto dehydrated films after swelling, similar trends of MC signal at bleached and colored states were recorded, with the degree of fatigue mainly dependent on the number of ring open-closure cycles. However, SP1 showed faster fatigue than SP2&3 after 10 cycles, especially in the dehydrated sample cycles (Figure 5b), although the time for SP1 ring closure was shorter than that for SP2&3 (Figure 4b).

Effect of Cross-Link Density on Color Activation in Water. It has been reported that swelling activation of SP nonpolar polymer in organic solvent is cross-link density-dependent.[33] Here, a series of SP3−PHEA with 1−10% cross-linker density were prepared, varying EGDMA content with a constant concentration of SP3, to study the effect of cross-link density on color activation in a polar polymer environment. The absorbance with time immersed in water and the corresponding mass change were recorded and are shown in Figure 6. All samples achieved maximum absorbance and mass after 50 and 2 h, respectively. The swelling ratio reduced with increasing cross-linking density, and consequently the absorption signal of MC also decreased. Although the SP chromophore would slowly form MC without swelling, here, the cross-linking density can be used to control the rate of color activation of SP3. This can be attributed to the reduced water content in the polymer network, causing a difference in the polarity of the matrix and free volume of the polymer chains. Interestingly, the absorption intensity in this instance

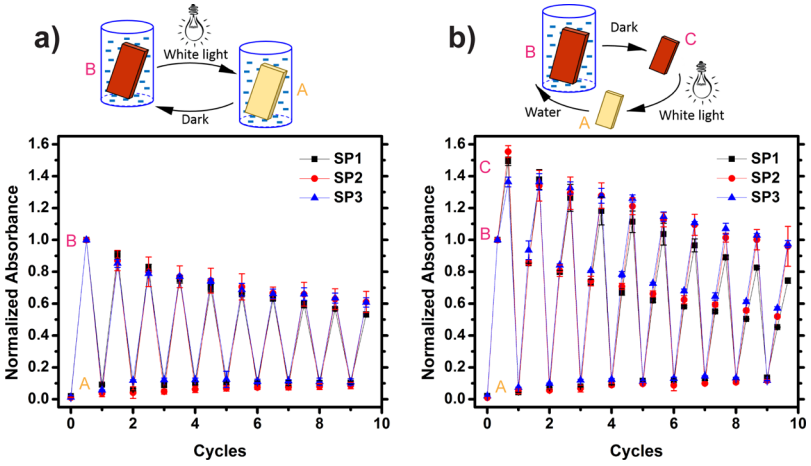

Figure 5. (a) Scheme of cyclic absorbance measurements between SP and MC by white light irradiation and subsequent storage in the dark for recovery, and the absorption plot of the SP1−3 films (1 mol % cross-linkers) in water; (b) scheme of cyclic absorbance measurements between SP and MC by swelling in water, dehydration in the dark at ambient conditions and white light irradiation, and the absorption plot of the SP1−3 films. The absorbance is normalized based on the maximum value in the swollen state.

DOI: 10.1021/acsami.9b09023
ACS Appl. Mater. Interfaces 2019, 11, 29268−29275

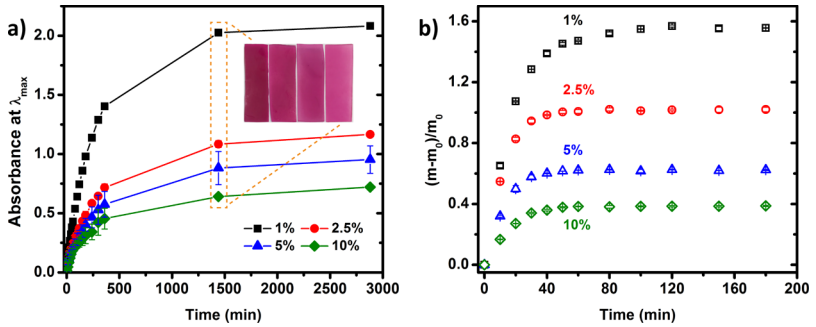

Figure 6. (a) Influence of cross-linking density on absorption intensity as a function of the swelling time for SP3−PHEA films (1 mol %, 2.5%, 5%, and 10%), and the inset images of different crosslinked films swelling over 1 day; (b) swelling ratio of the SP3−PHEA films at different cross-link densities.

because of the degree of cross-linking, does not follow the linear dependence reported for SP/nonpolar polymer systems in organic solvents.[33]

CONCLUSIONS

In summary, we have prepared three spiropyran molecules with two and three acrylate-attachment positions, which were subsequently covalently cross-linked with a polar HEA monomer via white light-induced polymerization. The effect of the polar environment on SP coloration (negative photochromism) was studied in the HEA solution and cross-linked PHEA bulk materials, with the latter having a much longer activation time. SP−PHEA polymer films showed activation by swelling in water due to mechanochromism. This was confirmed by incorporating a single functional SP into a PHEA matrix, which resulted in no color change during swelling. De-swelling in the dark could not reverse the colored MC to colorless SP because of the polar matrix. Under swollen conditions, the color reversibility can be achieved by exposure to visible light or storing in the dark, which was the same for dry bulk samples. It was determined that the tri-functional SP3 was least affected by negative photochromism, resulting in the lowest absorption intensity when stored in the dark; however, it displayed the fastest color activation by swelling. SP3 also exhibited a significantly slower decoloration rate relative to SP1 and SP2 once dehydrated after swelling. The color switchability was dependent on the number of cycles, with 45−60% remaining in the MC form after 10 cycles. The cross-linking density affected the rate and degree of SP ring-opening, with the absorption results showing that the lowest cross-linking density presented the highest absorption intensity. These results demonstrated that SP3 in PHEA has a greater resistance to the polar environment in switching to colored MC, and that the absorption can be regulated by controlling the degree of cross-linking. The switchable color triggering by swelling in water and light offer opportunities to tailor polar hydrophilic swellable films with color-changing properties suitable for biomedical applications such as biosensors or optical storage devices.

ASSOCIATED CONTENT

Supporting Information

The Supporting Information is available free of charge on the ACS Publications website at DOI: 10.1021/acsami.9b09023.

Absorbance spectra, linear fitting curves of absorption plots, and a control SP sample (PDF)

AUTHOR INFORMATION

Corresponding Author

*E-mail: gregghq@unimelb.edu.au.

ORCID

Greg G. Qiao: 0000-0003-2771-9675

Notes

The authors declare no competing financial interest.

ACKNOWLEDGMENTS

W.Q. thanks the University of Melbourne for providing the Melbourne International Research Scholarships. This research was funded partially by the Australian Government through the Australian Research Council. IH120100053 "Unlocking the Food Value Chain: Australian industry transformation for ASEAN markets."

REFERENCES

(1) Stuart, M. A. C.; Huck, W. T. S.; Genzer, J.; Müller, M.; Ober, C.; Stamm, M.; Sukhorukov, G. B.; Szleifer, I.; Tsukruk, V. V.; Urban, M.; Winnik, F.; Zauscher, S.; Luzinov, I.; Minko, S. Emerging applications of stimuli-responsive polymer materials. *Nat. Mater.* **2010**, *9*, 101−113.

(2) Ferrara, M.; Bengisu, M. *Materials That Change Color: Smart Materials, Intelligent Design*; Springer: New York, 2014; pp 47−52.

(3) Lötzsch, D.; Eberhardt, V.; Rabe, C. Chromogenic Materials. *Ullmann's Encyclopedia of Industrial Chemistry*; Wiley, 2000; pp 1−26.

(4) Wu, Z.; Pan, K.; Mo, S.; Wang, B.; Zhao, X.; Yin, M. Tetraphenylethene-Induced Free Volumes for the Isomerization of Spiropyran toward Multifunctional Materials in the Solid State. *ACS Appl. Mater. Interfaces* **2018**, *10*, 30879−30886.

(5) Liu, B.; Ranji-Burachaloo, H.; Gurr, P. A.; Goudeli, E.; Qiao, G. G. A Nontoxic Reversible Thermochromic Binary System via pi-pi Stacking of Sulfonephthaleins. *J. Mater. Chem. C* **2019**, *7*, 9335−9345.

(6) Potisek, S. L.; Davis, D. A.; Sottos, N. R.; White, S. R.; Moore, J. S. Mechanophore-linked addition polymers. *J. Am. Chem. Soc.* **2007**, *129*, 13808−13809.

(7) Bruns, N.; Pustelny, K.; Bergeron, L. M.; Whitehead, T. A.; Clark, D. S. Mechanical nanosensor based on FRET within a thermosome: damage-reporting polymeric materials. *Angew. Chem., Int. Ed.* **2009**, *48*, 5666−5669.

(8) Wang, T.; Zhang, N.; Dai, J.; Li, Z.; Bai, W.; Bai, R. Novel Reversible Mechanochromic Elastomer with High Sensitivity: Bond Scission and Bending-Induced Multicolor Switching. *ACS Appl. Mater. Interfaces* **2017**, *9*, 11874−11881.

(9) Kosuge, T.; Imato, K.; Goseki, R.; Otsuka, H. Polymer−Inorganic Composites with Dynamic Covalent Mechanochromophore. *Macromolecules* **2016**, *49*, 5903−5911.

(10) Li, M.; Zhang, Q.; Zhou, Y.-N.; Zhu, S. Let spiropyran help polymers feel force! *Prog. Polym. Sci.* **2018**, *79*, 26−39.

DOI: 10.1021/acsami.9b09023
ACS Appl. Mater. Interfaces 2019, 11, 29268−29275

(11) Davis, D. A.; Hamilton, A.; Yang, J.; Cremar, L. D.; Van Gough, D.; Potisek, S. L.; Ong, M. T.; Braun, P. V.; Martínez, T. J.; White, S. R.; Moore, J. S.; Sottos, N. R. Force-induced activation of covalent bonds in mechanoresponsive polymeric materials. *Nature* **2009**, *459*, 68−72.
(12) Zhang, H.; Chen, Y.; Lin, Y.; Fang, X.; Xu, Y.; Ruan, Y.; Weng, W. Spiropyran as a Mechanochromic Probe in Dual Cross-Linked Elastomers. *Macromolecules* **2014**, *47*, 6783−6790.
(13) O'Bryan, G.; Wong, B. M.; McElhanon, J. R. Stress sensing in polycaprolactone films via an embedded photochromic compound. *ACS Appl Mater Interfaces* **2010**, *2*, 1594−600.
(14) Gossweiler, G. R.; Hewage, G. B.; Soriano, G.; Wang, Q.; Welshofer, G. W.; Zhao, X.; Craig, S. L. Mechanochemical Activation of Covalent Bonds in Polymers with Full and Repeatable Macroscopic Shape Recovery. *ACS Macro Lett.* **2014**, *3*, 216−219.
(15) Li, M.; Liu, W.; Zhang, Q.; Zhu, S. Mechanical Force Sensitive Acrylic Latex Coating. *ACS Appl. Mater. Interfaces* **2017**, *9*, 15156−15163.
(16) Kempe, F.; Brügner, O.; Buchheit, H.; Momm, S. N.; Riehle, F.; Hameury, S.; Walter, M.; Sommer, M. A Simply Synthesized, Tough Polyarylene with Transient Mechanochromic Response. *Angew. Chem., Int. Ed.* **2018**, *57*, 997−1000.
(17) Shree, S.; Schulz-Senft, M.; Alsleben, N. H.; Mishra, Y. K.; Staubitz, A.; Adelung, R. Light, Force, and Heat: A Multi-Stimuli Composite that Reveals its Violent Past. *ACS Appl. Mater. Interfaces* **2017**, *9*, 38000−38007.
(18) Beiermann, B. A.; Davis, D. A.; Kramer, S. L. B.; Moore, J. S.; Sottos, N. R.; White, S. R. Environmental effects on mechanochemical activation of spiropyran in linear PMMA. *J. Mater. Chem.* **2011**, *21*, 8443−8447.
(19) Grady, M. E.; Beiermann, B. A.; Moore, J. S.; Sottos, N. R. Shockwave loading of mechanochemically active polymer coatings. *ACS Appl. Mater. Interfaces* **2014**, *6*, 5350−5355.
(20) Peterson, G. I.; Larsen, M. B.; Ganter, M. A.; Storti, D. W.; Boydston, A. J. 3D-printed mechanochromic materials. *ACS Appl. Mater. Interfaces* **2015**, *7*, 577−583.
(21) Such, G.; Evans, R. A.; Yee, L. H.; Davis, T. P. Factors Influencing Photochromism of Spiro-Compounds Within Polymeric Matrices. *J. Macromol. Sci., Polym. Rev.* **2003**, *43*, 547−579.
(22) Zhou, J.; Li, Y.; Tang, Y.; Zhao, F.; Song, X.; Li, E. Detailed investigation on a negative photochromic spiropyran. *J. Photochem. Photobiol., A* **1995**, *90*, 117−123.
(23) Tian, W.; Tian, J. An insight into the solvent effect on photo-, solvato-chromism of spiropyran through the perspective of intermolecular interactions. *Dyes Pigm.* **2014**, *105*, 66−74.
(24) Shiraishi, Y.; Itoh, M.; Hirai, T. Thermal isomerization of spiropyran to merocyanine in aqueous media and its application to colorimetric temperature indication. *Phys. Chem. Chem. Phys.* **2010**, *12*, 13737−13745.
(25) Sunamoto, J.; Iwamoto, K.; Akutagawa, M.; Nagase, M.; Kondo, H. Rate control by restricting mobility of substrate in specific reaction field. Negative photochromism of water-soluble spiropyran in AOT reversed micelles. *J. Am. Chem. Soc.* **1982**, *104*, 4904−4907.
(26) Kim, T. A.; Beiermann, B. A.; White, S. R.; Sottos, N. R. Effect of Mechanical Stress on Spiropyran-Merocyanine Reaction Kinetics in a Thermoplastic Polymer. *ACS Macro Lett.* **2016**, *5*, 1312−1316.
(27) Chen, H.; Yang, F.; Chen, Q.; Zheng, J. A Novel Design of Multi-Mechanoresponsive and Mechanically Strong Hydrogels. *Adv. Mater.* **2017**, *29*, 1606900.
(28) Abdollahi, A.; Alinejad, Z.; Mahdavian, A. R. Facile and fast photosensing of polarity by stimuli-responsive materials based on spiropyran for reusable sensors: a physico-chemical study on the interactions. *J. Mater. Chem. C* **2017**, *5*, 6588−6600.
(29) Feeney, M. J.; Thomas, S. W. Tuning the Negative Photochromism of Water-Soluble Spiropyran Polymers. *Macromolecules* **2018**, *51*, 8027−8037.
(30) Marini, A.; Muñoz-Losa, A.; Biancardi, A.; Mennucci, B. What is solvatochromism? *J. Phys. Chem. B* **2010**, *114*, 17128−17135.
(31) Julià-López, A.; Hernando, J.; Ruiz-Molina, D.; González-Monje, P.; Sedó, J.; Roscini, C. Temperature-Controlled Switchable Photochromism in Solid Materials. *Angew. Chem., Int. Ed.* **2016**, *55*, 15044−15048.
(32) Schaudel, B.; Guermeur, C.; Sanchez, C.; Nakatani, K.; Delaire, J. A. Spirooxazine-and spiropyran-doped hybrid organic−inorganic matrices with very fast photochromic responses. *J. Mater. Chem.* **1997**, *7*, 61−65.
(33) Lee, C. K.; Diesendruck, C. E.; Lu, E.; Pickett, A. N.; May, P. A.; Moore, J. S.; Braun, P. V. Solvent Swelling Activation of a Mechanophore in a Polymer Network. *Macromolecules* **2014**, *47*, 2690−2694.
(34) Li, M.; Lei, L.; Zhang, Q.; Zhu, S. CO_2-Breathing Induced Reversible Activation of Mechanophore within Microgels. *Macromol. Rapid Commun.* **2016**, *37*, 957−962.
(35) Qiu, W.; Gurr, P. A.; da Silva, G.; Qiao, G. G. Insights into the mechanochromism of spiropyran elastomers. *Polym. Chem.* **2019**, *10*, 1650−1659.
(36) Ziółkowski, B.; Florea, L.; Theobald, J.; Benito-Lopez, F.; Diamond, D. Self-protonating spiropyran-co-NIPAM-co-acrylic acid hydrogel photoactuators. *Soft Matter* **2013**, *9*, 8754−8760.
(37) Fang, X.; Zhang, H.; Chen, Y.; Lin, Y.; Xu, Y.; Weng, W. Biomimetic Modular Polymer with Tough and Stress Sensing Properties. *Macromolecules* **2013**, *46*, 6566−6574.
(38) Ellis, T. S.; Karasz, F. E. Interaction of epoxy resins with water: the depression of glass transition temperature. *Polymer* **1984**, *25*, 664−669.
(39) Balmond, E. I.; Tautges, B. K.; Faulkner, A. L.; Or, V. W.; Hodur, B. M.; Shaw, J. T.; Louie, A. Y. Comparative Evaluation of Substituent Effect on the Photochromic Properties of Spiropyrans and Spirooxazines. *J. Org. Chem.* **2016**, *81*, 8744−8758.
(40) Kemal, E.; Adesanya, K. O.; Deb, S. Phosphate based 2-hydroxyethyl methacrylate hydrogels for biomedical applications. *J. Mater. Chem.* **2011**, *21*, 2237−2245.
(41) Malatesta, V.; Renzi, F.; Wis, M. L.; Montanari, L.; Milosa, M.; Scotti, D. Reductive degradation of photochromic spiro-oxazines. Reaction of the merocyanine forms with free radicals. *J. Org. Chem.* **1995**, *60*, 5446−5448.
(42) Demadrille, R.; Rabourdin, A.; Campredon, M.; Giusti, G. Spectroscopic characterisation and photodegradation studies of photochromic spiro[fluorene-9,3′-[3′H]-naphtho[2,1-b]pyrans]. *J. Photochem. Photobiol., A* **2004**, *168*, 143−152.
(43) Radu, A.; Byrne, R.; Alhashimy, N.; Fusaro, M.; Scarmagnani, S.; Diamond, D. Spiropyran-based reversible, light-modulated sensing with reduced photofatigue. *J. Photochem. Photobiol., A* **2009**, *206*, 109−115.

DOI: 10.1021/acsami.9b09023
ACS Appl. Mater. Interfaces 2019, 11, 29268−29275